Alkali-Metal-Mediated Alumination

Development of *bis*-TMP Chemistry of [(THF)AM(TMP)$_2$Al(*i*Bu)$_2$] with Emphasis on Lithium

Elaine Crosbie

A thesis submitted to the Department of Pure and Applied Chemistry, University of Strathclyde, in part fulfilment of the regulations for the degree of Doctor of Philosophy.

May 2013

This thesis is the result of the author's original research. It has been composed by the author and has not been previously submitted for examination which has led to the award of a degree.

Acknowledgements

Firstly, I would like to thank my supervisor Professor Robert Mulvey for allowing me to join his research group and for believing in me when I was an undergraduate student working on my final year project. I am extremely grateful to have been given the opportunity to undertake such a fascinating area of chemistry. His support and continual encouragement has made it a pleasure to work for him. It has been a tough three and a half years but I have enjoyed every minute of it and it is a time I will always look back on fondly. I would also like to thank him for introducing me to Friday lunch, something which I never missed. I have had the pleasure of tasting some of Glasgow's finest food as well as being introduced to many different eating establishments from Mother India to Coia's Cafe! I couldn't write these acknowledgements without thanking him for allowing me to go to Hawaii on my international conference trip. What can I say other than, it was Hawaii!! It was a once in a life time trip which I will never forget and not just because we all got stuck there on Christmas Day. I would happily swap any future Christmas for a trip back there. Most importantly I would like to thank him for taking the time to read and correct this thesis and for all the ideas he has given me towards the project.

The most important person I would like to say a huge thank you to is my husband to be Graham (as I write this it is less than two months to our wedding!). I don't know what I would have done without him especially during the time I have had to write this thesis whilst also applying for jobs and planning the wedding. He has been a constant support and always knows how to make me laugh when times are tough. I consider myself very lucky to have him in my life and I know I have found a fantastic husband!

Someone else who should not go unnoticed is Dr Stuart Robertson, not only for spending numerous hours over at X-ray obtaining all my crystal structures but for the avid interest he has taken in my project. He has spent a great deal of time helping me out and giving me lots of ideas so for that I am extremely grateful. The standard of work within this thesis is a true reflection of Stuart's continual help and support.

I would also like to thank Dr Alan Kennedy for taking the time to check all the X-ray structures, Dr Dave Armstrong for the DFT calculations and Craig Irving for help with NMR spectroscopy.

A note of thanks must also go to Dr Charlie O'Hara (my second supervisor) and Dr Eva Hevia who were always on hand to provide ideas and suggestions at group meetings. I would also like to thank Eva for all the help with the work carried out in Chapter 5 as she would take time out of her day to sit in meetings to discuss the chemistry.

Lastly but certainly not least I would like to finish off by thanking my fellow lab colleagues and friends. The lab would have certainly been a dull place without you all! I would like to say a special thanks to Zoe (small fry), Jenni (posh spice), Donna (give me a blue WKD) and Emma (grumpy cat) who were my regular lunchtime buddies. Our lunchtime chats were always the highlight of my day (no one mention the D word or Innocent Smoothies ☺!). I must also thank all the girls (Jenni, Zoe, Donna, Emma, Silvia, Marina, Ana and Sarah) who came to my hen do in Newcastle, what a weekend! It was made extra special because I was able to celebrate it with you all. And who could forget Ross? He had no sense of smell and ate the same dinner every night for two weeks but that was Ross, one in a million (literally!). His random questions and bizarre comments always made me laugh and I miss working with him every day. I am very privileged to have met and worked with such a fantastic group of people and I know I have made some very good friends for life!

Abstract

Deprotonation, the exchange of an inert carbon-hydrogen bond for a more chemically useful carbon-metal bond, has long been one of the methods of choice for constructing substituted aromatic and heteroaromatic compounds. Organolithium reagents have been the standard for this purpose for many years; however, their many limitations mean that new reagents for deprotonative metallation are sought. Alkali-Metal-Mediated Metallation (AMM*M*) was developed as an alternative vehicle to functionalising a plethora of substrates. This project focuses on the synergic alumination chemistry generated by combining lithium amide LiTMP with low polarity aluminium reagent *i*Bu$_2$AlTMP exhibiting the reaction concept of Alkali-Metal-Mediated Alumination (AMM*Al*).

AMM*Al* reactions of lithium *bis*-TMP aluminate [(THF)Li(TMP)$_2$Al(*i*Bu)$_2$] were explored to learn more about the reactivity of this *bis*-amido base. Several functionalised aromatic substrates including anisole and *N*,*N*-diisopropylbenzamide were effectively *ortho*-aluminated in hexane solution at ambient temperature and quenched with iodine to generate the corresponding metal-free products in excellent yield. DFT calculations and DOSY NMR experiments were conducted to elucidate a possible structure for the base as it could not be isolated. A mechanism was proposed showing an open-structure with a *pseudo*-terminal TMP. This allowed a rationale for the intramolecular reactivity observed with a series of donor molecules including THF which could be deprotonated and the resulting anion trapped without ring opening.

Several key differences were observed between our *bis*-amido base [Li(TMP)$_2$Al(*i*Bu)$_2$] and Uchiyama's mono-amido base [Li(TMP)Al(*i*Bu)$_3$]. THF was deprotonated and its anion captured with the former; whereas the latter was found to be more stable in THF solution. Other donor molecules such as 1-methoxy-2-dimethylaminoethane (MDAE) and *bis*-[2-(*N*,*N*-dimethylamino)ethyl]ether (Me$_4$AEE) were deprotonated with the *bis*-amido base; whereas they were found to merely solvate lithium when the mono-amido base was employed. An investigation into the mono-amido base in THF solution revealed some interesting facts concluding us to believe that this base disproportionates to give our mono-amido base in THF solution.

Publications

Peer-reviewed papers arising from work carried out in this project:

1. *Structurally Engineered Deprotonation/Alumination of THF and THTP with Retention of Their Cycloanionic Structures*. **E. Crosbie**, P. García-Álvarez, A. R. Kennedy, J. Klett, R. E. Mulvey and S. D. Robertson, *Angew. Chem. Int. Ed.* **2010**, *49*, 9388 – 9391.

2. *Structurally Powered Synergic 2,2,6,6-tetramethylpiperidine Bimetallics: New Reflections Through Lithium-Mediated Ortho-Aluminations*. D. R. Armstrong, **E. Crosbie**, B. Conway, A. R. Kennedy, R. E. Mulvey and S. D. Robertson, *Inorg. Chem.* **2011**, *50*, 12241 – 12251.

3. *After-Effects of Lithium-Mediated Alumination of 3-iodoanisole: Isolation of Molecular Salt Elimination and Trapped Benzyne Products*. **E. Crosbie**, A. R. Kennedy, R. E. Mulvey and S. D. Robertson, *Dalton Trans.* **2012**, *41*, 1832 – 1839.

4. *Regioselective Heterohalogenation of 4-halo-anisoles via a Series of Sequential Ortho-Aluminations and Electrophilic Halogenations*. B. Conway, **E. Crosbie**, A. R. Kennedy, R. E. Mulvey and S. D. Robertson, *Chem. Commun.* **2012**, *48*, 4674 – 4676.

5. *Contrasting Reactivity of mono-TMP Versus bis-TMP (2,2,6,6-tetramethylpiperidide) Lithium Aluminates Towards Polydentate Lewis Bases: Co-complexation Versus Deprotonation.* R. Campbell, **E. Crosbie**, A. R. Kennedy, R. E. Mulvey, R. A. Naismith, S. D. Robertson, *Aust. J. Chem*. **2013** (accepted).

Conference Presentations

1. *Two TMP Ligands are Better Than One for Lithium-Mediated Alumination Reactions*, Prize for best Oral Presentation, Universities of Scotland Inorganic Chemistry Conference, Durham University, July 2010.

2. *Two TMP Ligands are Better Than One for Lithium-Mediated Alumination Reactions*, Poster Presentation, PacifiChem Conference, Hawaii, December 2010.

3. *FascinATES: Alkali Metals and Aluminium Working Together to Create Novel Metallation Chemistry*, Oral Presentation, West Brewery Inorganic Chemistry Postgraduate Presentations, Glasgow, June 2011.

4. *FascinATES: Alkali Metals and Aluminium Working Together to Create Novel Metallation Chemistry*, Oral Presentation, Inorganic Chemistry Conference, RSC London, July 2011.

5. *Two TMP Ligands are Better Than One for Lithium-Mediated Alumination Reactions*, Poster Presentation, Universities of Scotland Inorganic Chemistry Conference, Glasgow University, July 2011.

6. *FascinATES: Alkali Metals and Aluminium Working Together to Create Novel Metallation Chemistry*, Oral Presentation, WestCHEM Colloquia, University of Strathclyde, June 2012.

7. *FascinATES: Alkali Metals and Aluminium Working Together to Create Novel Metallation Chemistry*, Poster Presentation, Universities of Scotland Inorganic Chemistry Conference, St Andrews University, August 2012.

Abbreviations

AM	Alkali Metal
AMM*Al*	Alkali-Metal-Mediated Alumination
AMMM	Alkali-Metal-Mediated Metallation
*i*Bu	*iso*-butyl
*n*Bu	*n*-butyl
*t*Bu	*tert*-butyl
*t*BuOK	Potassium *tert*-butoxide
CCDB	Cambridge Crystallographic Database
C_6D_6	Deuterated benzene
C_6D_{12}	Deuterated cyclohexane
$CDCl_3$	Deuterated chloroform
CH_2SiMe_3	Monosilyl group
CIP	Contact Ion Pair
CIPE	Complex Induced Proximity Effect
COSY	Correlation Spectroscopy
Cp	Cyclopentadiene anion $(C_5H_5)^-$
DA	Diisopropylamide
DA(H)	Diisopropylamine
DFT	Density Functional Theory
DIBAH	Diisobutylaluminium hydride
DIPP	2,6-diisopropylphenol
DMAE	Dimethylaminoethanol
DME	1,2-dimethoxyethane
DMP	*cis*-2,6-dimethylpiperidide
DMP(H)	*cis*-2,6-dimethylpiperidine
D*o*M	Directed *ortho*-Metallation
DOSY	Diffusion Ordered Spectroscopy

Et	Ethyl
Fc	Ferrocene
GC-MS	Gas Chromatography-Mass Spectrometry
HMDS	1,1,1,3,3,3-hexamethyldisilazide
HMDS(H)	1,1,1,3,3,3-hexamethyldisilazane
HMPA	Hexamethylphosphoramide
HOESY	Heteronuclear Overhauser Effect Spectroscopy
HSQC	Heteronuclear Single Quantum Correlation Spectroscopy
LDA	Lithium diisopropylamide
LICKOR	Alkyllithium/potassium alkoxide superbase
MAD	Methylaluminium *bis*(2,6-di-*tert*-butyl-4-methylphenoxide)
MDAE	1-methoxy-2-dimethylaminoethane
Me	Methyl
Mes	Mesityl group
Me_4AEE	*bis*[2-(*N*,*N*-dimethylamino)ethyl]ether
Me_2TFA	*N*,*N*-dimethyltetrahydrofurfurylamine
Me_6-TREN	*tris*[2-(dimethylamino)ethyl]amine
MW	Molecular Weight
NMR	Nuclear Magnetic Resonance
NOE	Nuclear Overhauser Effect
OAc	Acetate group
OMe	Methoxy group
OTf	Trifluoromethanesulfonate
Ph	Phenyl
PhN	Phenylnaphthalene
PMDETA	*N*,*N*,*N*',*N*'',*N*''-pentamethyldiethylenetriamine
ppm	parts per million
*i*Pr	*iso*-propyl
R	Generic alkyl group

RLi	Generic alkyl lithium reagent
RMgX	Generic Grignard reagent
SPhos	2-dicyclohexylphosphino-2',6'-dimethoxybiphenyl
SSIP	Solvent Separated Ion Pair
TEDTA	Tetraethyldiethylenetriamine
THF	Tetrahydrofuran
THP	Tetrahydropyran
THT	Tetrahydrothiophene
THTP	Tetrahydrothiopyran
TMCDA	*N*,*N*,*N*',*N*'-(1*R*,2*R*)-tetramethylcyclohexane-1,2-diamine
TMEDA	*N*,*N*,*N*',*N*'-tetramethylethylenediamine
TMP	2,2,6,6-tetramethylpiperidide
TMP(H)	2,2,6,6-tetramethylpiperidine
TMS	Tetramethylsilane
TPP	Tetraphenylporphyrin
X	Halogen

Contents

Chapter 5: Comparison Between *bis*-TMP and *mono*-TMP Base

Chapter 6: General Experimental

Compounds

Chapter 2: Reactivity of *bis*-TMP Base

Number	Compound	Number	Compound
1.1	**[(THF)Li(TMP)$_2$Al(*i*Bu)$_2$]**	**1.2**	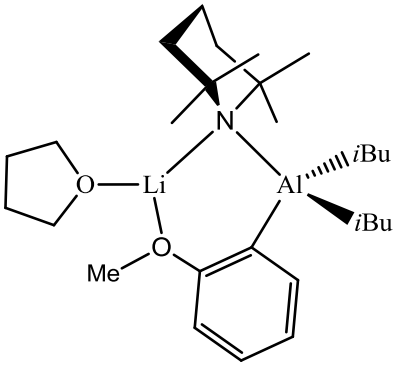
1.3	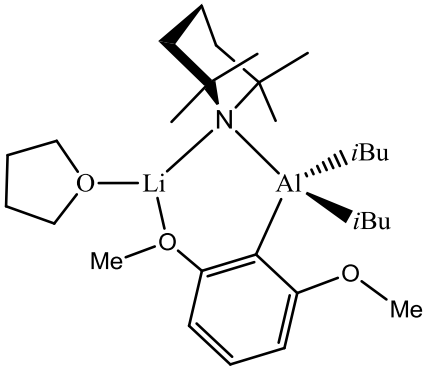	**1.4**	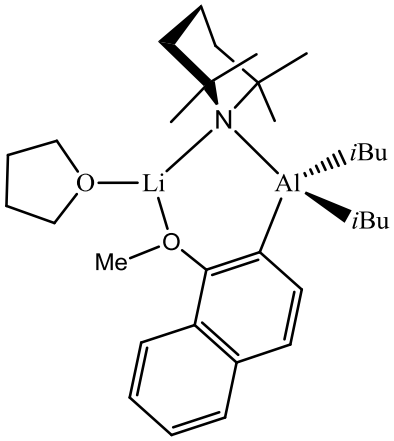
1.5	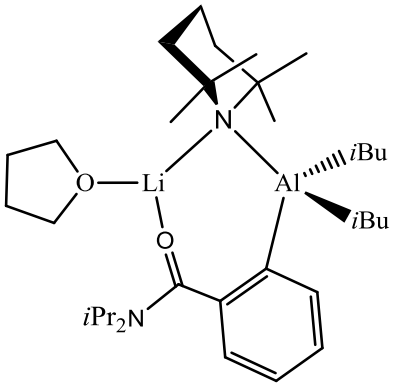	**1.6**	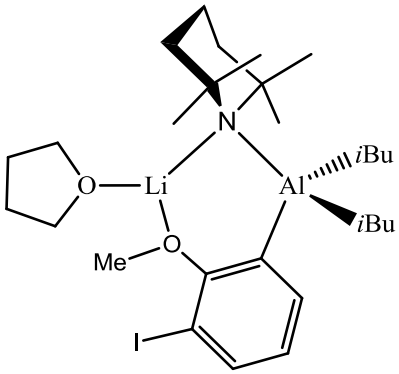

Number	Compound	Number	Compound
1.7	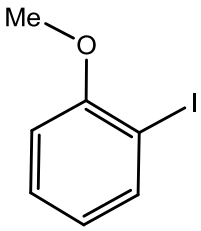	**1.8**	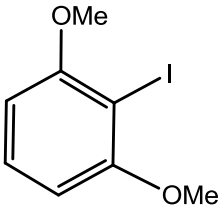
1.9	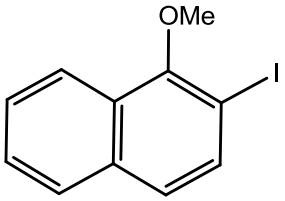	**1.10**	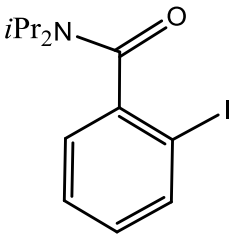
1.11	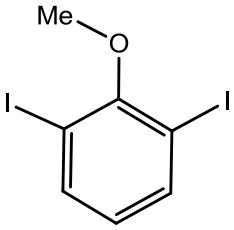	**1.12**	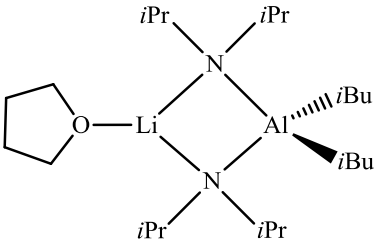
1.13	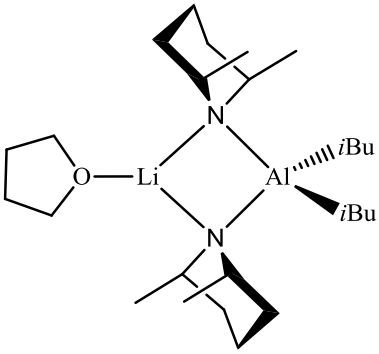	**1.14**	iBu$_2$Al(TMP)
1.15a	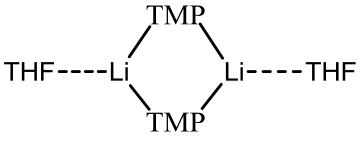	**1.15b**	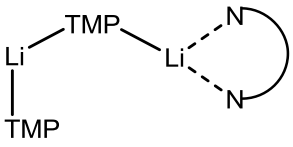

Number	Compound	Number	Compound
1.16	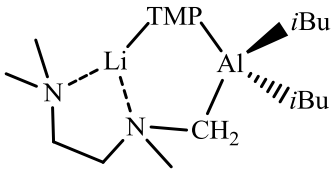	**1.17**	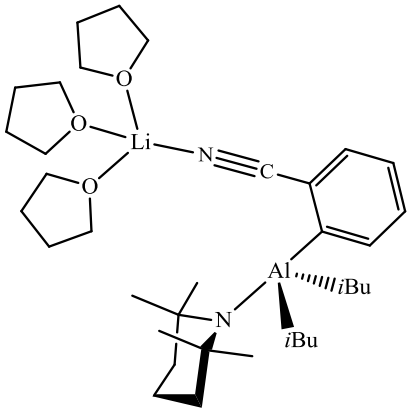
1.18	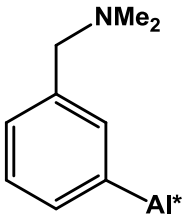	**1.19**	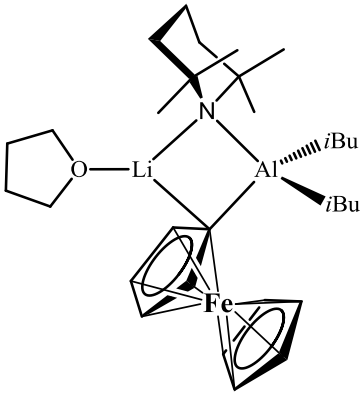
1.20	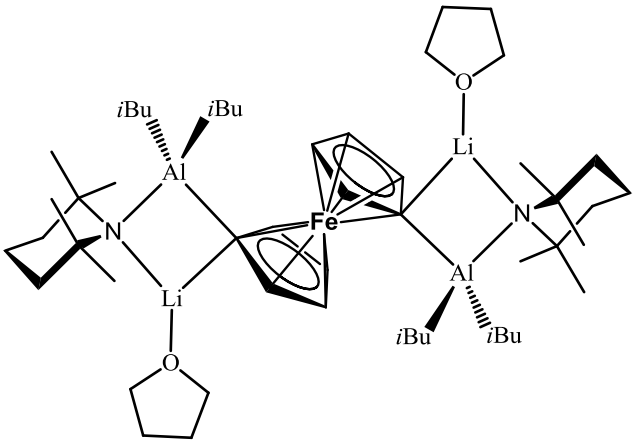		

Chapter 3: Donor Deprotonation

Number	Compound	Number	Compound
2.1	**[(THF)Li(TMP)$_2$Al(*i*Bu)$_2$]**	**2.2**	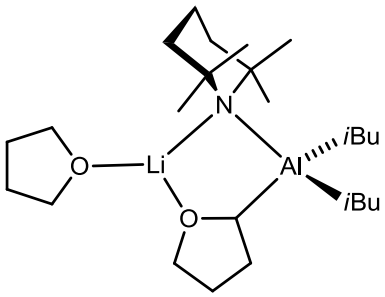
2.3	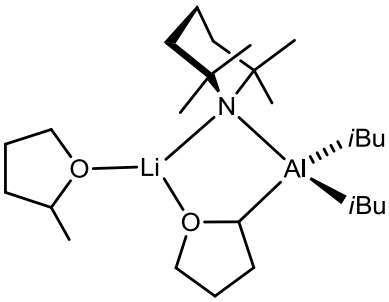	**2.4**	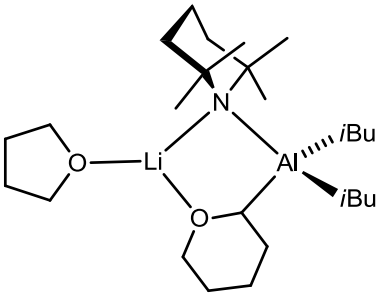
2.5	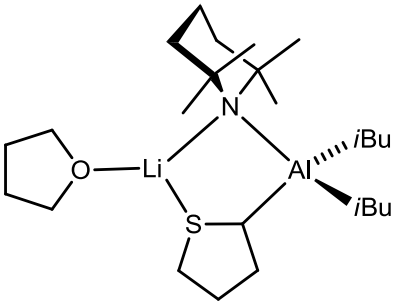	**2.6**	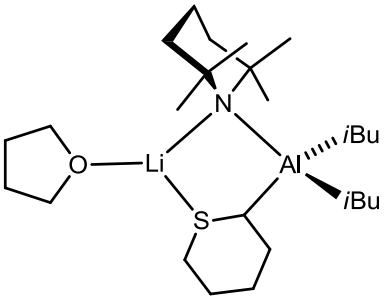
2.7	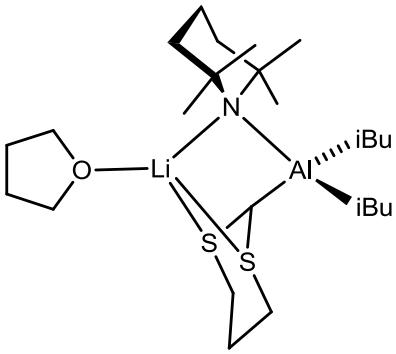	**2.8**	[Li(TMP)Al(*i*Bu)$_3$]

Number	Compound	Number	Compound
2.9	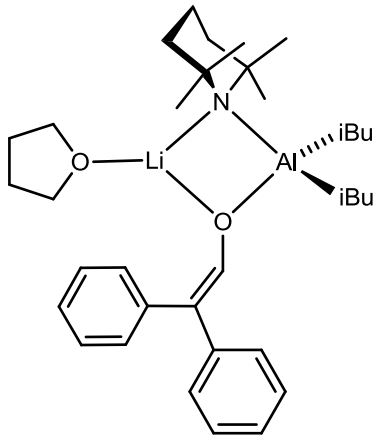	**2.10**	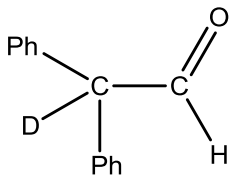
2.8C	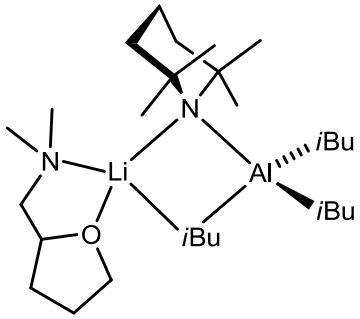	**2.8D**	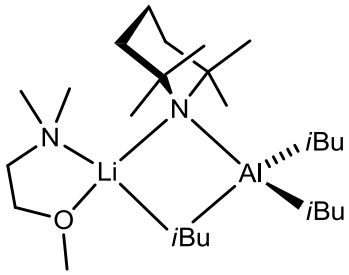
2.8F	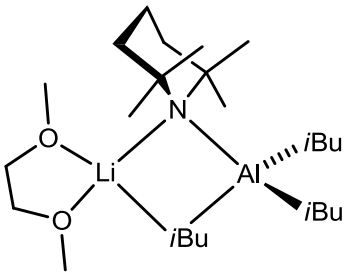	**2.1C**	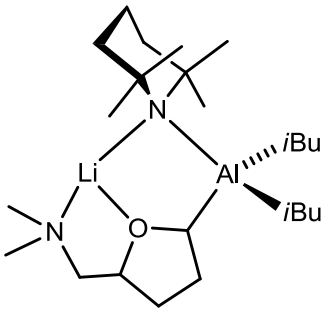
2.1D	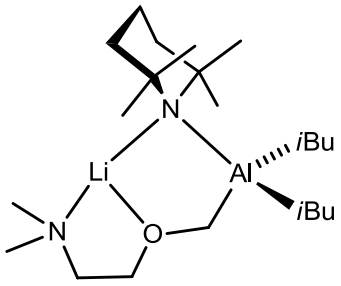	**2.1E**	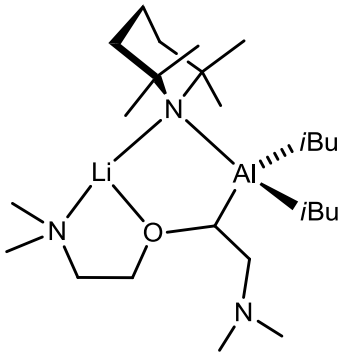

Number	Compound	Number	Compound
2.8H	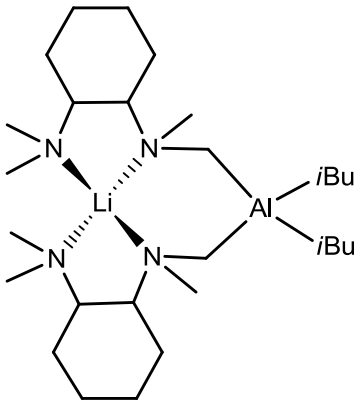		
2.1FA	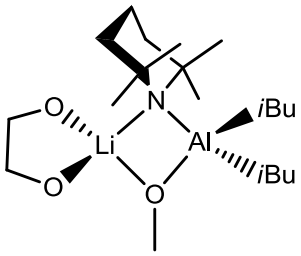	**2.1E'**	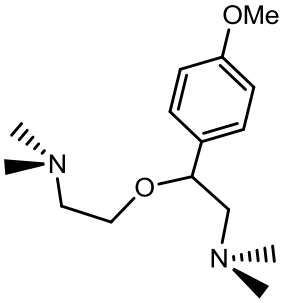
2.1F	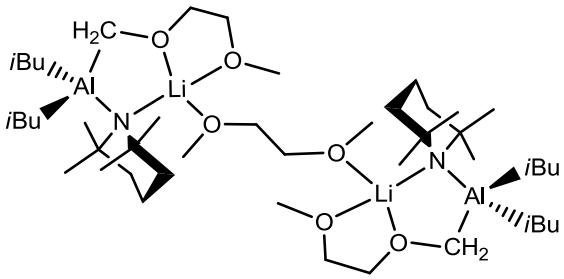		

Chapter 4: Halogen Substituted Aromatics

Number	Compound	Number	Compound
3.1	**$[(TMP)_3Al{\cdot}3LiCl]$**	**3.2**	$[Li(TMP)Al(iBu)_3]$
3.3	**$[Li(TMP)_2Al(iBu)_2]$**	**3.4**	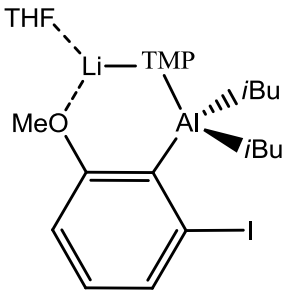
3.5	**$[LiI{\cdot}TMP(H)]_4$**	**3.6**	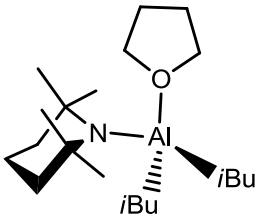
3.7	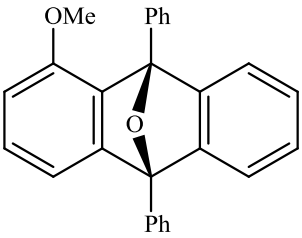	**3.8**	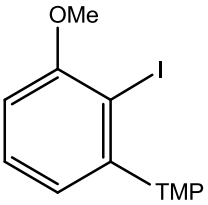
3.9	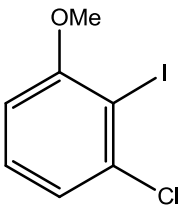	**3.10a**	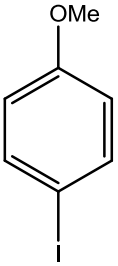

Number	Compound	Number	Compound
3.10b	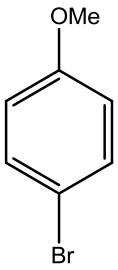	**3.10c**	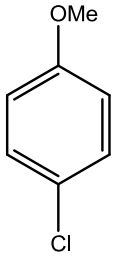
3.11a	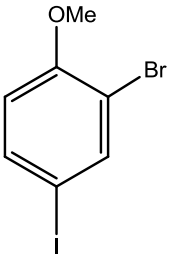	**3.11b**	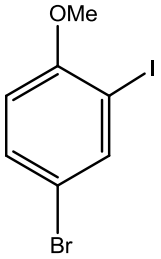
3.11c	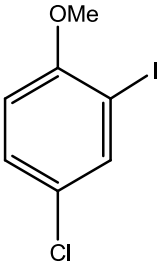	**3.12a**	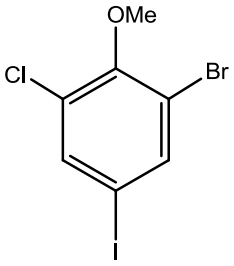
3.12b	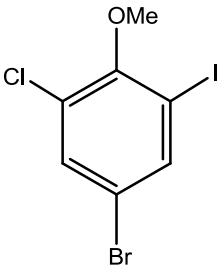	**3.12c**	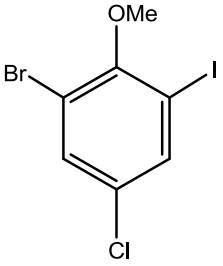
3.10-int	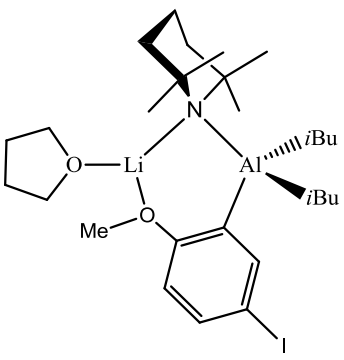	**3.11-int**	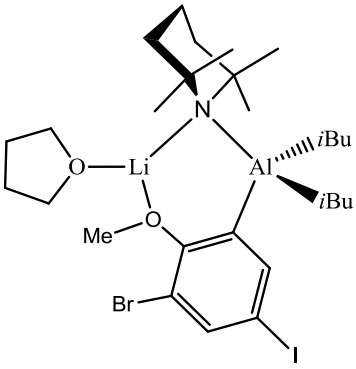

Number	Compound	Number	Compound
4.1	**[Li(TMP)$_2$Al(*i*Bu)$_2$]**	**4.2**	[Li(TMP)Al(*i*Bu)$_3$]
4.3	**[{Li(THF)$_4$}$^+${Al(*i*Bu)$_4$}$^-$]**	**4.4**	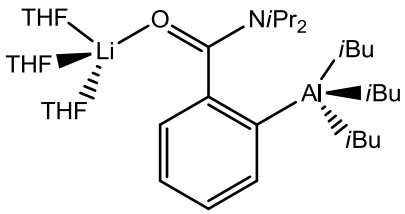
4.5	**[Na(TMP)Al(*i*Bu)$_3$]**	**4.6**	[Na(TMP)$_2$Al(*i*Bu)$_2$]

Chapter 1: Introduction

This chapter sets out to give an overview of special areas of organometallic chemistry including an in-depth look at organolithium reagents, directed *ortho*-metallation (D*o*M) and organoaluminium chemistry. These important classes of reagents will be examined individually before exploring the synergy these two metals can generate once combined in a mixed-metal complex. The concept of mixed-metal synergic chemistry and alkali-metal-mediated alumination will be unfolded.

1.1 Organometallic Reagents

Organometallic reagents are considered one of the most important synthetic tools for the regio-, chemo- and enantioselective functionalisation of aromatic and heteroaromatic substrates. The generated organometallic intermediates are quenched with a vast array of electrophiles giving compounds with applications in the pharmaceutical and agrochemical industries.[1–4] The pioneering work of Frankland (Et_2Zn)[5,6] and Grignard (RMgX),[7,8] who synthesised two of the most important types of organometallic reagent, paved the way for the development of many new methods for synthesising these reagents.[9] Nowadays, organometallic reagents can be picked from our synthetic toolbox to transform all manner of substrates depending on the desired regio-, chemo- and enantioselectivity.

The choice of organometallic reagent is the prime consideration when functionalising a given substrate. Altering the metal can influence the reactivity due to the nature of the carbon-metal bond. In general, the more ionic the bond the more reactive the organometallic reagent will be. For example, organolithium reagents have the most ionic C-M bonds due to the large difference in electronegativity between carbon (2.5 χ) and lithium (1.0 χ).[10] This is why organolithium reagents are so reactive and have a tendency to attack most functional groups even at low temperature.[11–14] Grignard reagents on the other hand can be utilised at higher temperatures as they have more covalent carbon-magnesium bonds hence are more tolerant of functional groups.[15–17] Organozinc reagents are the least reactive of the organometallic reagents as the C-Zn bond possesses the most covalent character. There are three main routes to access organometallic reagents: oxidative insertion, metal-halogen exchange and direct metallation. These are now summarised in turn.

1.1.1 Oxidative Insertion

Oxidative insertion involves the oxidative addition of a metallic element into an organic halide. Grignard reagents, developed by the Nobel Laureate Victor Grignard in 1900, are examples of organometallic reagents formed via oxidative insertion. It involves the insertion of Mg metal into a carbon-halogen bond via a single electron transfer radical mechanism (**Scheme 1.1**).[18–22] Although empirically formulated as R-Mg-X the structures of Grignard reagents in ethereal solvents are significantly more complex.[23] These air sensitive reagents are powerful synthetic tools for converting carbonyl compounds to alcohols, alkylating aldehydes and ketones and serving as nucleophiles for many electrophilic substrates.[24,25]

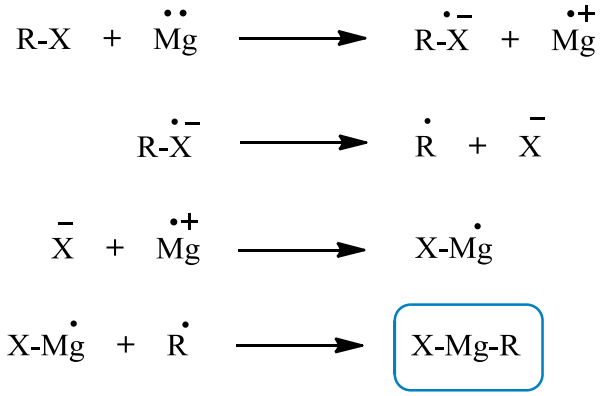

Scheme 1.1: Formation of Grignard reagent RMgX from Mg and R-X via a radical mechanism.

Similarly, Gilman and Wittig pioneered the application of organolithium reagents prepared by oxidative insertion of lithium metal into organic halides.[26] Overcoming the poor functional group tolerance inherent in organolithium reagents saw Rieke and co-workers develop Rieke metals for carrying out insertion reactions at low temperature. These metals are prepared by reducing metal halides with lithium-naphthalenide or elemental sodium or potassium.[27–32] More recently Knochel and co-workers have reported new routes to insertion products including the insertion of magnesium[33–35] and zinc[36–38] into carbon-halogen bonds in the presence of LiCl. In addition, they have also reported the direct insertion of Al powder into aryl halides in the presence of LiCl giving access to functionalised aromatic and heteroaromatic aluminium reagents.[39] These are just a selection of examples of routes to prepare organometallic reagents via oxidative insertion. Another important synthetic protocol for the same purpose is metal-halogen exchange.

1.1.2 Metal-Halogen Exchange

Developed back in the early 20th century, the metal-halogen exchange reaction, involves the exchange of a carbon-halogen bond for a carbon-metal bond which is synthetically more useful.[40] The reaction involves an organic halide and an organometallic reagent such as a Grignard or organolithium reagent. The reaction is in equilibrium (that is, it can be backwards as well as forwards) so its success lies in the formation of a more stable carbanion than that found in the starting organometallic reagent. Metal-halogen exchange reactions are therefore better applied to substrates with sp^2 carbon centres, such as aromatics, as these provide much more stable carbon-metal bonds. Prevost reported one of the first examples of metal-halogen exchange as long ago as 1931 where he reacted cinnamyl bromide with EtMgBr to generate cinnamylmagnesium bromide (**Scheme 1.2**).[41] Since then this concept has been studied at great length and it is now possible to generate lithium compounds bearing sensitive functional groups such as ketones and nitriles.[42,43]

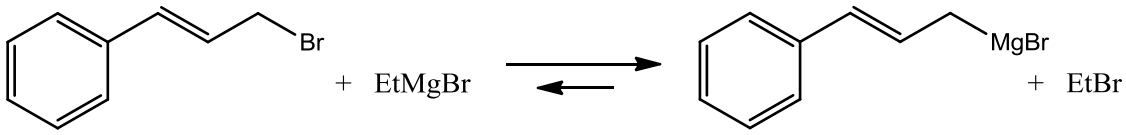

Scheme 1.2: Metal-halogen exchange reaction between cinnamyl bromide and EtMgBr to give cinnamylmagnesium bromide.

Many recent breakthroughs in this chemistry have come from Knochel who in 1998 reported a method for generating organomagnesium reagents from polyfunctional substrates bearing more than one sensitive group.[44] He also developed the "turbo-Grignard reagent" in 2004 by adding one equivalent of LiCl to *i*PrMgCl resulting in a superior reagent with a remarkably enhanced reactivity.[45] For example, reacting 4-bromoanisole with the normal Grignard reagent *i*PrMgCl produced only a poor yield of the desired metal-halogen exchange product. The new turbo-Grignard reagent *i*PrMgCl·LiCl on the other hand produced the 4-magnesiated anisole in excellent yield. LiCl is thought to coordinate to the magnesium reagent decreasing its aggregation state, increasing its solubility and hence increasing its reactivity (**Scheme 1.3**).[46]

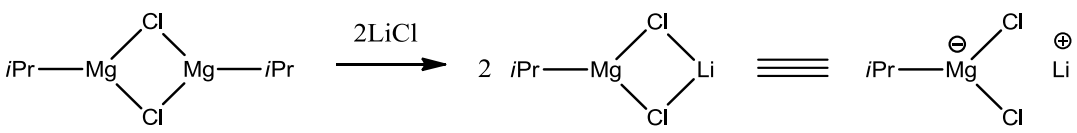

Scheme 1.3: Proposed deaggregation of *i*PrMgCl by LiCl.

1.1.3 Direct Metallation

The third common way to generate organometallic reagents is via the direct metallation of a substrate by alkyl or amide reagents (typically organolithium reagents). In contrast to oxidative insertion and metal-halogen exchange reactions a halogen-carbon bond is not required; instead a suitably acidic carbon-hydrogen bond is converted into a more reactive carbon-metal bond. Schlenk was the forerunner in metallation chemistry reporting the reaction of fluorene with EtLi in 1928 to give fluorenyllithium and ethane by abstraction of a bridgehead proton (**Scheme 1.4**).[47] As direct metallation using organolithium reagents forms part of this introduction it will be discussed in detail in the following pages.

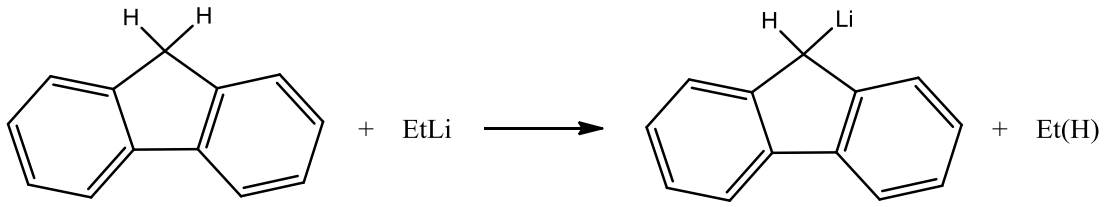

Scheme 1.4: Lithiation of fluorene by EtLi generating fluorenyllithium and ethane.

Aside from lithium reagents, magnesium bases of general formula "R_2NMgX" have also risen to prominence for direct metallation pioneered by Hauser.[48,49] Additionally, Eaton[50–52] and Mulzer[53–55] have reported the magnesium amide bases TMP_2Mg and TMPMgCl and have shown their effectiveness at functionalising aromatic and heterocycle substrates respectively. Similar to turbo-Grignard reagents, turbo-Hauser bases were synthesised by Knochel this time by mixing TMPMgCl and LiCl.[56] These bases demonstrate once again how the addition of LiCl can have a remarkable effect on the reactivity by solubilising and deaggregating the reagent. Another magnesium base found to be useful in direct metallation reactions is the more kinetically active *bis*-amido variant $TMP_2Mg{\cdot}2LiCl$ which was found to be good for functionalising less activated aromatic and heteroaromatic substrates.[57–59]

Direct metallation using organolithium reagents is by far the most widely studied methodology. A comprehensive look at the structure and reactivity of these reagents can help us understand better these powerful deprotonation agents.

1.2 Organolithium Reagents

The discovery of organolithium reagents such as methyl, ethyl and phenyllithium can be dated back to the Nobel Prize nominated work of Wilhelm Schlenk, a German chemist famous for his epochal work on air and moisture sensitive chemistry.[60] He was a pioneer, not only developing organolithium reagents but also the Schlenk flask and line which are now utilised routinely in chemical laboratories worldwide.

Synonymous with organolithium reagents is the deprotonative metallation reaction, one of the most important and globally used synthetic transformations, not only in industry but also in academia. Fundamentally, it describes the breaking of a relatively inert carbon-hydrogen bond by a metal-based reagent followed by the making of a more reactive and thus more chemically useful carbon-metal bond. The reaction is achieved by utilising polar organo alkali-metal reagents such as alkyl [R-Li e.g. *n*BuLi] or amido [R_2NLi e.g. $(Me_3Si)_2NLi$] lithium reagents or when the hydrogen atom to be abstracted is not acidic enough, LICKOR superbases.[61]

For the deprotonation reaction to be a useful synthetic tool it must firstly be selective, abstracting one specific proton often from many, and secondly requires a strong base to assist the hydrogen-metal exchange process. As a consequence highly reactive species are needed. Organolithium reagents are well equipped to carry out these (hydrogen-metal exchange) reactions due to the high electropositivity of lithium which creates a very reactive and polar carbon-lithium ($Li^{\delta+}$-$C^{\delta-}$) bond which can facilitate the deprotonation of a suitably acidic C-H substrate with relative ease. The resulting negatively charged carbanion can then be exposed to an electrophilic source, giving rise to the desired product. This can occur with a vast array of organic compounds. One of the most important applications of deprotonation chemistry, from a synthetic viewpoint, is the synthesis of pharmaceuticals. Smaller molecules act as building blocks with which to construct larger more complex molecules and it is the job of the deprotonation reaction and subsequent electrophilic quench to aid in synthesising these more useful compounds. For example, Schlosser has shown that the commonly used anti-inflammatory drug Ibuprofen (used for pain relief, fever and swelling) can be prepared by carrying out three sequential regioselective deprotonations (**Scheme 1.5**), emphasising the importance of this reaction type in synthetic chemistry.[62]

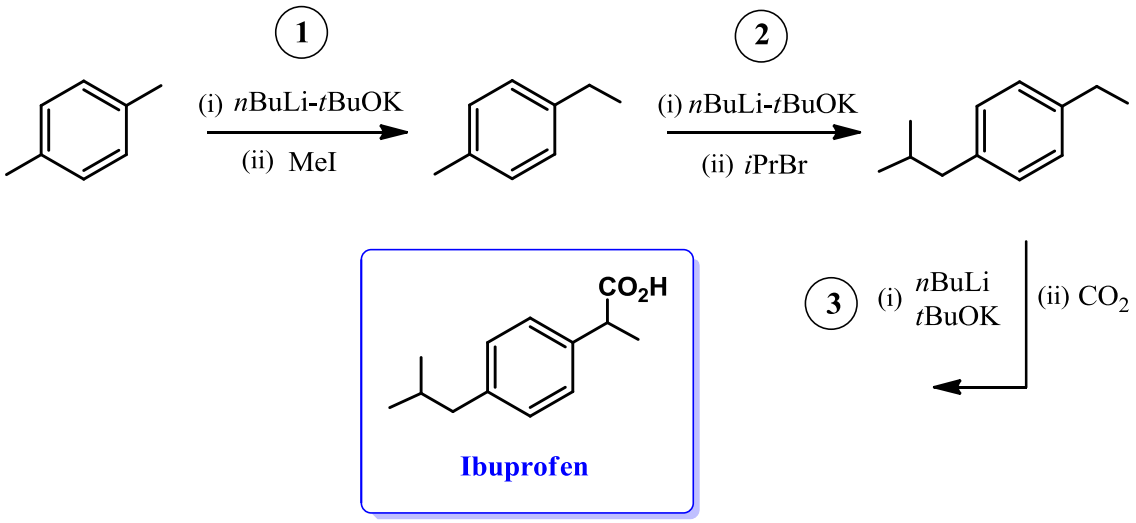

Scheme 1.5: Three sequential deprotonations leading to the synthesis of Ibuprofen.

The wide applicability of organolithium reagents lies in their simplicity and commercial availability. Although many are highly pyrophoric they are relatively easy to use and many can be purchased as hydrocarbon solutions. Reagents such as *n*-butyllithium (*n*BuLi) or the more sterically demanding metal amides, lithium diisopropylamide (LDA), lithium HMDS (HMDS = 1,1,1,3,3,3-hexamethyldisilazide) and lithium TMP (TMP = 2,2,6,6-tetramethylpiperidide) are examples of some of the most commonly used organolithium reagents.

An in depth understanding of the reactivity of organolithium reagents would not be complete without a discussion of the structural chemistry of these compounds. The structure of methyllithium, the simplest organolithium, was elucidated in 1964 by Weiss who solved the structures of many of the most important organolithium and polar organometallic compounds.[63,64] The structure is a body centred cubic array of tetrameric lithium units where each face is capped by a methyl group to form a distorted cubane with alternating carbon and lithium atoms. The methyl group of one cubane interacts with a lithium atom of another to form the infinite lattice. As a result of this polymeric network methyllithium is insoluble in hydrocarbon solvent unless polar additives are present. The ability of methyllithium to polymerise in this way is a direct consequence of the smallness of the organic group as other organolithium reagents such as hexameric *n*BuLi (*n*-butyllthium) or tetrameric *t*BuLi (*t*-butyllithium) which contain more sterically demanding groups do not display intermolecular interactions between

units.[65] The structure of the organolithium reagent is also altered depending on the solvent in which it is dissolved. For methyllithium the tetramer is favoured in polar solvents; whereas the structure switches to a hexamer in non-polar solvents such as benzene. The same is true about the structure of *n*-butyllithium which also adopts a discrete tetrameric structure in polar solvents such as tetrahydrofuran (THF) and a hexamer in non-polar solvents such as cyclohexane (**Figure 1.1**).[66]

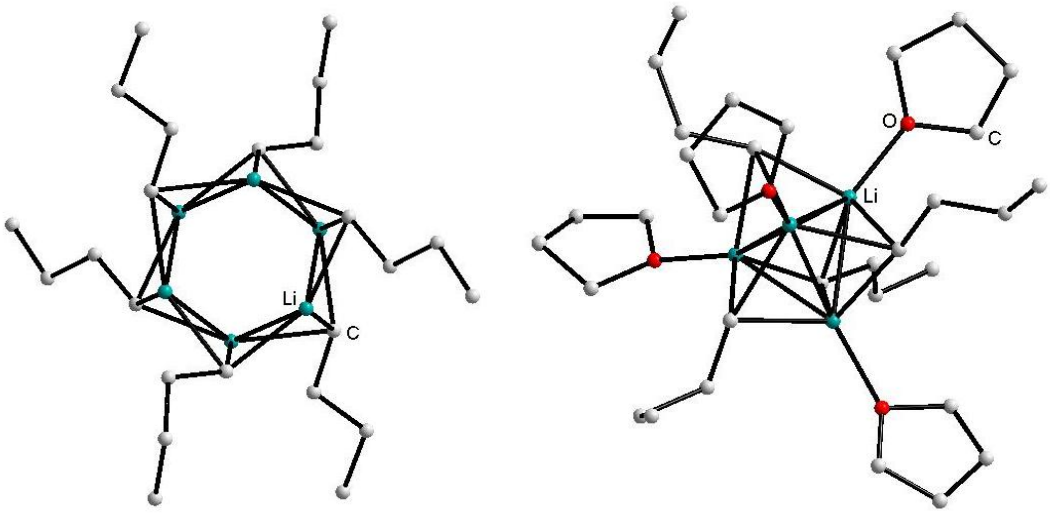

Figure 1.1: Hexameric structure of *n*-butyllthium in non-polar solvent (left) and tetrameric structure of *n*-butyllithium in polar THF (right).

Organolithium reagents are not only utilised directly they are also used to make another important class of deprotonation reagent. Deprotonation of relatively acidic secondary amines such as TMP(H) (2,2,6,6-tetramethylpiperidine), DA(H) (diisopropylamine) and HMDS(H) (1,1,1,3,3,3-hexamethyldisilazane) with *n*BuLi generates sterically encumbered lithium amide bases which can carry out deprotonations normally too challenging for alkyllithium reagents due their high nucleophilicity which leads to problems with side reactions. Contrastingly these bulky amide bases exhibit low nucleophilicity and high kinetic basicity which allows the deprotonation of more sensitive substrates. The effect of switching to bulky amide bases can be witnessed by treating 2-fluoropyridine with LDA. Metallation takes place preferentially in THF solution at -75^{o}C however, switching to *n*BuLi results in nuclophilic addition (**Scheme 1.6**).[67,68]

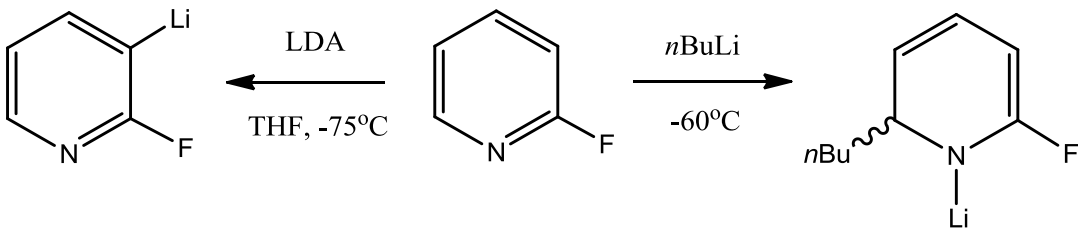

Scheme 1.6: Contrasting reactivity of *n*BuLi and LDA towards sensitive 2-fluoropyridine.

LDA is a popular, well-established regioselective deprotonating reagent capable of deprotonating a wide range of organic substrates bearing sensitive functional groups such as nitrile and ester groups.[69,70] LDA's strong presence in synthetic chemistry has seen many structural studies carried out, most notably the solution-state structural investigation by Collum.[71] These studies revealed the complexity of LDA in solution as up to five cyclic oligomers were detected by isotopic labelling. The structure of donor-free LDA adopts a helical, polymeric arrangement when crystallised from hexane solution in the presence of minute quantities of TMEDA.[72]

Due to the electropositive nature of lithium and the electronegative nature of nitrogen in lithium amides a highly polar bond results which, when coupled with the lone pair of electrons on nitrogen causes extensive aggregation of these species analogous to that seen with alkyllithium reagents. The metal and steric bulk of attached ligands on nitrogen greatly influences the extent of aggregation. For example, the less sterically bulky lithium amide LiHMDS is a cyclic trimer;[73] whereas LiTMP, which is more sterically demanding, adopts a tetrameric ring motif in the solid state (**Figure 1.2**).[74]

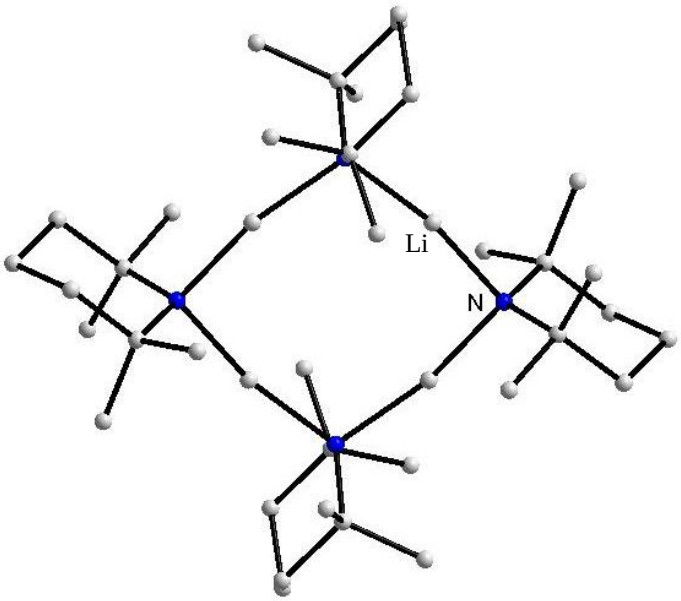

Figure 1.2: Tetrameric ring structure of LiTMP.

Lewis basic donor ligands are also able to affect the extent of aggregation by acting as an alternative source of electron-density for the Lewis acidic lithium atom. Donors such as amines and ethers can stabilise the lithium centre and also increase solubility in non-polar solvents. As discussed above, LDA crystallised from hexane has an infinite helical arrangement (**Figure 1.3**); whereas LDA crystallised from neat TMEDA is an infinite chain of dimers linked by TMEDA bridges.[75]

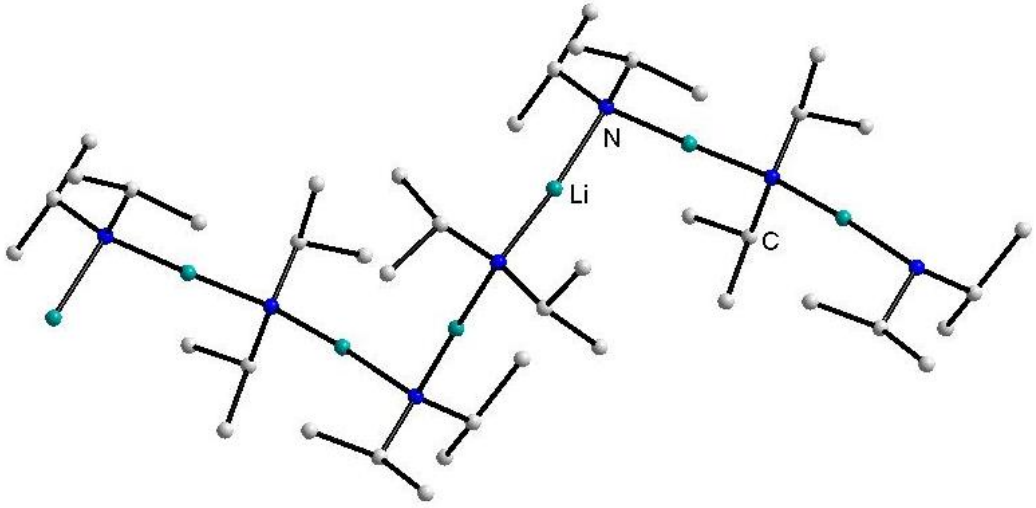

Figure 1.3: Structure of helical polymeric LDA crystallised from bulk hexane.

Addition of TMEDA to tetrameric LiTMP also has a noticeable effect on the structure producing a hemi-solvated open-dimer.[76] The structure provided evidence to back-up Collum's postulate of LiTMP open dimers in solution.[77] Further examples of LiTMP open-dimers with polydentate N-donors have been brought to light recently by our own group such as the potassium PMDETA (*N*,*N*,*N*',*N*'',*N*''-pentamethylethylenetriamine) LiTMP open dimer synthesised by a simple co-complexation approach (**Figure 1.4**).[78]

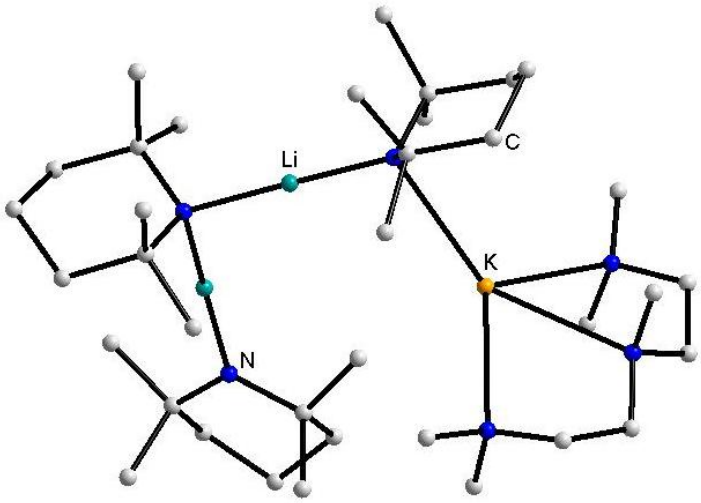

Figure 1.4: Potassium PMDETA-complexed LiTMP open dimer structure.

Donor solvents can also be considered essential to drive the reactivity of organolithium reagents. The reaction of anisole with *n*BuLi differs merely by the presence or absence of TMEDA. A tetrameric *n*BuLi-anisole complex is formed in the absence of TMEDA as the methoxy oxygen atom of anisole acts as a coordinating ligand breaking up the *n*BuLi hexamer. In the presence of TMEDA, deprotonation of anisole at the *ortho*-position occurs due to the acidifying effect of adjacent protons by the methoxy group. It is thought that TMEDA breaks down hexameric *n*BuLi to a kinetically more labile *n*BuLi·TMEDA dimer which is involved in the deprotonation mechanism.[79,80] The deaggregation of alkyllithium reagents by TMEDA can explain differences in reactivity in non-polar solution however, one must consider the effect of polar solvents such as THF. THF is a far better Lewis base donor for lithium and can deaggregate organolithium reagents in bulk solution to the same extent as TMEDA in hexane.

Tuning an organolithium reaction to facilitate the deprotonation of a selected hydrogen atom has been a hot topic for research groups for many years. It relies on a number of

important considerations, most obviously choice of reaction medium and base employed. For example, the position of metallation can be altered for 2-substituted pyridines by simply switching from LDA in THF to *n*BuLi/LiDMAE in hexane (**Scheme 1.7**).[81]

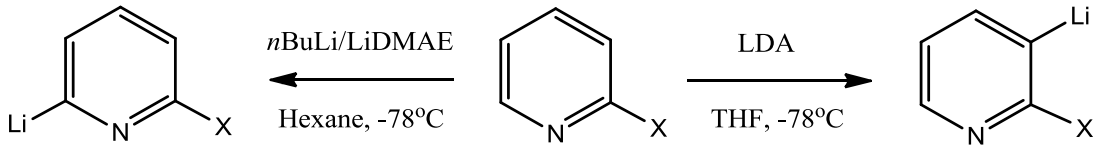

Scheme 1.7: Contrasting reactivity observed by switching base and solvent system for the deprotonation of 2-substituted pyridines (X = Cl and OMe).

When considering substrates with multiple hydrogen atoms it can be difficult to predict the outcome of the organolithium reaction without examining each controlling factor. The development and understanding of directed *ortho*-metallation (DoM) which will be discussed in detail in the coming pages has been a breakthrough in metallation chemistry and allows the regiospecific functionalisation of aromatic rings bearing directing groups.

1.3 Directed *ortho*-Metallation

Directed *ortho*-metallation (D*o*M), pioneered by Snieckus, Beak and others, is by far the most common and widely used deprotonative metallation (usually lithiation) methodology.[82–84] The hydrogen being replaced by a metal cation is *ortho* to a heteroatom containing functional group (directing group). The directing groups can be divided into strong, moderate or weak depending on their relative ability to direct metallation towards the *ortho* position (**Scheme 1.8**).

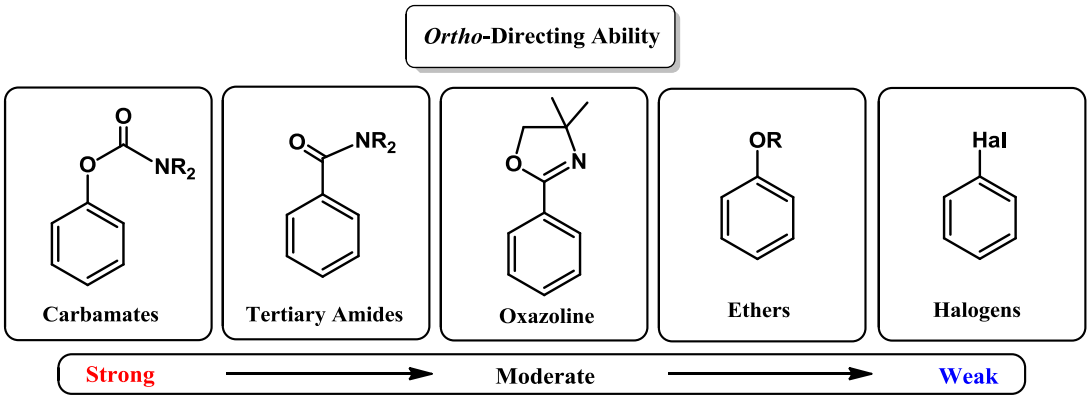

Scheme 1.8: A series of representative directing groups ranging from strong to weak showing a decreasing ability to "*ortho* direct" from left to right.

Commercial organolithium reagents (in particular *n*BuLi or LDA) have been used for this purpose for many years and DoM is now competing with conventional electrophilic aromatic substitution as the premier method for the synthesis of functionalised aromatic compounds. As mentioned above lithium coordinating additives most commonly THF or TMEDA are often required in order to increase the lithiation rate as these electron-rich lone pair donors help to break up the *n*BuLi aggregate to smaller, more kinetically active species. D*o*M is thought to work in part by providing the organolithium reagent with a coordination site hence increasing the reactivity at this site and directing the regioselectivity to the *ortho* position. Acidity plays a vital role when coordination to the directing group is hindered. Electron withdrawing groups which acidify adjacent protons via the inductive effect are usually deprotonated much more rapidly than those groups which are only weakly acidifying. 1-Substituted naphthalenes are deprotonated at *peri* or *ortho* sites depending on whether coordination or acidity is the dominant factor (**Scheme 1.9**). If the directing group operates by coordination deprotonation can

occur in the *ortho* or *peri* positions. If acidity drives the lithiation then only *ortho* deprotonation prevails.

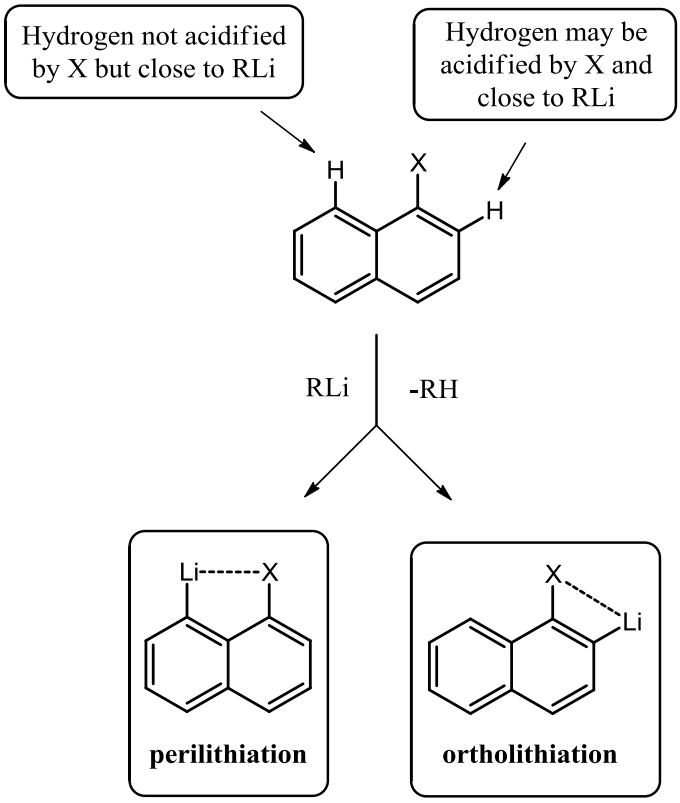

Scheme 1.9: *Ortho*-lithiation versus *peri*-lithiation depending on whether deprotonation occurs mainly via coordination or acidifying effects.

Solvents and other additives can also influence whether the deprotonation reaction is driven mainly by acidity or coordination. Lewis basic solvents such as TMEDA and THF coordinate strongly to organolithium reagents hence they become less Lewis acidic and deprotonation is less likely to be driven by coordination. For substrates such as 4-methoxy-*N*,*N*-dimethylaniline deprotonation occurs *ortho* to the more electronegative and hence more acidifying OMe group in the presence of TMEDA. In the absence of TMEDA deprotonation occurs *ortho* to the more Lewis basic NMe_2 group and coordination becomes the overriding factor.

Although organolithium reagents perform many successful D*o*M reactions they suffer from a number of significant limitations. The first major drawback is that sub-ambient temperatures are often required to carry out these reactions. Such cryogenic conditions incur huge costs to industry but are essential in order to supress the high reactivity of

organolithium reagents. Carrying out reactions at temperatures less than -40^{o}C can incur costs upwards of £250K per annum per batch process.[85] Poor functional group tolerance is another significant problem with organolithium reagents as they are prone to nucleophilically attack sensitive functional groups such as ketones, esters and nitriles. Once deprotonated the lithiated intermediates themselves are often too reactive to be useful, displaying poor kinetic stability. Lastly, organolithium reagents are utilised in ether solvents such as tetrahydrofuran (THF) and diethyl ether to increase their reactivity as mentioned above however, these solvents can form explosive peroxides on storage in air. There are obviously huge safety implications associated with using such solvents on a large industrial scale. Overcoming such drawbacks in organolithium chemistry, an inspiration shared by many research groups worldwide, would be of enormous benefit to both fundamental chemical synthesis and process chemistry. Progress towards this goal has been achieved by mixing together two different types of compound as now discussed.

1.4 LICKOR Superbase

The first type of reagent of this kind was coined the "superbase" by combining organolithium reagents and alkali-metal alkoxides. When the larger alkali-metal alkoxide is added to the organolithium reagent a transmetallation or partial transmetallation ensues bestowing a lithium alkoxide and organo alkali-metal compound with the mixture displaying an increase in reactivity over that of the parent organolithium reagent. The most popular example of such a reagent, the Lochmann-Schlosser superbase (LICKOR), is prepared by mixing *n*BuLi with *t*BuOK which gives far superior reactivity to *n*BuLi alone. This reagent is ideal for substrates with weakly acidifying groups or no acidifying groups such as benzene. The *ortho*-metallation of substrates such as trifluoromethylbenzene is also accomplished with relative ease employing LICKOR[86] as *n*BuLi gives poor yields and regioselectivity.[87,88]

Similarly, LICKOR deprotonates benzene without the need for any Lewis base donor activating agents[89] in contrast to *n*BuLi which requires TMEDA.[90] Most recently, the LICKOR superbase has also been employed to overcome D*o*M as described by O'Shea who found that by adding TMP(H) to the basic mixture resulted in benzylic metallation of substituted toluenes.[91] Schlosser has suggested that the enhanced reactivity observed

in LICKOR superbases is due to solvation, similar to that observed with organolithium reagents and Lewis base donors such as THF, where *n*BuLi is solvated by the oxygen atom of *t*BuOK.[92] There is not a lot of structural information known about LICKOR superbases however, our own group have synthesised the best example to date in the mixed lithium amide potassium alkoxide complex $[(t\text{BuNH})_4(t\text{BuO})_4\text{Li}_4\text{K}_4\cdot(\text{C}_6\text{H}_6)_n]$, which contains alternating $(\text{LiN})_2$ and $(\text{KO})_2$ rings (**Figure 1.5**).

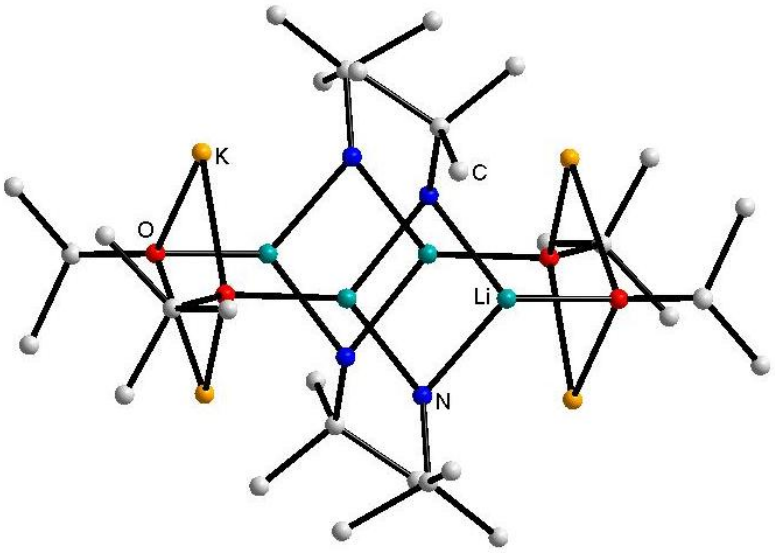

Figure 1.5: Structure of the LICKOR superbase relative $[(t\text{BuNH})_4(t\text{BuO})_4\text{Li}_4\text{K}_4\cdot(\text{C}_6\text{H}_6)_n]$.

The second type of reagent, forming the focus of this PhD study, developed to overcome the inherent problems associated with organolithium reagents is the 'ate' modification of organo alkali-metal bases. Superficially simple, this improved approach capitalizes on the juxtaposition of an alkali-metal with another softer, less reactive metal (such as Mg,[93–96] Zn,[97–100] Mn,[101–103] Fe and Cr[104] to name a few) within a basic ligand environment. These heterobimetallic reagents cannot only improve upon the limitations of organolithium reagents but in many cases they can generate special regio- and chemoselectivities. The origin of this special type of mixed-metal metallation chemistry appears to be synergic.

1.5 Mixed-Metal Synergic Metallation

Synergic mixed-metal chemistry has come to the forefront as a much superior method of converting a carbon-hydrogen bond into a carbon-metal bond.[105–107] It is now starting to rival the common industrial methods and with further improvement could even begin to supersede the use of organolithium reagents in laboratories. The reagents are special structurally engineered bases made up of an alkali metal such as Li, Na or K and a secondary metal (Mg, Zn, Al etc.) either within a single molecular framework or in a charge-separated variant. This combination can export the reactivity of the alkali-metal base to the softer less aggressive metal which, though reactivity enhanced, retains the superior selectivity and functional group tolerance of a softer metal compound. Although the alkali metal does not replace the hydrogen of the C-H bond of the organic substrate it is still essential for the deprotonation to take place. The alkali metal may appear to be merely a spectator however, it's bridging communication with the secondary metal or its role in generating a complexed ate anion of the second metal is essential in order to activate the attached base anions. It is through the structural design of the base that allows the alkali metal to impart its reactivity onto the less reactive secondary metal. In most cases enhanced reactivity exhibited by the base has been deemed to be synergic in origin as neither of the homometallic component parts, in general, are capable of deprotonating aromatic C-H bonds. This synergic mixed-metal chemistry encompasses a new type of reaction concept which our group have coined alkali-metal-mediated metallation (AMM*M*).

Typical ate reagents have a general formula (AM)MgR_3, (AM)ZnR_3, (AM)AlR_4 for magnesium, zinc, and aluminium respectively (AM = alkali metal). By definition alkali metal ate compounds (e.g., Li^+ MR_3^-, where M is a divalent metal or Na^+ MR_4^- where M is a trivalent metal) have their negative charge located on the molecular fragment containing the softer, less electropositive metal M, but while this is clearly a contributory factor for the observed reactivity transfer (historically Wittig[108] labelled this effect as "anionic activation") the full explanation must be significantly more complicated as many formulations labelled as ates do not exhibit reactivity enhancement. As most chemists would associate ate formulations with solvent separated ion pairs, our group have suggested it is more fitting to discuss this chemistry in terms of heterobimetallics or mixed-metal systems as the structures involved can often be

molecular and charge neutral contact ion pairs, though the bonding within them is usually highly polarised.[105,106]

The structural design of a typical ate base highlighting its three constituent parts is depicted in **Figure 1.6**. The subordinate metal is capped by terminal alkyl bases where the number is dependent on the valency of the metal. Metals are linked via two bridging anions, one of which is added as an alkali metal amide (commonly LiTMP as shown below), the other (R') can usually either be a molecule of the same amide or alternatively an alkyl base which comes from the subordinate metal reagent. Completing the structure is a donor molecule which solvates the alkali metal and stops the base from polymerising, thus aiding its solubility.

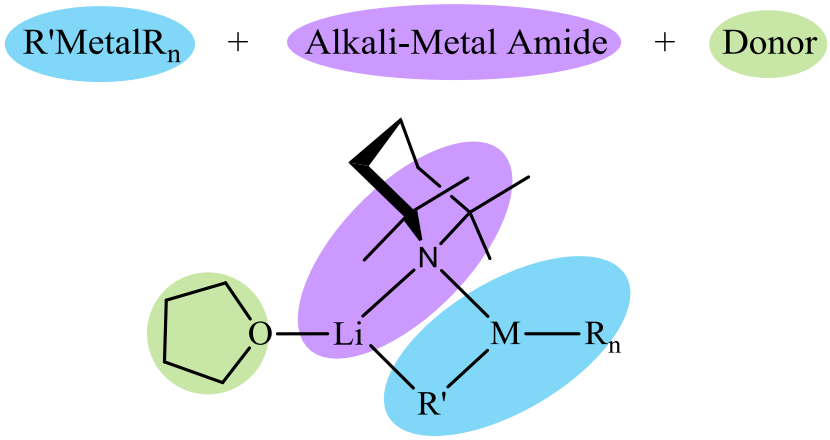

Figure 1.6: Structural design of an ate base emphasising its three component parts.

Several metals have been investigated in this context down the years but the spotlight has remained focused on magnesium and zinc with some emphasis on manganese and aluminium. The significance of AMM*M* as a deprotonation technique has increased ten-fold recently with publications in world-leading journals such as ***Science***[109] and ***Nature Chemistry***.[110] The limitations associated with organolithium reagents are much improved with these reagents as the reactions can be utilised in non-polar hexane at room temperature. Economic advantages aside, AMM*M* is also attractive from a fundamental chemistry standpoint since not only can it outperform many homometallic reagents, it can also deprotonate poorly acidic substrates (with high pK_a values) considered generally inert towards metal-hydrogen exchange. It is also possible to

polydeprotonate multi-C-H containing substrates or regioselectively deprotonate positions other than those *ortho* to directing groups.

At the vanguard of these heterometallic advances in deprotonative metallation lies two distinct methods: the organometallic salt supported approach (type **A**), pioneered by Knochel; and the mixed organic anion approach (type **B**), popularised by Kondo and Uchiyama,[111–116] Mongin,[117–122] Hevia[123,124] and our own group.

Originally proficient in halogen-metal exchange, the halide salt supported mixed-metal reagent mixtures (type **A** – for a typical example see **Scheme 1.10**) are now at the cutting edge of deprotonative metallation.

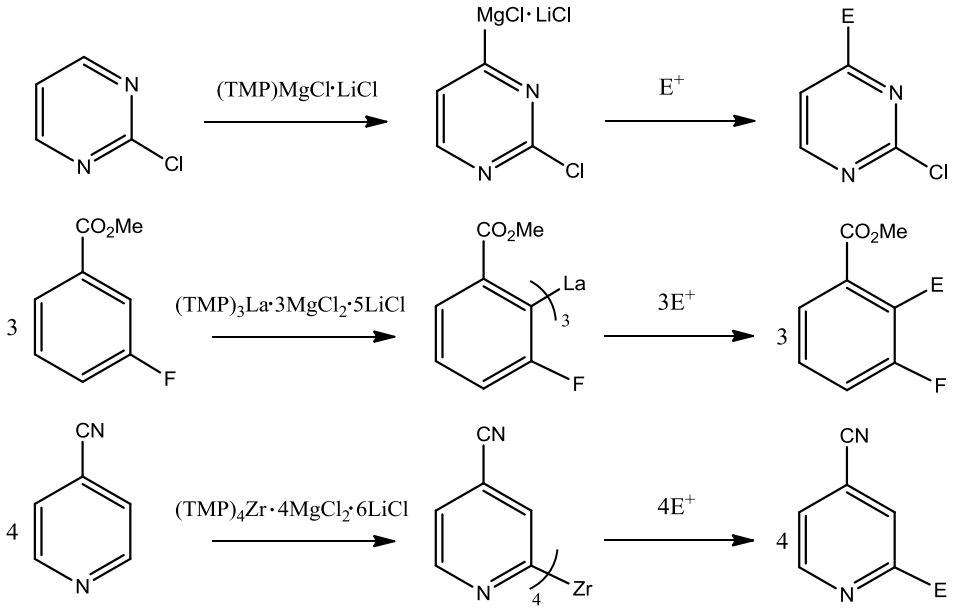

Scheme 1.10: Representative examples of metallation and electrophilic quenching of functionalised aromatics utilising halide salt supported mixed-metal reagent (type **A**) mixtures showing magnesiation (top), lanthanation (middle), and zirconation (bottom).

The pioneering research of the Knochel group has produced a plethora of examples whereby such reagents directly metallate substituted aromatics and heteroaromatics in an efficient manner in accord with the well-established principles of D*o*M.[83,84,125] Generally utilised in polar (THF) solvent, the introduction of LiCl (or $MgCl_2$[126] or $ZnCl_2$[127]) to the amido metal chloride or *bis*(amido) metal reagent is credited with enhancing reactivity at least in part by increasing solubility as previously described. What makes these mixed-metal reagent mixtures especially appealing is their excellent

tolerance of sensitive functional groups, as well as their improved kinetic basicity, regioselectivity and chemoselectivity with respect to the parent softer metal homometallic reagent. While the most common subordinate metals are magnesium and zinc in the form of (TMP)MCl·LiCl (M = Mg,[56,128–134] Zn[135–138]), $(TMP)_2Mg·2LiCl$[57,58,139] or $(TMP)_2Zn·2MgCl_2·2LiCl$,[140–142] Knochel has rapidly extended this concept to successfully initiate direct manganation,[143] alumination,[144] ferration,[145] lanthanation[146] and even zirconation[147] of functionalised aromatic molecules. In addition, incorporation of Lewis acidic BF_3 into a halide salt supported mixed-metal magnesiate was shown to activate previously unreactive C-H bonds in polyfunctional pyridines and related heterocycles.[148] The versatility of this class of reagent has been elaborated further by a recent report of the selective metallation of alkenes.[149]

While the ability of these reagent mixtures to induce regioselective or chemoselective direct metallations is undoubted, the mechanisms by which these reactions occur remain ambiguous since for example no metallated intermediates have been isolated or otherwise characterised. Typically, a bi- (or even tri- or tetra-) metallic cocktail is prepared in THF, reacted with a substrate and subsequently quenched with an electrophile or is cross-coupled with an aryl halide or related species. Recently, our group uncovered the solid state structure of a classical Knochel magnesiate base, THF solvated (TMP)MgCl·LiCl,[150] and its dimeric diisopropylamide [iPr$_2$N$^-$, DA] congener[151] (**Figure 1.7**), allowing the proposal of a structural rationale for the contrasting reactivities displayed by each compound.

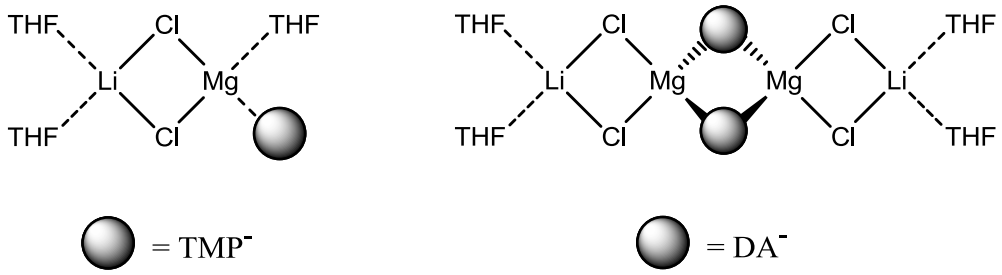

Figure 1.7: ChemDraw representations of the Turbo-Grignard reagent (TMP)MgCl·LiCl and its dimeric diisopropylamine congener $(DA)_2Mg_2Cl_2·2LiCl$.

On the basis of NMR spectroscopic evidence, including most informatively DOSY NMR experiments,[152–154] it was intimated that these LiCl supported complexes do not retain their structural integrity in solution. Instead their constitution is most likely in the form of solvent-separated ion pairs. These 'ates' are predisposed to metallating *ortho* to directing groups which in certain cases is in contrast to contacted-ion (type **B**) structures which can anchor a suitable substrate within a pre-metallation framework, opening up the possibility of less conventional metallation patterns occurring via a potentially intramolecular pathway.

Coupled with their ability to execute conventional *ortho* metallation of functionalised aromatic molecules containing a directing group, mixed organic anion (type **B**) heterometallic bases also have the capability of performing 'unusual' deprotonations. This can take the form of metallation at non-activated (less acidic) sites or through polymetallation of substrates which are not typically prone to experiencing more than a single deprotonation. A simple example of the former reaction is the special *meta* deprotonation of toluene with the mixed alkyl-amido sodium magnesiate base [TMEDA·Na(μ-TMP)(μ-Bu)Mg(TMP)][155] or the *meta* deprotonation of *N*,*N*-dimethylaniline (**Figure 1.8**) with the related zincate base [TMEDA·Na(μ-*t*Bu)(μ-TMP)Zn(*t*Bu)],[156] while the latter reaction is witnessed spectacularly via the regioselective tetra-deprotonation of ferrocene (**Figure 1.8**),[157] ruthenocene[158] and osmocene[158] with [NaMg(N*i*Pr$_2$)$_3$]. Novel host-guest ring compounds, referred to collectively as inverse crowns due to the antithetical location of the Lewis acidic/basic atoms with respect to a traditional crown ether complex, are often the result of such bimetallic-induced single or multiple deprotonations[159–161] although inverse crowns can also be prepared via co-complexation.[162] The contacted ion pair nature of these intermediate (with respect to metal-free organic final products) complexes plays a dominant role in their unconventional behaviour, as mentioned above.

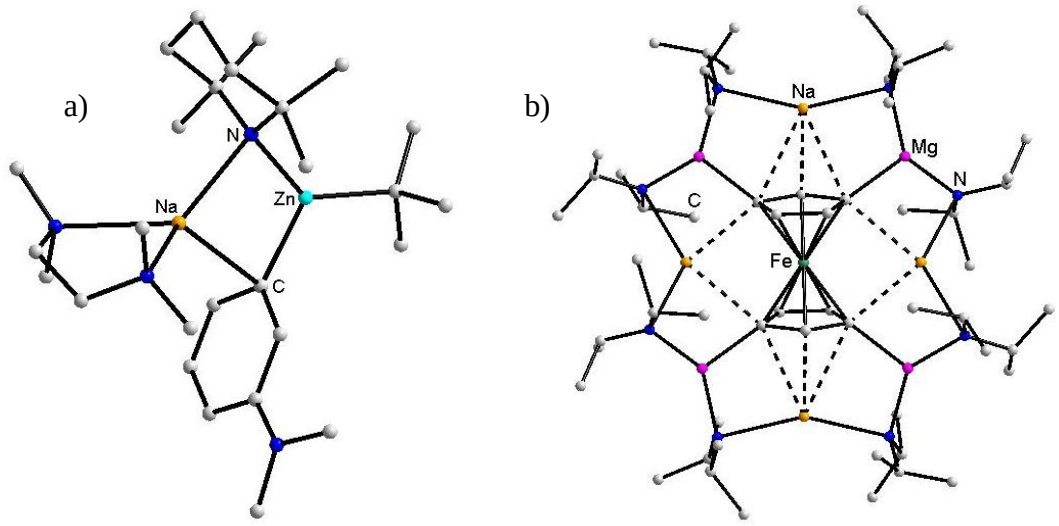

Figure 1.8: Crystal structures of (a) *meta*-deprotonated *N*,*N*-dimethylaniline compound and (b) *tetra*-deprotonated ferrocene compound.

Judicious selection of the subordinate metal, the anions and the donor molecule are clearly paramount if the desired reactivity towards any given substrate is to be achieved. With regards to the metal, this is eloquently demonstrated by the deprotonation of THF. When the mixed-metal sodium zincate base [TMEDA·Na(μ-TMP)(μ-CH_2SiMe_3) Zn(CH_2SiMe_3)][109] is employed the deprotonated highly sensitive cyclic ether molecule is captured with its OC_4 ring intact within the molecular framework. Switching to the magnesiate or manganate [TMEDA·Na(μ-TMP)(μ-CH_2SiMe_3)M(TMP)] (M = Mg, Mn)[110] causes cleavage of THF with its separated fragments being sequestered by residues of the base,[163–167] the oxygen containing fragment forming an oxo inverse crown (**Scheme 1.11**).[168–173]

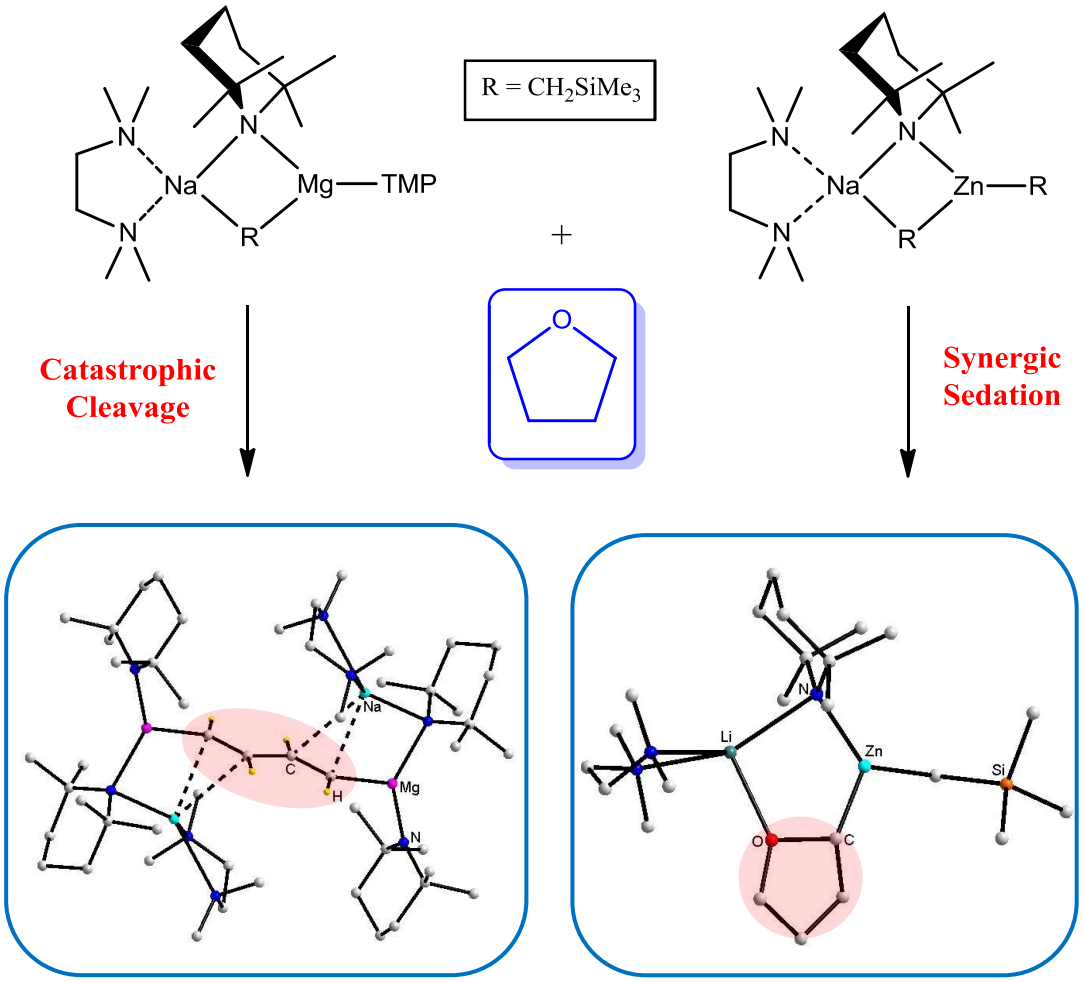

Scheme 1.11: Catastrophic cleavage (left) and synergic sedation (right) of THF by different sodium TMP ate reagents.

The choice of bridging anion is also an important consideration. Moving from the mono-TMP aluminate base [Li(TMP)Al(*i*Bu$_3$)] to one incorporating two TMP anions [Li(TMP)$_2$Al(*i*Bu)$_2$] results in the number of deprotonated donor TMEDA molecules within the complex being reduced from two to one as shown in [Li(μ-TMEDA*)$_2$Al(*i*Bu)$_2$] and [Li(μ-TMEDA*)(μ-TMP)Al(*i*Bu)$_2$] respectively.[174] Lewis donor identity is also a key factor, as articulated by Stalke who demonstrated that the MeLi/Me$_2$Zn combination yields a contact ion pair in the presence of PMDETA but a solvent separated ion pair in the presence of diglyme.[175]

One of the most significant recent advances in AMM*M* has involved the extension to a metal which is formally in the +3 oxidation state, namely Al^{III}. Aluminium has received much less attention in this field but it is worthy of more study as it promises a number

of advantages over magnesium and zinc. Firstly, it is the most abundant metallic element, an important consideration in a world with limited resources. It is relatively cheap, non-toxic and the reagents used to synthesise the base are all commercially available. These advantages coupled with a hexane/room temperature regime enable a much more environmentally benign deprotonation protocol. Secondly, preliminary work in the dominion of mixed-metal aluminium chemistry has exposed a myriad of unusual and novel metallation patterns which will be discussed later. Aluminium seemed the logical choice for exploitation as the development of alkali-metal-mediated alumination (AMM*Al*) is merely a drop in the ocean compared to magnesium and zinc.

1.6 Organoaluminium Reagents

1.6.1 Reactivity

Although the first organoaluminium compound [$(C_2H_5)_3Al_2I_3$] was discovered as long ago as 1859,[176] it was not until nearly 100 years later in the 1950s that organoaluminium compounds would win recognition as useful organometallic reagents. Ziegler and co-workers synthesised trialkylaluminium compounds including triethylaluminum as co-catalysts for application in olefin polymerisation which ultimately resulted in the 1963 Nobel Prize for Ziegler which was also shared with Giulio Natta.[177]

Over the years organoaluminium compounds have seen widespread utilisation in synthetic chemistry as, for example, reducing and alkylating agents, Lewis acid reagents,[178–180] organic synthetic building blocks[181–184] and co-catalysts for olefin polymerisation as mentioned above and have become popular reagents for this purpose as aluminium is the cheapest and most abundant of the active metals. Nowadays they have seen their way into Grignard type reactions where the insertion of Al into aryl halides[39] and propargylic bromides[185] is fast becoming a new route to functionalised aromatics and alcohols. The first iron-catalysed aluminium variant of a Negishi coupling reaction not employing an expensive palladium catalyst has also been reported recently.[186]

Organoaluminum reagents can be synthesised by various routes. A selection of these include, firstly, direct insertion of aluminium metal into alkyl halides via a similar

method as that seen for the synthesis of conventional Grignard reagents. Secondly, hydro- or carbo-alumination reactions can by employed where Al-powder reacts with alkenes in the presence of hydrogen in the former and organoaluminium compounds are treated with alkenes or alkynes in the latter. Finally, a transmetallation approach can be utilised where the corresponding more electropositive organolithium reagent is reacted with the appropriate aluminium source commonly a halide generating lithium halide via a salt metathesis reaction (**Scheme 1.12**).

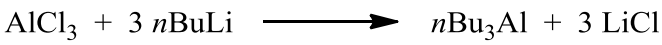

Scheme 1.12: A transmetallation reaction to give a new organoaluminum compound and LiCl.

The choice of reaction solvent can have a huge influence on the reactivity of organoaluminium reagents and the reaction outcome. In contrast to what is found with lithium and magnesium reagents, ether solvents can hinder the reactivity of organoaluminum compounds. For example, in a hydro-alumination reaction of an alkyne, altering the solvent switches the stereochemistry from *cis* to *trans*. If silylacetylene is reacted with DIBAH (diisobutylaluminium hydride) in hexane solution, the *cis*-product is formed initially but this readily isomerizes to the *trans*-isomer. If the reaction is carried out in diethyl ether the vacant orbital of aluminium is occupied by diethyl ether molecules and isomerisation is prohibited (**Scheme 1.13**).[187,188]

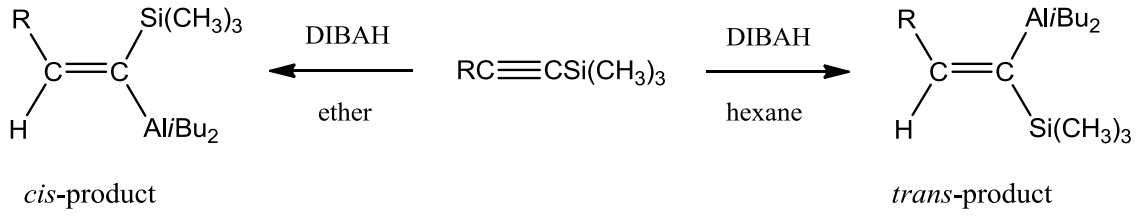

Scheme 1.13: Reaction of silylacetylene with DIBAH under different solvent conditions to generate *cis*- and *trans*-products.

The structures of simple trialkylaluminum compounds such as trimethylaluminium exist as dimers at room temperature where the two aluminium centres are connected via two methyl bridges (**Figure 1.9**). These compounds are electron-deficient and are described in terms of 3-centre 2-electron bonding.

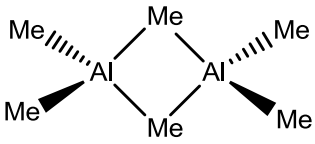

Figure 1.9: Dimeric structure of trimethylaluminium.

In the absence of solvating ligands trialkylaluminum dimers exist in a dynamic equilibrium where exchange occurs between bridging and terminal groups and between dimers. At low temperature the ^{1}H NMR spectrum of trimethylaluminium exhibits a 1:2 ratio of bridging to terminal Me groups consistent with the dimeric ring structure shown above. At room temperature only one signal is observed in the ^{1}H NMR spectrum because the exchange between bridging and terminal Me groups is too fast to be resolved on the NMR timescale hence implying a monomeric structure.[189–192] This association-dissociation problem has been overcome by utilising bulky ligands which prevent the association between monomers. Bulky ligands such as that derived from 2,6-di-*tert*-butyl-4-methylphenol reacts with trimethylaluminium to generate MAD [methylaluminium *bis*(2,6-di-*tert*-butyl-4-methylphenoxide)] which is totally monomeric in hydrocarbon solution (**Figure 1.10**).[193] Bulky organoaluminium compounds such as MAD are excellent reagents for converting carbonyl compounds to alcohols with a high degree of stereoselectivity.

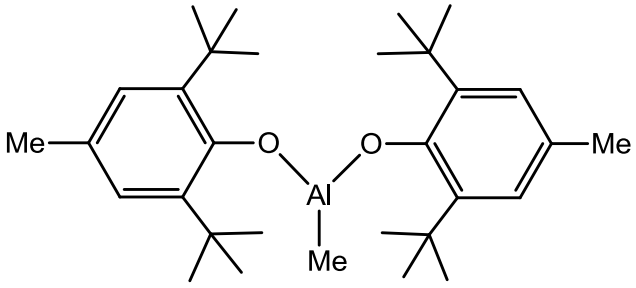

MAD

Figure 1.10: Structure of monomeric MAD [methylaluminium *bis*(2,6-di-tert-butyl-4-methylphenoxide)].

Organoaluminium reagents can also be employed to carry out ligand-exchange reactions where particular groups are transferred onto substrates. For example, an alkynylaluminium reagent can readily transfer the alkynyl group onto oxiranes in a *peri*-planar fashion and to enones via 1,4-addition in the presence of a nickel catalyst.[194] In

heterosubstituted organoaluminium reagents the group which is not the alkyl group is transferred preferentially due to a smaller activation energy. For example, reaction of diethylaluminium amide ($Et_2Al\text{-}NH_2$) with methanol (CH_3OH) produces ammonia and the alkoxide $Et_2Al\text{-}OCH_3$ by cleaving the more kinetically labile Al-N bond.[195] This ligand-exchange concept using R_2AlX has been widely exploited in organoaluminium chemistry for the transformation of many different substrates including esters to amides,[196,197] esters to nitriles[198] and epoxides to alcohols[199–203] to name but a few.

Organoaluminium reagents are highly reactive oxophilic compounds which can ignite spontaneously in air. Those with small alkyl groups are more reactive than those of greater molecular weight. In general, increasing the number of carbon atoms in the alkyl chain reduces the pyrophoric reactivity. The reagent named after Tebbe, the mixed titanium-aluminium complex $[Cp_2TiCl_2\text{-}Me_3Al]$ can be used for the transformation of esters to vinyl ethers utilising the oxophilicity of the aluminium reagent.[204] As a result organoaluminium reagents can be used in oxidation reactions producing epoxides from allyl alcohols and ketones from the dehydrogenation of secondary alcohols.[205] As an illustration, treatment of an aluminium reagent with *tert*-butyl hydroperoxide results in the strong coordination of oxygen to the aluminium atom producing a highly polarised structure where the oxygen is electrophilic. If an allyl alcohol is added to this reagent oxidation of the alkene generates an epoxide and for secondary alcohols the oxidation generates a ketone through the transition states shown in **Figure 1.11**.[206–208]

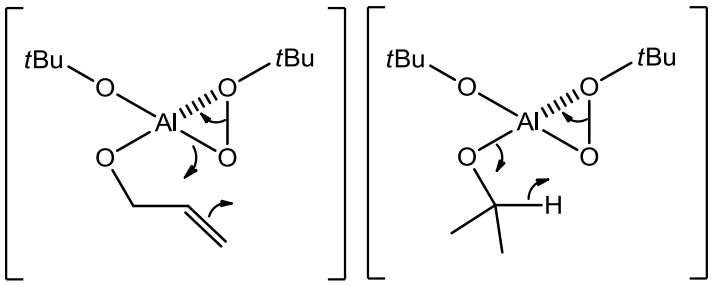

Figure 1.11: Transition states for epoxide formation from an allyl alcohol and a ketone from a secondary alcohol using a *tert*-butyl hydroperoxide aluminium reagent.[194]

The reverse reaction of transforming an epoxide to an allylic alcohol can be achieved with organoaluminium reagents under basic conditions. One of the hydrogen atoms next to the epoxide can be removed with a strong base. The organoaluminium reagent

requires a Lewis acidic site to coordinate oxygen and a Lewis basic site to remove the hydrogen. Organoaluminium amides are found to be the best reagents for this purpose. A proposed transition state of the reaction envisions the aluminium metal coordinating to the oxygen with the lone pair of electrons on nitrogen primed for the removal of the proton via a highly regioselective deprotonation (**Figure 1.12**).[202,203]

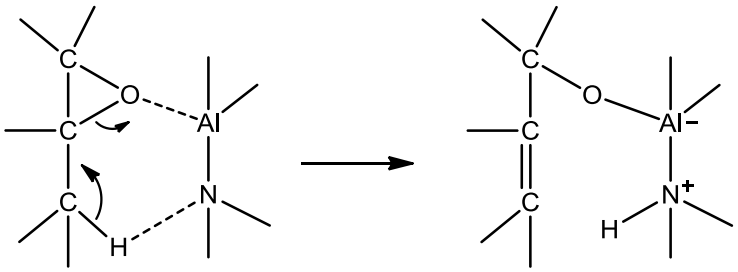

Figure 1.12: Transition state for the reaction between an organoaluminium amide and an epoxide for the conversion to an allyl alcohol.[194]

The extensively studied chemistry of organoaluminium amides can be exemplified by the bisalkyl-monamido reagent Et_2AlTMP reported by Yamamoto in 1974. This reagent has been utilised for the ring opening of epoxides[202,209] and oxetanes as well as for the formation of Al-enolates[210] and promoting regioselective Fischer indole synthesis.[211]

Aluminium ate compositions behave differently to neutral organoaluminium compounds as they act as nucleophiles rather than Lewis acids. For example, reduction of an α,β-unsaturated epoxide gives a different product on switching from a neutral aluminium reagent to an aluminium ate compound.[212] On reaction with the neutral species DIBAH 1,4-addition takes place; whereas when the ate species lithium aluminium hydride is employed a direct reduction product is formed (**Scheme 1.14**).

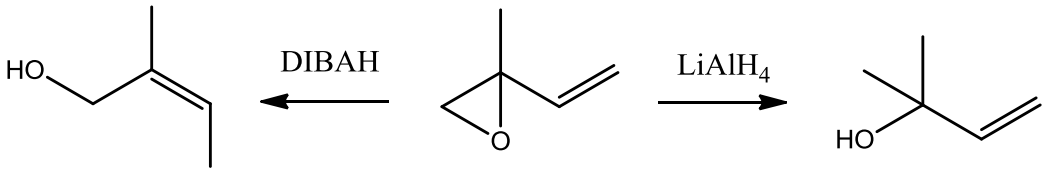

Scheme 1.14: Reactivity differences between the neutral aluminium compound DIBAH and the ate compound lithium aluminium hydride in their action towards an epoxide.

These few pages have given a brief overview of some of the more fundamental reactions carried out by organoaluminium reagents. The next section will review a

selection of the common structural motifs adopted by these reagents in particular organoaluminium amides.

1.6.2 Structures

Aluminium atoms in organoaluminium amides normally have coordination numbers of four or more; however, addition of bulky groups attached to aluminium or nitrogen can allow the isolation of compounds that are only three coordinate. The first structurally characterised three coordinate aluminium amide was $[Al\{N(SiMe_3)_2\}_3]$ containing three relatively bulky HMDS (1,1,1,3,3,3-hexamethyldisilazide) ligands.[213] Since then the synthesis of other three coordinate aluminium amides have emerged including the homoleptic *tris*-amide $[Al(NiPr_2)_3]$[214,215] and the heteroleptic amide $[Al(TMP)_2\{N(H)Ph\}]$.[216] Diorganoaluminium amides can be synthesised using the appropriate diorganoaluminium halide and lithium amide for example as in $[tBu_2AlN(Mes)_2]$.[217] Three coordinate *bis*-amido aluminium compounds containing the bulky amide TMP are also known which can be synthesised by salt elimination as for example was the case with $[(TMP)_2AlX]$ where X = Cl and ODipp (2,6-diisopropylphenyl) (**Figure 1.13**).[216,218]

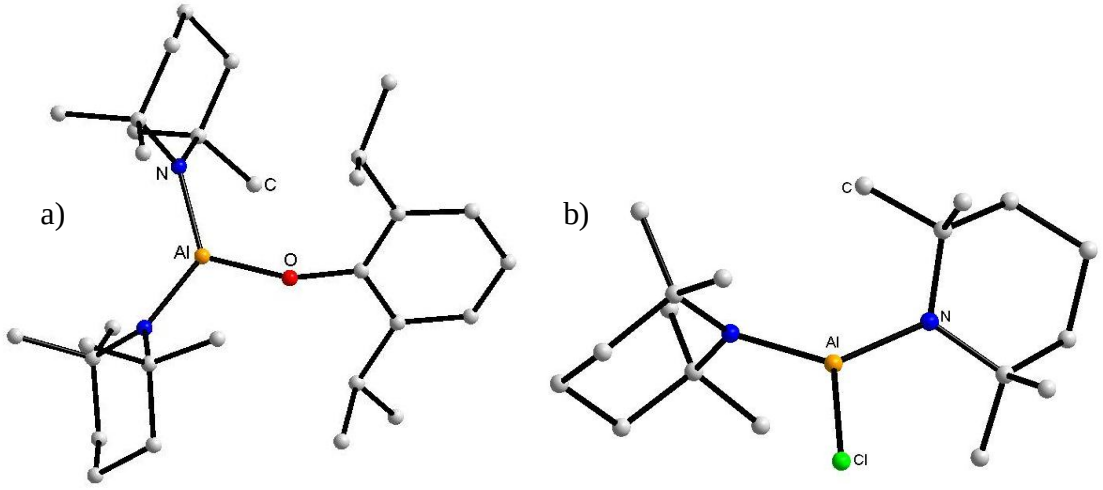

Figure 1.13: Examples of three coordinate aluminium amides (a) $[(TMP)_2AlODipp]$ and (b) $[(TMP)_2AlCl]$.

Four-coordinate organoaluminium amides can be divided into two separate categories; namely, Lewis base adducts and those complexed by chelating ligands. The Lewis base adducts generally have a distorted tetrahedral geometry and examples include

[(THF)Al{N(H)Si(NMe$_2$)$_3$}$_3$] (**Figure 1.14a**) [219] and [(THF)AlX(TMP)$_2$] where X = Cl or Br.[220] The most common four coordinate aluminium complexes are those possessing chelating ligands. Examples include the novel trigonal monopyramidal aluminium compound produced by a transamination route [Al{N(SiR$_3$)CH$_2$CH$_2$}$_3$N] (**Figure 1.14b**).[221,222] The three silylamido nitrogens are coordinated to aluminium in a trigonal planar fashion with the amine nitrogen in the axial position. Other examples include the tridentate chelate complex [(Me$_3$SiN{CH$_2$CH$_2$N(SiMe$_3$)}$_2$)AlCl] (**Figure 1.14c**).[223]

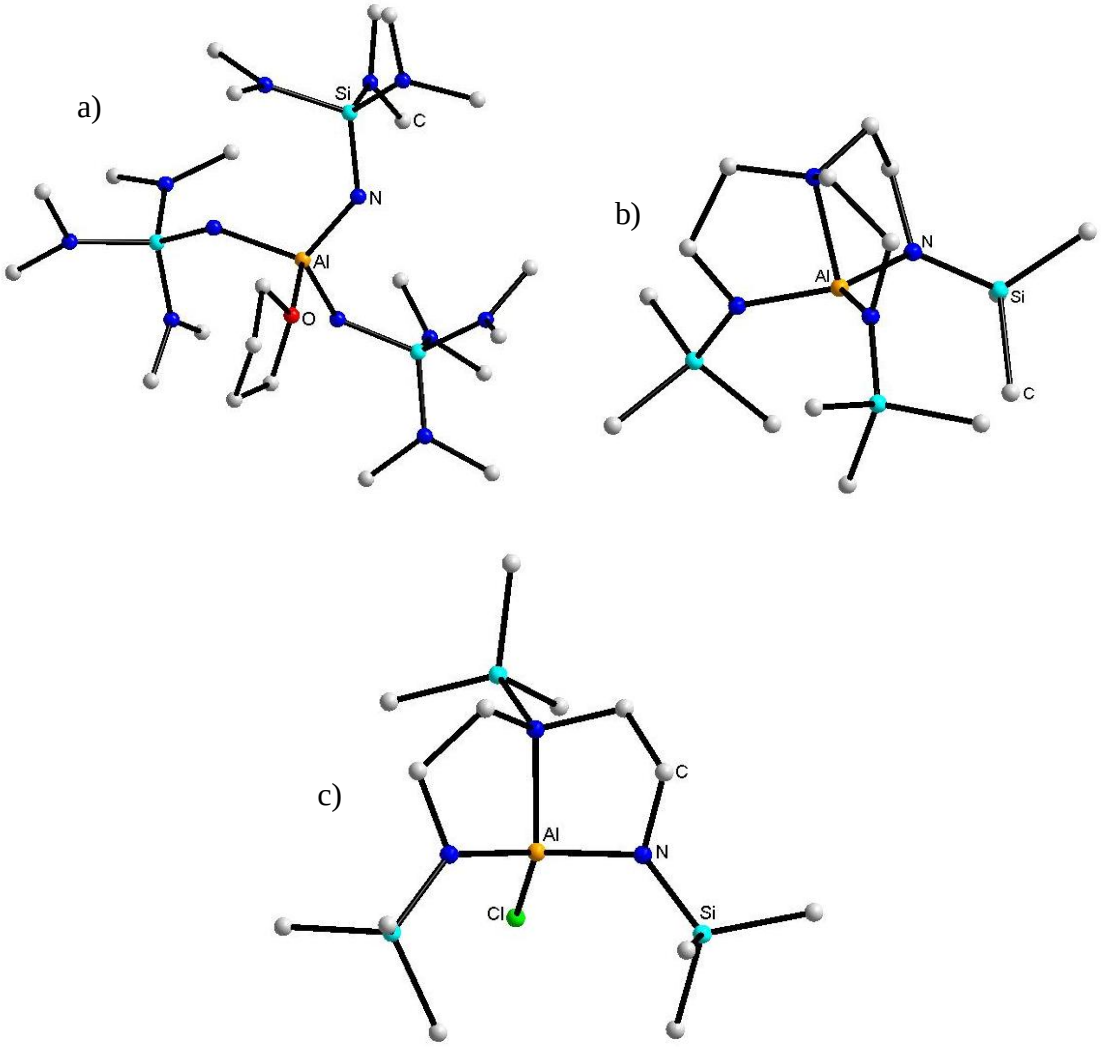

Figure 1.14: Examples of four coordinate aluminium complexes (a) [(THF)Al{N(H)Si(NMe$_2$)$_3$}$_3$], (b) [Al{N(SiR$_3$)CH$_2$CH$_2$}$_3$N] and (c) [(Me$_3$SiN{CH$_2$CH$_2$N(SiMe$_3$)}$_2$)AlCl].

Other geometries of aluminium complexes include the distorted square pyramidal complexes of [MeAl{OC(Me)C$_6$H$_4$NH-2}$_2$] (**Figure 1.15a**)[224] and [(Me$_2$N)Al {N(Me)$_2$C(N*i*Pr)$_2$}][225] which have their Me or NMe$_2$ groups in the apical position, the

trigonal bipyramidal complex [Me_2Al(TEDTA)] (**Figure 1.15b**)[226] (where TEDTA = tetraethyldiethylenetriamine) which also has apical methyl groups and the tridentate donor is in the equatorial position and the octahedral compound [Al{N(2-$C_5H_4N)_2$}$_3$][227] which incorporates three bidentate ligands around the aluminium atom (**Figure 1.15c**).

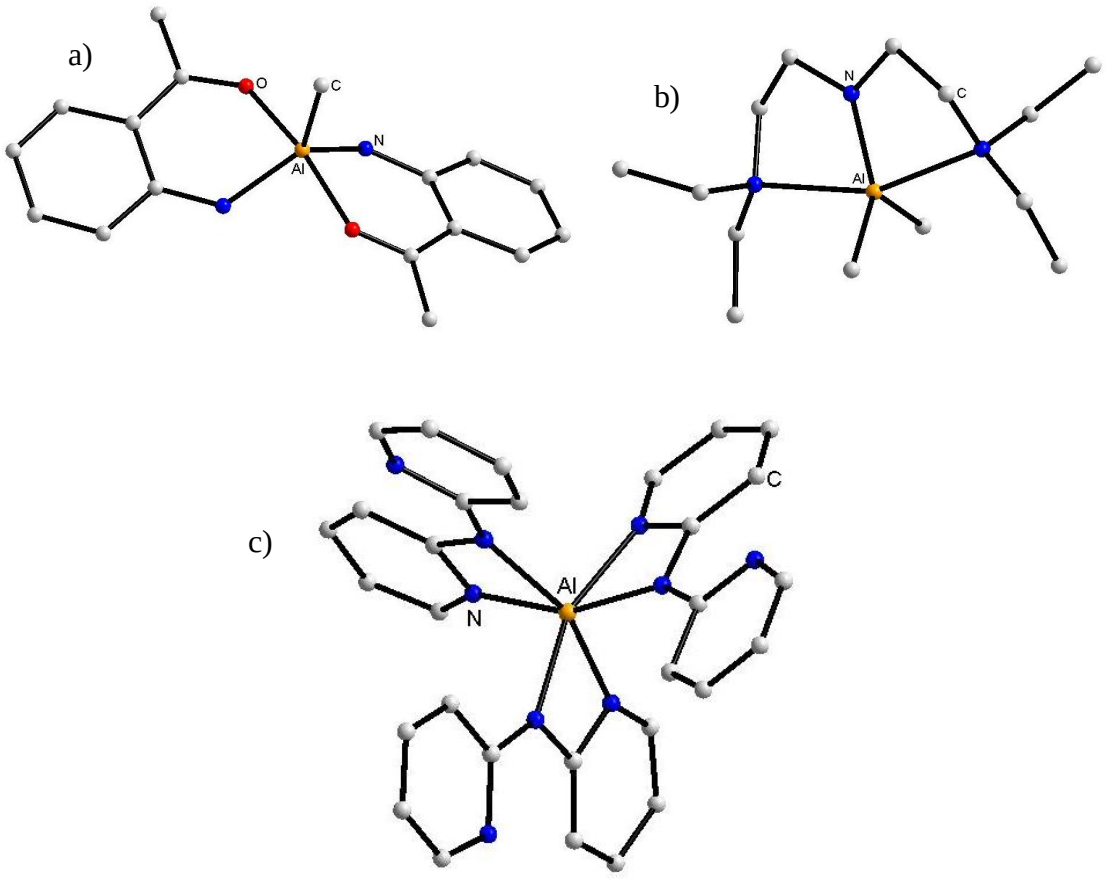

Figure 1.15: Other geometries of aluminium compounds including square pyramidal compound (a) [MeAl{OC(Me)$C_6H_4NH_2$}$_2$], trigonal bipyramidal (b) [Me_2Al(TEDTA)] and octahedral (c) [Al{N(2-$C_5H_4N)_2$}$_3$].

Amongst the largest class of aluminium amide are those which have a dimeric constitution. These compounds are generally either planar or non-planar four-atom $(AlN)_2$ or $(AlX)_2$ rings. The simplest of the aluminium amide dimers is the dimethylamide [{$Al(NMe_2)_3$}$_2$] (**Figure 1.16a**)[228,229] which exhibits a distorted tetrahedral geometry. Non-planar rings are usually due to steric effects of bulky groups such as in [($AlMe_2${μ-N-($SiMe_3$)C_6H_2*t*Bu-2,4,6)$_2$}].[230,231] Heteroleptic aluminium amides bridge through atoms other than nitrogen when the amido groups are sterically

demanding, for example a hydride in [{(μ-H)Al(TMP)$_2$}$_2$] (**Figure 1.16b**)[232] and a fluoride bridge in [{Al(μ-F)(TMP)$_2$}$_2$].[233] Compare these examples with the less sterically crowed amide in [{AlBr$_2$(μ-NEt$_2$)}$_2$][234] where bridging does occur via the amido N atom. Certain other aluminium amides can have two distinct bridging connections such as found in asymmetric [Ph$_2$Al{N*t*Bu$_2$SiMe$_2$}]$_2$ (**Figure 1.16c**) which has one amido and one phenyl bridge.[235] In this compound each aluminium has a different coordination environment - one with two terminal phenyl groups and the other with one terminal phenyl group and one terminal amido group. Other common structures include trimers, for example as witnessed in [{Al(μ-NH$_2$)Me$_2$}$_3$] (**Figure 1.16d**) [236,237] and [{H$_2$AlNMe$_2$}$_3$][238] which feature six-membered (AlN)$_3$ rings in a chair conformation.

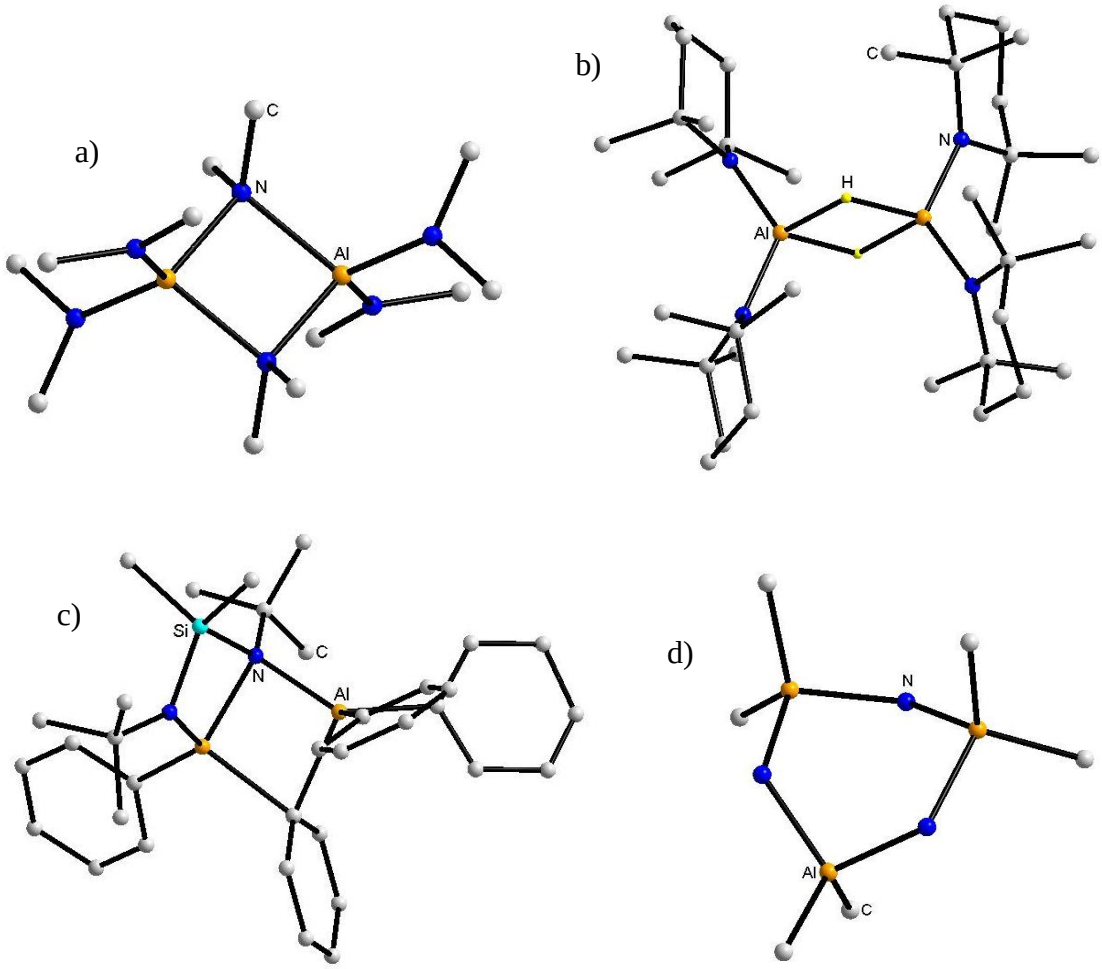

Figure 1.16: Structures of aluminium amide dimers (a) [{Al(NMe$_2$)$_3$}$_2$], (b) [{(μ-H)Al(TMP)$_2$}$_2$], (c) [Ph$_2$Al{N*t*Bu$_2$SiMe$_2$}]$_2$ and trimer aluminium compound (d) [{Al(μ-NH$_2$)Me$_2$}$_3$].

Mixed-metal aluminium amides make up the final class of reagent with the majority of these belonging to lithium aluminium amide compositions. The simplest structure is all inorganic [$LiAl(NH_2)_4$] which is synthesised from treatment of lithium and aluminium in liquid ammonia.[239] The common $(AlN)_2$ ring observed in the above structures also appear in lithium aluminium dimers such as [$(Me_2Al\{NLi(THF)tBu\})_2$] (**Figure 1.17a**)[240] where the planar $(AlN)_2$ ring contains a distorted tetrahedral aluminium centre and a terminal two-coordinate lithium atom. The related compound [$(Me_2Al\{NLi(THF)_2Ph\})_2$] has lithium in a distorted trigonal planar geometry.[241] Derived from a primary amine, the dimeric homoleptic complex [$\{Li(Al(NHtBu)_4\}_2$] has the lithium atoms bridging the two Al units.[242] Polymeric lithium aluminium amides such as [$LiN(SiMe_3)_2AlMe_3$] (**Figure 1.17b**) are also known which has infinite chains of $LiN(SiMe_3)_2AlMe_2$ linked by interactions between lithium and the methyl group from a neighbouring unit.[243] Solvent separated ion pair structures are also commonly observed as for example [$Li(THF)_4$][$Al\{N(CH_2Ph)_2\}_4$].[244]

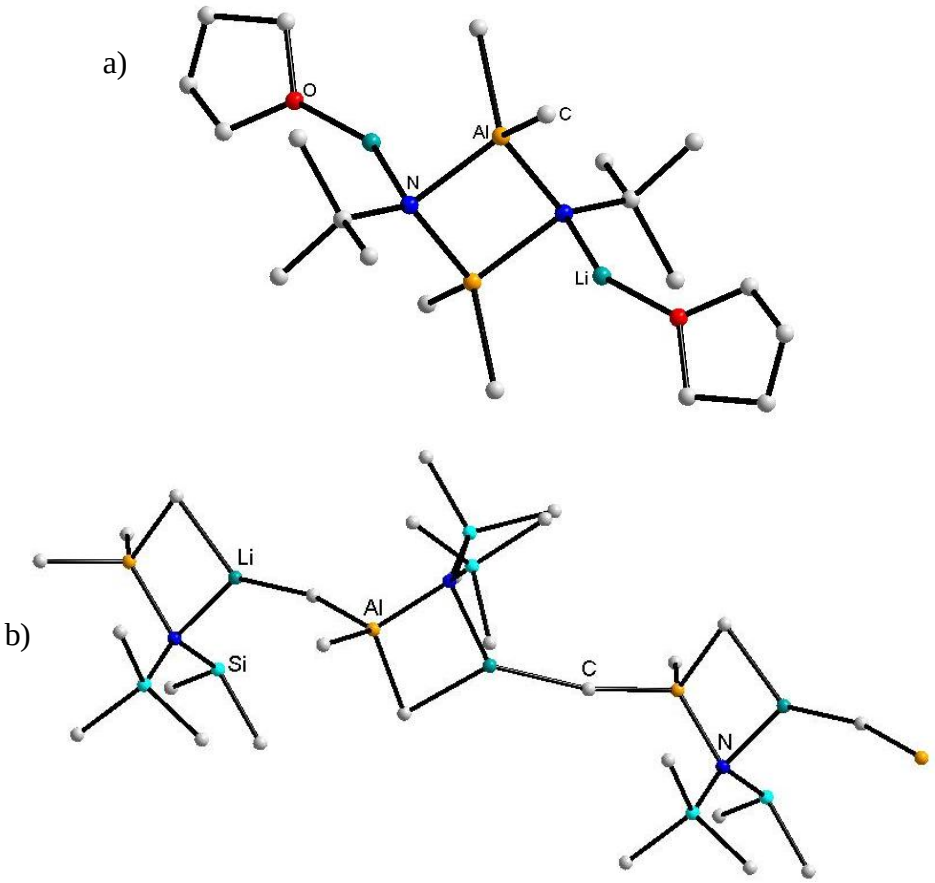

Figure 1.17: Examples of dimeric (a) [$(Me_2Al\{NLi(THF)tBu\})_2$] and polymeric (b) [$LiN(SiMe_3)_2AlMe_3$], lithium amidoaluminium complexes.

1.7 Alkali-Metal-Mediated Alumination

The application of organoaluminium reagents in organic synthesis has been geared towards the formation of aliphatic compounds with the focus on forming carbon-carbon and carbon-heteroatom bonds.[245–247] A simple transmetallation of organolithium or Grignard reagents is normally employed to generate the corresponding aliphatic aluminium compound.[248] However, when trying to extend this procedure to aromatic substrates it was realised that neither the reagent itself nor the reactive intermediate it generated could co-exist with sensitive functional groups (including, halogen, amide or cyano).[249] As aromatic compounds are invaluable synthetic building blocks, the effective deprotonation and functionalisation of such compounds with a newly designed aluminium ate base became an objective of Uchiyama and his co-workers in 2004 when they reported the first examples of regio- and chemoselective alumination of such substrates.[250] This insightful study has paved the way for the development of aluminium ate bases in deprotonative metallation reactions.

Uchiyama and co-workers synthesised the aluminate base, empirically formulated as Li(TMP)Al(*i*Bu)$_3$, by mixing together the trialkyl triisobutylaluminium (*i*Bu$_3$Al) and lithium TMP in THF solution. One notable feature was the high stability of the base in THF. Even after several weeks no decomposition was observed, which is in stark contrast to organolithium reagents which are known to decompose THF by ring-opening to form ethene gas and the lithium enolate of acetaldehyde[163] though other modes of decomposition are known. The focus of the study was the direct alumination of a variety of functionalised aromatic compounds to form aryl-aluminated intermediates which could be electrophilically quenched with iodine to generate the iodinated products in excellent yields. The scope of functionalising the *ortho*-aluminated intermediates could also be extended to include copper- and palladium-catalyzed carbon-carbon bond forming reactions giving successful examples of allylation, phenylation and benzoylation. Confirmation that an aryl-aluminated intermediate existed could be corroborated by the comparison of the ^{13}C NMR spectra of direct alumination products versus those of a similar co-complexation approach which revealed consistent chemical shifts. (**Scheme 1.15**).

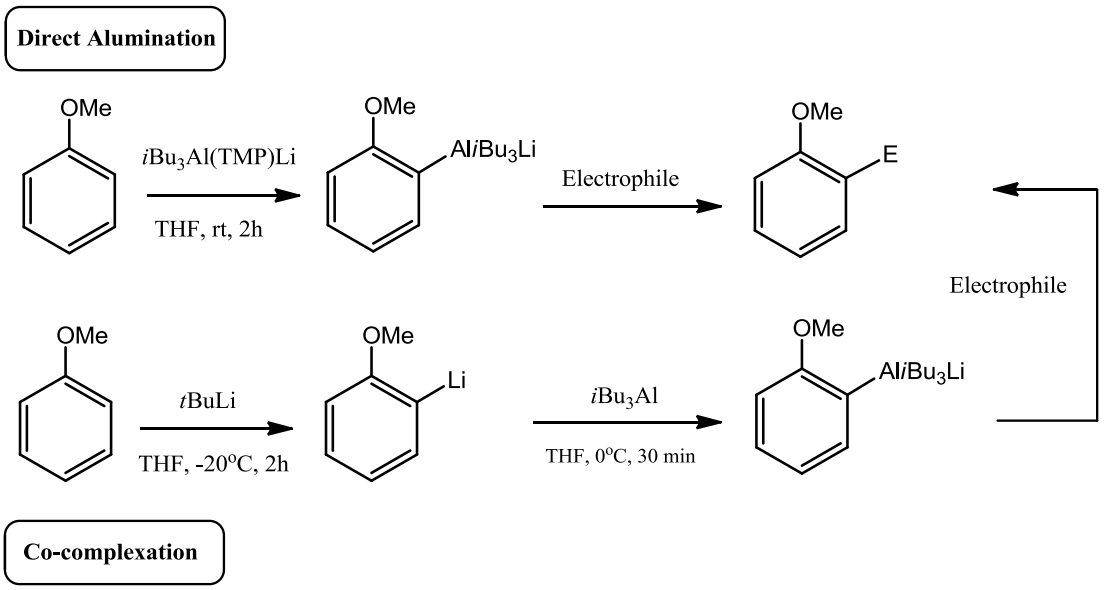

Scheme 1.15: *Ortho*-alumination of a functionalised aromatic substrate and subsequent quench.

Uchiyama and co-workers, the pioneers of AMM*Al* chemistry, developed a successful procedure for the alumination of aromatics tolerant of both electron-donating and electron-withdrawing functional groups. Zincate and magnesiate bases have been extensively studied in the context of aromatic deprotonation chemistry for a number of years however, what sets aluminium apart from these other metals is its superior chemoselectivity. Alkyllithium, Grignard and zincate reagents[111] are known to generally facilitate metal-halogen exchange when faced with the choice between removing an iodine or hydrogen from the same aromatic substrate.[251,252] On the other hand aluminium avoids metal-halogen exchange and chemoselectively *ortho*-aluminates substrates such as 4-iodoanisole and 4-iodobenzonitrile. Benzyne formation can be prevented in substrates (such as *meta*-dichlorobenzene) which bear a halogen next to the *ortho*-position as long the strength of the carbon-halogen bond is too great to facilitate its breakdown. Aluminium can control benzyne formation, if the carbon-halogen bond is weaker, by altering the temperature of the reaction. This is in contrast to zincate systems which control benzyne formation via drastic ligand effects.[113] Deprotonation and subsequent electrophilic trapping of *N*,*N*-diisopropyl-3-bromobenzamide with iodine (**Scheme 1.16**) at sub-ambient temperature produces the 2-iodo product. In contrast, by performing the deprotonation at room temperature, LiBr is expelled forming benzyne which could be trapped through a Diels-Alder cyclisation with 1,3-diphenylisobenzofuran.

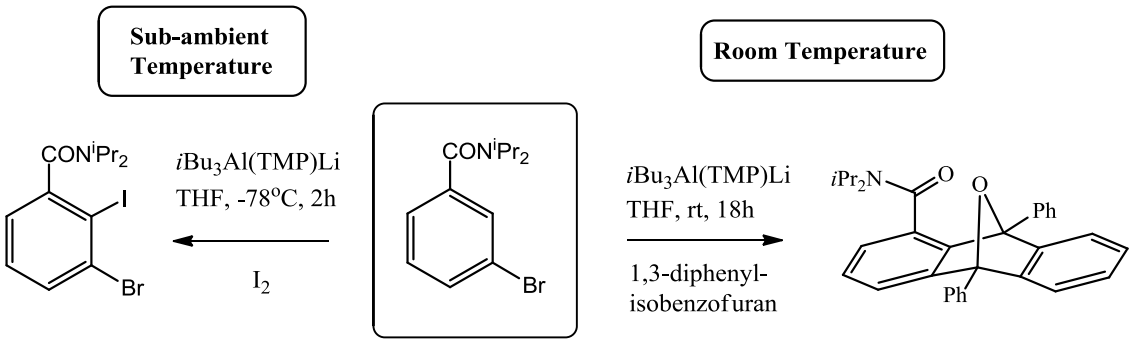

Scheme 1.16: Generation and suppression of 3-functionalised benzyne controlled via temperature.

Knochel and co-workers have also examined the potential of alumination chemistry. They synthesised neutral aluminium trisamide bases, base **1** formulated as "$Al(TMP)_3 \cdot 3LiCl$" prepared by reacting LiTMP with $AlCl_3$ in THF at -78°C and the more sterically encumbered base **2** prepared by treating the appropriate imine precursor with *t*BuLi in THF solution at -78°C followed by transmetallation with $AlCl_3$ (**Scheme 1.17**).[144]

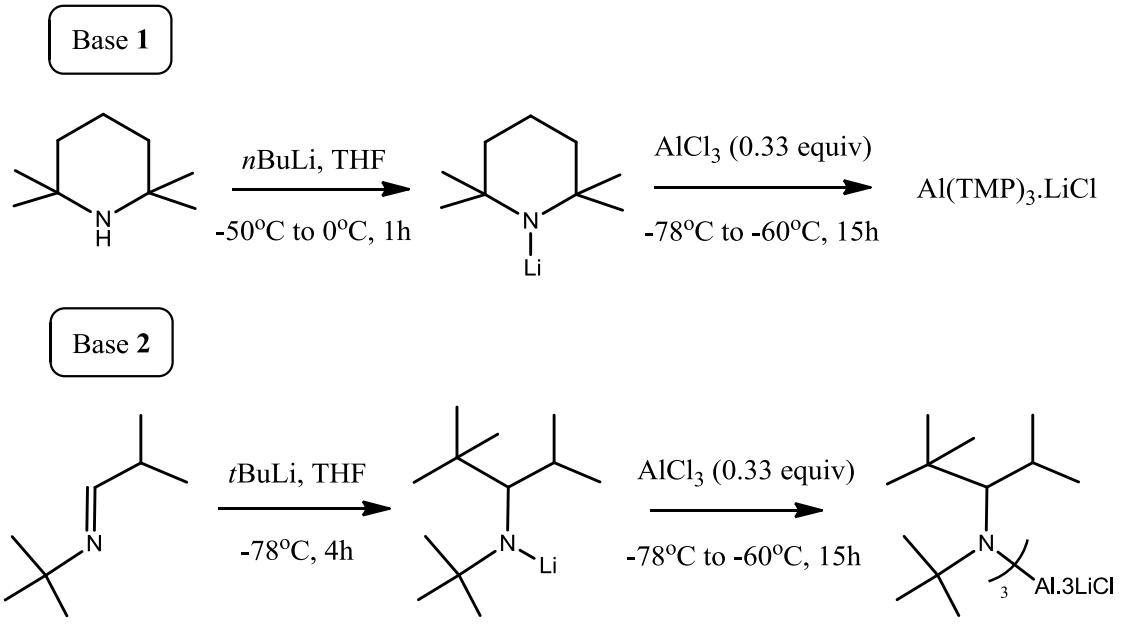

Scheme 1.17: Reactions showing preparation of the neutral trisamide aluminium bases **1** and **2**.

Several functionalised aromatic compounds were reacted with base **1** giving the desired alumination products within 3-6 hours at -5 to -10°C. After transmetallation of the aluminated intermediate with $ZnCl_2$, copper-mediated or palladium-catalysed cross-coupling reactions were carried out to give the final products in good yields (70-79%).

Though metallation often requires harsh cryogenic conditions, base **2** was found to aluminate difluorobenzenes regioselectively at a much milder temperature of -40°C. Additionally, aromatic and heteroaromatic ethers enabled the temperature to be increased further to between 0 and 25°C. Due to the regioselective nature of the alumination reaction even unusual substitution patterns could be obtained, metallating 2-(triisopropylsilyl) benzothiazole and 2-(triethylsilyl)benzothiazole *ortho* to the N atom instead of *ortho* to the S atom. The alumination procedure was found to be tolerant of ester, cyano and halo functional groups.

An understanding of the unique reactivity these reagents possess can be gained by examining their structure. The proposed structure of Uchiyama's base, confirming the presence of tetrahedrally coordinated aluminium (**Scheme 1.18**), could be determined by an NMR spectroscopic analysis.[115,116] All three isobutyl groups were chemically equivalent on the NMR time scale so the exact position of the lithium ion was impossible to pinpoint. Lithium can occupy one of two possible positions (**1**) coordinated to two bridging *i*Bu anions, or (**2**) to one *i*Bu and one TMP anion.

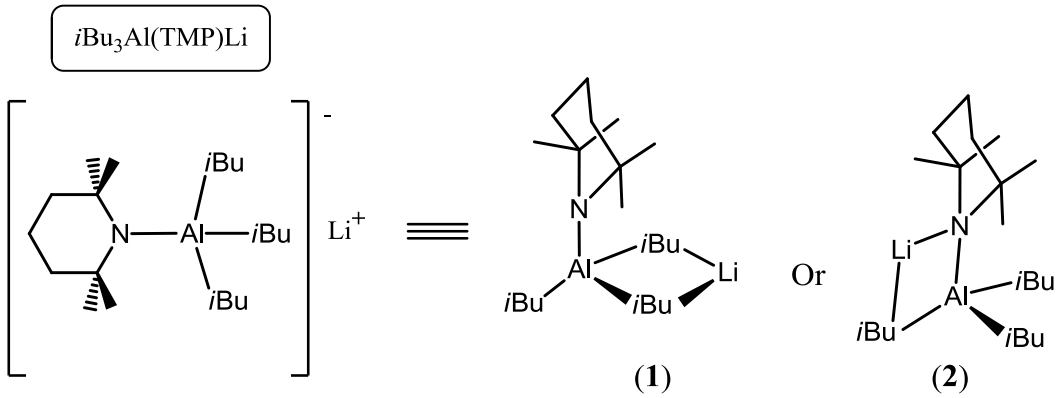

Scheme 1.18: Proposed structure of the aluminium base and the possible relative positions of lithium.

DFT calculations on the Me equivalent of the base [$Me_3Al(Me_2N)Li$] as the model compound were conducted to establish the more plausible isomer with Me_2O substituted for THF. Isomer (**2**) was found to be more energetically stable by 10-13 kcal/mol with the mono-solvated isomer being the most stable overall. These computational results were further backed up by the X-ray crystallographic structure (**Figure 1.18**) showing a distinct Li-N-Al-C core comprising one TMP and one *i*Bu bridge.

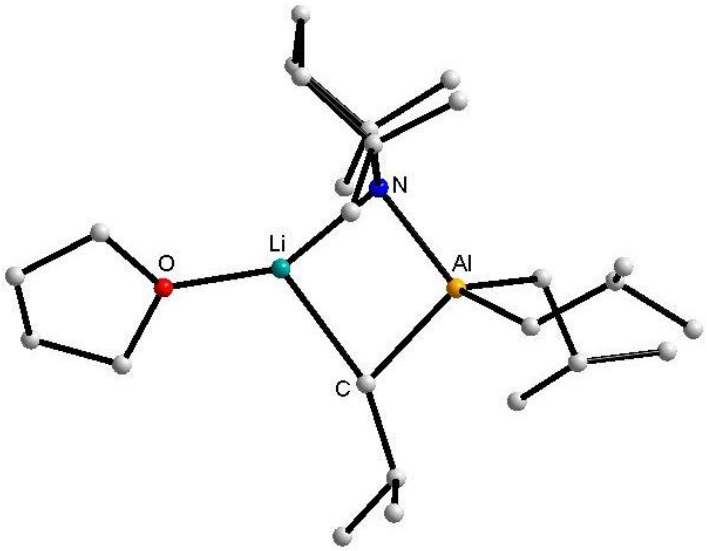

Figure 1.18: Molecular structure of Uchiyama's base [(THF)Li(TMP)Al(*i*Bu)$_3$].

In order to understand the mechanism behind directed *ortho*-alumination DFT calculations were conducted on possible reaction pathways. In D*o*M, a complex-induced proximity effect and/or an acidifying inductive effect is thought to be the driving force for *ortho*-regioselectivity as previously mentioned. That notwithstanding, the mechanisms involved in mixed-metal ate chemistry are a lot less clear cut.[253] Employing the same mono-solvated model compound [$Me_3Al(Me_2N)Li(OMe_2)$] with anisole as a model aromatic substrate, a single pathway leading to a reasonably stable initial complex was found. The results suggest that a coordinative proximity effect between the OMe group and Li can be used to explain the reason for *ortho*-alumination. Lithium forms an interaction with the oxygen atom forming a complex which can orientate itself towards the *ortho* hydrogen atom.

Although these calculations provide rationale for why deprotonations occur at the *ortho*-position, they tell us nothing about whether an overall alkyl or amido basicity applies. Logically one would expect TMP to be the active base as a consequence of its greater kinetic basicity over *i*Bu. Surprisingly, in the case of TMP-zincate systems, alkyl and amido basicity has been found to switch depending on the complex and reaction conditions employed,[254–256] though the former is generally thermodynamically preferred while the latter is the kinetic preference.

Once again utilising DFT calculations on the same model aluminate, only two transition states could be found corresponding to amido and alkyl basicity. The activation barrier leading to amido basicity was found to be much more energetically favourable by 18.1 kcal/mol implying that directed *ortho*-alumination occurs with loss of TMP(H) rather than *i*Bu(H) and occurs via a single step (**Scheme 1.19**). Unlike TMP-zincates, here TMP(H) does not facilitate the elimination of *i*Bu(H) via a two-step mechanism. A possible reason why a two-step mechanism cannot operate is because aluminium is coordinately saturated, due to its formal 3+ charge, and is relatively stable with four anionic groups. If TMP(H) were to interact with aluminium and form a 5-coordinate species this would be energetically unfavoured.

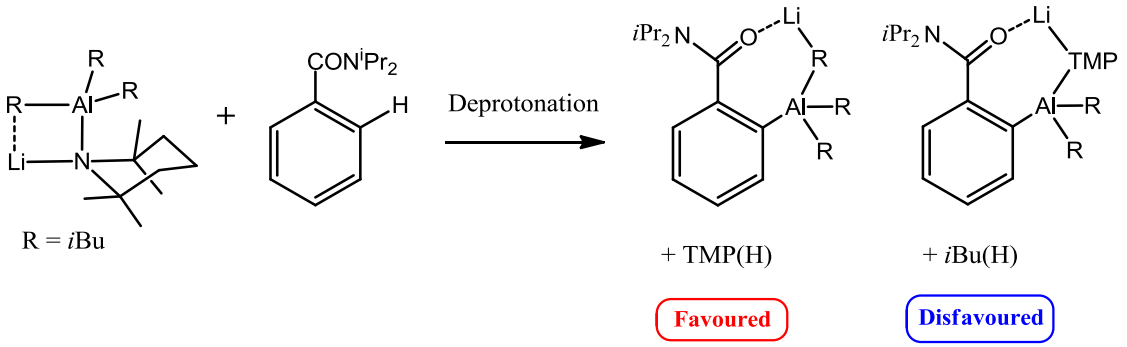

Scheme 1.19: *Ortho*-alumination of *N*,*N*-diisopropylbenzamide via the preferred TMP basicity route.

Stimulated by these investigations our own group began to examine the scope of alumination chemistry. Although it was demonstrated that [Li(TMP)Al(*i*Bu)$_3$] could facilitate the deprotonation of a wide range of functionalised aromatics, the structures of any intermediates prior to electrophilic quenching were unknown. Our own group began to probe the structural integrity of a similar sodium TMP-aluminate [(TMEDA)Na(μ-*i*Bu)(μ-TMP)Al(*i*Bu)$_2$], by mixing NaTMP, *i*Bu$_3$Al and TMEDA in hexane solution and examining its reaction with phenylacetylene.[257] The compound's molecular structure, analogous to Uchiyama's lithium version, was found to contain a single TMP and *i*Bu bridge. On reaction with phenylacetylene a compound containing two donor TMEDA molecules and deprotonated phenylacetylene [(TMEDA)$_2$Na(μ-*i*Bu)(μ-C≡CPh)Al(*i*Bu)$_2$] was synthesised, highlighting another example of TMP basicity. A TMEDA stabilised variation of Uchiyama's lithium base was also tested *in situ* with *N*,*N*-diisopropylbenzamide in the hope of synthesising the *ortho*-aluminated intermediate. Unexpectedly, a structure encompassing a fusion of products was generated

incorporating *ortho*-alumination of the amide, complexation of a neutral (non-metallated) amide to lithium and alumination of TMEDA on one of its terminal methyl arms (**Figure 1.19**).

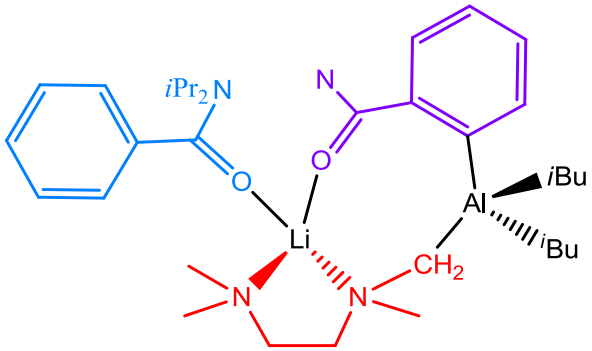

Figure 1.19: Product formed from the reaction between the TMEDA version of Uchiyama's base and *N*,*N*-diisopropylbenzamide highlighting deprotonated TMEDA in red, donor in blue and deprotonated *N*,*N*-diisopropylbenzamide in purple.

The first stage of the reaction is most probably *ortho*-deprotonation of *N*,*N*-diisopropylbenzamide, after prior coordination to lithium, via loss of TMP(H). The anchoring of the substrate, by coordination to lithium via its oxygen atom, puts it in an ideal position to be deprotonated by TMP(H). The second step must involve the solvation of lithium by a second benzamide molecule encouraging an intramolecular deprotonation of TMEDA at one of its methyl arms. This occurs via the remaining *i*Bu bridge which results in irreversible loss of butane. Surprisingly, a decrease in reactivity is observed as TMEDA, which is much less acidic, is deprotonated over a second benzamide molecule. This double deprotonation is the first authenticated example of dual alkyl/amido basicity exhibited by an aluminate base. It highlights how imperative it is to study these reactive intermediates as any electrophilic trapping would not have detected this unusual multiple component structure.

Another *N*,*N*-diisopropylbenzamide Lewis base stabilised complex of Li(TMP)Al(*i*Bu)$_3$ is known and is formed by a simple addition methodology to give the donor-acceptor complex [{PhC(=O)N*i*Pr$_2$}Li(μ-TMP)(μ-*i*Bu)Al(*i*Bu)$_2$].[258] Remarkably, although a straightforward synthesis, LiTMP is known to readily deprotonate benzamide even at sub-ambient temperature. This is regarded as a retarding synergic effect as the reactivity was found to decrease and not increase as usually the case. Unsurprisingly, complexes

with neutral donor tertiary aromatic amides were found to be rare because *ortho*-lithiation of the amide generally prevails.

One would envisage that addition of a stoichiometric amount of another Lewis base donor such as the bi-functional cyclic ether 1,4-dioxane to the benzamide complex would result in *ortho*-alumination of benzamide akin to Uchiyama's observed deprotonation utilising the base in THF. Solvation of lithium by 1,4-dioxane would force the neutral donor benzamide towards the bridging TMP anion facilitating its deprotonation. Instead, no *ortho*-alumination was observed and the isolated crystalline compound was found to be an unusual dilithium dialuminium hexaalkyl aggregate with alkoxy vinyl ether residues captured from the fragmentation of two 1,4-dioxane molecules. This pseudo-dimer structure is completed by two neutral benzamide molecules on lithium and a central intact 1,4-dioxane molecule bridging each lithium aluminium unit (**Figure 1.20**).[259]

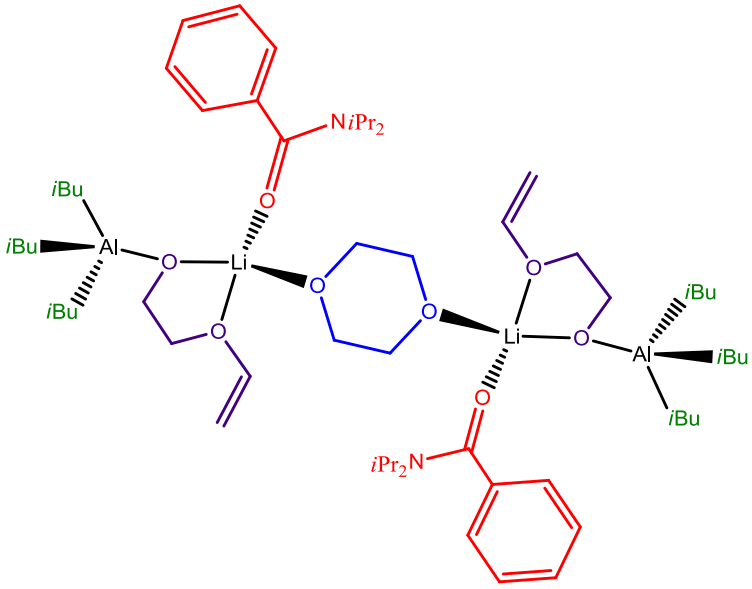

Figure 1.20: 1,4-dioxane cleave and capture product – two neutral benzamide molecules in red, six *i*Bu groups in green, central intact 1,4-dioxane in blue and two alkoxy vinyl ether residues from cleavage of 1,4-dioxane in purple.

As alluded to earlier ether cleavage is a frequent and problematic side reaction in organometallic chemistry especially in polar organolithium chemistry.[260] It is therefore surprising to find that the 1,4-dioxane product represents the first fully characterised structure incorporating captured alkoxy vinyl ether residues. The preferential

deprotonation and fragmentation of 1,4-dioxane was surprising as benzamide is such a strong C-acid and readily undergoes *ortho*-lithiation even at sub-ambient temperatures. Three of the proposed intermediates in the reaction pathway are shown in **Figure 1.21**.

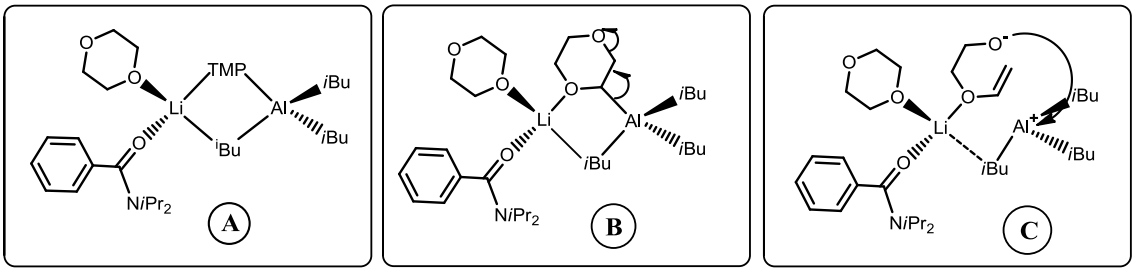

Figure 1.21: Three proposed intermediates in the pathway to the formation of the 1,4-dioxane cleave and capture product.

Intermediate **A**, the first proposed intermediate, could be generated as a consequence of the addition of 1,4-dioxane to the benzamide solvated lithium aluminate. A similar gallanate $[Li\{Ga(CH_2SiMe_3)_4\}\cdot 1.5(dioxane)]_2$ containing a four coordinate Li and ligated dioxane is known.[261] It is probable that the extra steric strain acquired by forming a four coordinate Li could stimulate an intramolecular deprotonation of the solvating 1,4-dioxane molecule by the neighbouring TMP anion to give intermediate **B**. Alternatively, an intermolecular deprotonation could take place on addition of a second 1,4-dioxane molecule. Due to the instability of the C-Al bond, as a result of the repulsion between the carbanionic centre and the electron rich oxygen atom, it is thought that the deprotonated 1,4-dioxane in intermediate **B** spontaneously opens up to give the vinyl form in intermediate **C**. The negatively charged alkoxy residue can nucleophilically attack Al to give the final product after dimerisation. Interestingly, benzamide was found to play an active role in the cleave and capture of 1,4-dioxane as repeating the reaction in its absence resulted in no such fragmentation. In this instance benzamide can be thought of as a key directing ligand and therefore essential for the cleavage of 1,4-dioxane.

To achieve a more thorough understanding of aluminate chemistry and the mechanisms at play, it is vital to comprehensively study the base $[Li(TMP)Al(i\text{Bu})_3]$, not only in the solid state but also in solution. Although Uchiyama's base is crystallised from hexane, its reaction with aromatic substrates is explored in THF solution. So the questions must be asked what is the structure of the base in THF and how does it behave? It is not

surprising to find that the base can only be crystallised from bulk hexane with a stoichiometric quantity of THF acting as a Lewis base donor. A bulk THF system is implemented in order to increase metallation efficiency, analogous to organolithium reagents. An attempt to ascertain some structural information of the reactive intermediates generated in THF solution following Uchiyama's synthetic protocol was performed by our own group. Employing the same substrate as before, *N*,*N*-diisopropylbenzamide was added to 2.2 molar equivalents of the base omitting the electrophilic quench step.[262] Although an intermediate containing deprotonated benzamide was anticipated, the actual isolated product was found to be a solvent-separated ionic homoleptic aluminate [{Li(THF)$_4$}$^+${Al(*i*Bu)$_4$}$^-$] which crystallised from solution even in the absence of *N*,*N*-diisopropylbenzamide. The need to use 2.2 molar equivalents of base becomes apparent as an unforeseen dismutation of the base must occur in solution leading to the product (**Scheme 1.20**).

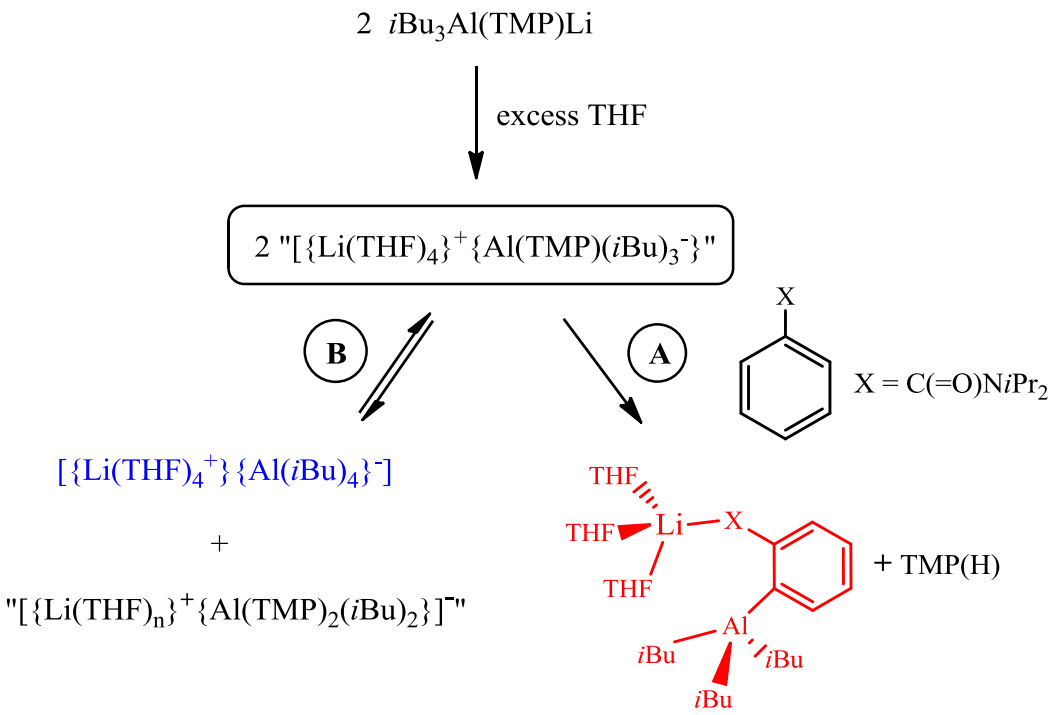

Scheme 1.20: Postulated pathway for the formation of the tris-THF solvated lithium trialkyl-monoarylaluminate [(THF)$_3$Li{O(=C)N(*i*Pr)$_2$(C$_6$H$_4$)}Al(*i*Bu)$_3$].

This inactive component does not react with *N*,*N*-diisopropylbenzamide in neat THF solution so as a result an excess of base must be employed in order to achieve high yields of metallated product. In addition to this dismutation product, the expected

deprotonated benzamide intermediate could also be isolated from the filtrate and was identified as the *tris*-THF solvated open lithium aluminate $[(THF)_3Li\{O(=C)N(iPr)_2(C_6H_4)\}Al(iBu)_3]$. The differences between this structure and those generated from bulk hexane are that it is heavily solvated and contains no second bridge between lithium and *i*Bu. This solution study has uncovered a more representative structural image of the base, its behaviour in THF solution and has become imperative to the understanding of its reactivity. Some of the species thought to be involved and a plausible explanation for the formation of the homoleptic aluminate $[\{Li(THF)_4\}^+\{Al(iBu)_4\}^-]$ are depicted in **Scheme 1.20**.

The presence of four *i*Bu groups in the solvent-separated homoleptic aluminate $[\{Li(THF)_4\}^+\{Al(iBu)_4\}^-]$ was cited as evidence that a dismutation process must be occurring. Balancing the stoichiometry the other component in the mixture was tentatively assigned as $[\{Li(THF)_n\}^+\{Al(TMP)_2(iBu)_2\}^-]$, a solvent-separated *bis*-TMP *bis*-*i*Bu aluminate. The composition of the characterised intermediate seems to verify the principal active base to be a mono-TMP *tris*-*i*Bu aluminate $[Li(THF)_xAl(TMP)(iBu)_3]$ with a stoichiometric excess of THF. The most likely base would probably incorporate four THF donor molecules however, a kinetically labile lower solvated analogue could not be ruled out. Pathway **A** is thought to dominate when a strong Lewis basic aromatic substrate such as *N*,*N*-diisopropylbenzamide is present, giving the expected deprotonated intermediate which can be subsequently quenched with a suitable electrophile. Pathway **B** is more likely to be followed when the base is left to stir in THF solution with no substrate for a period of time or when the substrate is less acidic and hence would be slower to react.

The potential of aluminum to act as a strong base within a mixed-metal formulation and facilitate an intramolecular deprotonation of a high pK_a ligand, was first realised when *N*,*N*-diisopropylbenzamide was added to the TMEDA analogue of $[Li(TMP)Al(iBu)_3]$. A novel complex incorporating the intramolecular deprotonation of a terminal TMEDA methyl group was witnessed. To facilitate a deeper understanding of this surprising deprotonation the reaction was repeated in the absence of the aromatic amide. Unexpectedly, the base operated as a dual alkyl/amido base to form a product containing two α-deprotonated molecules of TMEDA (**Scheme 1.21**).[174]

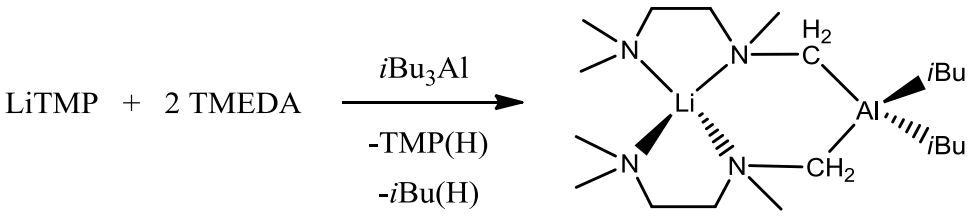

Scheme 1.21: Alumination of two molecules of TMEDA by Li(TMP)Al(*i*Bu)$_3$.

It is common that moderately acidic C-H bonds adjacent to nitrogen require superbasic reagents to affect their deprotonation in the α-position. It is usually extremely challenging with organolithium reagents due to the large repulsion between the lone pair of electrons on nitrogen and the negative charge developing upon deprotonation.[194,263,264] It is more possible however, when the lone pair is involved in conjugation with a carbonyl group or delocalised within an aromatic ring.[62] The amine may also require prior activation with BF_3[265] or a transmetallation approach[266–269] to facilitate its deprotonation. TMEDA can be readily deprotonated at one terminal methyl group using either *t*BuLi or *n*BuLi as the alkyllithium reagent.[270–272] When the more reactive superbasic LICKOR is used instead the regioselectivity is altered to give methylene (CH_2) deprotonation. The intramolecular deprotonation of TMEDA is thought to occur by firstly coordination to Li then subsequent deprotonation at the α-position by the attached bridging anions. Increasing the concentration of TMEDA to three or four equivalents has no effect on the product as TMEDA is unable to bind to Li because it is coordinatively saturated. This explains the lack of basicity by the two terminal *i*Bu bases. This unusual TMEDA deprotonation prompted the exploration of the reactivity of a new amide rich base [Li(TMP)$_2$Al(*i*Bu)$_2$], prepared by mixing a solution of LiTMP with *i*Bu$_2$AlTMP in hexane solution. On addition of one molar equivalent of TMEDA to this base a single TMEDA methyl deprotonation was observed giving rise to a complex incorporating a TMP bridge and a deprotonated methyl group (**Scheme 1.22**).

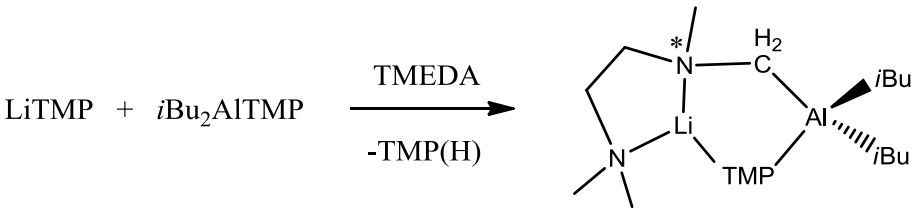

Scheme 1.22: Alumination of one molecule of TMEDA by the amido rich aluminium base.

This single-step deprotonation displaying amido basicity exclusively is in contrast to the twofold alkyl/amido basicity witnessed with the alkyl rich base. Repeating the reaction with an excess of TMEDA produced the same isolated product even under reflux conditions. The bridging TMP and terminal *i*Bu bases are incapable of deprotonating subsequent TMEDA molecules. **Scheme 1.23** provides a rationale for the formation of the di-TMEDA aluminated compound via two intramolecular deprotonation steps.

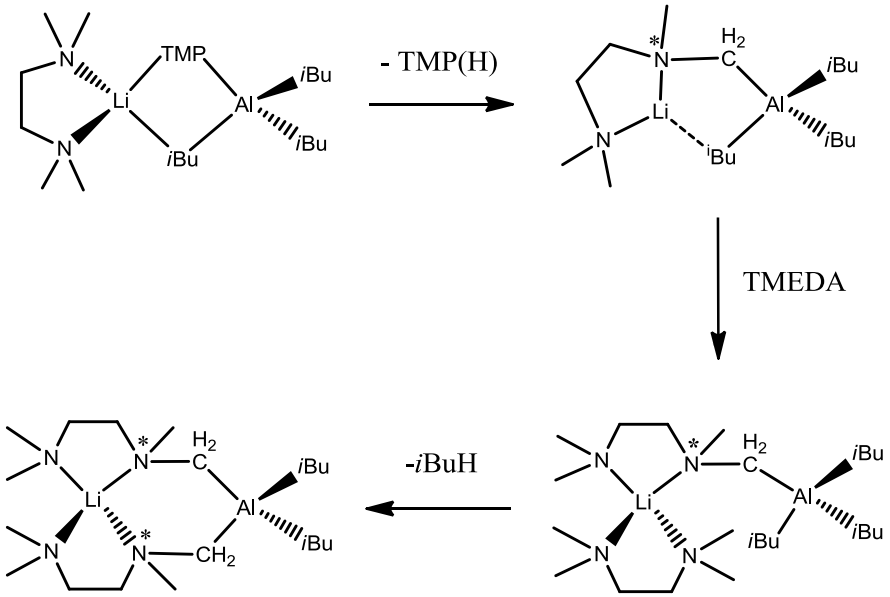

Scheme 1.23: Proposed stepwise reaction pathway for formation of the di-TMEDA aluminated compound.

Although the structure of the lithium/TMEDA alkyl rich base remains unknown it is thought to exhibit a related structure to its sodium analogue with a solvating TMEDA molecule completing the Li coordination environment. A presumed reasonable explanation for the intramolecular mechanism is that the smaller Li atom creates a closer contact between TMEDA and TMP resulting in the deprotonation of a TMEDA methyl group with loss of TMP(H). The generated intermediate can react with a second molecule of TMEDA via coordination to lithium eliminating *i*Bu(H) as the final step in the formation of the di-TMEDA aluminated compound. A rationale for the formation of the mono-TMEDA aluminated compound via a single intramolecular deprotonation step without further reaction could come from the formation of three strong Li-N bonds. Lithium is therefore not only coordinatively but electronically saturated thus a second TMEDA molecule is excluded from reacting further with the aluminate. The base with

more amido groups was also found to react with PMDETA in a similar fashion producing another example of an intramolecular deprotonation product in [Li{$Me_2NCH_2CH_2N(Me)CH_2CH_2N(Me)CH_2$}(μ-TMP)Al(*i*Bu)$_2$]. Significantly this set of metallation reactions illustrate a reversal of the usual reactivity pattern displayed by a synergic base as a nonacidic C-H bond is broken over the acidic N-H bond of TMP(H).

These special intramolecular deprotonations extended the investigation into the possibility of deprotonating other attached anions, in particular TMP.[273] The TMP anion formed from proton abstraction from the cyclic secondary amine 2,2,6,6-tetramethylpiperidine has been popular in organometallic chemistry as a very strong deprotonating agent for decades.[274–278] This is due to its high steric bulk, low nucleophilicity and absence of β-hydrogen atoms. As described above the incorporation of this anion into mixed-metal systems has been increasingly studied. It is commonly the active base ingredient deprotonating the substrate and forming TMP(H), at least initially. Although this may appear intermolecular in origin, a more accurate mechanism is one which involves coordination of the substrate to the alkali metal prior to deprotonation.

By tuning the steric properties of the alkali-metal, any attached donor ligands and the anionic bridging ligands it is possible to influence the deprotonation of an attached donor. This situation has been shown by the deprotonation of the neutral tertiary amine donor TMEDA which, as a consequence of the small steric needs of lithium, can encroach into the vicinity of the bridging bases. Altering the size of the alkali metal to one which is more sterically demanding such as potassium, prevents small dative ligands such as TMEDA being deprotonated as it is significantly further away from bridging anions. An example of this occurs when KTMP was reacted with *i*Bu$_2$Al(TMP) and TMEDA in hexane solution. Surprisingly N-H and CH_3-deprotonation of TMP(H) occurs to give the dianion TMP^{2-} compound [(TMEDA)K(μ-*i*Bu)(μ-TMP*)Al(*i*Bu)] in **Figure 1.22**.

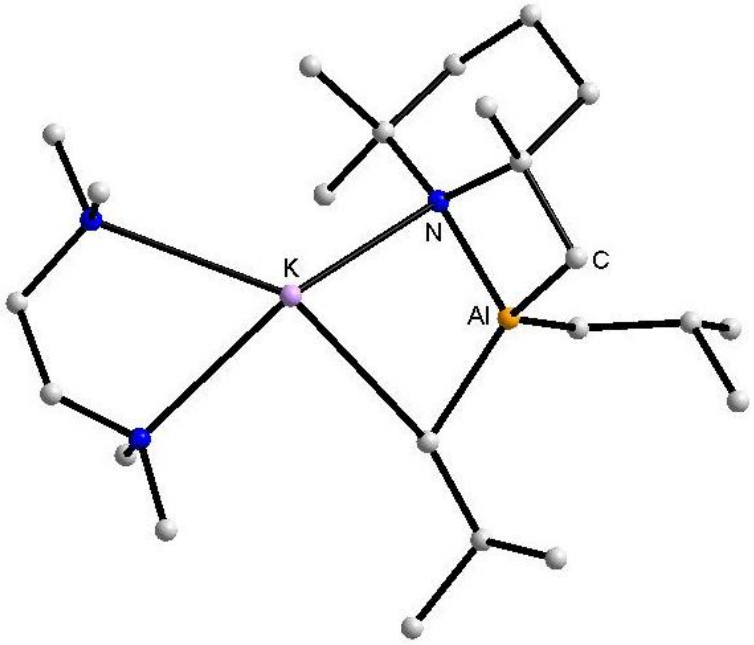

Figure 1.22: TMP dianion complex [(TMEDA)K(μ-*i*Bu)(μ-TMP*)Al(*i*Bu)].

This extraordinary reaction can be interpreted as a self-deprotonation of the TMP anion, where one bridging TMP in its need to cleave a hydrogen atom from a suitably acidic source takes it from the remaining TMP, thus one TMP molecule reacts with the other. This is believed to take place because the larger size of potassium compared to lithium pushes the anion bridges closer together and as TMEDA is further away from these anions it escapes C-H deprotonation. This unexpected C-H bond activation of a high pK_a character has opened up the scope of intramolecular deprotonation in alkali-metal-mediated alumination chemistry and the research conducted within this Ph.D project follows on from this concept.

1.8 Principal Aims of Ph.D. research project

The main aim of this research project was to undertake a comprehensive study of the reaction and solution chemistry of the synergic presumed *bis*-TMP *bis*-alkyl lithium-aluminium reagent "[(THF)Li(TMP)$_2$Al(*i*Bu)$_2$]". Aluminium-hydrogen exchange reactions of a variety of organic substrates were the primary focus of our investigations.

Specific objectives are outlined as follows:

- To study and understand the reacitivty of "[(THF)Li(TMP)$_2$Al(*i*Bu)$_2$]" by investigating its structure and reaction with a series of substrates including functionalised aromatics, Lewis base donor molecules and halogenated aromatic compounds.

- To prepare and where possible isolate crystalline aluminated intermediates of these reactions and in specific cases perform electrophilic trapping of these intermediates with a series of electrophiles to generate the metal-free product.

- To fully characterise the aluminated and metal-free products by NMR spectroscopy, elemental analysis and where possible X-ray crystallography.

- To carry out DFT calculations and DOSY NMR experiments to understand more about the structures and solution chemistry in these alumination reactions.

- To shed light on the mechanisms and reactivities within alkali-metal-mediated alumination reactions.

- To compare and contrast the reactivity of our *bis*-amido base "[Li(TMP)$_2$Al(*i*Bu)$_2$]" with Uchiyama's mono-amido base "[Li(TMP)Al(*i*Bu)$_3$]".

- To rationalise any differences observed in reactivity between these two aluminate bases.

1.9 References

[1] K. C. Nicolaou, J. S. Chen, D. J. Edmonds, A. A. Estrada, *Angew. Chem. Int. Ed.* **2009**, *48*, 660.

[2] R. Chinchilla, C. Najera, M. Yus, *Tetrahedron* **2005**, *61*, 3139.

[3] K. C. Nicolaou, E. J. Sorensen, Eds., *Classics in Total Synthesis*, Wiley-VCH, Weinheim, Germany, **1996**.

[4] K. C. Nicolaou, S. A. Synder, Eds., *Classics in Total Synthesis II*, Wiley-VCH, Weinheim, Germany, **2003**.

[5] E. Frankland, *Liebigs Ann. Chem.* **n.d.**, *71*, 171.

[6] E. Frankland, *J. Chem. Soc.* **n.d.**, *2*, 263.

[7] V. Grignard, *Compt. Rend. Acad. Sci. Paris* **1900**, *130*, 1322.

[8] V. Grignard, *Ann. Chim.* **1901**, *24*, 433.

[9] P. Knochel, Ed., *Handbook of Functionalized Organometallics Vol 1 and 2*, Wiley-VCH, Weinheim, Germany, **2005**.

[10] D. D. Ebbing, S. D. Gammon, *General Chemistry*, Houghton Mifflin Company, Boston, **2005**.

[11] P. Stanetty, M. D. Mihovilovic, *J. Org. Chem.* **1997**, *62*, 1514.

[12] P. Buck, G. Kobrich, *Chem. Ber.* **1970**, *103*, 1420.

[13] H. A. Brune, B. Stapp, G. Schmidtberg, *Chem. Ber.* **1986**, *119*, 1845.

[14] W. E. Parham, R. M. Piccirilli, *J. Org. Chem.* **1976**, *41*, 1976.

[15] P. Knochel, W. Dohle, N. Gommermann, F. F. Kneisel, F. Kopp, T. Korn, I. Sapountzis, V. A. Vu, *Angew. Chem. Int. Ed.* **2003**, *42*, 4302.

[16] G. S. Silverman, P. E. Rakita, Eds., *Handbook of Grignard Reagents*, CRC Press, New York, **1996**.

[17] H. G. Richey, Ed., *Grignard Reagents, New Developments*, Wiley-VCH, Weinheim, Germany, **2000**.

[18] J. F. Garst, F. Ungvary, *Grignard Reagents*, John Wiley & Sons, New York, **2000**.

[19] F. A. Carey, R. J. Sundberg, *Advanced Organic Chemistry Part B: Reactions and Synthesis*, **1983**.

[20] H. R. Rogers, C. L. Hill, Y. Fujiwara, R. J. Rogers, H. L. Mitchell, G. M. Whitesides, *J. Am. Chem. Soc.* **1980**, *120*, 217.

[21] H. J. R. De Boer, O. S. Akkerman, F. Bickelhaupt, *Angew. Chem. Int. Ed.* **1988**, *27*, 687.

[22] G. P. M. van Klink, H. J. R. De Boer, G. Schat, O. S. Akkerman, F. Bickelhaupt, A. Spek, *Organometallics* **2002**, *21*, 2119.

[23] T. Holm, I. Crossland, *Grignard Reagents - New Developments*, Wiley, New York, **2000**.

[24] A. Inoue, K. Oshima, *Main Group Metals in Organic Synthesis: Magnesium in Organic Synthesis*, John Wiley & Sons, **2004**.

[25] L. Ackermann, A. Althammer, *Chem. Unserer Zeit* **2009**, *43*, 74.

[26] R. G. Jones, H. Gilman, *Chem. Rev.* **1954**, *54*, 835.

[27] R. D. Rieke, *Science* **1989**, *246*, 1260.

[28] R. D. Rieke, *Aldrichim Acta* **2000**, *33*, 52.

[29] T. P. Burns, R. D. Rieke, *J. Org. Chem.* **1987**, *52*, 3674.

[30] R. D. Rieke, P. T.-J. Li, T. P. Burns, S. T. Uhm, *J. Org. Chem.* **1981**, *46*, 4323.

[31] J. Lee, R. Velarde-Ortiz, A. Guijarro, J. R. Wurst, R. D. Rieke, *J. Org. Chem.* **2000**, *65*, 5428.

[32] S.-H. Kim, R. D. Rieke, *J. Org. Chem.* **2000**, *65*, 2322.

[33] F. M. Piller, P. Appukkuttan, A. Gavryushin, M. Helm, P. Knochel, *Angew. Chem. Int. Ed.* **2008**, *47*, 6802.

[34] F. M. Piller, A. Metzger, M. A. Schade, B. A. Haag, A. Gavryushin, P. Knochel, *Chem. Eur. J.* **2009**, *15*, 7192.

[35] A. Metzger, F. M. Piller, P. Knochel, *Chem. Commun.* **2008**, 5824.

[36] A. Krasovskiy, V. Malakhov, A. Gavryushin, P. Knochel, *Angew. Chem. Int. Ed.* **2006**, *45*, 6040.

[37] N. Boudet, S. Sase, P. Sinha, C.-Y. Liu, A. Krasovskiy, P. Knochel, *J. Am. Chem. Soc.* **2007**, *129*, 12358.

[38] A. Metzger, M. A. Schade, P. Knochel, *Org. Lett.* **2008**, *10*, 1107.

[39] T. Blumke, Y.-H. Chen, Z. Peng, P. Knochel, *Nature Chemistry* **2010**, *2*, 313.

[40] R. G. Jones, H. Gilman, *Organic Reactions: Halogen Metal Interconversion Reactions with Organolithium Compounds*, John Wiley & Sons, New York, **1951**.

[41] C. Prevost, *Bull. Soc. Chem. Fr.* **1931**, *49*, 1372.

[42] C. E. Tucker, T. N. Majid, P. Knochel, *J. Am. Chem. Soc.* **1992**, *114*, 3983.

[43] P. A. Wender, L. A. Wessjohann, B. Peschke, D. B. Rawlins, *Tetrahedron Lett.* **1995**, *36*, 7181.

[44] L. Boymond, M. Rottlander, G. Cahiez, P. Knochel, *Angew. Chem. Int. Ed.* **1998**, *37*, 1701.

[45] A. Krasovskiy, P. Knochel, *Angew. Chem. Int. Ed.* **2004**, *43*, 3333.

[46] A. Krasovskiy, B. F. Straub, P. Knochel, *Angew. Chem. Int. Ed.* **2005**, *44*, 159.

[47] W. Schlenk, E. Bergmann, *Ann.* **1928**, *463*, 98.

[48] C. R. Hauser, H. G. Walker, *J. Am. Chem. Soc.* **1947**, *69*, 295.

[49] C. R. Hauser, F. C. Frostick, *J. Am. Chem. Soc.* **1949**, *71*, 1350.

[50] P. E. Eaton, C.-H. Lee, Y. Xiong, *J. Am. Chem. Soc.* **1989**, *111*, 8016.

[51] M.-X. Zhang, P. E. Eaton, *Angew. Chem. Int. Ed.* **2002**, *41*, 2169.

[52] P. E. Eaton, K. A. Lukin, *J. Am. Chem. Soc.* **1993**, *115*, 11375.

[53] W. Schlecker, A. Huth, E. Ottow, J. Mulzer, *J. Org. Chem.* **1995**, *60*, 8414.

[54] W. Schlecker, A. Huth, E. Ottow, J. Mulzer, *Liebigs Ann.* **1995**, 1441.

[55] W. Schlecker, A. Huth, E. Ottow, J. Mulzer, *Synthesis* **1995**, 1225.

[56] A. Krasovskiy, V. Krasovskaya, P. Knochel, *Angew. Chem. Int. Ed.* **2006**, *45*, 2958.

[57] G. C. Clososki, C. J. Rohbogner, P. Knochel, *Angew. Chem. Int. Ed.* **2007**, *46*, 7681.

[58] C. J. Rohbogner, G. C. Clososki, P. Knochel, *Angew. Chem. Int. Ed.* **2008**, *47*, 1503.

[59] C. J. Rohbogner, A. J. Wagner, G. C. Clososki, P. Knochel, *Org. Synth.* **2009**, *86*, 374.

[60] W. Schlenk, J. Holtz, *Ber. Dtsch. Chem. Ges.* **1917**, *50*, 262.

[61] D. Seyferth, *Organometallics* **2009**, *28*, 2.

[62] J. Clayden, *Organolithiums: Selectivity for Synthesis*, Elsevier Science Ltd, Oxford, **2002**.

[63] E. Weiss, E. A. C. Lucken, *J. Organomet. Chem.* **1964**, *2*, 197.

[64] E. Weiss, *Angew. Chem. Int. Ed.* **1993**, *32*, 1501.

[65] C. Elschenbroich, *Organometallics*, Wiley-VCH, Weinheim, Germany, **2006**.

[66] H. L. Lewis, T. L. Brown, *J. Am. Chem. Soc.* **1970**, *92*, 4664.

[67] F. Marsais, P. Granger, G. Queguiner, *J. Org. Chem.* **1981**, *46*, 4494.

[68] T. Gungor, F. Marsais, G. Queguiner, *J. Organomet. Chem.* **1981**, *215*, 139.

[69] M. Hammell, R. Levine, *J. Org. Chem.* **1950**, *15*, 162.

[70] G. Stork, L. Maldonado, *J. Am. Chem. Soc.* **1971**, *93*, 5286.

[71] Y. J. Kim, M. P. Bernstein, A. S. G. Roth, F. E. Romesberg, P. G. Williard, D. J. Fuller, A. T. Harrison, D. B. Collum, *J. Org. Chem.* **1991**, *56*, 4435.

[72] N. D. R. Barnett, R. E. Mulvey, W. Clegg, P. A. O'Neil, *J. Am. Chem. Soc.* **1991**, *113*, 8187.

[73] A. Mootz, A. Zinnius, B. Bottcher, *Angew. Chem. Int. Ed.* **1969**, *8*, 378.

[74] M. F. Lappert, M. J. Slade, A. Singh, J. L. Atwood, R. D. Rogers, R. Shakir, *J. Am. Chem. Soc.* **1983**, *105*, 302.

[75] M. P. Bernstein, F. E. Romesberg, D. J. Fuller, A. T. Harrison, D. B. Collum, Q. Y. Liu, P. G. Williard, *J. Am. Chem. Soc.* **1992**, *114*, 5100.

[76] P. G. Williard, Q. Y. Liu, *J. Am. Chem. Soc.* **1993**, *115*, 3380.

[77] J. F. Remenar, B. L. Lucht, D. Kruglyak, F. E. Romesberg, J. H. Gilchrist, D. B. Collum, *J. Org. Chem.* **1997**, *62*, 5748.

[78] D. R. Armstrong, A. R. Kennedy, R. E. Mulvey, S. D. Robertson, *Chem. Eur. J.* **2011**, *17*, 8820.

[79] R. A. Rennels, A. S. Maliakal, D. B. Collum, *J. Am. Chem. Soc.* **1998**, *120*, 421.

[80] S. T. Chadwick, R. A. Rennels, J. L. Rutherford, D. B. Collum, *J. Am. Chem. Soc.* **2000**, *1222*, 8640.

[81] P. Gros, S. Choppin, J. Mathieu, Y. Fort, *J. Org. Chem.* **2002**, *67*, 234.

[82] P. Beak, V. Snieckus, *Acc. Chem. Res.* **1982**, *15*, 306.

[83] V. Snieckus, *Chem. Rev.* **1990**, *90*, 879.

[84] H. W. Gschwend, H. R. Rodriguez, *Org. React.* **1979**, *26*, 1.

[85] L. S. Bennie, W. J. Kerr, M. Middleditch, A. J. B. Watson, *Chem. Commun.* **2011**, *47*, 2264.

[86] M. Schlosser, G. Katsoulos, S. Takagishi, *Synlett* **1990**, 747.

[87] J. D. Roberts, D. Y. Curtin, *J. Am. Chem. Soc.* **1946**, *68*, 1658.

[88] D. A. Shirley, J. R. Johnson, J. P. Hendrix, *J. Organomet. Chem.* **1968**, *11*, 209.

[89] M. Schlosser, H. C. Jung, S. Takagishi, *Tetrahedron* **1990**, *46*, 5633.

[90] M. D. Rausch, D. J. Ciappenelli, *J. Organomet. Chem.* **1967**, *10*, 127.

[91] P. Fleming, D. F. O'Shea, *J. Am. Chem. Soc.* **2011**, *133*, 1698.

[92] M. Schlosser, *J. Organomet. Chem.* **1967**, *8*, 9.

[93] A. R. Kennedy, R. E. Mulvey, R. B. Rowlings, *J. Am. Chem. Soc.* **1998**, *120*, 7816.

[94] D. R. Armstrong, A. R. Kennedy, R. E. Mulvey, R. B. Rowlings, *Angew. Chem. Int. Ed.* **1999**, *38*, 131.

[95] W. Clegg, K. W. Henderson, A. R. Kennedy, R. E. Mulvey, C. T. O'Hara, R. B. Rowlings, D. M. Tooke, *Angew. Chem. Int. Ed.* **2001**, *40*, 3902.

[96] V. L. Blair, A. R. Kennedy, R. E. Mulvey, C. T. O'Hara, *Chem. Eur. J.* **2010**, *16*, 8600.

[97] W. Clegg, G. C. Forbes, A. R. Kennedy, R. E. Mulvey, S. T. Liddle, *Chem. Commun.* **2003**, 406.

[98] H. R. L. Barley, W. Clegg, S. H. Dale, E. Hevia, G. W. Honeyman, A. R. Kennedy, R. E. Mulvey, *Angew. Chem. Int. Ed.* **2005**, *44*, 6018.

[99] E. Hevia, G. W. Honeyman, A. R. Kennedy, R. E. Mulvey, *J. Am. Chem. Soc.* **2005**, *127*, 13106.

[100] D. R. Armstrong, W. Clegg, S. H. Dale, E. Hevia, L. M. Hogg, G. W. Honeyman, R. E. Mulvey, *Angew. Chem. Int. Ed.* **2006**, *45*, 3775.

[101] J. Garcia-Alvarez, A. R. Kennedy, J. Klett, R. E. Mulvey, *Angew. Chem. Int. Ed.* **2007**, *46*, 1105.

[102] L. M. Carrella, W. Clegg, D. V. Graham, L. M. Hogg, A. R. Kennedy, J. Klett, R. E. Mulvey, E. Rentschler, L. Russo, *Angew. Chem. Int. Ed.* **2007**, *46*, 4662.

[103] V. L. Blair, W. Clegg, B. Conway, E. Hevia, A. R. Kennedy, J. Klett, R. E. Mulvey, L. Russo, *Chem. Eur. J.* **2008**, *14*, 65.

[104] P. Albores, L. M. Carrella, W. Clegg, P. Garcia-Alvarez, A. R. Kennedy, J. Klett, R. E. Mulvey, E. Rentschler, L. Russo, *Angew. Chem. Int. Ed.* **2009**, *48*, 3317.

[105] R. E. Mulvey, *Organometallics* **2006**, *25*, 1060.

[106] R. E. Mulvey, F. Mongin, M. Uchiyama, Y. Kondo, *Angew. Chem. Int. Ed.* **2007**, *46*, 3802.

[107] R. E. Mulvey, *Acc. Chem. Res.* **2009**, *42*, 743.

[108] G. Wittig, *Angew. Chem.* **1958**, *70*, 65.

[109] A. R. Kennedy, J. Klett, R. E. Mulvey, D. S. Wright, *Science* **2009**, *326*, 706.

[110] R. E. Mulvey, V. L. Blair, W. Clegg, A. R. Kennedy, J. Klett, L. Russo, *Nature Chemistry* **2010**, *2*, 588.

[111] Y. Kondo, M. Shilai, M. Uchiyama, T. Sakamoto, *J. Am. Chem. Soc.* **1999**, *121*, 3539.

[112] T. Imahori, M. Uchiyama, T. Sakamoto, Y. Kondo, *Chem. Commun.* **2001**, 2450.

[113] M. Uchiyama, T. Miyoshi, Y. Kajihara, T. Sakamoto, Y. Otani, T. Ohwada, Y. Kondo, *J. Am. Chem. Soc.* **2002**, *124*, 8514.

[114] Y. Kondo, J. V. Morey, J. C. Morgan, H. Naka, D. Nobuto, P. R. Raithby, M. Uchiyama, A. E. H. Wheatley, *J. Am. Chem. Soc.* **2007**, *129*, 12734.

[115] H. Naka, M. Uchiyama, Y. Matsumoto, A. E. H. Wheatley, M. McPartlin, J. V. Morey, Y. Kondo, *J. Am. Chem. Soc.* **2007**, *129*, 1921.

[116] H. Naka, J. V. Morey, J. Haywood, D. J. Eisler, M. McPartlin, F. Garcia, H. Kudo, Y. Kondo, M. Uchiyama, A. E. H. Wheatley, *J. Am. Chem. Soc.* **2008**, *130*, 16193.

[117] A. Seggio, M.-I. Lannou, F. Chevallier, D. Nobuto, M. Uchiyama, S. Golhen, T. Roisnel, F. Mongin, *Chem. Eur. J.* **2007**, *13*, 9982.

[118] A. Seggio, F. Chevallier, M. Vaultier, F. Mongin, *J. Org. Chem.* **2007**, *72*, 6602.

[119] J.-M. L'Helgoual'ch, G. Bentabed-Ababsa, F. Chevallier, M. Yonehara, M. Uchiyama, A. Derdour, F. Mongin, *Chem. Commun.* **2008**, 5375.

[120] J.-M. L'Helgoual'ch, A. Seggio, F. Chevallier, M. Yonehara, E. Jeanneau, M. Uchiyama, F. Mongin, *J. Org. Chem.* **2008**, *73*, 177.

[121] K. Snegaroff, J.-M. L'Helgoual'ch, G. Bentabed-Ababsa, T. T. Nguyen, F. Chevallier, M. Yonehara, M. Uchiyama, A. Derdour, F. Mongin, *Chem. Eur. J.* **2009**, *15*, 10280.

[122] G. Dayaker, F. Chevallier, P. C. Gros, F. Mongin, *Tetrahedron* **2010**, *66*, 8904.

[123] E. Hevia, A. R. Kennedy, J. Klett, M. D. McCall, *Chem. Commun.* **2009**, 3240.

[124] W. Clegg, B. Conway, E. Hevia, M. D. McCall, L. Russo, R. E. Mulvey, *J. Am. Chem. Soc.* **2009**, *131*, 2375.

[125] M. C. Whisler, S. MacNeil, V. Snieckus, P. Beak, *Angew. Chem. Int. Ed.* **2004**, *43*, 2206.

[126] A. Metzger, S. Bernhardt, G. Manolikakes, P. Knochel, *Angew. Chem. Int. Ed.* **2010**, *49*, 4665.

[127] Z. Dong, G. C. Clososki, S. H. Wunderlich, A. Unsinn, J. Li, P. Knochel, *Chem. Eur. J.* **2009**, *15*, 457.

[128] W. Lin, O. Baron, P. Knochel, *Org. Lett.* **2006**, *8*, 5673.

[129] N. Boudet, J. R. Lachs, P. Knochel, *Org. Lett.* **2007**, *9*, 5525.

[130] A. H. Stoll, P. Mayer, P. Knochel, *Organometallics* **2007**, *26*, 6694.

[131] M. Mosrin, P. Knochel, *Org. Lett.* **2008**, *10*, 2497.

[132] M. Mosrin, N. Boudet, P. Knochel, *Org. Biomol. Chem.* **2008**, *6*, 3237.

[133] M. Mosrin, P. Knochel, *Chem. Eur. J.* **2009**, *15*, 1468.

[134] C. Despotopoulou, L. Klier, P. Knochel, *Org. Lett.* **2009**, *11*, 3326.

[135] M. Mosrin, P. Knochel, *Org. Lett.* **2009**, *11*, 1837.

[136] M. Mosrin, T. Bresser, P. Knochel, *Org. Lett.* **2009**, *11*, 3406.

[137] M. Mosrin, G. Monzon, T. Bresser, P. Knochel, *Chem. Commun.* **2009**, 5615.

[138] T. Bresser, M. Mosrin, G. Monzon, P. Knochel, *J. Org. Chem.* **2010**, *75*, 4686.

[139] C. J. Rohbogner, S. Wirth, P. Knochel, *Org. Lett.* **2010**, *12*, 1984.

[140] S. H. Wunderlich, P. Knochel, *Angew. Chem. Int. Ed.* **2007**, *46*, 7685.

[141] S. H. Wunderlich, P. Knochel, *Org. Lett.* **2008**, *10*, 4705.

[142] S. H. Wunderlich, P. Knochel, *Chem. Commun.* **2008**, 6387.

[143] S. H. Wunderlich, M. Kienle, P. Knochel, *Angew. Chem. Int. Ed.* **2009**, *48*, 7256.

[144] S. H. Wunderlich, P. Knochel, *Angew. Chem. Int. Ed.* **2009**, *48*, 1501.

[145] S. H. Wunderlich, P. Knochel, *Angew. Chem. Int. Ed.* **2009**, *48*, 9717.

[146] S. H. Wunderlich, P. Knochel, *Chem. Eur. J.* **2010**, *16*, 3304.

[147] M. Jeganmohan, P. Knochel, *Angew. Chem. Int. Ed.* **2010**, *49*, 8520.

[148] M. Jaric, B. A. Haag, A. Unsinn, K. Karaghiosoff, P. Knochel, *Angew. Chem. Int. Ed.* **2010**, *49*, 5451.

[149] T. Bresser, P. Knochel, *Angew. Chem. Int. Ed.* **2011**, *50*, 1914.

[150] P. Garcia-Alvarez, D. V. Graham, E. Hevia, A. R. Kennedy, J. Klett, R. E. Mulvey, C. T. O'Hara, S. Weatherstone, *Angew. Chem. Int. Ed.* **2008**, *47*, 8079.

[151] D. R. Armstrong, P. Garcia-Alvarez, A. R. Kennedy, R. E. Mulvey, J. A. Parkinson, *Angew. Chem. Int. Ed.* **2010**, *49*, 3185.

[152] D. Li, I. Keresztes, R. Hopson, P. G. Willard, *Acc. Chem. Res.* **2009**, *42*, 270.

[153] A. Macchioni, G. Ciancaleoni, C. Zuccaccia, D. Zuccaccia, *Chem. Soc. Rev.* **2008**, *37*, 479.

[154] B. Antalek, *Concepts Magn. Reson., Part A* **2007**, *30*, 219.

[155] P. C. Andrikopoulos, D. R. Armstrong, D. V. Graham, E. Hevia, A. R. Kennedy, R. E. Mulvey, C. T. O'Hara, C. Talmard, *Angew. Chem. Int. Ed.* **2005**, *44*, 3459.

[156] D. R. Armstrong, W. Clegg, S. H. Dale, E. Hevia, L. M. Hogg, G. W. Honeyman, R. E. Mulvey, *Angew. Chem. Int. Ed.* **2006**, *45*, 3775.

[157] W. Clegg, K. W. Henderson, A. R. Kennedy, R. E. Mulvey, C. T. O'Hara, R. B. Rowlings, D. M. Tooke, *Angew. Chem. Int. Ed.* **2001**, *40*, 3902.

[158] P. C. Andrikopoulos, D. R. Armstrong, W. Clegg, C. J. Gilfillan, E. Hevia, A. R. Kennedy, R. E. Mulvey, C. T. O'Hara, J. A. Parkinson, D. M. Tooke, *J. Am. Chem. Soc.* **2004**, *126*, 11612.

[159] A. R. Kennedy, R. E. Mulvey, C. L. Raston, B. A. Roberts, R. B. Rowlings, *Chem. Commun.* **1999**, 353.

[160] P. C. Andrews, A. R. Kennedy, R. E. Mulvey, C. L. Raston, B. A. Roberts, R. B. Rowlings, *Angew. Chem. Int. Ed.* **2000**, *39*, 1960.

[161] D. J. Gallagher, K. W. Henderson, A. R. Kennedy, C. T. O'Hara, R. E. Mulvey, R. B. Rowlings, *Chem. Commun.* **2002**, 376.

[162] R. Bomparola, R. P. Davies, S. Hornauer, A. J. P. White, *Angew. Chem. Int. Ed.* **2008**, *47*, 5812.

[163] R. B. Bates, L. M. Kroposki, D. E. Potter, *J. Org. Chem.* **1972**, *37*, 560.

[164] A. M. Corrente, T. Chivers, *Dalton Trans.* **2008**, 4840.

[165] S. J. Geier, D. W. Stephan, *J. Am. Chem. Soc.* **2009**, *131*, 3476.

[166] T. Kottke, R. J. Lagow, D. Hoffman, R. D. Thomas, *Organometallics* **1997**, *16*, 789.

[167] B. Walfort, S. K. Pandey, D. Stalke, *Chem. Commun.* **2001**, 1640.

[168] M. Westerhausen, *Dalton Trans.* **2006**, 4755.

[169] N. M. Clark, P. Garcia-Alvarez, A. R. Kennedy, C. T. O'Hara, G. M. Robertson, *Chem. Commun.* **2009**, 5835.

[170] E. Velez, A. Alberola, V. Polo, *J. Phys. Chem. A.* **2009**, *113*, 14008.

[171] X.-H. Lu, M.-T. Ma, Y.-M. Yao, Y. Zhang, Q. Shen, *Inorg. Chem. Commun.* **2010**, *13*, 1566.

[172] J. Wu, X. Pan, N. Tang, C.-C. Lin, *Inorg. Chem.* **2010**, *49*, 5362.

[173] C. V. Cardenas, M. A. M. Hernandez, J.-M. Grevy, *Dalton Trans.* **2010**, *39*, 6441.

[174] B. Conway, J. Garcia-Alvarez, E. Hevia, A. R. Kennedy, R. E. Mulvey, S. D. Robertson, *Organometallics* **2009**, *28*, 6462.

[175] S. Merkel, D. Stern, J. Henn, D. Stalke, *Angew. Chem. Int. Ed.* **2009**, *48*, 6350.

[176] W. Hallwachs, A. Schafarik, *Liebigs Ann. Chem.* **1859**, *109*, 206.

[177] J. Boor, *Ziegler Natta Catalysts and Polymerisations*, Academic Press: New York, **1979**.

[178] S. Saito, *Main Group Metals in Organic Synthesis: Aluminium in Organic Synthesis*, Wiley-VCH, Weinheim, Germany, **2004**.

[179] M. S. Taylor, D. N. Zalatan, A. M. Lerchner, E. N. Jacobsen, *J. Am. Chem. Soc.* **2005**, *127*, 1313.

[180] L. C. Wieland, H. Deng, M. L. Snapper, A. H. Hoveyda, *J. Am. Chem. Soc.* **2005**, *127*, 15453.

[181] W. Nagata, M. Yoshioka, S. Hirai, *J. Am. Chem. Soc.* **1972**, *94*, 4635.

[182] E. Y. –X. Chen, M. J. Cooney, *J. Am. Chem. Soc.* **2003**, *125*, 7150.

[183] K. Maruoka, H. Sano, K. Shinoda, H. Yamamoto, *Chem. Lett.* **1987**, 73.

[184] G. W. Kabalka, R. J. Newton, *J. Organomet. Chem.* **1978**, *156*, 65.

[185] L.-N. Guo, H. Gao, P. Mayer, P. Knochel, *Chem. Eur. J.* **2010**, *16*, 9829.

[186] S. Kawamura, K. Ishizuka, H. Takaya, M. Nakamura, *Chem. Commun.* **2010**, *46*, 6054.

[187] J. J. Eisch, G. A. Damasevitz, *J. Org. Chem.* **1976**, *40*, 2214.

[188] K. Uchida, K. Utimoto, H. Nozaki, *J. Org. Chem.* **1976**, *40*, 2215.

[189] N. S. Ham, T. Mole, *Prog. Nucl. Magn. Reson. Spectrosc.* **1961**, *4*, 91.

[190] K. C. Ramey, J. F. O. Brien, I. Hasegawa, A. E. Borchert, *J. Phys. Chem.* **1965**, *69*, 3418.

[191] K. C. Williams, T. L. Brown, *J. Am. Chem. Soc.* **1966**, *88*, 5460.

[192] E. A. Jeffery, T. Mole, *Aust. J. Chem.* **1969**, *22*, 1129.

[193] K. Maruoka, T. Itoh, M. Sakurai, K. Nonoshita, H. Yamamoto, *J. Am. Chem. Soc.* **1988**, *110*, 3588.

[194] M. Schlosser, *Organometallics in Synthesis: A Manual*, Wiley, New York, **2002**.

[195] K. Gosling, J. D. Smith, D. H. W. Wharmby, *j. Chem. Soc. A* **1969**, 1738.

[196] A. Basha, M. Lipton, S. M. Winreb, *Tetrahedron Lett.* **1977**, *18*, 4171.

[197] E. J. Corey, D. J. Beames, *J. Am. Chem. Soc.* **1973**, *95*, 5829.

[198] J. L. Wood, N. A. Khatri, S. M. Weinreb, *Tetrahedron Lett.* **1979**, *17*, 4907.

[199] L. E. Overman, L. A. Flippin, *Tetrahedron Lett.* **1981**, *22*, 195.

[200] A. Yasuda, M. Takahashi, H. Takaya, *Tetrahedron Lett.* **1981**, *22*, 2413.

[201] A. P. Kozikowski, A. Ames, *J. Org. Chem.* **1978**, *43*, 2735.

[202] A. Yasuda, S. Tanaka, K. Oshima, H. Yamamoto, H. Nozaki, *J. Am. Chem. Soc.* **1974**, *96*, 6513.

[203] S. Tanaka, A. Yasuda, H. Yamamoto, H. Nozaki, *J. Am. Chem. Soc.* **1975**, *97*, 3252.

[204] S. H. Pine, R. Zahler, D. A. Evans, R. H. Grubbs, *J. Am. Chem. Soc.* **1980**, *102*, 3270.

[205] K. Takai, K. Oshima, H. Nozaki, *Tetrahedron Lett.* **1980**, *21*, 1657.

[206] T. Katsuki, K. B. Sharpless, *J. Am. Chem. Soc.* **1980**, *102*, 5974.

[207] B. E. Rossiter, T. Katsuki, K. B. Sharpless, *J. Am. Chem. Soc.* **1981**, *103*, 464.

[208] V. S. Matin, S. S. Woodard, T. Katsuki, Y. Yamada, M. Ikeda, K. B. Sharpless, *J. Am. Chem. Soc.* **1981**, *103*, 6237.

[209] H. Yamamoto, H. Nozaki, *Angew. Chem. Int. Ed.* **1978**, *3*, 169.

[210] K. Maruoka, M. Oishi, H. Yamamoto, *J. Org. Chem.* **1993**, *58*, 7638.

[211] K. Maruoka, S. Hashimoto, Y. Kitagawa, H. Yamamoto, H. Nozaki, *J. Am. Chem. Soc.* **1977**, *99*, 7705.

[212] R. S. Lenox, J. A. Katzenellenbogen, *J. Am. Chem. Soc.* **1973**, *95*, 957.

[213] G. M. Sheldrick, W. S. Sheldrick, *j. Chem. Soc. A* **1969**, 2297.

[214] C.-C. Chang, M.-D. Li, M. Y. Chiang, S. M. Peng, Y. Wang, G.-H. Lee, *Inorg. Chem.* **1997**, *36*, 1955.

[215] P. J. Brothers, R. J. Wehmschulte, M. M. Olmstead, K. Ruhlandt-Senge, S. R. Parkin, P. P. Power, *Organometallics* **1994**, *13*, 2792.

[216] K. Knabel, I. Krossing, H. Noth, H. Schwenk-Kirchner, M. Schmidt-Amelunxen, T. Seifert, *Eur. J. Inorg. Chem.* **1998**, 1095.

[217] M. A. Petrie, K. Ruhlandt-Senge, P. P. Power, *Inorg. Chem.* **1993**, *32*, 1135.

[218] I. Krossing, H. Noth, C. Tacke, M. Schmidt, *Chem. Ber. Recl.* **1997**, *130*, 1047.

[219] J. S. Bradley, F. Cheng, S. J. Archibald, R. Suppilit, R. Rovai, C. W. Lehmann, C. Kruger, F. Lefebvre, *Dalton Trans.* **2003**, 1846.

[220] I. Krossing, H. Noth, H. Schwenk-Kircher, *Eur. J. Inorg. Chem.* **1998**, 927.

[221] J. Pinkas, B. Gaul, J. Verkade, *J. Am. Chem. Soc.* **1993**, *115*, 3925.

[222] J. Pinkas, T. Wang, R. A. Jacobson, J. G. Verkade, *Inorg. Chem.* **1994**, *33*, 4202.

[223] N. Emig, H. Nguyen, H. Krautscheid, R. Reau, J. B. Cazaux, G. Bertrand, *Organometallics* **1998**, *17*, 3599.

[224] J. Lewinski, J. Zachara, T. Kopec, Z. Ochal, *Polyhedron* **1997**, *16*, 1337.

[225] A. P. Kenney, G. P. A. Yap, D. S. Richeson, S. T. Barry, *Inorg. Chem.* **2005**, *44*, 2926.

[226] S. J. Trepanier, S. N. Wang, *Organometallics* **1994**, *13*, 2213.

[227] L. M. Engelhardt, M. G. Gardiner, C. Jones, P. C. Junk, C. L. Raston, A. H. White, *J. Chem. Soc.* **1996**, 3053.

[228] E. Wiberg, A. May, *Z. Naturforsch* **1955**, *10B*, 681.

[229] K. M. Waggoner, M. M. Olmstead, P. P. Power, *Polyhedron* **1990**, *9*, 257.

[230] J.-P. Bezombes, B. Gehrhus, P. B. Hitchcock, M. F. Lappert, P. G. Merle, *Dalton Trans.* **2003**, 1821.

[231] P. B. Hitchcock, H. A. Jasim, M. F. Lappert, H. D. Williams, *Polyhedron* **1990**, *9*, 245.

[232] C. Klein, H. Noth, M. Tacke, M. Thomann, *Angew. Chem. Int. Ed.* **1993**, *32*, 886.

[233] M. Schiefer, H. Hatop, H. W. Roesky, H.-G. Schmidt, M. Noltemeyer, *Organometallics* **2002**, *21*, 1300.

[234] T. Y. Her, C. C. Cheng, J. U. Ysai, Y. Y. Lai, L. K. Lui, H. C. Chang, J. H. Chen, *Polyhedron* **1993**, *12*, 731.

[235] M. Veith, H. Lange, O. Recktenwald, W. Frank, *J. Organomet. Chem.* **1985**, *294*, 273.

[236] L. V. Interrante, G. A. Sigel, M. Garbauskas, C. Hejna, G. A. Slack, *Inorg. Chem.* **1989**, *28*, 252.

[237] F. C. Sauls, L. V. Interrante, Z. Jiang, *Inorg. Chem.* **1990**, *29*, 2989.

[238] K. Ouzounis, H. Riffel, H. Hess, U. Kohler, J. Weidlein, *Z. Anorg. Allg. Chem.* **1983**, *504*, 67.

[239] H. Jacobs, K. Jaenichen, C. Hadenfeldt, R. Juza, *Z. Anorg. Allg. Chem.* **1985**, *531*, 125.

[240] D. Rutherford, D. A. Atwood, *J. Am. Chem. Soc.* **1996**, *118*, 11535.

[241] D. A. Atwood, D. Rutherford, *Organometallics* **1996**, *15*, 436.

[242] J. S. Silverman, C. J. Carmalt, D. A. Neumayer, A. H. Cowley, B. G. McBurnett, A. Decken, *Polyhedron* **1998**, *17*, 977.

[243] M. Niemeyer, P. P. Power, *Organometallics* **1995**, *14*, 5488.

[244] J. Pauls, B. Neumuller, *Z. Anorg. Allg. Chem.* **2001**, *627*, 583.

[245] T. Mole, E. A. Jeffrey, *Organoaluminium Compounds*, Elsevier, Amsterdam, **1972**.

[246] S. Hashimoto, Y. Kitagawa, S. Iemura, H. Yamamoto, H. Nozaki, *Tetrahedron Lett.* **1976**, *30*, 2615.

[247] E. Negishi, *J. Organomet. Chem. Libr.* **1976**, *1*, 93.

[248] J. J. Eisch, *Comprehensive Organometallic Chemistry*, Pergamon Press, Oxford, **1982**.

[249] C. J. Upton, P. Beak, *J. Org. Chem.* **1975**, *40*, 1094.

[250] M. Uchiyama, H. Naka, Y. Matsumoto, T. Ohwada, *J. Am. Chem. Soc.* **2004**, *126*, 10527.

[251] D. J. Gallagher, P. Beak, *J. Am. Chem. Soc.* **1991**, *113*, 7984.

[252] P. Beak, T. J. Musick, C. W. Chen, *J. Am. Chem. Soc.* **1988**, *110*, 3538.

[253] D. Nobuto, M. Uchiyama, *J. Org. Chem.* **2008**, *73*, 1117.

[254] W. Clegg, S. H. Dale, A. M. Drummond, E. Hevia, G. W. Honeyman, R. E. Mulvey, *J. Am. Chem. Soc.* **2006**, *128*, 7434.

[255] D. R. Armstrong, W. Clegg, S. H. Dale, E. Hevia, L. M. Hogg, G. W. Honeyman, R. E. Mulvey, *Angew. Chem. Int. Ed.* **2006**, *45*, 3775.

[256] M. Uchiyama, Y. Matsumoto, D. Nobuto, T. Furuyama, K. Yamaguchi, K. Morokuma, *J. Am. Chem. Soc.* **2006**, *126*, 8748.

[257] J. Garcia-Alvarez, D. V. Graham, A. R. Kennedy, R. E. Mulvey, S. Weatherstone, *Chem. Commun.* **2006**, 3208.

[258] J. Garcia-Alvarez, E. Hevia, A. R. Kennedy, J. Klett, R. E. Mulvey, *Chem. Commun.* **2007**, 2402.

[259] R. E. Mulvey, *Dalton Trans.* **2013**, *42*, 6676.

[260] A. Maercker, *Angew. Chem. Int. Ed.* **1987**, *26*, 972.

[261] W. Uhl, K.-W. Klinkhammer, M. Layh, V. Massa, *Chem. Ber.* **1991**, *124*, 279.

[262] B. Conway, E. Hevia, J. Garcia-Alvarez, D. V. Graham, A. R. Kennedy, R. E. Mulvey, *Chem. Commun.* **2007**, 5241.

[263] G. Boche, J. C. W. Lohrenz, A. Opel, A.-M. Sapse, P. v. R. Schleyer, *Lithium Chemistry*, John Wiley & Sons, New York, **1995**.

[264] R. N. Bordwell, R. Vanler, X. Zhang, *J. Am. Chem. Soc.* **1991**, *113*, 9856.

[265] S. V. Kessar, P. Singh, *Chem. Rev.* **1997**, *97*, 721.

[266] D. Seyferth, M. A. Weiner, *J. Org. Chem.* **1959**, *24*, 1395.

[267] D. J. Peterson, *J. Organomet. Chem.* **1970**, *21*, 63.

[268] D. J. Peterson, *J. Am. Chem. Soc.* **1971**, *93*, 4027.

[269] X. Tian, M. Woski, C. Lustig, T. Pape, R. Frohlich, D. Le Van, K. Bergander, N. W. Mitzel, *Organometallics* **2005**, *24*, 82.

[270] F. H. Kohler, N. Hertkorn, J. Blumel, *Chem. Ber.* **1987**, *120*, 2081.

[271] S. Harder, M. Lutz, *Organometallics* **1994**, *13*, 5173.

[272] A. Hildebrand, P. Lonnecke, L. Silaghi-Dumitrescu, I. Silaghi-Dumitrescu, E. Hey-Hawkins, *Dalton Trans.* **2006**, 967.

[273] B. Conway, A. R. Kennedy, R. E. Mulvey, S. D. Robertson, J. Garcia-Alvarez, *Angew. Chem. Int. Ed.* **2010**, *49*, 3182.

[274] C. L. Kissel, B. Rickborn, *J. Org. Chem.* **1972**, *37*, 2060.

[275] M. W. Rathke, R. Kow, *J. Am. Chem. Soc.* **1972**, *94*, 6854.

[276] R. A. Olofson, C. M. Dougherty, *J. Am. Chem. Soc.* **1973**, *95*, 581.

[277] R. A. Olofson, C. M. Dougherty, *J. Am. Chem. Soc.* **1973**, *95*, 582.

[278] M. Campbell, V. Snieckus, *Encyclopedia of Reagents for Organic Synthesis*, Wiley, Chichester, **1995**.

Chapter 2: Reactivity of *bis*-TMP Base

2.1 Introduction

The active base of most alkali-metal-mediated deprotonations is the anion of 2,2,6,6-tetramethylpiperidine, TMP (**Figure 2.1**), and it communicates through the bonds it forms with the different metal centres.

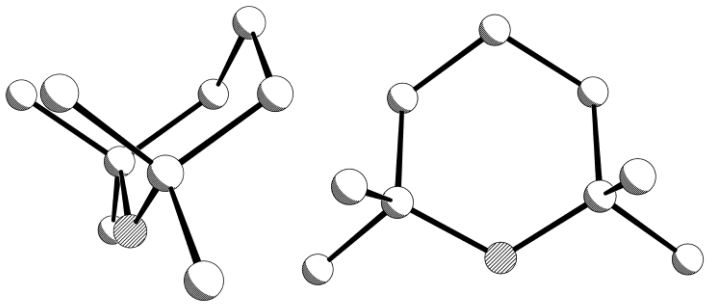

Figure 2.1: A side on (left) and front on (right) representation of the chair-shaped TMP anion showing how its anionic nitrogen (shaded) is sterically protected.

Four flanking methyl groups provide steric protection for its N reactive centre which, since it bonds only to saturated sp^3-C atoms, retains most of the negative charge associated with its anionic status. This combination of steric and electronic features gives TMP its key synthetically exploitable qualities of low nucleophilicity and high Brønsted basicity. In the vast majority of its synthetic applications, TMP has been dispensed in the form of its lithium derivative LiTMP.[1–7] What is evident, especially from the rapidly growing literature on heterometallic systems, is that the reactivity profile of TMP is profoundly sensitive to the form in which it is dispensed. Multi-component systems containing TMP can have markedly different reactivity profiles. Each component in the system (e.g., alkali-metal, softer metal, supporting anions, neutral solvent ligands) to a smaller or larger extent, can influence reactivity and selectivity and therefore must be taken explicitly into consideration along with the usual discriminatory experimental factors (such as stoichiometry, solubility, bulk solvent, concentration and temperature) when rationalising a reaction involving TMP. O'Shea recently provided a pertinent example observing that the Schlosser-Lochmann superbase *n*BuLi-KO*t*Bu executed *ortho*-metallation of OMOM-substituted/activated toluenes but changed to selective benzylic metallation on introducing stoichiometric or

catalytic quantitities of TMP(H)[8] (implying a metal or more likely a mixed-metal TMP species, not identified by the authors, is essential for the selectivity switch). Uchiyama has shown that the aluminate base [Li(TMP)Al(*i*Bu)$_3$] utilised in THF solution (**Figure 2.2** shows the molecular structure of THF solvate crystallised from hexane) incorporating one TMP anion is an effective *ortho*-aluminator deprotonating many functionalised aromatic and heteroaromatic substrates.[9–11] Our own group have demonstrated that by incorporating an additional TMP anion into this motif or more accurately into the reaction mixture that it crystallised from, a remarkable effect is observed on the reactivity, such that attached donors such as TMEDA[12] or anions such as TMP[13] itself (potassium analogue) can be deprotonated intramolecularly.

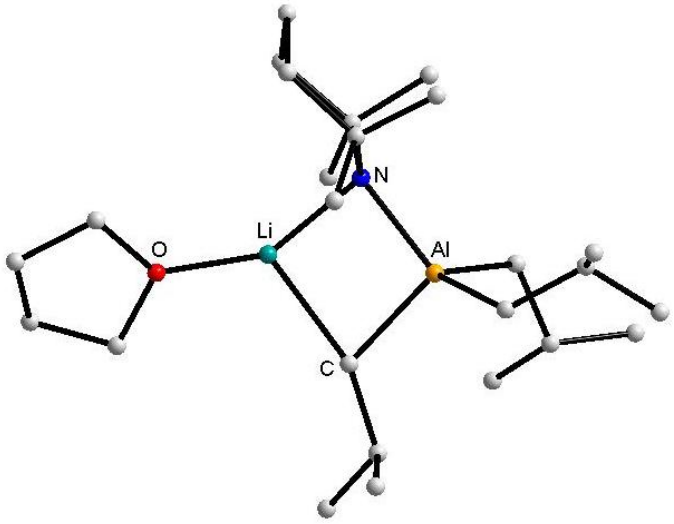

Figure 2.2: Molecular structure of the THF solvate of Uchiyama's base [Li(TMP)Al(*i*Bu)$_3$].

Towards gaining a greater understanding of alkali-metal-mediated alumination (AMM*Al*), this chapter documents a detailed investigation of the reactivity of this new aforementioned *in situ* generated *bis*-alkyl *bis*-amido aluminium base "[(THF)Li(TMP)$_2$Al(*i*Bu)$_2$]" **1.1** towards a variety of substituted aromatic substrates resulting in a series of extensively characterised mixed-metal complexes of general formula [THF·Li(μ-TMP)(μ-R)Al(*i*Bu)$_2$] (where R is the deprotonated substrate) and the products of such metallated intermediates upon electrophilic quenching with elemental iodine. Adding to the knowledge already acquired on AMM*Al*, we provide some theoretical and mechanistic insight into some of the potential reasons why ligand/metal choice is so fundamentally important in these intriguing heterometallic systems.

2.2 Results and Discussion

The new dialkyl-diamido aluminium base was synthesised by mixing the commercially available reagents *n*BuLi, TMP(H) and *i*Bu_2AlCl (*n*BuLi and *i*Bu_2AlCl were purchased from Sigma Aldrich and TMP(H) from Merck) in hexane producing soluble *i*Bu_2Al(TMP) and insoluble LiCl which was filtered through Celite and glass wool. A hexane solution of LiTMP was prepared from *n*BuLi and TMP(H) and cannulated into the solution of *i*Bu_2Al(TMP). Finally, one molar equivalent of THF was added to form the new base empirically formulated as "[(THF)Li$(TMP)_2$Al(*i*$Bu)_2$]" **1.1**. Several attempts were made to crystallise the base but all that could be gleaned from the reaction mixture was an orange/brown oil. **Figure 2.3** shows the ^{1}H NMR spectrum of this oil highlighting the resonances associated with THF, *i*Bu and TMP.

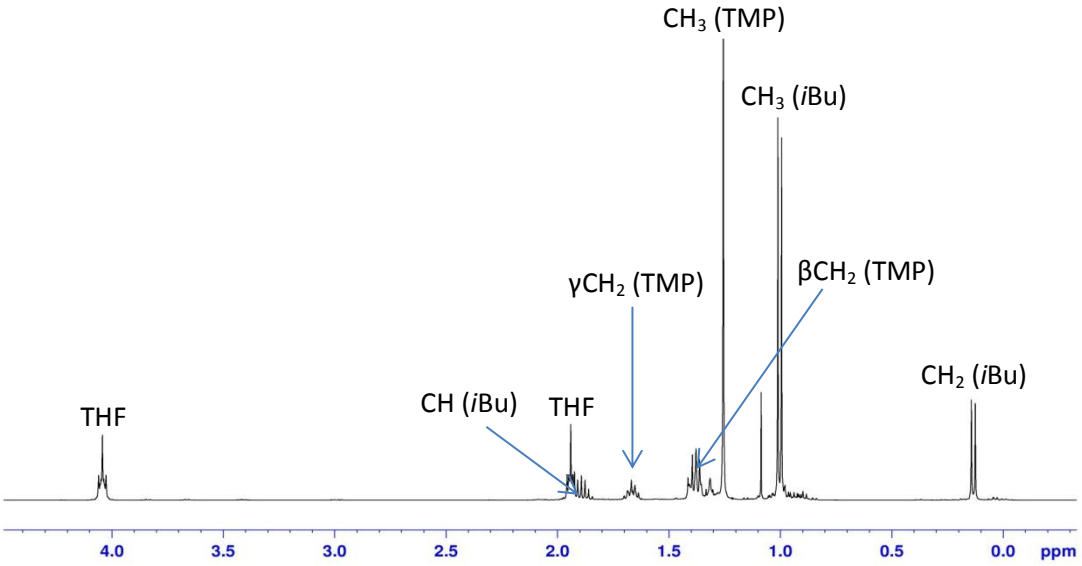

Figure 2.3: ^{1}H NMR spectrum of new *bis*-alkyl *bis*-TMP aluminium base [(THF)Li$(TMP)_2$Al(*i*$Bu)_2$] **1.1** in C_6D_6 solution.

The ability of **1.1** to effect the room temperature deprotonation of some representative functionalised aromatic molecules according to the reactions in **Scheme 2.1** was probed. Specifically, anisole, 1,3-dimethoxybenzene, 1-methoxynaphthalene and *N*,*N*-diisopropylbenzamide were chosen as representative substituted aromatic substrates for this task.

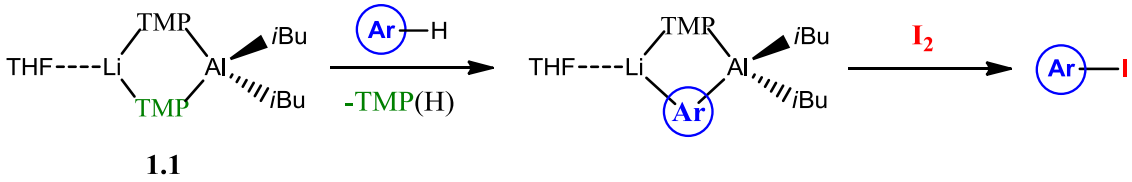

1.1

Scheme 2.1: Deprotonation of aromatic substrates by **1.1** and iodine quenching.

Given that Uchiyama[11] and Knochel[14] have previously observed that Al/Li bases prefer deprotonative metallation over metal halogen exchange, 2-iodoanisole was also considered in this study. The outcomes of these reactions were monitored by both the identification of the crystalline intermediates and also the identification of their subsequent metal-free organic products obtained via electrophilic quenching with iodine. In each case, the site of alumination was shown to be *ortho* to the functional group (for 1,3-dimethoxybenzene, the metallation occurred at the site mutually *ortho* to both OMe groups). As anticipated, the base **1.1** tolerated the carboxamide functionality of *N*,*N*-diisopropylbenzamide and the iodo functionality of 2-iodoanisole. Such *ortho*-deprotonations have taken place via directed *ortho*-metallation (D*o*M), that is the heteroatomic functional group can play a dual role by both acidifying the *ortho*-proton inductively and providing a lone pair of electrons on which to anchor the incoming metal. Of key importance in these reactions is that they were all achieved in non-polar hexane solution at room temperature, obviating the need for more expensive more dangerous (e.g. ethers can form explosive peroxides) polar solvents or non-ambient temperature regimes which are generally required for homometallic, organolithium based D*o*M applications. The crystalline products could be isolated in decent yields (44-71%) but in fact the metallation was nearly quantitative as shown by electrophilic quenching (*vide infra*).

While mixed-metal bases have routinely been employed to deprotonate a plethora of organic substrates, the identity of the metal which actually displaces the proton is often assumed since usually the metallated intermediate is not in itself characterised but rather used *in situ* and quenched with an electrophile. Although this assumption is not necessarily untrue, the solid state structures of complexes **1.2** [(THF)Li(μ-TMP)(μ-C_6H_4OMe)Al(*i*Bu)$_2$], **1.3** [(THF)Li(μ-TMP)(μ-C_6H_3{OMe}$_2$)Al(*i*Bu)$_2$], **1.4** [(THF)Li(μ-TMP)(μ-$C_{10}H_6$OMe)Al(*i*Bu)$_2$], **1.5** [(THF)Li(μ-TMP)(μ-C_6H_4C(=O)N*i*Pr$_2$)Al(*i*Bu)$_2$] and **1.6** [(THF)Li(μ-TMP){μ-(1-OMe)C_6H_3(6-I)}Al(*i*Bu)$_2$] (**Figure 2.4**) unambiguously

confirm in these cases that it is *direct alumination* of the substrate that is occurring. However, the presence of lithium is of paramount importance since the parent homometallic reagent, *i*Bu_2Al(TMP) does not deprotonate the substrates by itself [in confirmation of this, each aromatic substrate with *i*Bu_2Al(TMP) in C_6D_{12} solution was found not to react by ^{1}H NMR spectroscopy after two hours at room temperature followed by one hour at 70^{o}C] and thus these alumination reactions can be considered synergic in origin, operating via Li···Al communication through a TMP bridge.

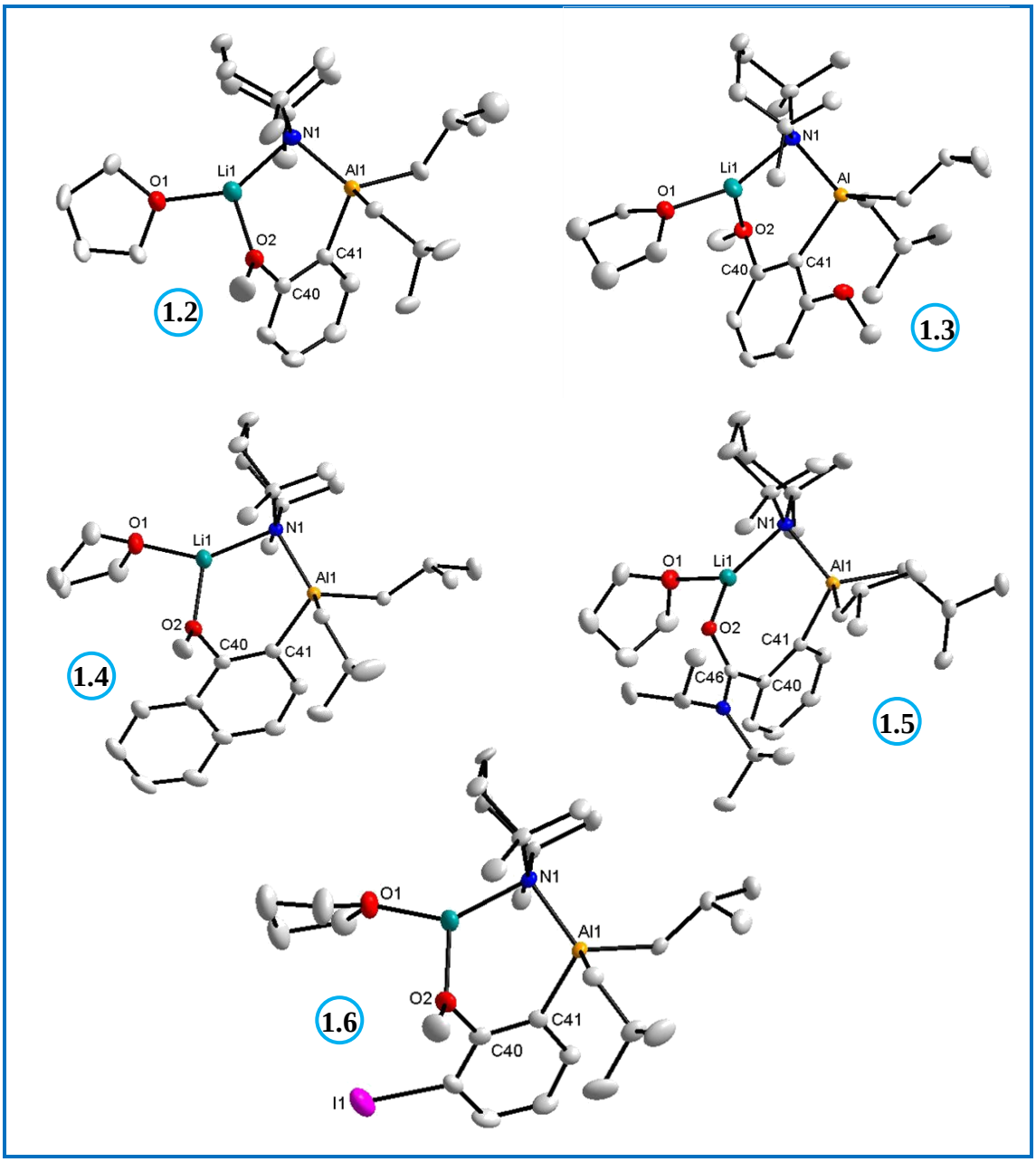

Figure 2.4: Molecular structures of complexes **1.2-1.6** with thermal ellipsoids displayed at the 50% probability level. Hydrogen atoms and any minor disorder components are omitted for clarity.

The molecular structures of complexes **1.2-1.6** share many features: for example they are all bimetallic (Li/Al) molecular contacted ion-pair arrangements incorporating two *i*Bu groups terminal on aluminum, a TMP ligand bridge (with the substituted piperidide ring leaning towards lithium in the chair formation), a bridging C-H deprotonated aromatic molecule and one molecule of THF solvating the lithium. This motif results in a distorted tetrahedral (C_3N) aluminum centre, and a trigonal planar lithium centre. The substrate has clearly been aluminated *ortho* to the functional group, with the heteroatom donating via its lone pair of electrons to the electropositive lithium resulting in a six-membered $LiNAlC_2O$ ring (or, in the case of carboxamide **1.5**, a seven-membered $LiNAlC_3O$ ring). That notwithstanding, the gross features of these structures are unspectacular and require no further discussion (see **Table 2.1** for pertinent bond parameters). The spread of corresponding bond lengths is very small for example, Al1-C41 ranges from 2.047 to 2.088Å and Al1-N1 ranges from 1.974 to 1.985Å for compounds **1.2-1.6**. Multinuclear NMR data confirm that these structures maintain their integrity in the solution state (see ^{1}H NMR spectrum of **1.2** in **Figure 2.5**), while purity of the bulk sample was evidenced via satisfactory elemental analyses.

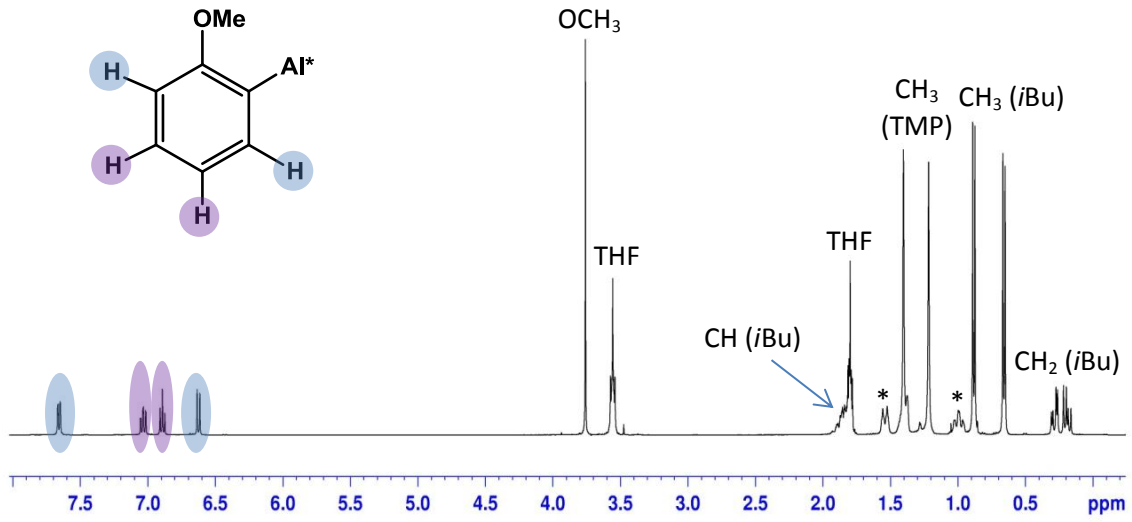

Figure 2.5: ^{1}H NMR spectrum of aluminated anisole product **1.2** in C_6D_{12} solution highlighting resonances consistent with the four remaining aromatic protons (βCH_2 and γCH_2 protons of TMP are marked with a *).

Table 2.1: Selected bond parameters of complexes **1.2-1.6** (in Å and °)

	1.2	1.3	1.4	1.5	1.6
Al1-N1	1.981(1)	1.985(1)	1.975(1)	1.985(1)	1.974(3)
N1-Li1	2.036(3)	2.032(3)	2.039(2)	2.064(2)	2.015(6)
Li1-O1	1.929(3)	1.940(2)	1.943(2)	1.941(2)	1.906(7)
Li1-O2	1.922(3)	1.991(4)	1.909(2)	1.905(2)	1.904(6)
O2-C40	1.415(2)	1.409(2)	1.422(1)	-	1.402(4)
O2-C46	-	-	-	1.250(1)	-
C46-C40	-	-	-	1.500(1)	-
C40-C41	1.391(2)	1.394(2)	1.367(2)	1.418(1)	1.384(4)
C41-Al1	2.049(1)	2.082(2)	2.057(1)	2.088(1)	2.047(3)
O1-Li1-O2	103.5(1)	102.5(1)	99.8(1)	102.8(1)	102.0(3)
O1-Li1-N1	142.7(1)	145.1(1)	142.5(1)	133.4(1)	140.2(3)
N1-Li1-O2	113.8(1)	112.3(1)	117.6(1)	121.4(1)	117.7(3)
Li1-N1-Al1	97.1(1)	88.9(1)	98.7(1)	87.7(1)	98.7(2)

Of course, while a crystallographic determination gives a clear snapshot of the salient metal containing intermediates, it may not be correct to assume the structure determined is representative of the bulk solution. Consequently, the reactions were repeated and the *in situ* generated intermediates **1.2-1.6** were subjected to elemental iodine as the electrophilic quenching agent to give **1.7** (2-iodoanisole), **1.8** (2-iodo-1,3-dimethoxybenzene), **1.9** (2-iodo-1-methoxynaphthalene), **1.10** (2-iodo-*N*,*N*-diisopropyl benzamide) and **1.11** (2,6-diiodoanisole) in good to excellent (70-96%) yield (**Table 2.2**). The iodinated products were purified via column chromatography to give the final products whose identities were confirmed by ^{1}H NMR spectroscopy[10] (see ^{1}H NMR spectrum of purified iodinated anisole **1.7** in **Figure 2.6**).

Table 2.2: Substrates and products upon electrophilic quenching of aluminated aromatic intermediates with iodine. [a] The identity of iodinated products was confirmed by comparison of their ^{1}H NMR spectra with those published previously by Uchiyama.[9]

Entry	1	2	3	4	5
Substrate	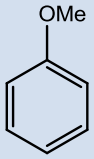	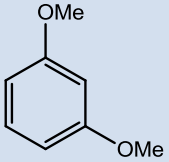	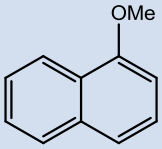	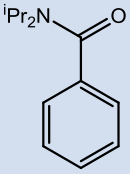	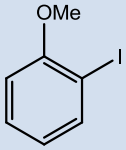
Product	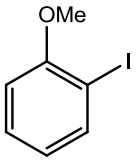	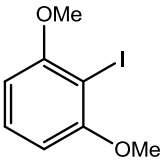	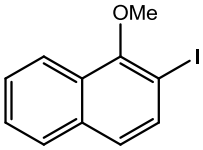	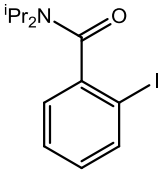	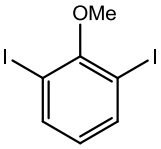
Yield (%)	77	81	70	88	96

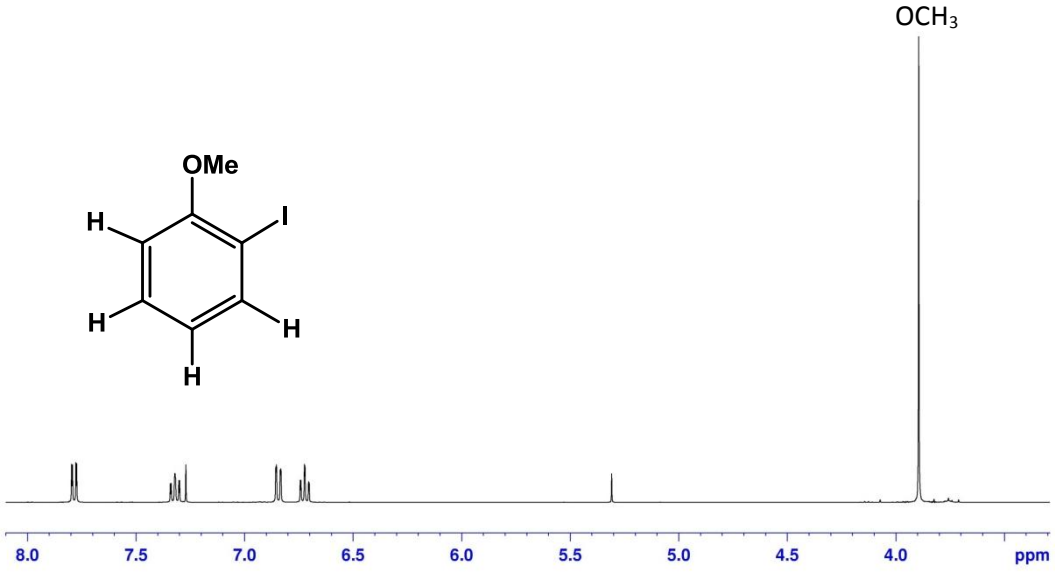

Figure 2.6: ^{1}H NMR spectrum in $CDCl_3$ solution of purified iodinated anisole compound **1.7**.

Although these reactions, both at the metallic intermediate stage and electrophilic quenching stage, have been well defined structurally, the structure of the active base **1.1** remains elusive. However a clue is provided by a closely related system. The *in situ* generation and reaction with two molar equivalents of diisopropylamine [*i*Pr$_2$NH, DA(H)] yields the diisopropylamide derivative THF·Li(μ-DA)$_2$Al(*i*Bu)$_2$ (**1.12**),

produced in a crystalline yield of 55%. The molecular structure of **1.12** (**Figure 2.7**) shows that the electron rich amide groups occupy the bridging positions between the two metals, with the alkyl groups residing in the terminal positions on aluminium. A search of the literature did not uncover any examples of related lithium aluminium DA complexes. A related aluminium DA dimer compound with terminal hydrogen atoms $[H_2Al(DA)_2AlH_2]$[15] has very similar Al-N bond distances of 1.964(8) and 1.968(8)Å when compared to **1.12** [1.935(1) and 1.936(1)Å].

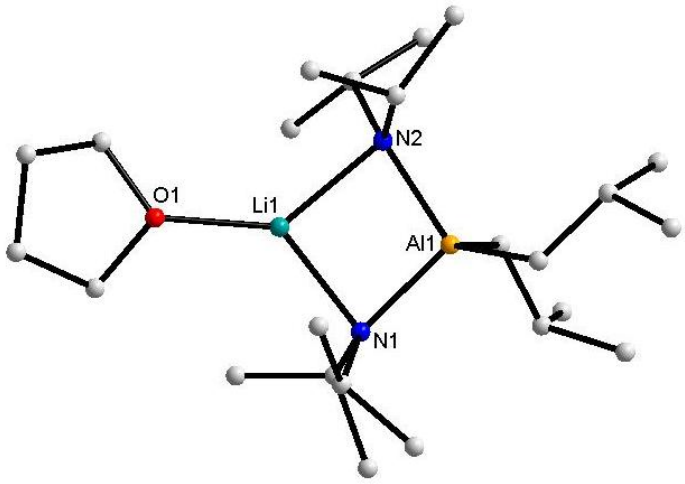

Figure 2.7: Molecular structure of complex **1.12** with thermal ellipsoids displayed at 50% probability level. Hydrogen atoms are omitted for clarity. Selected bond parameters (in Å and °): Al1-N1 1.935(1), Al1-N2 1.936(1), Li1-N1 2.075(3), Li1-N2 2.086(3), Li1-O1 1.969(3); N1-Al1-N2 100.67(5), Al1-N1-Li1 84.10(8), Al1-N2-Li1 83.78(8), N1-Li1-N2 91.45(10), N1-Li1-O1 132.8(1), N2-Li1-O1 135.7(1).

The ^{1}H NMR spectrum of **1.12** in **Figure 2.8** shows that the compound retains its strucural integrity in solution.

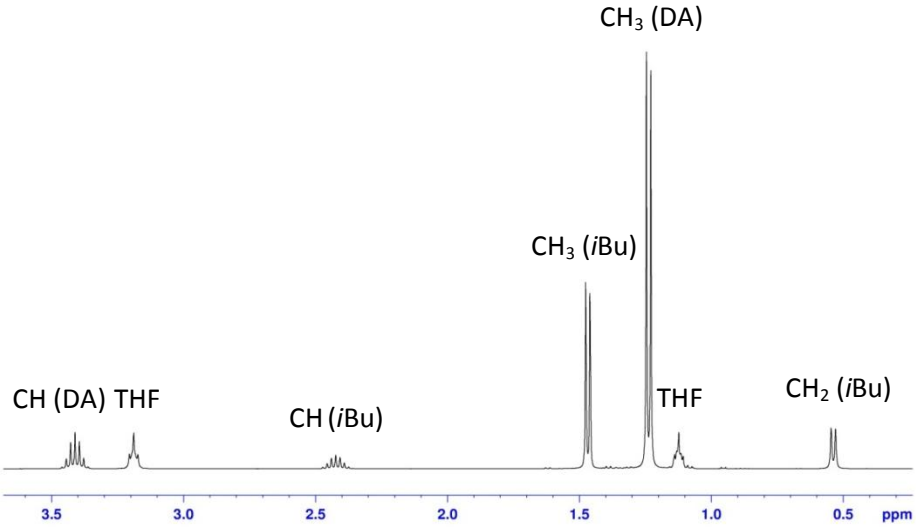

Figure 2.8: ^{1}H NMR spectrum of DA aluminium base **1.12** $[(THF)Li(DA)_2Al(iBu)_2]$ in C_6D_6 solution.

2.2.1 Theoretical and Mechanistic Examination of AMM*Al*

On considering the preceding results in the field of Alkali-Metal-Mediated Alumination (*vide supra*) an important question is worth asking: why can the THF solvated *bis*-DA *bis*-alkyl lithium aluminate complex **1.12** be isolated and crystallographically characterised, yet its TMP analogue (**1.1**) remains only a putative intermediate? Therefore what is its structure? To try and find a possible answer we next carried out a series of density functional theory (DFT) calculations, which coupled with other experimental observations, allow us to propose a potential rationale for the witnessed reactivity described in the preceding section.

DFT calculations were performed using the Gaussian 03 package with geometry optimisation using the B3LYP density functionals[16–18] and the 6-311(*d*,*p*) basis set[19,20] with a frequency analysis being performed after each geometry optimization. The energy values quoted include the zero point energy contribution. We investigated the relative energies of three potential structural manifestations of **1.1**, that is with the bridging positions occupied by either (**a**) both TMP anions, (**b**) both *i*Bu anions or (**c**) a mixture of one TMP and one *i*Bu anion (**1.1a-1.1c**, **Figure 2.9**).

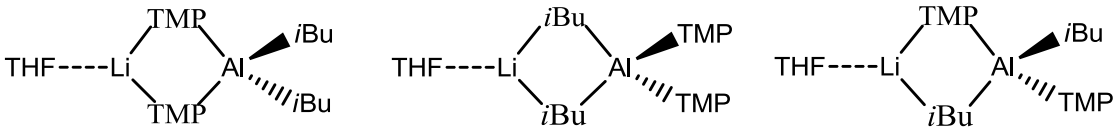

1.1a **1.1b** **1.1c**

Figure 2.9: modelled structures of complex **1.1** studied via DFT calculations.

Hypothetical mixed bridge complex **1.1c** was also studied for two alternative conformations, namely with the bridging TMP group having its γ-C apex pointing towards the Al (**1.1c'**) or towards the Li centre (**1.1c''**). Unsurprisingly, given that complexes **1.2-1.6** all have terminal *i*Bu groups, complex **1.1a** is the most energetically favourable by 14.75, 4.85 and 10.06 kcal mol^{-1} compared to **1.1b** **1.1c'** and **1.1c''** respectively. However, perhaps surprisingly, this study also reveals that the product is energetically unfavourable with respect to the homometallic starting materials of which it is composed (a combination of THF solvated and unsolvated starting materials were computed – **Equations 1a-1c**). That is all three reactions appear endothermic.

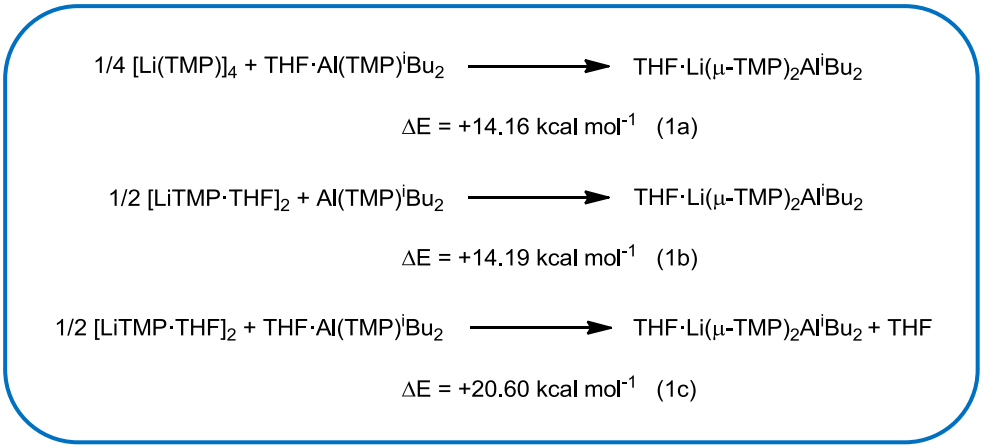

The inability to isolate a stable compound of composition **1.1** is perhaps attributable to the steric protection of the nitrogen atom in the TMP being too much to allow the necessary $AlN_{TMP}LiN_{TMP}$ closed ring to form since clearly, as the molecular structure of **1.12** shows, an AlNLiN ring can be obtained with a slightly less bulky secondary amide. This is further supported by our comparative study of homometallic iBu_2AlNR_2 (NR_2 = DMP, *cis*-2,6-dimethylpiperidide **1.13 Figure 2.10**; TMP **1.14**) which were prepared by mixing an equimolar amount of iBu_2AlCl with the appropriate $LiNR_2$ in hexane solution.

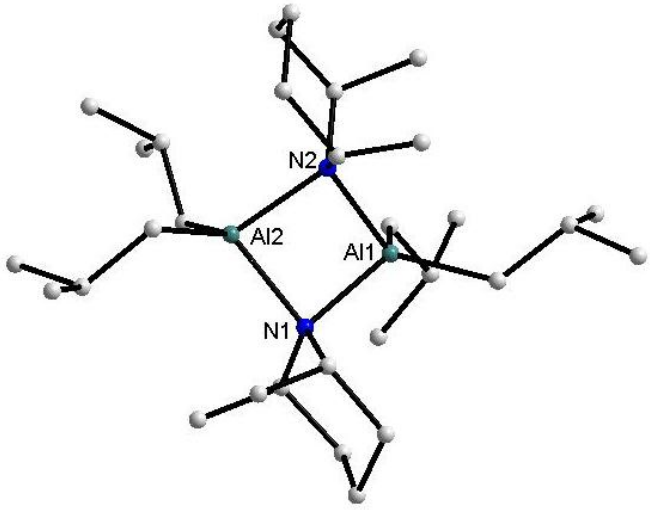

Figure 2.10: Molecular structure of complex **1.13** with thermal ellipsoids displayed at 50% probability level. Hydrogen atoms are omitted for clarity. Selected bond parameters (in Å and °): Al1-N1 2.009(2), Al1-N2 2.021(2), Al2-N1 2.020(2), Al2-N2 2.003(2); N1-Al1-N2 86.34(8), N1-Al2-N2 86.51(8), Al1-N1-Al2 87.76(8), Al1-N2-Al2 87.89(8).

DMP has only 2 of TMP's 4 methyl substituents so its anionic N centre is significantly less sterically protected.[21] In these homometallic reactions after filtering the mixture to

remove LiCl, the product was obtained in excellent yield as a crystalline solid (**1.13**) or yellow oil (**1.14**). Ascertained through a single crystal X-ray diffraction study, the molecular structure of **1.13** exists as a cyclodimer with the alkyl groups in the terminal positions and the DMP ligands bridging the two trivalent metal atoms.

Since the molecular structure of the oily complex **1.14** could not be determined, we turned to a DOSY NMR study in an attempt to gain further information on the aggregation of these two species in solution. Using this NMR technique, different components present in solution can be separated according to their diffusion coefficients which can be linked to their molecular weights.

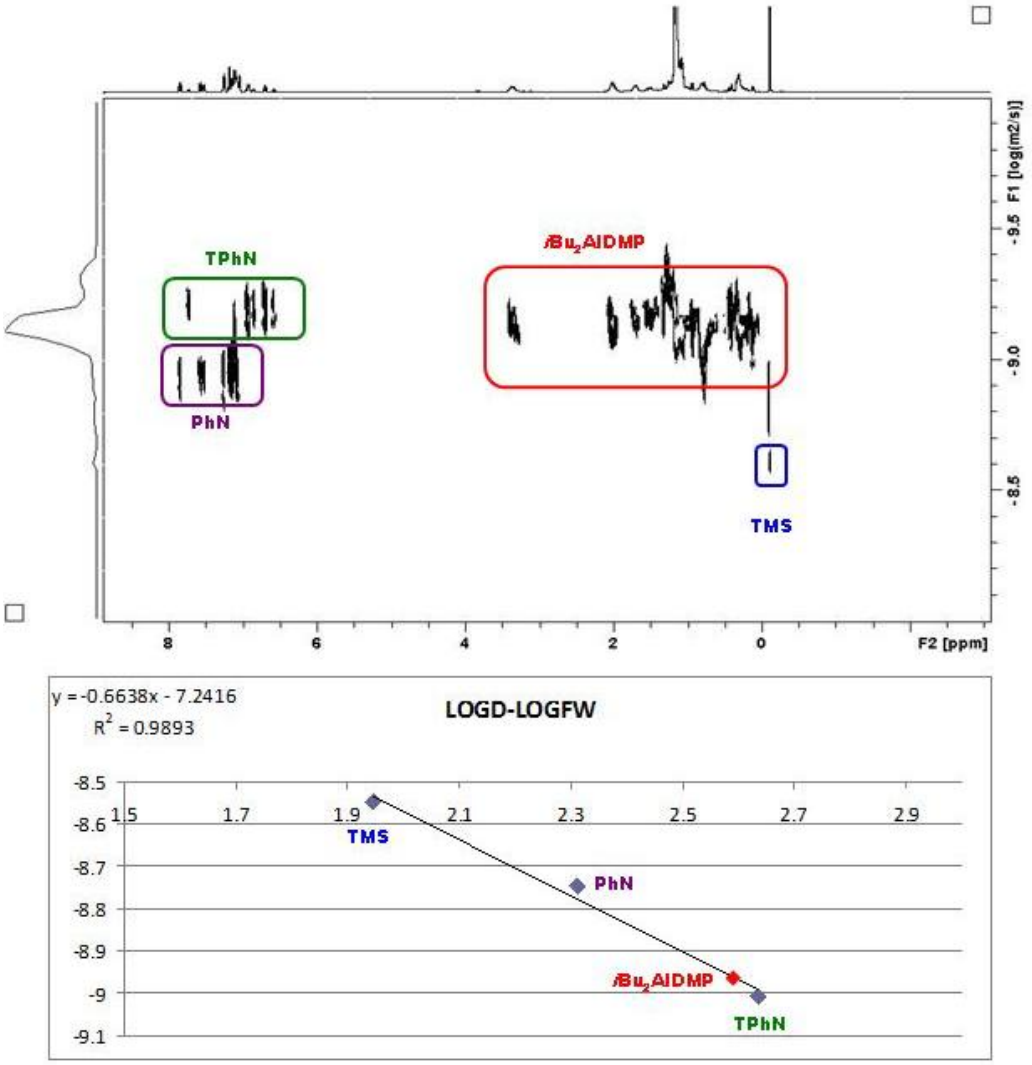

Figure 2.11: (top) ^{1}H DOSY NMR spectrum of *i*Bu$_2$Al(DMP) (**1.13**), TPhN, PhN and TMS at 25 °C in C_6D_6 solution and (bottom) log *D* – log FW representation from the ^{1}H DOSY data obtained for the mixture of *i*Bu$_2$Al(DMP) (**1.13**), TPhN, PhN and TMS at 25 °C in C_6D_6 solution.

Such component(s) can then have their molecular weights estimated provided inert samples of known molecular weight are also present in the solution for calibration purposes since the log of molecular weight can be linearly correlated to log *D* (diffusion coefficient). The ^{1}H DOSY NMR spectra and plots of log *D* – log FW for compounds **1.13** and **1.14** are shown in **Figures 2.11** and **2.12** respectively.

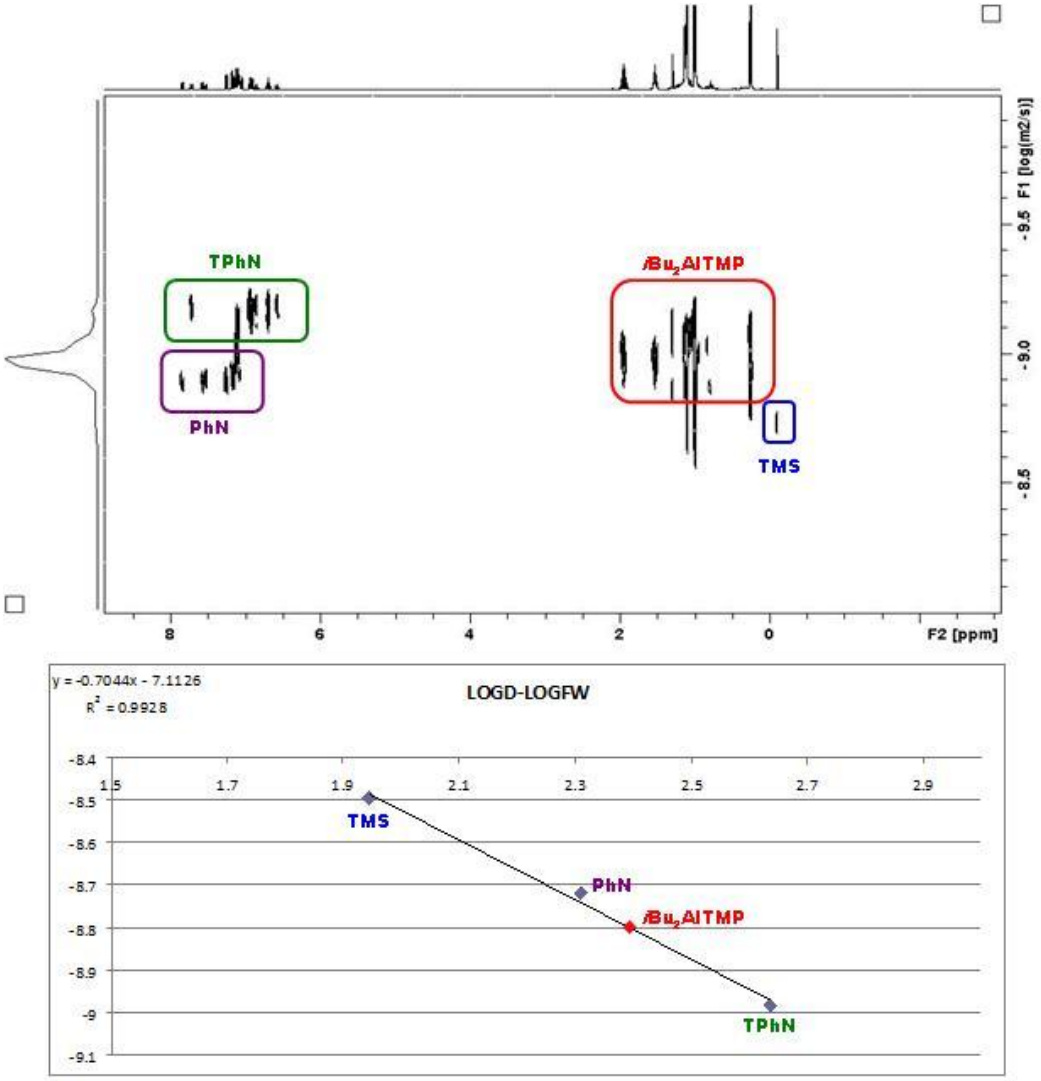

Figure 2.12: (top) ^{1}H DOSY NMR spectrum of *i*Bu$_2$Al(TMP) (**1.14**), TPhN, PhN and TMS at 25 °C in C_6D_6 solution and (bottom) log *D* – log FW representation from the ^{1}H DOSY data obtained for the mixture of *i*Bu$_2$Al(TMP) (**1.14**), TPhN, PhN and TMS at 25 °C in C_6D_6 solution.

The results gave a predicted molecular weight (MW_{DOSY}) of 395 and 243 g mol^{-1} for **1.13** and **1.14** respectively. Clearly, **1.13** seems to have a higher solution molecular weight than **1.14** despite having a smaller empirical molecular weight. The value of MW_{DOSY} for **1.13** is intermediate between that of monomeric *i*Bu$_2$Al(DMP) and dimeric

[*i*Bu$_2$Al(DMP)]$_2$ [253 and 507 g mol^{-1} respectively] and is therefore consistent with a monomer-dimer equilibrium. The corresponding value for **1.14** is within 13% error of the molecular weight for a monomeric species (MW = 281 g) and as it is on the lower side of the predicted value it is likely to exist as a monomer in arene solution.

We appear to have located a point at which steric bulk around the anion will prevent dimerisation from taking place. Indeed, the Al_2N_2 ring of **1.13** is extremely strained, as evidenced by the movement of the ring away from planarity. For comparison, a search of the Cambridge Crystallographic database[22] for dialkylamidoaluminum structures which have dimerised through their amido ligands reveals 124 positive matches. While the N-Al-N angles [86.34(8) and 86.51(8)^o] of **1.13** are consistent with those previously reported [mean = 86.63^o, median = 87.56^o], the Al-N-Al angles [87.76(8) and 87.89(8)^o] are considerably tighter than expected [mean = 91.91^o, median = 91.82^o], resulting in a butterfly motif [hinge angle = 36.23(6)^o]. Likewise, the Al-N bond lengths are relatively long, coming in the range 2.003(2)-2.021(2)Å (average 2.013Å) when compared with those reported in the literature [1.883-2.045Å, with a mean value of 1.974Å and a median value of 1.977Å]. Clearly, the presence of two additional methyl groups (that is by substituting DMP by TMP) close to the bridging point is sufficient to inhibit dimerisation. The inability of **1.14** to dimerize is consistent with the accomplished work of Nöth who has crystallographically characterised a variety of solvated and unsolvated TMP containing aluminum complexes of general formula (TMP)$_2$AlX (X includes halides,[23] phosphides,[24,25] amides,[24] alkoxides,[24] thiolates[24] and borazinyl[26]) which are primarily monomeric. Of the dimers known, such as the fluoride [(TMP)$_2$AlF]$_2$ or the chloride [(TMP)AlCl(OEt)]$_2$,[23] none dimerise through TMP bridges. Dimeric species with a dianionic [(CH$_2$)$^{2-}$ or (PPh)$^{2-}$][25,27] bridge or trimeric species with a N=N=N or C≡N bridge have also been reported.[28] Nöth established that the hydride [(TMP)AlH$_2$]$_3$ is a trimer with hydride bridges while [(DMP)AlH$_2$]$_2$ is a dimer with DMP bridges.[29]

It is pertinent to note that thus far there have been no reported examples of a LiN_{TMP}LiN_{TMP} closed ring in the literature containing a four coordinate lithium centre. While such a ring can be formed, each lithium cation is only monosolvated (trigonal planar {THFLiTMP}$_2$ **1.15a**),[7] while an attempt to use a bidentate donor (namely TMEDA) resulted in an open, hemisolvated dinuclear structure ({LiTMP}$_2$TMEDA

1.15b – **Figure 2.13**) with a mixture of two and three coordinate lithium centres.[5] TMEDA solvated Li(DMP) forms a central four membered ring but TMEDA binds in a unidentate fashion, bridging between adjacent Li_2N_2 rings to give a polymeric motif.[30]

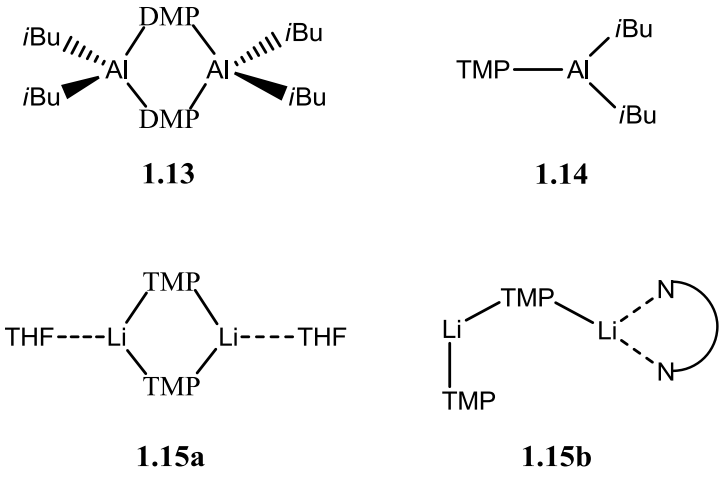

Figure 2.13: known solid state structures of some pertinent DMP/TMP complexes (**1.13**, **1.15a**, **1.15b**) and the proposed structure of **1.14** as predicted from DOSY NMR spectroscopy.

Since bridging Al-N(amide) bonds are shorter than bridging Li-N(amide) bonds (see **Table 2.1**), coupled with the fact that a $[LiN_{TMP}]_2$ ring cannot be formed with four-coordinate lithium for presumably steric reasons, it is unlikely that the $Li\text{-}N_{TMP}\text{-}Al\text{-}N_{TMP}$ ring is obtainable and any species with the empirical formula of **1.1** should therefore exist in an open form. This suggestion is further supported by the change from dimeric (four-coordinate Al) to monomeric (three-coordinate Al) on slightly increasing the amide bulk from DMP to TMP in the homometallic complexes **1.13** and **1.14** (*vide supra*).

With this increasing body of indirect evidence supporting an open structure, we are now in a position to propose a hypothetical mechanism for the deprotonation of the NCH_3 unit of TMEDA to yield complex **1.16** (**Scheme 2.2**),[12] the proposed open intermediate brings the TMEDA molecule into partial proximity allowing one of its α-Me groups to be deprotonated by the reactive *pseudo*-terminal TMP anion. Formation of a more stable five membered $[AlN_{TMP}LiNC]$ ring would provide a driving force for the reaction.

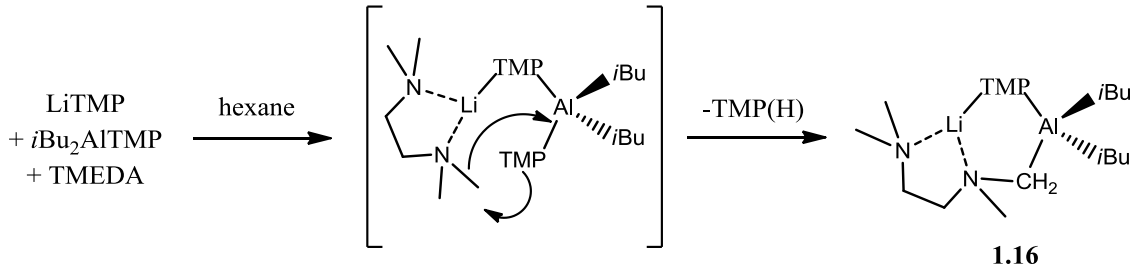

1.16

Scheme 2.2: Proposed mechanism for deprotonation of coordinated TMEDA via an open structure to afford heterotrianionic complex **1.16**.

This accumulated evidence allows us to propose a plausible hypothesis to answer our question: the combined bulk of two TMP molecules with their tetrasubstituted α-carbon atoms is just sufficient to prevent the formation of a stable four-membered ring; whereas with less bulky *i*Bu or N*i*Pr$_2$ groups such a ring is feasible in either [Li(TMP)Al(*i*Bu)$_3$] or **1.12**. It is this open structure, with a '*pseudo*-terminal' TMP ligand, which may confer increased reactivity on heterometallic bases of this type, consequently leading to the deprotonation of other donor molecules at relatively non-acidic sites normally considered resistant towards deprotonative metallation.

2.2.2 Unconventional Alumination Reactions

2.2.2.1 *m*-Tolunitrile

In a previous study by our group of nitriles with a sodium zincate base some interesting structural motifs were observed. For example, when reacted with the base [(TMEDA)Na(μ-TMP)(μ-*t*Bu)Zn(*t*Bu)], *m*-tolunitrile, trimethylacetonitrile and 1-cyanonaphthalene all produced unusual structures, two of which were solvent separated ion-pair arrangements (**Figure 2.14**).[31]

Returning to the work of this project *m*-tolunitrile, an important molecular building block in biomedicinal chemistry,[32] was studied with base **1.1** to establish if it was possible to move away from the normal aforementioned *ortho*-aluminated closed ring motifs observed in compounds **1.2-1.6** and to determine if regioselectivity would be an issue due to the possibility of competing addition across the nitrile triple bond. To explore this, *m*-tolunitrile was added to base **1.1** in a 1:1 stoichiometry in hexane solution, which instantly produced a bright orange/red solution with a small amount of precipitate. Approximately 5 mL of THF was added to dissolve the solid though this

caused the solution to turn dark brown. The solution was then allowed to stand overnight after which large yellow crystals grew on the side wall of the Schlenk flask.

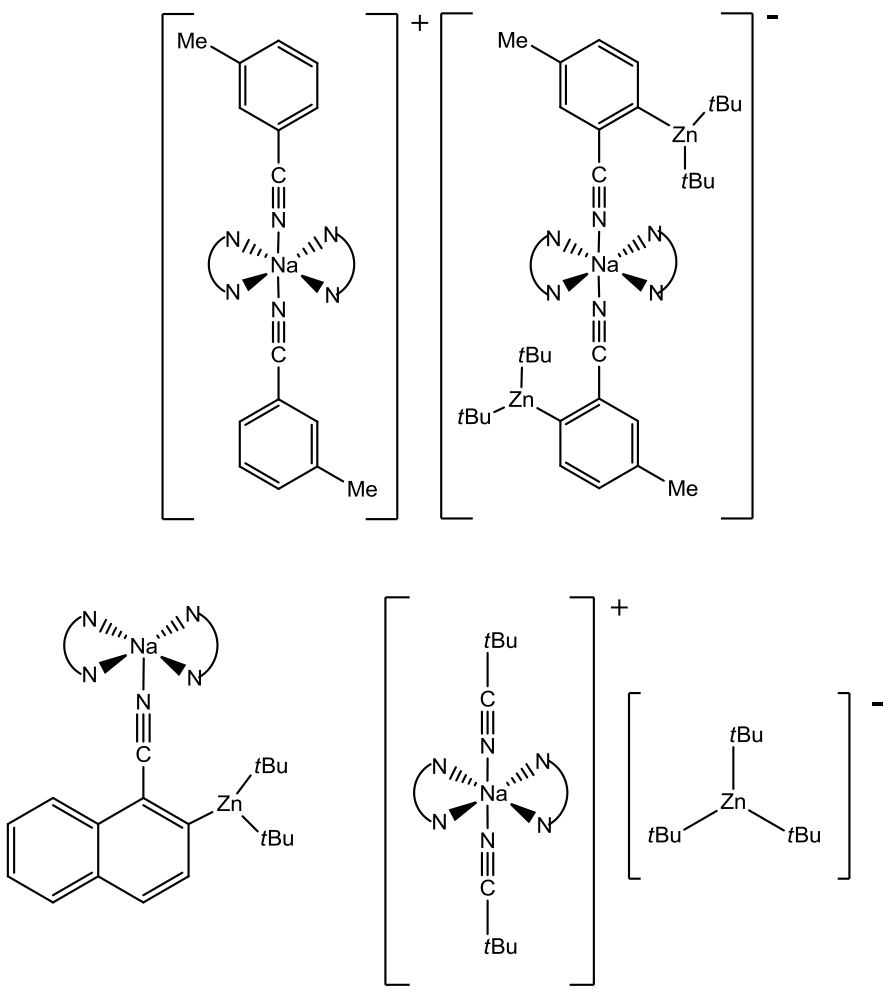

Figure 2.14: Novel metallo-nitrile structures obtained from the reaction between [(TMEDA)Na(μ-TMP)(μ-*t*Bu)Zn(*t*Bu)] and *m*-tolunitrile (top), trimethylacetonitrile (bottom right) and 1-cyanonaphthalene (bottom left).

X-ray crystallographic analysis of these crystals revealed them to be an open *ortho*-aluminated *m*-tolunitrile-derived complex with a terminal TMP anion having the formula $[(THF)_3Li\{(N{\equiv}C)C_6H_3(Me)\}Al(iBu)_2(TMP)]$ **1.17** (**Figure 2.15**). Owing to the high reactivity of **1.1** with *m*-tolunitrile a good reproducible yield could not be obtained as the reaction mixture would decompose over time even when transferred to the freezer after addition of *m*-tolunitrile.

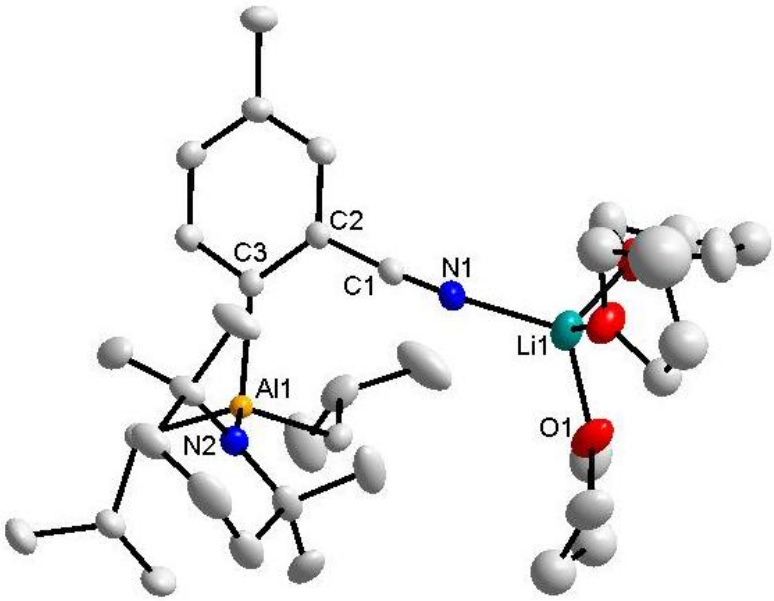

Figure 2.15: Open motif structure of $[(THF)_3Li\{(N{\equiv}C)C_6H_3(Me)Al(iBu)_2(TMP)]$ **1.17** with selective atom labelling. Hydrogen atoms are omitted for clarity. Selected bond lengths [Å] and bond angles [°]: Li1-O1, 1.945(5); Li1-N1, 2.021(4); Al1-C3, 2.0691(19); Al1-N2, 1.9022(18); Al1-C(*i*Bu), 2.026(8); Al1-C(*i*Bu), 2.020(5); C(*i*Bu)-Al1-C(*i*Bu), 110.42(9); C(*i*Bu)-Al1-N2, 109.38(8); N2-Al1-C(*i*Bu), 119.66(8); C(*i*Bu)-Al1-C3, 98.34(8); C(*i*Bu)-Al1-C3, 105.78(8); C3-Al1-N2, 112.07(8); N1-Li1-O1, 105.8(2); Li1-N1-C1, 174.9(2).

This structural motif differs quite markedly from previously described compounds **1.2-1.6** as three donor THF molecules solvate Li with the only bridging communication between Li and Al being an *ortho*-aluminated *m*-tolunitrile molecule deprotonated adjacent to the electron-withdrawing nitrile substituent. This regioselectivity is in accord with the stronger directing ability of C≡N versus the electron donating Me. This is in contrast to **1.3** where *ortho*-alumination occurred directly between both OMe groups. The most distinctive structural features of **1.17** are the Li-N1-C1 bond angle which approaches linearity at 174.9(2)° and the lack of contact between TMP and Li as it forms an open structural motif with a terminal TMP anion. As expected, the terminal Al-N(TMP) bond [1.9022(18)Å] is shorter than the bridging Al-N(TMP) bonds in aluminates **1.2-1.6** (e.g. **1.2** [1.9807(12)Å] and **1.3** [1.9853(13)Å]) reflecting the higher coordination number of the bridging TMP ligand. The Li atom in **1.17** adopts a distorted tetrahedral geometry due to solvation by three Lewis donor THF molecules which is in contrast to the distorted trigonal planar geometry observed for Li in complexes **1.2-1.6**. A common feature between **1.17** and the nitrile zincate structures discussed above is

that in each case Li binds to the nitrile N atom and *ortho*-metallation occurs exclusively without any addition product. A possible explanation for the observed open motif could come from the orientation of the lone pair on the nitrile N atom which in coordinating to the Li atom keeps it well away from the TMP ligand (the non-bonding distance between Li1 and N2 is 5.849Å). Compound **1.17** is the first example of a terminal TMP aluminate so future work should focus on examining the reactivity of this terminal TMP anion. An interesting question to ask is "as the bridging communication between Li and Al has been broken on one side, will this enable the terminal TMP anion to become active towards subsequent deprotonations?"

The ^{1}H NMR spectrum of **1.17** in C_6D_{12} solution (**Figure 2.16**) shows the expected two doublets at 7.02 and 7.99 ppm and a singlet at 7.04 ppm corresponding to the remaining aromatic protons (see insert showing enlarged region of spectrum) confirming *ortho*-alumination. The remainder of the ^{1}H NMR spectrum is consistent with the crystal structure and confirms that it retains its structural integrity in solution. The two signals for the α and β protons of THF (1.85 and 3.79 ppm) shows an increase in integration due to the presence of two extra THF molecules solvating lithium (this is in comparison to ^{1}H NMR spectrum of aluminated anisole compound **1.2** in **Figure 2.5** with only one THF ligand).

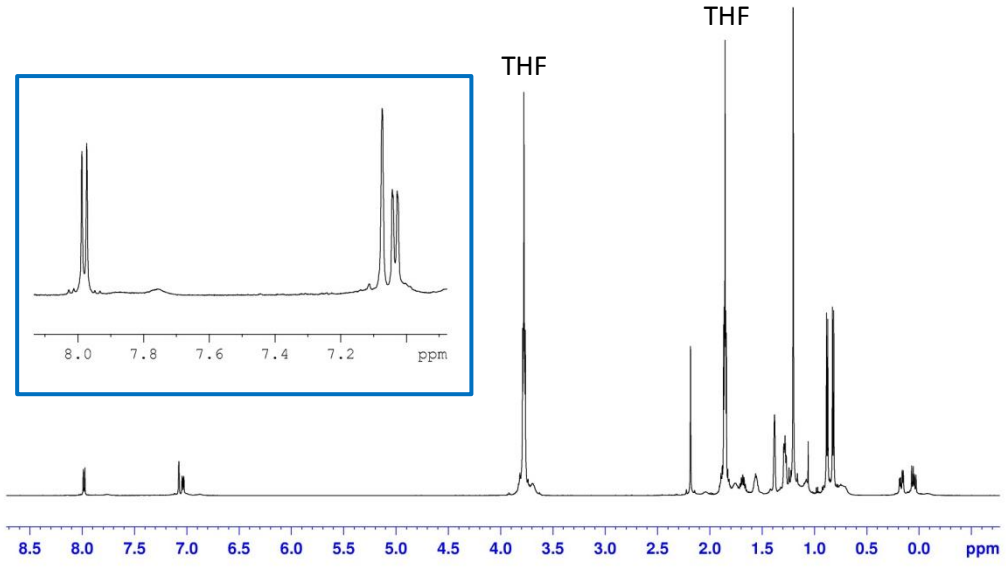

Figure 2.16: ^{1}H NMR spectrum of *ortho*-aluminated *m*-tolunitrile compound **1.17** in C_6D_{12} solution.

Uchiyama has deprotonated the parent unsubstituted nitrile benzonitrile, PhC≡N, utilising [Li(TMP)Al(*i*Bu)$_3$] as the aluminium base. Note, however, that this was achieved at low temperature (-78^{o}C) and after 2 hours was quenched with iodine to give 100% of the iodinated product (two equivalents of the base were employed meaning that the actual yield was 50%).[10] Deprotonation of other aromatic substrates could be achieved at room temperature or 0^{o}C highlighting the high reactivity of nitriles with the aluminium base and the need to supress this reactivity by cooling the reaction mixture. Future work should include repeating this reaction at low temperature to try and supress decomposition in order to isolate the compound. A search of the CCDB confirms that **1.17** is the first crystallographically elucidated example of *ortho*-alumination of *m*-toluntrile with the only other example of *ortho*-metallation being the *ortho*-zincated example described above. The isolation of **1.17** demonstrates the need to isolate reactive intermediates as any electrophilic quenching of the *in situ* solution would have masked this novel structure and not allowed us to gain more valuable information about the pathways involved in TMP aluminate chemistry.

2.2.2.2 *N,N*-dimethylbenzylamine

In addition to *ortho*-metallation of aromatic substrates there are several examples by our group where the regioselectivity can been directed away from the *ortho*- (*N,N*-dimethylaniline)[33] or even the benzylic-position (toluene)[34] to the *meta*-position. In reality however, these systems are a lot less straightforward than a simple *meta*-metallation with the *N,N*-dimethylaniline reaction showing evidence of *ortho*- and *para*-isomers as well as *meta*-isomers in solution.[35] Additionally, treatment of the sodium zincate base [(TMEDA)Na(TMP)(*t*Bu)Zn(*t*Bu)] with trifluoromethyl benzene results in a complex mixture of products at room temperature, namely the *ortho*-, *meta*- and *para*-metallated isomers.[36] As all reported compounds thus far feature *ortho*-alumination of the aromatic substrate it was decided that a good candidate to probe the possibility of *meta*-alumination would be the investigation of aromatic amines. *N,N*-dimethylbenzylamine was selected as a suitable substrate for this purpose and was added to base **1.1** in a 1:1 stoichiometry in hexane solution. As base **1.1** did not react with *N,N*-dimethylbenzylamine at room temperature, as evidenced by a ^{1}H NMR spectrum of the reaction filtrate, the reaction solution was heated to reflux for two hours. The solution was left in the refrigerator at 0^{o}C for several weeks eventually

affording colourless crystals. However, due to the poor quality of these crystals an X-ray crystallographic analysis could not be conducted, but the ^{1}H NMR spectrum (**Figure 2.17**) of the crystals in C_6D_6 solution clearly shows deprotonation has occurred regioselectively at the *meta*-position as evidenced by the singlet at 8.06 ppm (compound **1.18**).

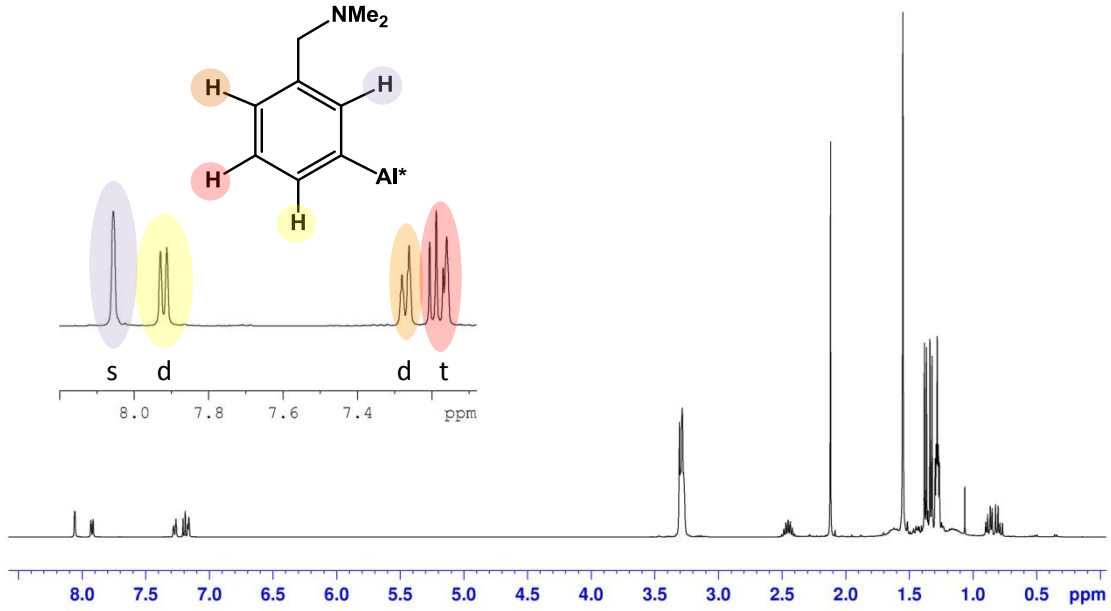

Figure 2.17: ^{1}H NMR spectrum of **1.18** in C_6D_6 solution.

To elaborate, the singlet corresponds to the single non-coupled hydrogen atom situated between Al and the CH_2NMe_2 substituent. Even though no crystal structure has been obtained thus far we can state with certainty that the deprotonation has occurred at the *meta*-position as this is the only deprotonation that would produce a singlet in the ^{1}H NMR spectrum. It is worth pointing out at this stage that although a *meta*-deprotonation is observed in the ^{1}H NMR spectrum of the crystals, a ^{1}H NMR spectrum of the reaction filtrate remains for future work as a consequence of the poor reproducibility of the reaction, so we therefore cannot rule out the possibility of other regio-isomers being present in the solution.

Due to the lack of structural information the exact arrangement of the deprotonated *N*,*N*-dimethylbenzylamine in the structure can only be postulated. Aluminate **1.18** could adopt one of two possible geometries, namely where the N atom of the NMe_2 group coordinates to Li or one where it remains uncoordinated and pointing away from Li (**Figure 2.18**). It is more likely that Li will not coordinate to the Me_2N substituent as

this would form a strained 8-atom $LiNAlC_4N$ ring as shown. A more probable structure is one containing a 4-atom LiNAlC ring, something commonly observed in lithium aluminates such as Uchiyama's THF solvated base [Li(TMP)Al(*i*Bu)$_3$] and **1.12**, with the NMe_2 group pointing away from Li. This structural motif is observed in [(TMEDA)Na(μ-TMP)(μ-{NMe_2}C_6H_4)Zn(*t*Bu)] discussed above.[33]

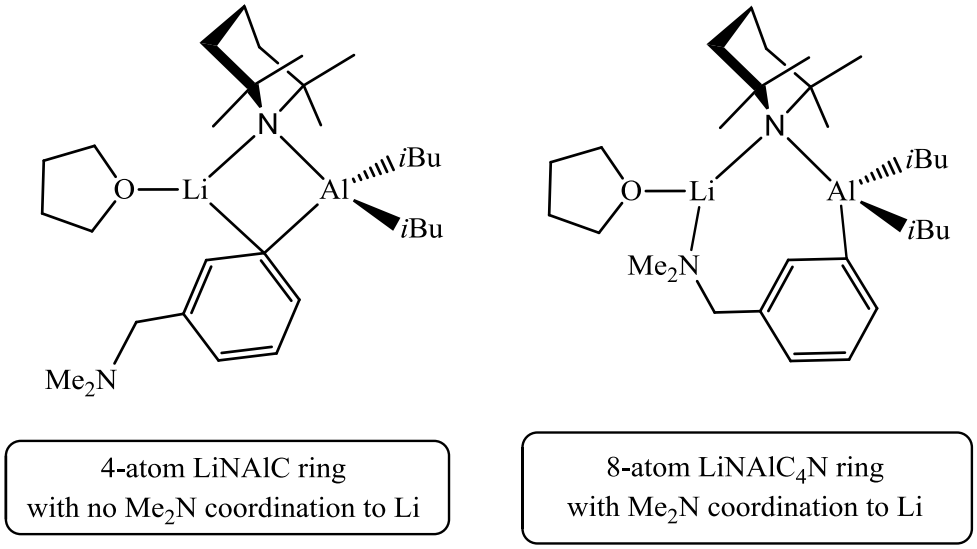

Figure 2.18: Possible structural motifs of the *meta*-aluminated *N*,*N*-dimethylbenzylamine aluminate **1.18**.

It was surprising to find that *N*,*N*-dimethylbenzylamine would become deprotonated preferentially at the *meta*-position as several literature examples show that *ortho*-deprotonation is the common hydrogen abstraction pathway.[37] Organolithum reagents such as *n*BuLi invariably coordinate to the N atom allowing an orientation towards the *ortho*-position via a coordinative proximity effect as described by the basic principles within D*o*M. A simple explanation for the observed *meta*-selectivity in aromatic amines such as *N*,*N*-dimethylaniline and *N*,*N*-dimethylbenzylamine is probably due to the N atom being a less attractive donor for the alkali-metal and also in the latter case since it is a remote amine (the Me_2N function is separated from the aromatic ring by a CH_2 spacer). The inductive effect on the *ortho* C-H bond is not strong. As described previously in this chapter the first step in directed *ortho*-alumination of aromatic substrates is thought to be coordination of the substrate to the alkali-metal prior to deprotonation, if coordination is less favourable then this opens up the possibility of regioselectively deprotonating sites other than *ortho*. This can be exemplified by the reaction of the sodium TMP-zincate [(TMEDA)Na(TMP)(*t*Bu)Zn(*t*Bu)] with the related

oxygen containing substrate benzyl methyl ether. As oxygen is a far better Lewis base donor than nitrogen, coordination of the oxygen atom to sodium results in the position of zincation being directed to the *ortho*-position.[38] Zincation at the *meta*-position would have resulted in a strained 8-atom ring which would be highly unfavourable. Future work should focus on obtaining the crystal structure of this intriguing product and establishing if any other regio-isomers are present in solution. At present this is the only evidence of the direct *meta*-metallation of *N*,*N*-dimethylbenzylamine with no structural examples present in the CCDB.

2.2.2.3 Ferrocene

Deprotonation of metallocene compounds (notably the most popular example of this type, ferrocene) is of particular importance as the metallated intermediates once functionalised provide a vast array of ring-substituted derivatives that are useful across different areas of science and medicine.[39] Organolithium reagents are generally used for this purpose with mono-lithiated ferrocene obtained via deprotonation with *t*BuLi in THF.[40,41] Even di-lithiated ferrocenes can be obtained using two molar equivalents of the alkyllithium base in the presence of TMEDA.[42] Our group have reported the potential to obtain a higher metallation efficiency using a sodium-magnesium base [NaMg{N*i*Pr$_2$}$_3$] to give polymetallated metallocenes (of the group 8 triad ferrocene, ruthenocene and osmocene) of general formula [{M(C$_5$H$_3$)$_2$}Na$_4$ Mg$_4$(N*i*Pr$_2$)$_8$] (where M = Fe, Ru, Os) where the metallocene has lost a total of four hydrogen atoms and its tetra-anionic derivative is captured within an inverse crown ether structure.[43,44] The TMP anologue of this base [NaMg{TMP}$_3$] has also provided an example of 1,1'-twofold deprotonation of ferrocene producing trinuclear ferrocenophanes.[45] Direct zincation of ferrocene is also achieved producing compounds with two or three deprotonated ferrocenes within the zincate structure.[46] There is obviously the potential for multi-deprotonations with ferrocene hence the next task for AMM*Al* within this project was to establish if it was possible to activate the other attached bases in our *bis*-TMP Al system towards ferrocene.

To investigate this possibility, one molar equivalent of ferrocene was added to base **1.1** in hexane solvent producing an orange coloured solution which was allowed to stir overnight. A crop of orange coloured needle crystals were formed upon leaving the

solution to stand at room temperature. X-ray crystallographic analysis of these crystals revealed them to be a new mono-aluminated ferrocene-derived compound in [(THF)Li($C_5H_4FeC_5H_5$)Al(*i*Bu)$_2$] **1.19**, isolated in a reasonable crystalline yield of 48%. Mimicking the situation with the aromatic substrates **1.2-1.6** discussed above the molecular structure of **1.19** (**Figure 2.19**) shows a single mono-aluminated substrate (ferrocene in this case) captured as the bridging anion between lithium and aluminium. The central planar four-membered ring comprises Li, N, Al and C atoms with Al in its usual distorted tetrahedral environment. The structure is completed in the usual way with two *i*Bu groups on Al, a bridging TMP anion connecting Al to the distorted trigonal planar Li and a Lewis base THF molecule terminally solvating Li.

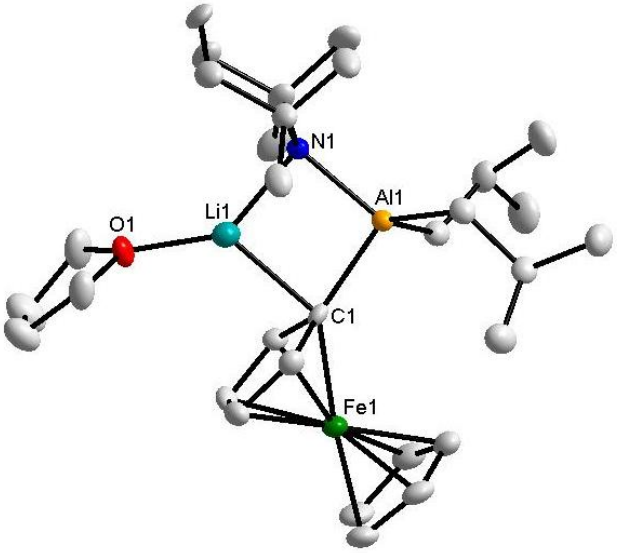

Figure 2.19: Molecular structure of ferrocenylaluminate [(THF)Li(μ-TMP)(μ-$C_{10}H_9Fe$)Al(*i*Bu)$_2$] **1.19** with selective atom labelling. Hydrogen atoms are omitted for clarity. Selected bond lengths [Å] and bond angles [°]: Al1-N1, 1.994(2); Al1-C1, 2.039(3); Al1-C(*i*Bu), 2.018(1); Al1-C(*i*Bu), 2.023 (1); Li1-N1, 2.004(5); Li1-C1, 2.188(5); Li1-O1, 1.866(5); C1-Al-C(*i*Bu), 101.31(12); C1-Al-C(*i*Bu), 117.30(12); N1-Al1-C(*i*Bu), 120.76(11); N1-Al1-C(*i*Bu), 114.99(12); N1-Al1-C1, 96.08(9); C(*i*Bu)-Al1-C(*i*Bu), 105.92(2); N1-Li1-C1, 91.24(19); O1-Li1-N1, 139.20(3); O1-Li1-C1, 129.60(3); Al1-N1-Li1, 45.18(11); Li1-C1-Al1, 46.08(11).

The ^{1}H NMR spectrum of **1.19** (**Figure 2.20**) in C_6D_{12} solution clearly shows a mono-deprotonated ferrocene as three distinct hydrogen resonances at 4.00 ppm, 4.08 ppm and 4.28 ppm in a 1:2:1 integration ratio correspond to the β-protons of the deprotonated C_5H_4 ring, intact C_5H_5 ring and α-protons of the deprotonated C_5H_4 ring respectively.

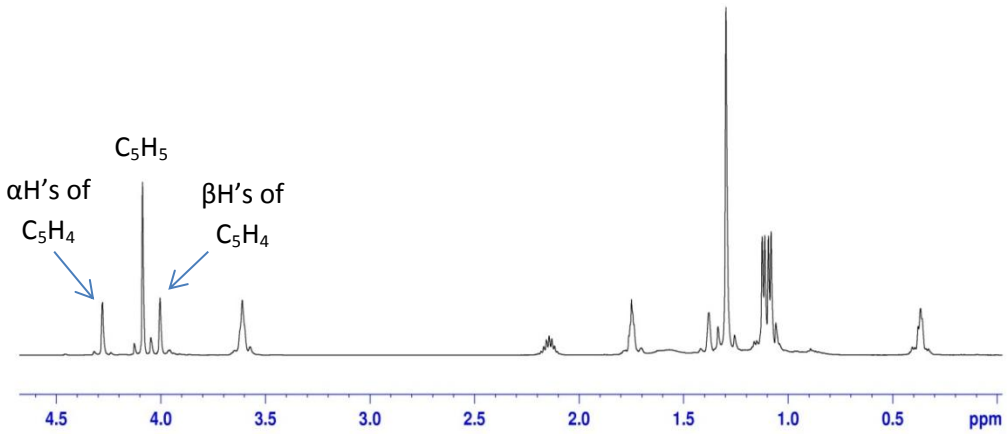

Figure 2.20: ^{1}H NMR spectrum of [(THF)Li(μ-TMP)(μ-$C_5H_4FeC_5H_5$)Al(*i*Bu)$_2$] **1.19** in C_6D_{12} solution.

To explore the possibility of achieving multiple deprotonations of a single ferrocene molecule the reaction was repeated but this time with 0.5 molar equivalents of ferrocene added to **1.1**. As the ^{1}H NMR spectrum of the reaction filtrate after stirring the reaction at room temperature showed a mixture of the mono-aluminated product **1.19** and a new di-aluminated product **1.20**, the reaction mixture was heated to reflux for two hours. Large orange cubic crystals were grown from solution upon cooling to 0^{o}C. An X-ray crystallographic analysis of these crystals showed them to be the di-aluminated ferrocene complex [(THF)$_2$Li$_2$(μ-TMP)$_2$($C_5H_4FeC_5H_4$)Al$_2$(*i*Bu)$_4$] **1.20** (yield = 28%) observed in the filtrate NMR spectrum. The fact that this product was obtained after harsh refluxing conditions highlights the high stability of this lithium-aluminium system.

The salient feature of **1.20** (**Figure 2.21**) is the incorporation of a di-aluminated ferrocene skeleton sandwiched between two Al base units. A single molecule of ferrocene is deprotonated twice, once on the upper and once on the lower Cp ring, by two equivalents of **1.1**. The molecular structure is penta-nuclear consisting of 2 x Li, 2 x Al and 1 x Fe atoms. The two Al units are analogous to the one observed in **1.19** so for brevity no further discussion is warrented.

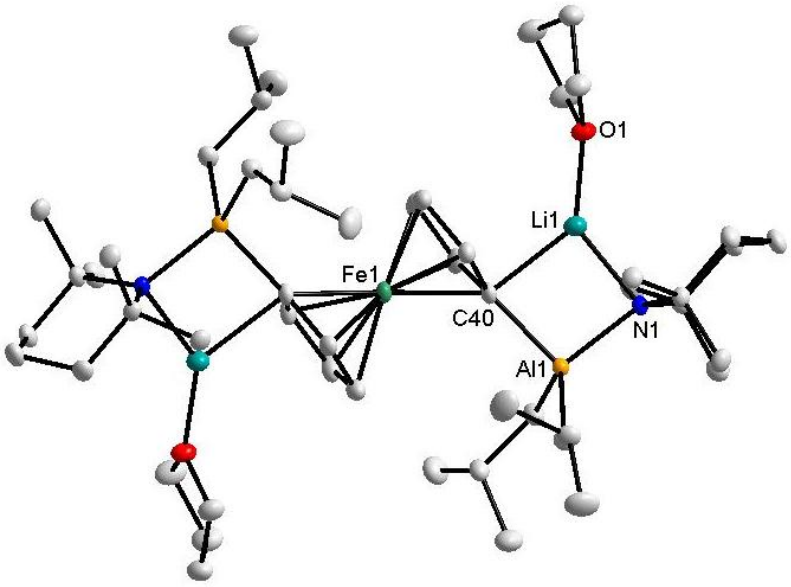

Figure 2.21: Molecular structure of the di-aluminated ferrocene compound $[(THF)_2Li_2(\mu\text{-}TMP)_2(\mu\text{-}C_5H_4FeC_5H_4)Al_2(i\text{Bu})_4]$ **1.20** with selective atom labelling. Hydrogen atoms are omitted for clarity. Selected bond lengths [Å] and bond angles [°]: Al1-N1, 1.9956(10); Al1-C40, 2.0528(13); Li1-N1, 2.033(2); Li1-C40, 2.194(3); Li1-O1, 1.884(2); C40-Al1-C(*i*Bu), 117.17(5); C40-Al1-C(*i*Bu), 104.40(5); N1-Al1-C(*i*Bu), 115.04(5); N1-Al1-C(*i*Bu), 117.81(5); N1-Al1-C40, 97.28(5); Al1-N1-Li1, 88.17(7); C(*i*Bu)-Al1-C(*i*Bu), 104.75(5); O1-Li1-N1, 135.48(13); O1-Li1-C40, 132.65(12); N1-Li1-C40, 91.85(9); Al1-C40-Li1, 82.51(6).

The ^{1}H NMR spectrum of **1.20** (**Figure 2.22**) shows the presence of two distinct resonances at 3.97 ppm and 4.47 ppm corresponding to the α and β hydrogen's of the two deprotonated Cp rings. Only two resonances appear in this metallocene region as both Cp rings are now equivalent.

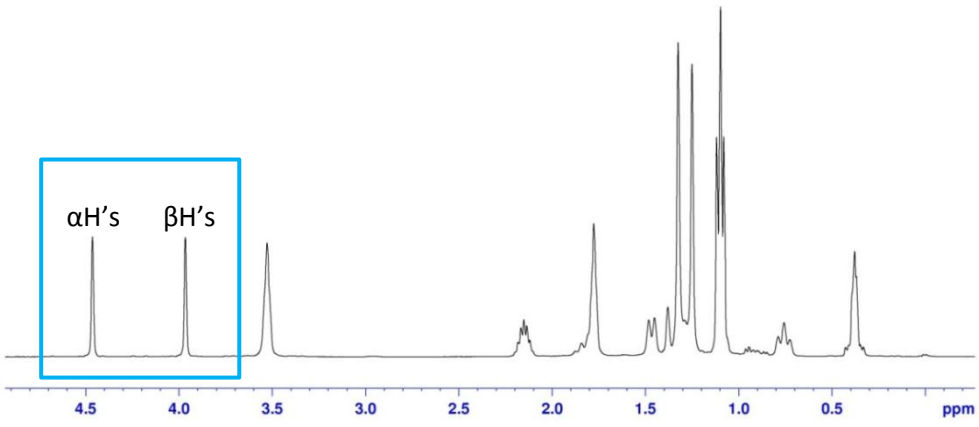

Figure 2.22: ^{1}H NMR spectrum of **1.20** $[(THF)_2Li_2(\mu\text{-}TMP)_2(C_5H_4FeC_5H_4)Al_2(i\text{Bu})_4]$ in C_6D_{12} solution.

The resonance for the β-hydrogen atoms (3.98 ppm) is consistent with that seen for mono-aluminated ferrocene compound **1.19** (4.00 ppm). The resonance for the α-hydrogen atoms (4.46 ppm), on the other hand, is shifted slightly downfield compared to that of **1.19** (4.39 ppm).

The reaction was also attempted using 0.25 molar equivalents of ferrocene to ascertain whether further deprotonation above twofold was possible. However, in this case only **1.20** was crystallised in a lower yield. There are several examples of aluminium ferrocene compounds in the literature. The Al-C(Fc') bonds lengths in the related alkyl-halide compounds $[(\eta\text{-}C_5H_5)Fe(\eta\text{-}C_5H_3)Al_2Me_3Cl]_2$[47] [2.12(3)Å] and $[(\eta^5\text{-}C_5H_5)Fe(\eta^5\text{-}C_5H_4Al_2(Me)_4Cl]$[48] [2.116(8)Å] are in good agreement with those observed in aluminates **1.19** [2.039(3)Å] and **1.20** [2.0528(13)Å].

2.3 Conclusions

The lithium aluminate base $[(THF)Li(TMP)_2Al(i\text{Bu})_2]$ **1.1** shows excellent regio- and chemoselectivity towards *ortho*-alumination of a range of substituted aromatic molecules. Operating at room temperature, this bimetallic but as yet structurally undefined complex directly aluminates (converting C-H bonds to C-Al bonds) the substrate in an efficient manner and is tolerant of sensitive functionality (for example carboxamide and halide functionalities), as proven by the isolation and identification of a series of novel aluminated aryl intermediates. The presence of a second TMP anion in this *bis*-alkyl *bis*-amido base with respect to its more alkyl rich counterpart $[Li(TMP)Al(i\text{Bu})_3]$ clearly plays an important role in reactivity since this seemingly innocent alteration to the composition of the base has previously induced less conventional metallation patterns. DFT calculations, in conjunction with some new observations in the domain of aluminium and lithium alkyl/amide chemistry, have allowed us to propose a potential hypothesis for this increased reactivity. The steric bulk of the TMP anion when considered against less bulky *i*Bu might inhibit formation of a stable four-membered ring, leaving an open intermediate structure with greater reactivity imparted via easier access of the organic substrate possibly involving a *pseudo*-terminal TMP anion. This *pseudo*-terminal TMP having a lower coordination number would be thus more reactive as it would cleave more easily from a single metal than when held in the grip of two metals.

It has also been shown that we can open up the possibility of forming unconventional aluminate structures such as that seen in the cyano-toluene derivative **1.17**. The terminal TMP anion in this structure has the possibility to react further due to the lack of bridging communication so this reaction could provide the first example of a di-deprotonation by the same TMP-aluminate base if studied further. We could also advance this methodology to unconventional metallation patterns given the right choice of substrate such as the *meta*-metallation observed utilising the aromatic amide *N*,*N*-dimethylbenzylamine. Finally, the scope of AMM*Al* has been extended to include the deprotonation of the popular metallocene compound ferrocene with the ability to di-deprotonate this substrate by increasing the number of equivalents of **1.1** employed.

2.4 Future Work

Research following this project should focus on investigating a wider range of aromatic substrates including more electron-rich substrates and those which are poor *ortho*-directors as well as poor coordinating groups. The range of substrates should be exhausted to determine the scope of our *bis*-TMP base **1.1**. Heteroaromatic substrates should also be tested such as benzothiophene, pyridine and indole for comparison. The question to address is "do we get novel structures and any differences in reactivity?"

As nitrile compound **1.17** is the first example of a terminal TMP aluminate, new work should concentrate on examining the reactivity of this terminal TMP anion. Is it possible to deprotonate another aromatic substrate using this aluminated intermediate? The reaction should be repeated at low temperature to try and supress decomposition in order to isolate the compound. Other nitriles including benzonitrile, substituted aryl nitriles and acetonitrile could also be tested to establish if other novel aluminium nitrile compounds can be isolated.

The reaction generating *meta*-aluminated compound **1.18** should be repeated to try and obtain the crystal structure and NMR monitoring should be carried out on the filtrate solution to establish if any other regio-isomers are present in solution.

Looking to the bigger picture, the reactivity of related aluminium bases should be explored including switching to larger alkali-metals such as sodium. How does this affect the reactivity? Additionally how does the reactivity of a tri-TMP base compare?

The reactivity of the related *bis*-DMP *bis*-alkyl base should also be explored to determine any differences in reactivity by moving to a less bulky secondary amine.

The grandest challenge will be to make alkali-metal-mediated alumination catalytic as to date all these reactions have been performed stoichiometrically.

2.5 Experimental

2.5.1 General Experimental

Due to the acute air and moisture sensitivity of the organometallic reagents and products studied in this project, all reactions and manipulations of compounds were performed under a protective argon atmosphere using either standard Schlenk techniques or a glove box. To remove traces of moisture all solvents were dried over Na/benzophenone[49] and freshly distilled prior to use. Anisole, 2-iodoanisole, 1-methoxynapthalene, *m*-tolunitrile, ferrocene, *n*BuLi and *i*Bu_2AlCl were purchased from Aldrich and used as received. 1,3-Dimethoxybenzene, *N*,*N*-diisopropylbenzamide and *cis*-DMP(H) were purchased from Alfa Aesar and used as received. TMP(H) was purchased from Merck and stored over 4Å molecular sieves. *N*,*N*-Dimethylbenzylamine was purchased from Aldrich and distilled over calcium hydride prior to use.

^{1}H and ^{13}C NMR spectra were recorded on a Bruker AV400 MHz spectrometer (operating at 400.03 MHz for ^{1}H and 100.58 MHz for ^{13}C). All ^{13}C NMR spectra were proton decoupled. DOSY experiments were performed on a Bruker AVANCE 400 NMR spectrometer operating at 400.13 MHz for proton resonance under TopSpin (version 2.0, Bruker Biospin, Karlsruhe) and equipped with a BBFO-z-atm probe with actively shielded z-gradient coil capable of delivering a maximum gradient strength of 54 G/cm. Diffusion ordered NMR data were acquired using the Bruker pulse program dstegp3s employing a double stimulated echo with three spoiling gradients. Sine-shaped gradient pulses were used with a duration of 4 ms (P30) together with a diffusion period of 100 ms (D20). Gradient recovery delays of 200 μs followed the application of each gradient pulse. Data were systematically accumulated by linearly varying the diffusion encoding gradients over a range from 2% to 95% for 64 gradient increment values. The signal decay dimension on the pseudo-2D data was generated by Fourier transformation of the time-domain data. DOSY plots were generated by use of the DOSY processing

module of TopSpin. Parameters were optimised empirically to find the best quality of data for presentation purposes. Diffusion coefficients were calculated by fitting intensity data to the Stejskal-Tanner expression with estimates of errors taken from the variability in the calculated diffusion coefficients by consideration of different NMR responses for the same molecules of interest.

Synthesis of [(THF)Li(TMP)$_2$Al(*i*Bu)$_2$] 1.1

Hexane (10 mL) was added to an oven-dried Schlenk tube. Next, 1.6M *n*BuLi (1.25 mL, 2 mmol) was added, followed by TMP(H) (0.34 mL, 2 mmol) at room temperature. The reaction mixture was left to stir for 10 min and then *i*Bu$_2$AlCl (0.38 mL, 2 mmol) was injected into the Schlenk tube, producing a white suspension almost immediately. The reaction was left to stir for 1 hour and was then filtered through Celite and glass wool, which was then washed with more hexane (10 mL). To a separate Schlenk tube containing a solution of freshly prepared LiTMP in hexane (10 mL) [from a mixture of *n*BuLi (1.25 mL, 2 mmol) and TMP(H) (0.34 mL, 2 mmol)], the solution was added through cannula to give a colourless solution. Finally, THF (0.16 mL, 2 mmol) was injected and the reaction mixture was left to stir for 5 mins. Base **1.1** could not be isolated as a solid and was instead used as an *in situ* mixture.

^{1}H NMR data (400.13 MHz, 298 K, C$_6$D$_{12}$)

δ = 0.12 [4H, d, ^3J(H,H) = 6.81 Hz, 2 x CH$_2$ of *i*Bu], 1.10 [12H, d, ^3J(H,H) = 6.49 Hz, 4 x CH$_3$ of *i*Bu], 1.26 [12H, s, 4 x CH$_3$ of TMP], 1.38 [4H, m, 2 x βCH$_2$ of TMP], 1.65 [2H, m, γCH$_2$ of TMP], 1.90 [2H, sept, ^3J(H,H) = 6.60 Hz, 2 x CH of *i*Bu], 1.95 [4H, m, 2 x CH$_2$ of THF], 4.04 ppm [4H, m, 2 x CH$_2$ of THF].

Synthesis of [(THF)Li(μ-TMP)(μ-C$_6$H$_4$OMe)Al(*i*Bu)$_2$] 1.2

Anisole (0.22 mL, 2 mmol) was injected into a 20 mL hexane solution containing 2 mmol of **1.1** and this mixture was then stirred overnight at room temperature. This mixture was reduced *in vacuo* and cooled to -30^{o}C. A crop (0.41 g, 44 %) of colourless crystals of **1.2** formed in solution that was suitable for X-ray crystallographic analysis.

^{1}H NMR data (400.13 MHz, 298 K, C$_6$D$_{12}$)

δ = 0.24 [4H, m, 2 x CH$_2$ of *i*Bu], 0.66 [6H, d, ^3J(H,H) = 6.45 Hz, 2 x CH$_3$ of *i*Bu], 0.88 [6H, d, ^3J(H,H) = 6.45 Hz, 2 x CH$_3$ of *i*Bu], 0.97 [2H, m, 1 x βCH$_2$ of TMP], 1.38 [6H,

s, 2 x CH_3 of TMP], 1.38 [1H, s, γCH of TMP], 1.41 [6H, s, 2 x CH_3 of TMP], 1.54 [2H, m, 1 x βCH_2 of TMP], 1.80 [4H, m, 2 x βCH_2 of THF], 1.84 [1H, m, γCH of TMP] and [2H, m, 2 x CH of *i*Bu], 3.56 [4H, m, αCH_2 of THF], 3.76 [3H, s, CH_3O], 6.62 [1H, d, ^3J(H,H) = 8.05 Hz, 1 x H of anisole], 6.89 [1H, t, ^3J(H,H) = 7.05 Hz, 1 x H of anisole], 7.03 [1H, m, 1 x H of anisole], 7.65 ppm [1H, d, ^3J(H,H) = 7.02 Hz, 1 x H of anisole].

^{13}C {1H} NMR data (100.62 MHz, 298 K, C_6D_{12})

δ = 19.2 [γCH_2 of TMP], 26.0 [2 x βCH_2 of THF], 27.7 [2 x CH of *i*Bu], 27.9 [2 x CH_3 of *i*Bu], 28.6 [2 x CH_2 of *i*Bu], 30.3 [2 x CH_3 of TMP], 30.5 [2 x CH_3 of *i*Bu], 37.8 [2 x CH_3 of TMP], 45.4 [2 x βCH_2 of TMP], 53.7 [2 x quaternary C of TMP], 55.7 [CH_3O of anisole], 69.5 [2 x αCH_2 of THF], 110.2 [1 x CH of anisole], 124.2 [1 x CH of anisole], 128.3 [1 x CH of anisole], 142.1 [1 x CH of anisole], 163.6 ppm [*ipso* C of anisole OCH_3–C].

El. Analysis calc. for $C_{28}H_{51}AlLiNO_2$ (Mr = 467.62) C, 71.92; H, 10.99; N, 3.00; found: C, 71.61; H, 11.27; N, 2.99%.

Synthesis of [(THF)Li(μ-TMP)(μ-C_6H_3{OMe}$_2$)Al(*i*Bu)$_2$] 1.3

1,3-Dimethoxybenzene (0.26 mL, 2 mmol) was injected into a 20 mL hexane solution containing 2 mmol of **1.1** and this mixture was stirred overnight at room temperature. This solution was then cooled to -30^{o}C. A crop (0.65 g, 65%) of colourless crystals of **1.3** formed in solution that was suitable for X-ray crystallographic analysis.

^{1}H NMR data (400.13 MHz, 298 K, C_6D_6)

δ = 0.63 [2H, m, 1 x CH_2 of *i*Bu], 0.85 [2H, m, 1 x CH_2 of *i*Bu], 1.00 [2H, m, 1 x βCH_2 of TMP], 1.04 [4H, m, 2 x βCH_2 of THF], 1.15 [6H, m, 2 x CH_3 of *i*Bu], 1.45 [1H, m, 1 x γCH of TMP], 1.47 [12H, s, 2 x CH_3 of TMP and *i*Bu], 1.60 [2H, m, 1 x βCH_2 of TMP], 1.73 [6H, s, 2 x CH_3 of TMP], 1.95 [1H, m, 1 x γCH of TMP], 2.41 [2H, broad s, 2 x CH of *i*Bu], 2.95 [4H, m, 2 x αCH_2 of THF], 3.46 [6H, s, 2 x OCH_3], 6.34 [2H, d, ^3J(H,H) = 8.06 Hz, 2 x aromatic CH], 7.14 ppm [1H, t, ^3J(H,H) = 8.05 Hz, 1 x aromatic CH].

^{13}C {1H} NMR data (100.62 MHz, 298 K, C_6D_6)

δ = 19.0 [γCH_2 of TMP], 25.0 [2 x βCH_2 of THF], 27.6 [2 x CH_3 of *i*Bu], 27.7 [2 x CH of *i*Bu], 29.9 [2 x CH_3 of TMP], 30.4 [2 x CH_2 of *i*Bu], 31.5 [2 x CH_3 of *i*Bu], 36.5 [2 x CH_3 of TMP], 44.6 [2 x βCH_2 of TMP], 53.3 [quaternary C of TMP], 54.8 [2 x OCH_3], 68.4 [2 x αCH_2 of THF], 104.5 [2 x aromatic CH], 129.5 [1 x aromatic CH], 166.2 ppm [2 x *ipso* C-OMe].

El. Analysis calc. for $C_{29}H_{53}AlLiNO_3$ (Mr = 497.64) C, 69.99; H, 10.73; N, 2.81; found: C, 69.65; H, 11.18; N, 2.80%.

Synthesis of [(THF)Li(μ-TMP)(μ-$C_{10}H_6$OMe)Al(*i*Bu)$_2$] 1.4

1-Methoxynaphthalene (0.29 mL, 2 mmol) was injected into a 20 mL hexane solution containing 2 mmol of **1.1** and this mixture was stirred overnight at room temperature. This was cooled to -30^{o}C. A crop (0.54 g, 52 %) of colourless crystals of **1.4** formed in solution that was suitable for X-ray crystallographic analysis.

^{1}H NMR data (500.13 MHz, 298 K, C_6D_{12})

δ = 0.43 [4H, m, 2 x CH_2 of *i*Bu], 1.00 [12H, s, 4 x CH_3 of *i*Bu], 1.25 [2 x βCH_2 of TMP], 1.30 [12H, broad m, 4 x CH_3 of TMP], 1.62 [1 x γCH_2 of TMP], 1.74 [4H, m, 2 x βCH_2 of THF], 2.04 [2H, broad s, 2 x CH of *i*Bu], 3.61 [4H, m, 2 x αCH_2 of THF], 4.15 [3H, s, 1 x OCH_3], 7.23 [1H, t, ^3J(H,H) = 7.30 Hz, 1 x aromatic CH], 7.29 [1H, t, ^3J(H,H) = 7.91 Hz, 1 x aromatic CH], 7.45 [1H, d, ^3J(H,H) = 7.82 Hz, 1 x aromatic CH], 7.69 [1H, d, ^3J(H,H) = 7.99 Hz, 1 x aromatic CH], 7.74 [1H, d, ^3J(H,H) = 8.34 Hz, 1 x aromatic CH], 7.83 ppm [1H, d, ^3J(H,H) = 7.91 Hz, 1 x aromatic CH].

^{13}C {1H} NMR data (100.62 MHz, 298 K, C_6D_{12})

δ = 19.2 [1 x γCH_2 of TMP], 25.3 [2 x βCH_2 of THF], 27.5 [2 x CH_2 of *i*Bu], 27.9 [2 x CH of *i*Bu], 31.2 [4 x CH_3 of *i*Bu], 37.6 [4 x CH_3 of TMP], 44.8 [2 x βCH_2 of TMP], 53.4 [2 x quaternary C of TMP], 62.9 [1 x OCH_3], 67.3 [2 x αCH_2 of THF], 120.8 [1 x aromatic CH], 124.7 [1 x aromatic CH], 125.2 [1 x aromatic CH], 125.3 [1 x aromatic CH], 126.8 [1 x quaternary aromatic C], 129.3 [1 x aromatic CH], 136.2 [1 x quaternary aromatic C], 137.8 [1 x aromatic CH], 152.2 [1 x quaternary aromatic C-Al], 157.0 ppm [1 x *ipso* C-OMe].

El. Analysis calc. for $C_{32}H_{53}AlLiNO_2$ (Mr = 517.67) C, 74.25; H, 10.32; N, 2.71; found: C, 73.53; H, 10.3; N, 2.82%.

Synthesis of [(THF)Li(μ-TMP)(μ-$C_6H_4C(=O)N$*i*Pr_2)Al(*i*Bu)$_2$] 1.5

N,*N*-Diisopropylbenzamide (0.41 g, 2 mmol) was introduced into a 20 mL hexane solution that contained 2 mmol of freshly prepared **1.1** and this mixture was stirred overnight at ambient temperature. This solution was then cooled to -30^{o}C. A crop (0.57 g, 47 %) of colourless crystals of **1.5** formed in solution that was suitable for X-ray crystallographic analysis.

^{1}H NMR data (400.13 MHz, 298 K, C_6D_{12})

δ = -0.14 [2H, m, CH_2 of *i*Bu], 0.26 [2H, m, CH_2 of *i*Bu], 0.84 [3H, d, ^3J(H,H) = 6.62 Hz, 1 x CH_3 of *i*Bu], 1.00 [9H, m, 3 x CH_3 of *i*Bu], 1.08 [1H, m, 1 x βCH of TMP], 1.09 [1H, m, 1 x βCH of TMP], 1.17 [3H, broad s, 1 x CH_3 of TMP], 1.26 [3H, d, ^3J(H,H) = 6.52 Hz, 1 x CH_3 of *i*Pr], 1.31 [3H, d, ^3J(H,H) = 6.52 Hz, 1 x CH_3 of *i*Pr], 1.32 [1H, m, 1 x βCH of TMP], 1.38 [3H, m, 1 x CH_3 of TMP], 1.39 [4H, m, 1 x γCH of TMP and 1 x CH_3 of TMP], 1.47 [3H, d, ^3J(H,H) = 6.78 Hz, 1 x CH_3 of *i*Pr], 1.54 [3H, broad s, 1 x CH_3 of TMP], 1.65 [7H, m, 1 x CH_3 of *i*Pr and 2 x βCH_2 of THF], 1.66 [1H, m, 1 x βCH of TMP], 1.89 [1H, m, 1 x γCH of TMP], 2.01 [2H, m, 1 x CH_2 of *i*Bu], 2.14 [2H, m, 1 x CH_2 of *i*Bu], 3.32 [4H, m, 2 x αCH_2 of THF], 3.52 [1H, sept, ^3J(H,H) = 6.86 Hz, 1 x CH of *i*Pr], 4.18 [1H, sept, ^3J(H,H) = 6.64 Hz, 1 x CH of *i*Pr], 6.97 [2H, m, 2 x aromatic CH], 7.13 [1H, td, ^3J(H,H) = 7.06 Hz, 1 x aromatic CH], 8.23 ppm [1H, d, ^3J(H,H) = 7.44 Hz, 1 x aromatic CH].

^{13}C {1H} NMR data (100.62 MHz, 298 K, C_6D_{12})

δ = 19.5 [1 x γCH_2 of TMP], 20.7 [1 x CH_3 of *i*Pr], 21.1 [1 x CH_3 of *i*Pr], 21.3 [1 x CH_3 of *i*Pr], 22.0 [1 x CH_3 of *i*Pr], 25.9 [2 x βCH_2 of THF], 27.4 [1 x CH_3 of *i*Bu], 28.1 [1 x CH_3 of *i*Bu], 28.3 [2 x CH of *i*Bu], 29.1 [1 x CH_2 of *i*Bu], 29.6 [1 x CH_2 of *i*Bu], 30.3 [1 x CH_3 of TMP], 30.9 [1 x CH_3 of *i*Bu], 31.3 [1 x CH_3 of *i*Bu], 31.9 [1 x CH_3 of TMP], 37.7 [1 x CH_3 of TMP], 38.2 [1 x CH_3 of TMP], 44.4 [1 x βCH_2 of TMP], 45.4 [1 x βCH_2 of TMP], 46.8 [1 x CH of *i*Pr], 52.3 [1 x CH of *i*Pr], 54.0 [2 x quaternary C of TMP], 68.5 [2 x αCH_2 of THF], 123.4 [1 x aromatic CH], 124.9 [1 x aromatic CH], 127.5 [1 x aromatic CH], 145.9 [1 x *ipso* C-C=O], 146.5 [1 x aromatic CH], 179.4 ppm [1 x carbonyl C(=O)].

El. Analysis calc. for $C_{37}H_{69}AlLiN_2O_2$ (Mr = 607.86) C, 73.11; H, 11.44; N, 4.61; found: C, 72.08; H, 11.23; N, 5.00%.

Synthesis of [(THF)Li(μ-TMP){μ-(OMe)C_6H_3(I)}Al(*i*Bu)$_2$] 1.6

2-Iodoanisole (0.26 mL, 2 mmol) was added into a 20 mL hexane solution containing 2 mmol of **1.1** and this mixture was stirred overnight at ambient temperature. This mixture was cooled to -30^{o}C. A crop (0.84 g, 71 %) of colourless crystals of **1.6** formed in solution that was suitable for X-ray crystallographic analysis.

^{1}H NMR data (400.13 MHz, 298 K, C_6D_6)

δ = 0.65 [2H, m, 1 x CH_2 of *i*Bu], 0.77 [2H, m, 1 x CH_2 of *i*Bu], 0.91 [2H, m, 1 x βCH_2 of TMP], 1.11 [6H, broad s, 2 x CH_3 of TMP], 1.20 [6H, broad m, 2 x CH_3 of *i*Bu], 1.28 [4H, m, 2 x βCH_2 of THF], 1.35 [1H, m, 1 x γCH of TMP], 1.45 [2H, m, 1 x βCH_2 of TMP], 1.46 [6H, d, ^3J(H,H) = 6.37 Hz, 2 x CH_3 of *i*Bu], 1.84 [1H, m, 1 x γCH of TMP], 1.58 [6H, s, 2 x CH_3 of TMP], 2.43 [2H, broad m, 2 x CH of *i*Bu], 3.29 [4H, m, 2 x αCH_2 of THF], 3.85 [3H, s, 1 x OCH_3], 6.68 [1H, t, ^3J(H,H) = 7.23 Hz, 1 x aromatic CH], 7.55 [1H, dd, ^3J(H,H) = 7.54 Hz, 1 x aromatic CH], 7.99 ppm [1H, dd, ^3J(H,H) = 7.13 Hz, 1 x aromatic CH].

^{13}C {1H} NMR data (100.62 MHz, 298 K, C_6D_6)

δ = 18.7 [1 x γCH_2 of TMP], 25.3 [2 x βCH_2 of THF], 27.5 [2 x CH_3 of *i*Bu], 27.6 [2 x CH of *i*Bu], 28.9 [2 x CH_2 of *i*Bu], 29.9 [2 x CH_3 of TMP], 31.3 [2 x CH_3 of *i*Bu], 37.8 [2 x CH_3 of TMP], 44.4 [2 x βCH_2 of TMP], 53.0 [2 x quaternary C of TMP], 62.7 [OCH3], 68.9 [2 x αCH_2 of THF], 88.7 [quaternary aromatic C-I], 128.1 [1 x aromatic CH], 138.5 [1 x aromatic CH], 140.3 [1 x aromatic CH], 160.8 ppm [quaternary aromatic C-OMe].

El. Analysis calc. for $C_{28}H_{50}AlLiNO_2I$ (Mr = 593.51) C, 56.66; H, 8.49; N, 2.36; found: C, 56.61; H, 8.89; N, 2.36%.

Iodine quenching of aluminated complexes 1.2-1.6 to give metal free products 1.7-1.11

Aluminate compounds **1.2-1.6** were prepared *in situ* as described by the methods above. A solution of I_2 in dry THF (10 mL of a 1 M solution) was added at 0^{o}C and this

mixture was stirred overnight. The resulting mixture was diluted was saturated aq. $NaHS_2O_3$ (20 mL) and saturated aq. NH_4Cl (40 mL) and extracted with $CHCl_3$ (30 mL x 3). The organic layer was dried over $MgSO_4$ and solvent removed under reduced pressure to give crude compounds **1.7-1.11.**

Purification of iodinated compounds 1.7-1.11

2-iodoanisole 1.7

The residue was purified by SiO_2 column chromatography using petroleum ether (100%) as an eluent to give 2-iodoanisole **1.7** (0.36 g, 77%).

2-iodo-1,3-dimethoxybenzene 1.8

The residue was purified by SiO_2 column chromatography using diethyl ether:petroleum ether (1:10) as an eluent to give 2-iodo-1,3-dimethoxybenzene **1.8** (0.43 g, 81%).

2-iodo-1-methoxynaphthalene 1.9

The residue was purified by SiO_2 column chromatography using diethyl ether:petroleum ether (1:10) and diethyl ether (100%) as an eluent to give 2-iodo-1-methoxynaphthalene **1.9** (0.4 g, 70%).

2-iodo-*N*,*N*-diisopropylbenzamide 1.10

The residue was purified by Al_2O_3 column chromatography using petroleum ether (100%), petroleum ether:diethyl ether (1:1) and finally diethyl ether (100%) as an eluent to give 2-iodo-*N*,*N*-diisopropylbenzamide **1.10** (0.58 g, 88%).

2,6-diiodoanisole 1.11

The residue was purified by SiO_2 column chromatography using petroleum ether (100%) as an eluent to give 2,6-diiodoanisole **1.11** (0.69 g, 96%).

^{1}H NMR data (400.13 MHz, 298 K, $CDCl_3$)

δ = 3.87 [3H, s, OCH_3], 6.55 [1H, t, ^3J(H,H) = 7.76 Hz, 1 x aromatic H], 7.76 ppm [2H, d, ^3J(H,H) = 7.76 Hz, 2 x aromatic H].

^{13}C {1H} NMR data (100.62 MHz, 298 K, $CDCl_3$)

δ = 60.6 [OCH_3], 90.7 [2C, C-I], 127.6 [2C, *meta*-aromatic CH], 139.8 [1C, *para*-aromatic CH], 158.8 ppm [C-OCH_3].

El. Analysis calc. for $C_7H_6OI_2$ (Mr = 359.93) C, 23.36; H, 1.68; found: C, 24.20; H, 2.08%.

Synthesis of diisopropylamine base [(THF)Li(μ-DA)$_2$Al(*i*Bu)$_2$] 1.12

Diisopropylamine (0.56 mL, 4 mmol) was injected into a 20 mL hexane solution containing 2 mmol of **1.1** and this solution was stirred overnight at room temperature. The solution was reduced *in vacuo* and cooled to -30^{o}C. A crop (0.46 g, 55%) of colourless crystals of **1.12** formed in solution which was suitable for X-ray crystallographic analysis.

^{1}H NMR data (400.13 MHz, 298 K, C_6D_6)

δ = 0.54 [4H, d, ^3J(H,H) = 6.70 Hz, 2 x CH_2 of *i*Bu], 1.12 [4H, m, 2 x βCH_2 of THF], 1.24 [24H, d, ^3J(H,H) = 6.65 Hz, 8 x CH_3 of *i*Pr], 1.47 [12H, d, ^3J(H,H) = 6.46 Hz, 4 x CH_3 of *i*Bu], 2.42 [2H, sept, ^3J(H,H) = 6.55 Hz, 2 x CH of *i*Bu], 3.19 [4H, m, 2 x αCH_2 of THF], 3.41 ppm [4H, sept, ^3J(H,H) = 6.63 Hz, 4 x CH of *i*Pr].

^{13}C {1H} NMR data (100.62 MHz, 298 K, C_6D_6)

δ = 25.0 [2 x βCH_2 of THF], 26.4 [8 x CH_3 of *i*Pr], 27.4 [2 x CH of *i*Bu and 2 x CH_2 of *i*Bu], 29.9 [4 x CH_3 of *i*Bu], 46.7 [4 x CH of *i*Pr], 68.8 ppm [2 x αCH_2 of THF].

El. Analysis calc. for $C_{24}H_{54}AlLiN_2O$ (Mr = 420.63) C, 68.53; H, 12.94; N, 6.66; found: C, 67.27; H, 13.06; N, 6.56%.

Synthesis of [*i*Bu$_2$Al(DMP)]$_2$ 1.13

*n*BuLi (1.25 mL, 1.6 M in hexanes, 2.0 mmol) was added to a solution of DMP(H) (0.27 mL, 2 mmol) in hexane (10 mL). After stirring for 1 h, *i*Bu$_2$AlCl (0.38 mL, 2 mmol) was introduced to the solution via syringe. After 1 h, this solution was filtered, reduced in volume and cooled to -30^{o}C. A crop (0.49 g, 48%) of colourless crystals of **1.13** formed in solution that was suitable for X-ray crystallographic analysis.

^{1}H NMR data (400.13 MHz, 298 K, C_6D_{12})

δ = 0.31-0.47 [8H, m, 4 x CH_2 of *i*Bu], 1.11-1.34 [24H, m, 8 x CH_3 of *i*Bu], 1.46 [4H, m, βCH_2 of DMP], 1,47-1.50 [12H, m, 4 x CH_3 of DMP], 1.52 [2H, m, 1 x γCH_2 of DMP], 1.95 [2H, m, 1 x γCH_2 of DMP], 1.96 [4H, m, 2 x βCH_2 of DMP], 2.05 [4H, sept, ^3J(H,H) = 6.44 Hz, 4 x CH of *i*Bu], 3.61 ppm [4H, m, 4 x CH of DMP].

^{13}C {1H} NMR data (100.62 MHz, 298 K, C_6D_{12})

δ = 14.0 [γCH_2 of DMP], 24.4 [CH_3 of DMP], 26.4 [CH_2 of *i*Bu], 27.0 [CH of *i*Bu], 29.3 [CH_3 of *i*Bu], 29.5 [CH_3 of *i*Bu], 32.7 [βCH_2 of DMP], 49.8 ppm [CH of DMP].

El. Analysis calc. for $C_{30}H_{64}Al_2N_2$ (Mr = 506.82) C, 71.10; H, 12.73; N, 5.53; found: C, 68.89; H, 13.23; N, 5.22%.

Synthesis of *i*Bu_2Al(TMP) 1.14

This was prepared in an identical manner to that described above for **1.13** using TMP(H) (0.34 mL, 2 mmol). After filtration, the solvent was completely removed *in vacuo* to give the final product as a yellow oil (0.42 g, 75 %).

^{1}H NMR data (400.13 MHz, 298 K, C_6D_{12})

δ = 0.26 [4H, d, ^{3}J(H,H) = 7.19 Hz, 2 x CH_2 of *i*Bu], 0.97 [12H, d, ^{3}J(H,H) = 6.53 Hz, 4 x CH_3 of *i*Bu], 1.25 [12H, s, 4 x CH_3 of TMP], 1.27 [4H, m, 2 x βCH_2 of TMP], 1.69 [2H, m, 1 x γCH_2 of TMP], 1.95 ppm [2H, sept, ^{3}J(H,H) = 6.68 Hz, 2 x CH of *i*Bu].

^{13}C {1H} NMR data (100.62 MHz, 298 K, C_6D_{12})

δ = 19.8 [γCH_2 of TMP], 26.7 [CH of *i*Bu], 28.5 [CH_3 of *i*Bu], 29.4 [CH_2 of *i*Bu], 33.3 [CH_3 of TMP], 40.0 [βCH_2 of TMP], 51.7 ppm [quaternary C of TMP].

El. Analysis could not be satisfactorily obtained as the product was an air sensitive oil and could not be subjected to conventional purification techniques.

Synthesis of [$(THF)_3$Li{(N≡C)C_6H_3(Me)}Al(*i*$Bu)_2$(TMP] 1.17

m-tolunitrile (0.24 mL, 2 mmol) was injected into a 20 mL hexane solution containing 2 mmol of **1.1** instantly producing a bright orange/red solution with a small amount of precipitate. Approximately 5 mL of THF was added to dissolve the solid however, the solution turned dark brown. The solution was allowed to stand overnight where large yellow crystals grew onto the side of the Schlenk flask. These were subjected to X-ray crystallographic analysis. Owing to the high reactivity of **1.1** with *m*-tolunitrile and the formation of a dark brown solution upon addition of THF a good reproducible yield could not be obtained.

^{1}H NMR data (400.13 MHz, 298 K, C_6D_{12})

δ = 0.00-0.20 [4H, m, 2 x CH_2 of *i*Bu], 0.81 [6H, d, ^{3}J(H,H) = 6.33 Hz, 2 x CH_3 of *i*Bu], 0.89 [6H, d, ^{3}J(H,H) = 6.33 Hz, 2 x CH_3 of *i*Bu], 1.20 [12H, s, 4 x CH_3 of TMP], 1.38 [4H, m, 2 x βCH_2 of TMP], 1.55 [2H, m, γCH_2 of TMP], 1.69 [2H, m, 2 x CH of *i*Bu], 1.85 [12H, m, 6 x CH_2 of THF], 2.19 [3H, s, CH_3 of aromatic], 3.79 [12H, m, 6 x CH_2 of THF], 7.02 [1H, d, ^{3}J(H,H) = 7.74 Hz, 1 x aromatic H], 7.04 [1H, s, 1 x aromatic H], 7.99 ppm [1H, d, ^{3}J(H,H) = 7.74 Hz, 1 x aromatic H].

Synthesis of [(THF)Li(μ-TMP){μ-$C_6H_4(CH_2NMe_2)$}Al(*i*Bu)$_2$] 1.18

N,*N*-dimethylbenzylamine (0.30 mL, 2 mmol) was injected into a 20 mL hexane solution containing 2 mmol of **1.1** and this mixture was stirred overnight at room temperature. This was cooled to 0^{o}C and a crop of colourless crystals formed in solution after several weeks. As a result of the poor quality of these crystals X-ray crystallographic data could not be obtained.

^{1}H NMR data (400.13 MHz, 298 K, C_6D_{12})

δ = 0.77-0.90 [4H, m, 2 x CH_2 of *i*Bu], 1.16 [4H, broad s, 2 x βCH_2 of TMP], 1.28 [4H, m, 2 x βCH_2 of THF], 1.33 [6H, d, ^{3}J(H,H) = 6.43 Hz, 2 x CH_3 of *i*Bu], 1.37 [6H, d, ^{3}J(H,H) = 6.43 Hz, 2 x CH_3 of *i*Bu], 1.55 [12H, s, 4 x CH_3 of TMP], 1.62 [2H, broad s, γCH_2 of TMP], 2.12 [6H, s, 2 x CH_3 of NMe_2], 2.45 [2H, sept, ^{3}J(H,H) = 6.94 Hz, 2 x CH of *i*Bu], 3.28 [4H, m, 2 x αCH_2 of THF], 3.31 [2H, s, 1 x CH_2 next to NMe_2], 7.19 [1H, t, ^{3}J(H,H) = 7.34 Hz, 1 x aromatic CH], 7.27 [1H, d, ^{3}J(H,H) = 7.62 Hz, 1 x aromatic CH], 7.92 [1H, d, ^{3}J(H,H) = 6.77 Hz, 1 x aromatic CH], 8.06 ppm [1H, s, 1 x aromatic CH].

^{13}C {^{1}H} NMR data (100.62 MHz, 298 K, C_6D_{12})

δ = 18.4 [γCH_2 of TMP], 25.5 [2 x βCH_2 of THF], 28.0 [2 x CH of *i*Bu], 28.7 [2 x CH_3 of *i*Bu], 29.4 [2 x CH_2 of *i*Bu], 30.0 [2 x CH_3 of *i*Bu], 33.3 [4 x CH_3 of TMP], 44.8 [2 x βCH_2 of TMP], 45.5 [$N(CH_3)_2$], 52.6 [2 x quaternary C of TMP], 65.1 [CH_2 next to NMe_2], 68.0 [2 x αCH_2 of THF], 128.4 [1 x aromatic CH], 138.3 [1 x aromatic CH], 141.0 ppm [1 x aromatic CH].

Synthesis of [(THF)Li(μ-TMP)(μ-$C_{10}H_9Fe$)Al(*i*Bu)$_2$] 1.19

Ferrocene (0.37 g, 2 mmol) was added into a 20 mL hexane solution containing 2 mmol of **1.1** producing an orange solution which was stirred overnight at room temperature. A crop of orange coloured needle crystals (0.52 g, 48%) were obtained by allowing the Schlenk flask to stand at room temperature. These crystals were suitable for X-ray crystallographic analysis.

^{1}H NMR data (400.13 MHz, 298 K, C_6D_{12})

δ = 0.37 [4H, m, 2 x CH_2 of *i*Bu], 1.09 [6H, d, ^3J(H,H) = 6.28 Hz, 2 x CH_3 of *i*Bu], 1.12 [6H, d, ^3J(H,H) = 6.28 Hz, 2 x CH_3 of *i*Bu], 1.15 [4H, m, 2 x βCH_2 of TMP], 1.30 [12H, s, 4 x CH_3 of TMP], 1.57 [2H, broad s, γCH_2 of TMP], 1.75 [4H, m, 2 x βCH_2 of THF], 2.14 [2H, sept, ^3J(H,H) = Hz, 2 x CH of *i*Bu], 3.61 [4H, m, 2 x αCH_2 of THF], 4.00 [2H, s, 2 x βCH of ferrocene], 4.08 [5H, s, Cp ring of ferrocene], 4.28 ppm [2H, s, 2 x αCH of ferrocene].

^{13}C {^{1}H} NMR data (100.62 MHz, 298 K, C_6D_{12})

δ = 18.7 [1 x γCH_2 of TMP], 28.0 [2 x CH of *i*Bu], 29.2 [4 x CH_3 of *i*Bu], 29.9 [2 x CH_2 of *i*Bu], 31.0 [2 x CH_3 of TMP], 39.2 [2 x CH_3 of TMP], 45.0 [2 x βCH_2 of TMP], 53.1 [2 x quaternary C of TMP], 69.5 [Cp ring of ferrocene], 71.8 [2 x βCH of ferrocene], 77.1 ppm [2 x αCH of ferrocene].

Synthesis of [(THF)$_2$Li$_2$(μ-TMP)$_2$(μ-$C_5H_4FeC_5H_4$)Al$_2$(*i*Bu)$_4$] 1.20

Ferrocene (0.19 g, 1 mmol) was added into a 20 mL hexane solution containing 2 mmol of **1.1** producing an orange solution which was heated to reflux for 2 hours. Once the solution was allowed to cool the Schlenk flask was placed in the freezer at -30^{o}C. A crop of orange coloured cubic crystals (0.50 g, 28%) of **1.20** formed in solution that were suitable for X-ray crystallographic analysis.

^{1}H NMR data (400.13 MHz, 298 K, C_6D_{12})

δ = 0.38 [8H, m, 4 x CH_2 of *i*Bu], 0.75 [4H, m, 2 x βCH_2 of TMP], 1.10 [24H, m, 8 x CH_3 of *i*Bu], 1.25 [12H, s, 4 x CH_3 of TMP], 1.29 [2H, m, 2 x γCH of TMP], 1.32 [12H, s, 4 x CH_3 of TMP], 1.47 [4H, d, ^3J(H,H) = 12.38 Hz, 2 x βCH_2 of TMP], 1.78 [8H, s, 4 x βCH_2 of THF], 1.84 [2H, m, 2 x γCH of TMP], 2.15 [4H, sept, ^3J(H,H) = 6.37 Hz, 4 x

CH of *i*Bu], 3.53 [8H, s, 4 x αCH$_2$ of THF], 3.97 [4H, s, 4 x H of Cp ferrocene ring], 4.47 ppm [4H, s, 4 x H of Cp ferrocene ring].

^{13}C {^{1}H} NMR data (100.62 MHz, 298 K, C$_6$D$_{12}$)

δ = 18.7 [γCH$_2$ of TMP], 25.9 [4 x βCH$_2$ of THF], 28.1 [4 x CH of *i*Bu], 29.4 [8 x CH$_3$ of *i*Bu], 29.7 [4 x CH$_3$ of TMP], 29.8 [4 x CH$_2$ of *i*Bu], 36.8 [4 x CH$_3$ of TMP], 45.1 [4 x βCH$_2$ of TMP], 53.0 [4 x quaternary C of TMP], 69.2 [4 x αCH$_2$ of THF], 74.7 [4 x CH of Cp ferrocene ring], 77.4 ppm [4 x CH of Cp ferrocene ring].

X-ray diffraction data

Crystallographic data was collected at 123(2) K on Oxford Diffraction instruments with 0.71073Å wavelength radiation. Structures were refined to convergence against F^2 and with all independent reflections by the full-matrix least-squares method using the *SHELXL-97* program.[50] Selected crystallographic and refinement parameters are given in **Table 1.3**.

Table 1.3: Crystallographic data and refinement details for compounds **1.2-1.6, 1.12, 1.13, 1.17, 1.19** and **1.20**.

	1.2	**1.3**	**1.4**	**1.5**	**1.6**	**1.12**	**1.13**	**1.17**	**1.19**	**1.20**
Empirical Formula	$C_{28}H_{51}AlLiNO_2$	$C_{29}H_{53}AlLiNO_3$	$C_{32}H_{53}AlLiNO_2$	$C_{37}H_{69}AlLiN_2O_2$	$C_{28}H_{50}AlILiNO_2$	$C_{24}H_{54}AlLiN_2O$	$C_{30}H_{64}Al_2N_2$	$C_{37}H_{66}AlLiN_2O_3$	$C_{31}H_{53}AlFeLiNO$	$C_{52}H_{96}Al_2FeLi_2N_2O_2$
M_r	467.62	497.64	517.67	607.86	593.51	420.61	506.79	620.84	545.51	905.00
Crystal System	monoclinic	monoclinic	monoclinic	monoclinic	monoclinic	monoclinic	Triclinic	monoclinic	Triclinic	Monoclinic
Space Group	P 21/n	P 21/n	P 21/c	P 21/c	P 21/n	P 21/n	P -1	P 21/n	P -1	I 2/a
a [Å]	11.6847(5)	11.3436(2)	9.9464(3)	11.4941(2)	11.1865(5)	11.3522(2)	10.2455(5)	13.1665(4)	10.6687(7)	16.3217(8)
b [Å]	19.6467(9)	23.3577(5)	15.9170(4)	19.1867(3)	14.3886(8)	17.0080(4)	10.6589(5)	17.5146(5)	11.1600(6)	14.7125(4)
c [Å]	12.9662(6)	11.6850(3)	19.7960(6)	17.9794(4)	19.3615(8)	14.0982(4)	16.0232(10)	17.0373(5)	13.8524(7)	22.5707(12)
α [°]	90	90	90	90	90	90	101.147(4)	90	94.846(4)	90
β [°]	101.987(4)	104.261(2)	93.414(3)	106.101(2)	103.485(4)	90.351(3)	96.316(5)	103.376(3)	95.578(5)	98.785(10)
γ [°]	90	90	90	90	90	90	109.340(4)	90	108.439(5)	90
V [Å^3]	2911.7(2)	3000.65(11)	3128.48(16)	3809.53(12)	3030.5(2)	2722.00(11)	1591.05(15)	3822.32(19)	1545.58(15)	5356.4(4)
Z	4	4	4	4	4	4	2	4	2	4
P_{calcd} [g cm^{-3}]	1.067	1.102	1.099	1.060	1.301	1.026	1.058	1.079	1.172	1.122

Reflns Measured	22283	21173	20987	31771	13679	11593	9348	18827	19710	17936
Unique Reflns	7290	7042	8860	10910	6701	5793	9348	9921	6073	6218
R int	0.0282	0.0284	0.0281	0.0264	0.0317	0.0232	0.000	0.0236	0.0852	0.0191
GooF	1.098	1.067	0.907	1.059	0.944	0.939	0.994	1.078	0.797	1.103
R [on F, obs rflns only]	0.0499	0.0461	0.0414	0.0409	0.0441	0.0400	0.0502	0.0696	0.0482	0.0299
wR [on F^2, all data]	0.1438	0.1255	0.0956	0.1075	0.1232	0.1003	0.1199	0.2168	0.0731	0.0864
Largest diff. peak/hole [$eÅ^{-3}$]	0.491/-0.409	0.667/-0.500	0.279/-0.272	0.337/-0.270	0.696/-0.804	0.326/-0.239	0.461/-0.421	0.788/-0.431	0.691/-0.360	0.335/-0.386

2.6 References

[1] J. Clayden, *Organolithiums: Selectivity for Synthesis*, Elsevier Science Ltd, Oxford, U.K., **2002**.

[2] M. F. Lappert, M. J. Slade, A. Singh, J. L. Atwood, R. D. Rogers, R. Shakir, *J. Am. Chem. Soc.* **1983**, *105*, 302.

[3] P. Renaud, M. A. Fox, *J. Am. Chem. Soc.* **1988**, *110*, 5702.

[4] F. E. Romesberg, D. B. Collum, *J. Am. Chem. Soc.* **1992**, *114*, 2112.

[5] P. G. Williard, Q. Y. Liu, *J. Am. Chem. Soc.* **1993**, *115*, 3380.

[6] B. L. Lucht, D. B. Collum, *J. Am. Chem. Soc.* **1994**, *116*, 7949.

[7] D. R. Armstrong, P. Garcia-Alvarez, A. R. Kennedy, R. E. Mulvey, S. D. Robertson, *Chem. Eur. J.* **2011**, *17*, 6725.

[8] P. Fleming, D. F. O'Shea, *J. Am. Chem. Soc.* **2011**, *133*, 1698.

[9] M. Uchiyama, H. Naka, Y. Matsumoto, T. Ohwada, *J. Am. Chem. Soc.* **2004**, *126*, 10527.

[10] H. Naka, M. Uchiyama, Y. Matsumoto, A. E. H. Wheatley, M. McPartlin, J. V. Morey, Y. Kondo, *J. Am. Chem. Soc.* **2007**, *129*, 1921.

[11] H. Naka, J. V. Morey, J. Haywood, D. J. Eisler, M. McPartlin, F. Garcia, H. Kudo, Y. Kondo, M. Uchiyama, A. E. H. Wheatley, *J. Am. Chem. Soc.* **2008**, *130*, 16193.

[12] B. Conway, J. Garcia-Alvarez, E. Hevia, A. R. Kennedy, R. E. Mulvey, S. D. Robertson, *Organometallics* **2009**, *28*, 6462.

[13] B. Conway, A. R. Kennedy, R. E. Mulvey, S. D. Robertson, J. Garcia-Alvarez, *Angew. Chem. Int. Ed.* **2010**, *49*, 3182.

[14] S. H. Wunderlich, P. Knochel, *Angew. Chem. Int. Ed.* **2009**, *48*, 1501.

[15] M. M. Hansmann, R. L. Melen, D. S. Wright, *Chem. Sci.* **2011**, *2*, 1554.

[16] W. Kohn, A. D. Becke, R. G. Parr, *J. Phys. Chem.* **1996**, *100*, 12974.

[17] A. D. Becke, *Phys. Rev. A.* **1988**, *38*, 3098.

[18] C. T. Lee, W. Yang, R. G. Parr, *Phys. Rev. B.* **1988**, *37*, 785.

[19] A. D. McLean, G. S. Chandler, *J. Chem. Phys.* **1980**, 5639.

[20] R. Krishnan, J. S. Binkley, R. Seeger, J. A. Pople, *J. Chem. Phys.* **1980**, *72*, 650.

[21] R. Campbell, B. Conway, G. S. Fairweather, P. Garcia-Alvarez, A. R. Kennedy, J. Klett, R. E. Mulvey, C. T. O'Hara, G. M. Robertson, *Dalton Trans.* **2010**, *39*, 511.

[22] F. H. Allen, *Acta Crystallogr.* **2002**, *B58*, 380.

[23] I. Krossing, H. Noth, C. Tacke, M. Schmidt, H. Schwenk, *Chem. Ber.* **1997**, *130*, 1047.

[24] K. Knabel, I. Krossing, H. Noth, H. Schwenk-Kircher, M. Schmidt-Amelunxen, T. Siefert, *Eur. J. Inorg. Chem.* **1998**, 1095.

[25] T. Habereder, H. Noth, R. T. Paine, *Eur. J. Inorg. Chem.* **2007**, 4298.

[26] B. Gemund, B. Gunther, J. Knizek, H. Noth, *Z. Naturforsch. B: Chem. Sci.* **2008**, *63*, 23.

[27] K. Knabel, H. Noth, T. Siefert, *Z. Naturforsch. B: Chem. Sci.* **2002**, *57*, 830.

[28] K. Knabel, H. Noth, *Z. Naturforsch. B: Chem. Sci.* **2005**, *60*, 155.

[29] C. Klein, H. Noth, M. Tacke, M. Thomann, *Angew. Chem. Int. Ed.* **1993**, *32*, 886.

[30] W. Clegg, L. Horsburgh, S. A. Couper, R. E. Mulvey, *Acta Crystallogr.* **1999**, *C55*, 867.

[31] W. Clegg, S. H. Dale, E. Hevia, L. M. Hogg, G. W. Honeyman, R. E. Mulvey, C. T. O'Hara, L. Russo, *Angew. Chem. Int. Ed.* **2008**, *47*, 731.

[32] E. Elzein, R. Kalla, X. Li, T. Perry, E. Parkhill, V. Palle, V. Varkhedkar, A. Gimbel, D. Zeng, D. Lustig, et al., *Bioorg. Med. Chem. Lett.* **2006**, *16*, 302.

[33] D. R. Armstrong, W. Clegg, S. H. Dale, E. Hevia, L. M. Hogg, G. W. Honeyman, R. E. Mulvey, *Angew. Chem. Int. Ed.* **2006**, *45*, 3775.

[34] P. C. Andrikopoulos, D. R. Armstrong, D. V. Graham, E. Hevia, A. R. Kennedy, R. E. Mulvey, C. T. O'Hara, C. Talmard, *Angew. Chem. Int. Ed.* **2005**, *44*, 3459.

[35] D. R. Armstrong, L. Balloch, E. Hevia, A. R. Kennedy, R. E. Mulvey, C. T. O'Hara, S. D. Robertson, *Beilstein J. Org. Chem.* **2011**, *7*, 1234.

[36] D. R. Armstrong, V. L. Blair, W. Clegg, S. H. Dale, J. Garcia-Alvarez, G. W. Honeyman, E. Hevia, R. E. Mulvey, L. Russo, *J. Am. Chem. Soc.* **2010**, *132*, 9480.

[37] E. Rijnberg, J. T. B. H. Jastrzebski, J. Boersma, H. Kooijman, N. Veldman, A. L. Spek, G. van Koten, *Organometallics* **1997**, *16*, 2239.

[38] L. Balloch, A. R. Kennedy, J. Klett, R. E. Mulvey, C. T. O'Hara, *Chem. Commun.* **2010**, *46*, 2319.

[39] A. Togni, T. Hayashi, *Ferrocenes*, Wiley-VCH, Weinheim, Germany, **1995**.

[40] F. Rebiere, O. Samuel, H. B. Kagan, *Tetrahedron Lett.* **1990**, *31*, 3121.

[41] R. Sanders, U. T. Mueller-Westerhoff, *J. Organomet. Chem.* **1996**, *512*, 219.

[42] I. R. Butler, W. R. Cullen, J. Ni, S. J. Rettig, *Organometallics* **1985**, *4*, 2196.

[43] W. Clegg, K. W. Henderson, A. R. Kennedy, R. E. Mulvey, C. T. O'Hara, R. B. Rowlings, D. M. Tooke, *Angew. Chem. Int. Ed.* **2001**, *40*, 3902.

[44] P. C. Andrikopoulos, D. R. Armstrong, W. Clegg, C. J. Gilfillan, E. Hevia, A. R. Kennedy, R. E. Mulvey, C. T. O'Hara, J. A. Parkinson, D. M. Tooke, *J. Am. Chem. Soc.* **2004**, *126*, 11612.

[45] K. W. Henderson, A. R. Kennedy, R. E. Mulvey, C. T. O'Hara, R. B. Rowlings, *Chem. Commun.* **2001**, 1678.

[46] H. R. L. Barley, W. Clegg, S. H. Dale, E. Hevia, G. W. Honeyman, A. R. Kennedy, R. E. Mulvey, *Angew. Chem. Int. Ed.* **2005**, *44*, 6018.

[47] J. L. Atwood, A. L. Shoemaker, *Chem. Commun.* **1976**, 536.

[48] R. D. Rodgers, W. J. Cook, J. L. Atwood, *Inorg. Chem.* **1979**, *18*, 279.

[49] D. F. Shriver, M. A. Derezdzon, *The Manipulation of Air-Sensitive Compounds*, Wiley And Sons, New York, **1986**.

[50] G. M. Sheldrick, *Acta Cryst.* **2008**, *A64*, 112.

Chapter 3: Donor Deprotonation

3.1 Introduction

A spectacular demonstration of the special reactivity of bimetallic bases came with the α-zincation of tetrahydrofuran (THF) by the sodium dialkyl(amido)zincate [(TMEDA)Na(μ-TMP)(μ-CH_2SiMe_3)Zn(CH_2SiMe_3)] to produce [(TMEDA)Na(μ-TMP)(μ-OC_4H_7)Zn(CH_2SiMe_3)].[1] Conventional metallation of THF invariably initiates decomposition via ring opening,[2–5] but in this low polarity zincation the 5-atom ring of the sensitive α-deprotonated THF anion remains intact. Due to the surprising intramolecular aluminations of attached donors such as TMEDA[6] and anions such as TMP[7] we decided to examine the deprotonation of donor molecules by our new lithium aluminate base [Li(TMP)$_2$Al(*i*Bu)$_2$] **2.1** which has a higher amido content than the alkyl-rich zincate reagent. The question to be answered was - is it possible to intramolecularly deprotonate other donors attached to Li? Several donors were screened in this reaction ranging from polyfunctional examples such as dioxane and DABCO, to monodentate donors including THF and triethylamine.

3.2 Results and Discussion

As discussed in **Chapter 2** the base **2.1** empirically formulated as [(THF)Li(TMP)$_2$Al(*i*Bu)$_2$] can be prepared straightforwardly by mixing the commercially available chemicals *n*BuLi, TMP(H), *i*Bu$_2$AlCl, and THF in a 2:2:1:1 stoichiometry in hexane with co-products butane and lithium chloride easily separated from the mixture. Aluminate **2.1** cannot be isolated as a pure solid as it forms as an oil in hexane solution (**see Chapter 2**). Previously a modified version of it not containing THF was found to metallate TMEDA[6] so it appeared to be a good candidate bimetallic reagent to metallate other attached donors. The potency of **2.1** as a base was obvious on standing as it begins to self-metallate, by deprotonating its THF ligand (evidenced by slow growth of resonances attributed to deprotonated THF) hence THF was tested first. To accomplish the desired alumination of THF, only one molar equivalent of "reactant THF" was added to an *in situ* hexane solution of **2.1** which already contained one "ligand THF" molecule. Leaving it to stir overnight, before cooling in a freezer at -30^{o}C

afforded a crop of colourless crystals. This crystalline product (isolated yield, 35%) was subsequently characterised by X-ray crystallography, NMR spectroscopy, and elemental analysis as the lithium tetrahydro-2-furanylaluminate [(THF)Li(μ-TMP)(μ-OC_4H_7) Al(*i*Bu)$_2$], **2.2** (**Scheme 3.1**).

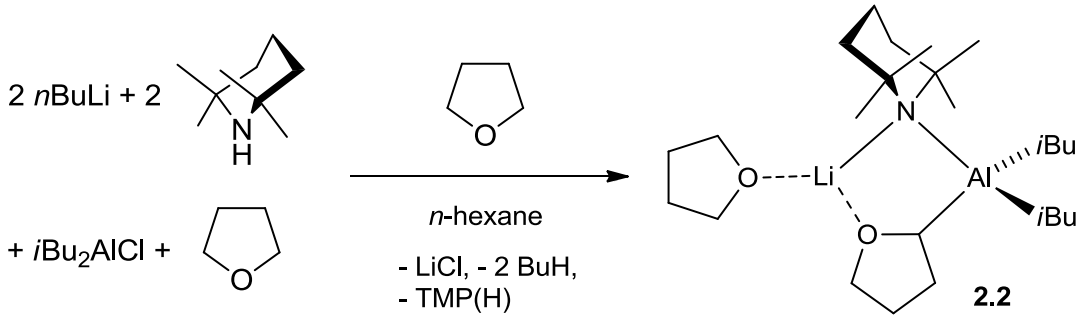

Scheme 3.1: Synthesis of complex **2.2** through reaction of stoichiometric THF with *in situ* generated **2.1**.

Crystalline **2.2** (**Figure 3.1**) exists as a discrete molecular contacted ion pair structure as elucidated by X-ray crystallography. The structure displayed extensive disorder over all organic fragments, resulting in a detailed discussion of specific bond parameters being unwarranted. However it is clear that retention of the heterocyclic OC_4 ring of THF, deprotonated at the 2-position, is the salient feature. Stabilization of the sensitive cyclic ether anion occurs through both its O atom and deprotonated α-C atom, binding to lithium and aluminium respectively. Though racemic overall, this α-C atom is rendered stereogenic on deprotonation as it bonds to four different atoms (Al, C, H, O). In addition to the THF anion bridge, lithium and aluminium are connected by the TMP N atom to complete a five-element (LiNAlCO) ring which fuses to the O-αC junction of the deprotonated THF molecule. Possessing a full complement of hydrogen atoms, a neutral, terminal THF ligand completes the distorted trigonal planar (1xN; 2xO) coordination of lithium, while two terminal *i*Bu ligands complete the distorted tetrahedral (3xC; 1xN) coordination of aluminium. The fused cyclic core architecture of **2.2** closely resembles that of [(TMEDA)Na(μ-TMP)(μ-OC_4H_7)Zn(CH_2SiMe_3)] though substitution of Na by Li and Zn by Al does force exocyclic distinctions with a monodentate THF ligand on Li replacing a bidentate TMEDA ligand on the larger Na and with the single terminal monosilyl alkyl ligand on Zn replacing the two such *i*Bu ligands on the larger Al center.

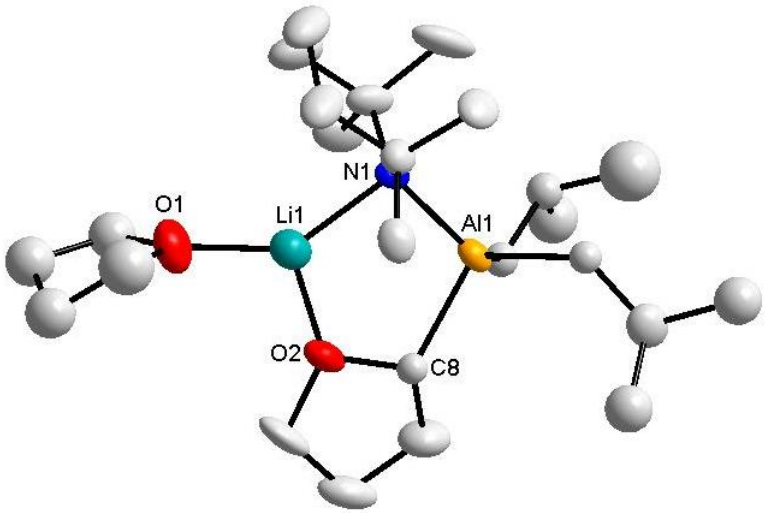

Figure 3.1: Molecular structure of **2.2** with hydrogen atoms omitted for clarity. Thermal ellipsoids are drawn at 50% probability. Selected bond lengths (Å) and angles (°): Al1-N1, 1.981(3); Al1-C8, 2.091(4); O2-C8, 1.421(5); Li1-N1, 2.024(7); Li1-O2, 1.826(7); Li1-O1, 1.896(7); C8-Al1-C(*i*Bu), 109.70(18); C8-Al1-C(*i*Bu), 101.42(17); N1-Al1-C(*i*Bu), 114.30(15); N1-Al1-C(*i*Bu), 121.32(16); N1-Al1-C8, 102.98(3); C(*i*Bu)-Al1-C(*i*Bu), 105.23(1); O2-Li1-N1, 109.3(3); O1-Li1-O2, 109.6(3); N1-Li1-O1, 110.94(3); Li1-N1-Al1, 98.53(3); Li1-O2-C8, 110.77(13).

Like the zincate example, this deprotonation and trapping is surprising as organolithium reagents deprotonate THF resulting in a carbanion in the α-position adjacent to the electron rich oxygen atom. This repulsion causes a severe destabilisation that incites the spontaneous ring opening of THF to cause decomposition. Depending on conditions and the base used, THF can decompose in different ways however, the products are commonly ethene gas and the enolate of acetylaldehyde (**Scheme 3.2**).

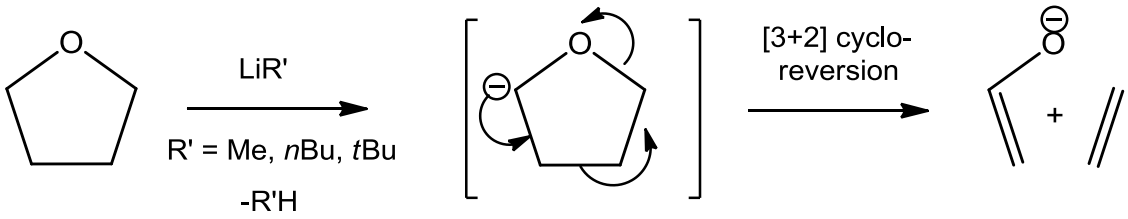

Scheme 3.2: Common metallation-induced decomposition pathway of THF via organolithium reagents.

This new aluminium trapping of THF has a number of significant advantages over the zincate method. Firstly, the reaction is fast and only takes a couple of hours to obtain a reasonable crystalline yield of 35 %. A ^{1}H NMR spectrum of the reaction filtrate reveals that much more of the compound remains in solution due to its high solubility in hexane

so its absolute yield is significantly higher. In stark contrast the zinc analogue takes a total of two weeks to obtain a yield of 52 %. Secondly, the reaction can be heated to reflux for two hours and still produces the compound in a reasonable crystalline yield. Normally a THF anion would decompose rapidly at these high temperatures so the high stability of this system is noteworthy. Thirdly, the most important advantage is that the reaction is stoichiometric as only two molar equivalents of THF are required. The zinc reaction, on the other hand, requires a bulk THF solvent system. Lastly, all of the reagents used in the alumination approach are commercially available whereas several days are required to prepare the zinc starting materials *n*BuNa and (TMEDA)Zn(CH_2SiMe_3)$_2$. The stoichiometric nature, commercial availability of starting materials and speed of reaction marks this alumination reaction as a significant improvement over the zincation method.

Aluminate **2.2** was also characterized in d_{12}-cyclohexane solution by ^{1}H and ^{13}C NMR spectroscopy with all resonances easily assignable with the assistance of both COSY and HSQC spectra. Of principal importance was the resonance of the hydrogen on the metallated C atom at 2.96 ppm which is shielded by the metal (highlighted in red in **Figure 3.2**).

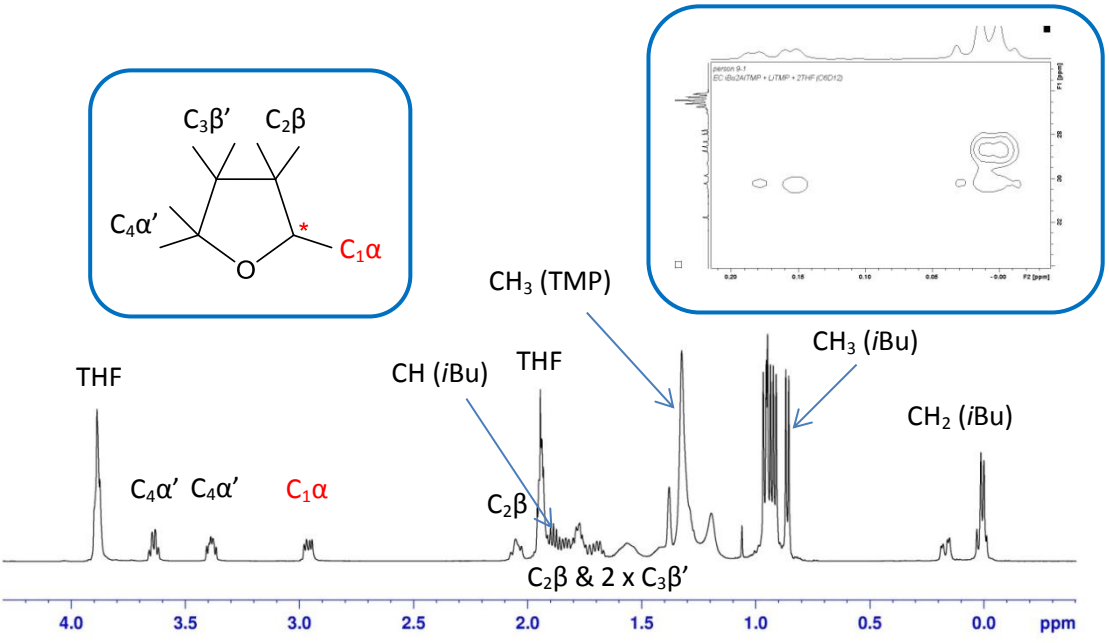

Figure 3.2: ^{1}H NMR spectrum of [(THF)Li(μ-TMP)(μ-C_4H_7O)Al(*i*Bu)$_2$] **2.2** in C_6D_{12} (β and γCH_2 proton labels of TMP have been omitted for clarity) with expansion of HSQC (inset) showing splitting of one CH_2 group. Note that the two *i*Bu CH_2 groups separate into two distinct resonances which have an integration of 1:3. HSQC experiment (inset) shows that one of the groups has inequivalent protons (as a

possible consequence of being closer to stereogenic C8 of the deprotonated THF group) and the other CH_2 resonance is at a coincidental chemical shift.

For more solution structural elaboration **2.2** was also studied using diffusion-ordered NMR spectroscopy (DOSY).[8] A ^{1}H DOSY NMR spectrum run at 300K (**Figure 3.3**) reveals cross points for all ligand (THF, TMP, C_4H_7O, *i*Bu) resonances of **2.2** approximately in the same line of the second dimension (average diffusion coefficient, D, 5.42±9 x 10^{-10} m^2s^{-1}). Consistent with all four ligands belonging to the same molecule, this observation implies the solid state structure of **2.2** is retained in this solution medium.[9] It does not break up into separated ion pairs as would be implied by observing different diffusion coefficients.

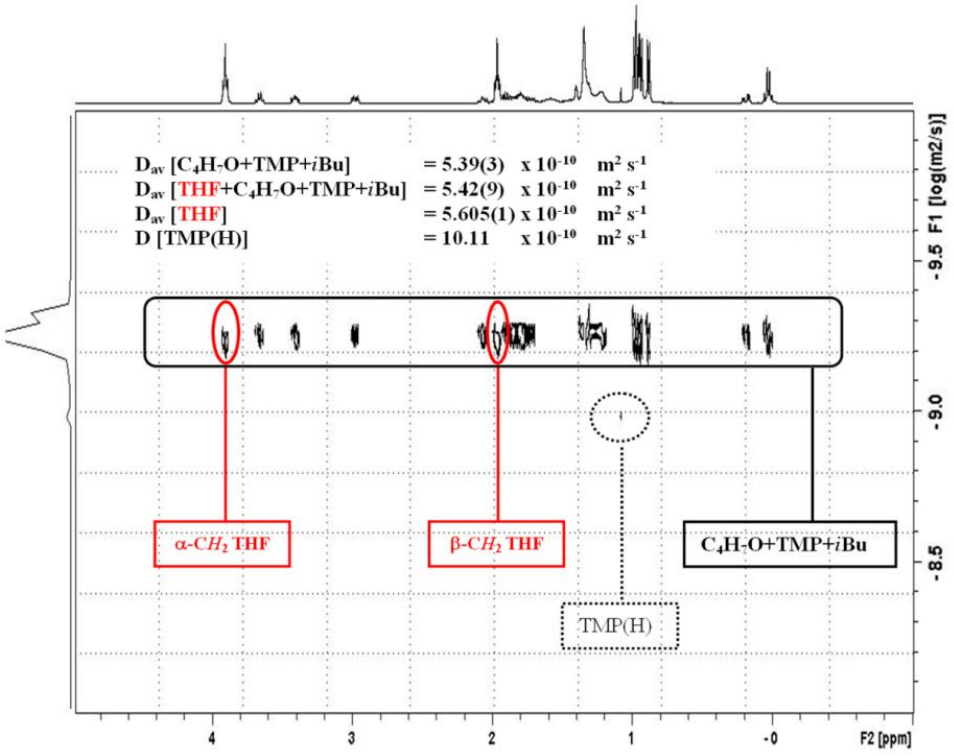

Figure 3.3: ^{1}H DOSY-NMR spectrum of **2.2** (50 mg) at 300 K in C_6D_{12} (0.7 mL). X-axis represents the ^{1}H chemical shift, and y-axis represents the diffusion dimension (log D).

Closer inspection of the DOSY NMR data hints at an equilibrium involving a fast decoordination-recoordination of the neutral THF ligand attached to Li as its D value (5.605±1 x 10^{-10} m^2s^{-1}) is slightly higher than the average D value of the other three ligands (5.39±3 x 10^{-10} m^2s^{-1} for TMP, C_4H_7O and *i*Bu), a possibility supported by the broadness of the singlet in the ^{7}Li NMR spectrum. The fact that the D_{av} of neutral THF is far away from the diffusion coefficient expected for free THF (see in **Figure 3.3** how

a larger molecule than free THF, namely TMP(H), arising from a trace amount of hydrolysis, has a much higher D value of 10.11 x 10^{-10} m^2 s^{-1}), indicates how this equilibrium is strongly displaced to the retention of **2.2** in solution.

Further evidence for the predominant retention of the solid state structure of **2.2** in d_{12}-cyclohexane solution came from ^1H-^7Li heteronuclear NOE (HOESY)[10] experiments which show a good accordance between the H…Li separation distances in the crystal structure and the intensities of the ^1H-^7Li NOE responses (**Figure 3.4** and **Table 3.1**).

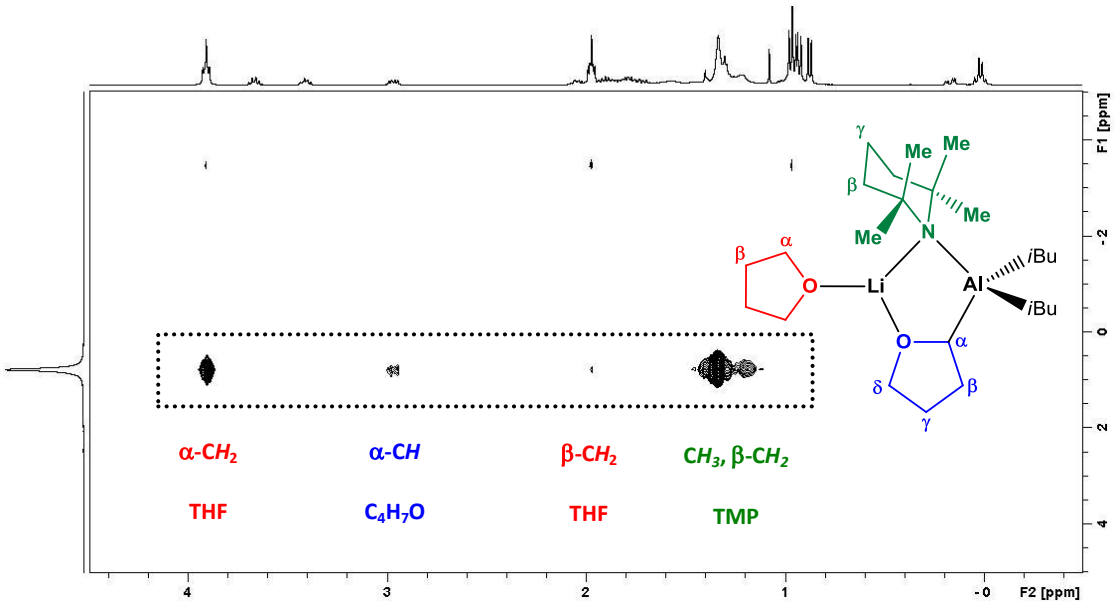

Figure 3.4: $^1H\{^7Li\}$ HOESY-NMR spectrum of the complex **2.2** (100 mg) at 300 K in C_6D_{12} (0.7 mL). Picture is amplified, from absence of signal, two (top) and three (bottom) times.

Table 3.1: Average shortest H···Li contacts distances (Å) in the solid X-ray structure of **2.2** and qualitative $^1H\{^7Li\}$HOESY response.

Li-H interaction	d(Å)	$^1H\{^7Li\}$HOESY response
CH_3-TMP	2.32(6)	very strong
β-CH_2-TMP	2.70(2)	strong
α-CH_2-THF	2.90(20)	strong
α-CH-C_4H_7O	3.07(20)	medium
δ-CH_2-C_4H_7O	3.31(12)	very weak
β-CH_2-THF	4.26(20)	weak
β-CH_2-C_4H_7O	4.11	not observed

CH_2-*i*Bu	4.12(31)	very weak
γ-CH_2-TMP	4.38	non observed
γ-CH_2-C_4H_7O	4.77(9)	non observed
C*H*-*i*Bu	5.30(20)	non observed
CH_3-*i*Bu	5.60(31)	non observed

Other more sterically demanding ethers such as 2-methyltetrahydrofuran, tetrahydropyran (THP) and oxepane were also reacted with base **2.1**. Crystals were obtained from the reactions of 2-methyltetrahydrofuran (compound **2.3**) and THP (compound **2.4**). The molecular structure of **2.3** (**Figure 3.5**) was highly disordered so a detailed discussion is unwarranted, it does however, show us that THF is deprotonated preferentially over 2-methyltetrahydrofuran which instead acts as the donor ligand to give [(2-MeTHF)Li(μ-TMP)(μ-C_4H_7O)Al(*i*Bu)$_2$]. The reason for this comes from the extra steric bulk attributed to the methyl group attached to the 2-position.

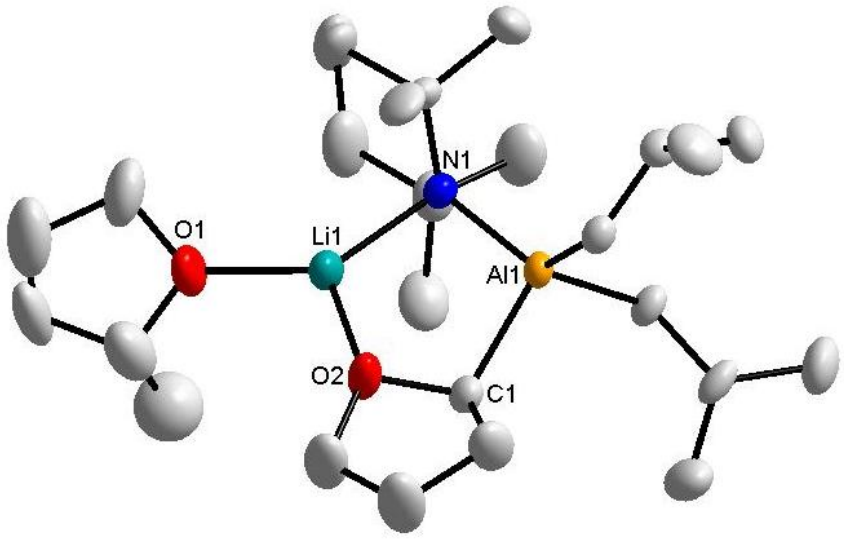

Figure 3.5: Molecular structure of α-aluminated THF/donor 2-methylTHF compound **2.3**.

Compound **2.4** was also obtained in crystalline form however, these were of poor quality and an X-ray crystal structure could not be obtained. The ^{1}H NMR spectrum in C_6D_{12} (**Figure 3.6**) of these crystals reveals that **2.4**, analogous to **2.2**, contains an α-deprotonated cyclic ether molecule and one donor THF molecule, confirming that it is possible to deprotonate bigger cyclic ether molecules without ring opening. This is

evidenced by the identification of the 9 individual proton resonances on the deprotonated cyclic ring. The ^{1}H NMR spectrum shows the same splitting of the isobutyl protons as was observed for **2.2**. It is assumed that **2.4** will adopt the same structure as **2.2** with the only difference being the incorporation of an additional CH_2 group into the cyclic ring.

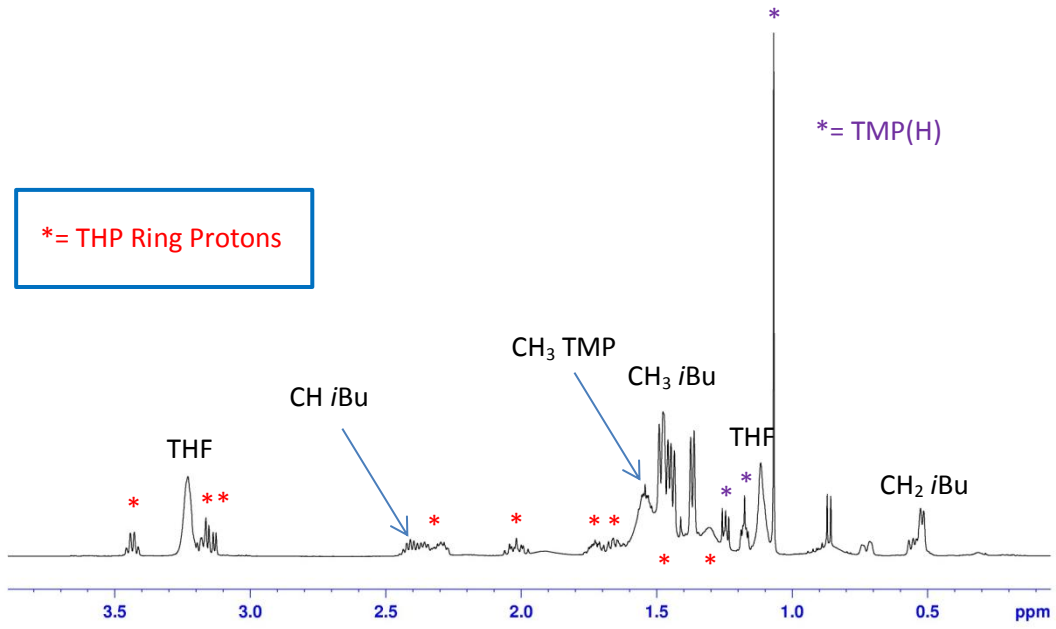

Figure 3.6: ^{1}H NMR spectrum in C_6D_{12} of α-aluminated THP compound **2.4** (β and γCH_2 protons of TMP have been omitted from labelling for clarity).

Since THF and THP can be readily deprotonated by **2.1** without ring opening decomposition, its reactivity was considered against other difficult to deprotonate and trap, but synthetically useful substrates. Thioethers were considered as the next logical step since these sulphur compounds suffer from the same problems as THF. The problem arises due to the combination of low thermodynamic stability of the resulting carbanion upon deprotonation and the moderate kinetic activity of the α-CH_2 group adjacent to the sulfur atom. The sulfur heterocycle tetrahydrothiophene (THT) was considered first and this was also smoothly aluminated by **2.1** with retention of its α-deprotonated anionic SC_4H_7 ring in the crystalline product [(THF)Li(μ-TMP)(μ-SC_4H_7)Al(iBu)$_2$], **2.5**. This was confirmed by ^{1}H and ^{13}C NMR spectroscopy which showed no evidence of deprotonated THF (*cf.* complex **2.2**) or "ligand" THT. Mimicking the synthesis of **2.2**, this reaction was also stoichiometric, thus involving a 1:1 mixture of

THF (present in *in situ* generated **2.1**) and THT. The latter heterocycle is aluminated as seen through the molecular structure of **2.5** (crystalline yield = 34%) and from NMR analysis of the reaction filtrate which suggested that the reaction was virtually quantitative. Contrary to the ease in which it is accomplished here, THT is usually challenging to metallate on account of the low kinetic acidity of its α-CH_2 atoms. Previously Glass reported[11] that metallation was possible with superbasic *n*BuLi/KO*t*Bu at -40^{o}C though the Li/K-metallated intermediate decomposed completely to a thioenolate and ethene at 5^{o}C. Obviously, carrying out reactions at these low temperatures incurs huge costs when undertaking them on a large scale for example when preparing pharmaceuticals. Magnesiation of THT is also possible via [(TMEDA)Na(μ-TMP)(μ-CH_2SiMe_3)Mg(TMP)][12] but similar to the disadvantages of the aforementioned zincate base the components of this sodium magnesiate base *n*BuNa and $Mg(CH_2SiMe_3)_2$ have to be preprepared. From a search of the literature and Cambridge Crystallographic Database (CCDB)[13] there is only one other structurally characterised THT complex known out with our own research group, namely the triosmium complex $[Os_3(CO)_{10}(C_4H_7S)(\mu\text{-}H)]$ which was isolated as an intermediate during the ring opening of THT.[14] Aluminated thiophene **2.5** has been characterized by ^{1}H and ^{13}C NMR spectroscopy in d_{12}-cyclohexane solution. The ^{1}H NMR spectral data (**Figure 3.7**) fits the molecular structure and clearly shows the presence of the seven individual hydrogen atoms remaining on the deprotonated THT ring. Each ^{1}H resonance is split due to the chirality of the α-C atom. All of the resonances were assigned quantitatively using ^{1}H-^{1}H COSY NMR techniques. The ^{1}H NMR spectrum shows no evidence of THF deprotonation or donor THT.

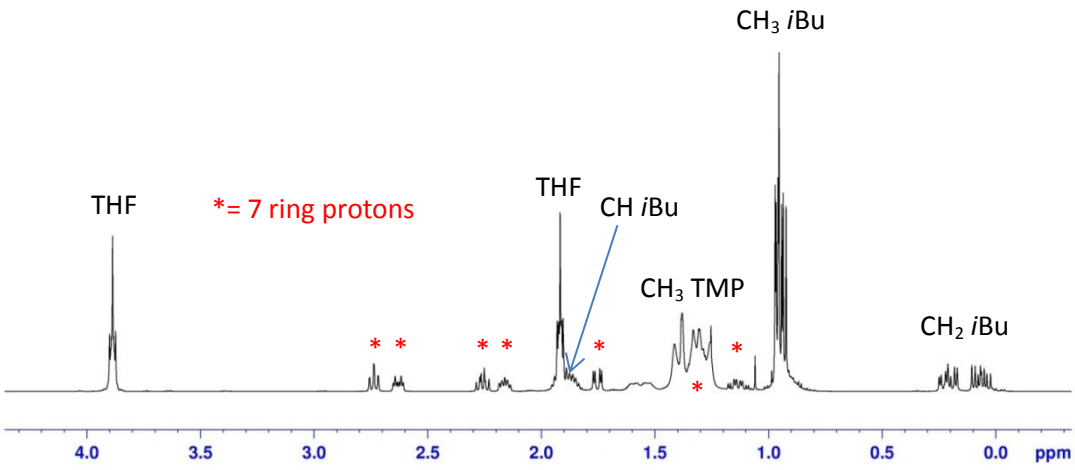

Figure 3.7: ^{1}H NMR spectrum of [(THF)Li(μ-TMP)(μ-C_4H_7S)Al(*i*Bu)$_2$] **2.5** in C_6D_{12} (β and γCH_2 protons of TMP have been omitted from labelling for clarity).

As with **2.2**, the proton bound to the aluminated carbon resonates upfield at 1.75 ppm. Determined by X-ray crystallography, the molecular structure of **2.5** (**Figure 3.8**) is essentially identical to that of **2.2** with retention of the α-deprotonated anionic ring with a Li-S dative bond instead of a Li-O dative bond closing its five-element (LiNAICS) ring. As with **2.2** deprotonation at the α-C atom generates a stereogenic centre with C, H, S and Al, though overall the crystals are racemic. The Li-S [2.414(4)Å] and Li-O [1.925(6)Å] bond lengths are in accord with those seen in an α-metallated 1,3-dithiane which also contains an S-coordinated Li(THF) fragment.[15] This confirms our assertion that metallation has occurred exclusively to the thiophene and that no mutual substitution disorder exists between the THF and THT.

THT was also added to the reaction mixture in reverse order (that is prior to THF addition) to establish if THF would deprotonate preferentially. As expected THT was still deprotonated over THF generating **2.5**. It is thought that the Li atom prefers smaller and harder donors such as oxygen than larger and softer donors such as sulfur.

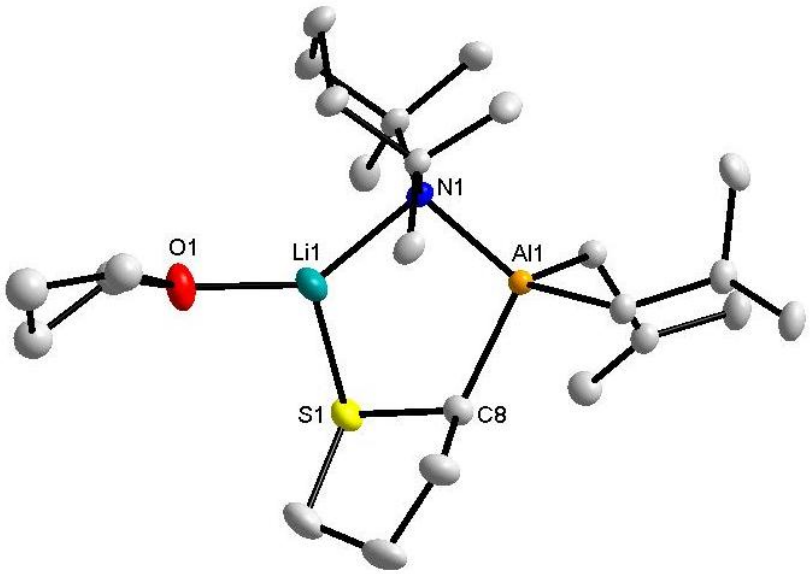

Figure 3.8: Molecular structure of **2.5** with hydrogen atoms omitted for clarity. Thermal ellipsoids are drawn at 50% probability. Selected bond lengths (Å) and angles (°): Li1-O1 1.925(6), Li1-S1 2.413(3), Li1-N1 2.025(5), S1-C8 1.829(2), Al1-C8 2.054(2), Al1-N1 1.979(2); C(*i*Bu)-Al1-C8, 109.21(5); C(*i*Bu)-Al1-C8, 101.83(4); N1-Al1-C8, 105.74(5); N1-Al1-C(*i*Bu), 116.75(4); N1-Al1-C(*i*Bu), 119.13(5); C(*i*Bu)-Al1-C(*i*Bu), 102.99(3); N1-Li1-O1 138.9(2), N1-Li-S1 111.3(2), O1-Li1-S1 108.5(2).

Other thioethers were also tested with **2.1** including the more sterically demanding tetrahydrothiopyran (THTP). THTP was added to base **2.1** in a 1:1 stoichiometry and the solution was allowed to stir overnight. Colourless crystals were grown from solution at -30°C and these were subjected to X-ray crystallographic analysis. The structure was found to be the new THTP deprotonated complex **2.6** [(THF)Li(μ-TMP)(μ-C_5H_9S) Al(*i*Bu)$_2$] obtained in a good crystalline yield of 60 %. The molecular structure of **2.6** (**Figure 3.9**) bears a close resemblance to aluminate **2.5** with the only difference being an additional CH_2 group within the cycloanionic ring. This is analogous to **2.4** where the ^{1}H NMR spectrum showed that it was possible to deprotonate the 6-membered cyclic ether THP. Analogous to **2.5** its salient feature is the presence of a central 5-membered 5-element LiNAlCS ring. Deprotonation at the α-C atom [C9] once again generates a stereogenic centre though overall the crystals are racemic. The Al-αC bond length in **2.5** [2.056(2)Å] is in good agreement with the Al-αC bond length in **2.6** [2.067(2)Å]. Additionally, the Li-S bond lengths are also in good agreement as expected e.g. [2.414(4)Å] **2.5** and [2.451(5)Å] **2.6**.

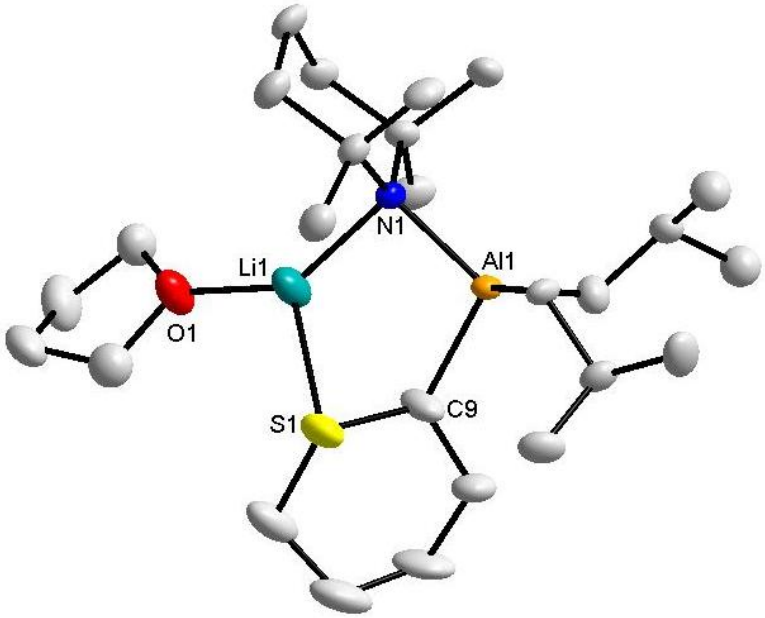

Figure 3.9: Molecular structure of **2.6** [(THF)Li(μ-TMP)(μ-C_5H_9S)Al(*i*Bu)$_2$] with selective atom labelling. Hydrogen atoms omitted for clarity. Selected bond lengths [Å] and bond angles [°]: Al1-N1, 1.992(2); Al1-C9, 2.067(2); Li1-N1, 2.046(5); Li1-S1, 2.451(5); Li1-O1, 1.892(5); S1-C9, 1.812(3); C9-Al1-C(*i*Bu), 98.77(11); C9-Al1-C(*i*Bu), 113.27(11); N1-Al1-C(*i*Bu), 120.96(10); N1-Al1-C(*i*Bu), 115.50(9); C(*i*Bu)-Al1-C(*i*Bu), 104.51(5); N1-Al1-C9, 102.79(11); Li1-N1-Al1, 41.87(11); O1-Li1-N1, 140.2(3); O1-Li1-S1, 108.34(19); N1-Li1-S1, 110.7(2); Li1-S1-C9, 74.54(6); S1-C9-Al1, 114.63(13).

The key feature of the ^{1}H NMR spectrum of **2.6** (**Figure 3.10**) in C_6D_{12} solution is the presence of the individual proton resonances corresponding to those attached to the trapped THTP ring as seen previously in compounds **2.2**, **2.4** and **2.5**. The splitting of these proton resonances is again due to the chirality of the α-C atom.

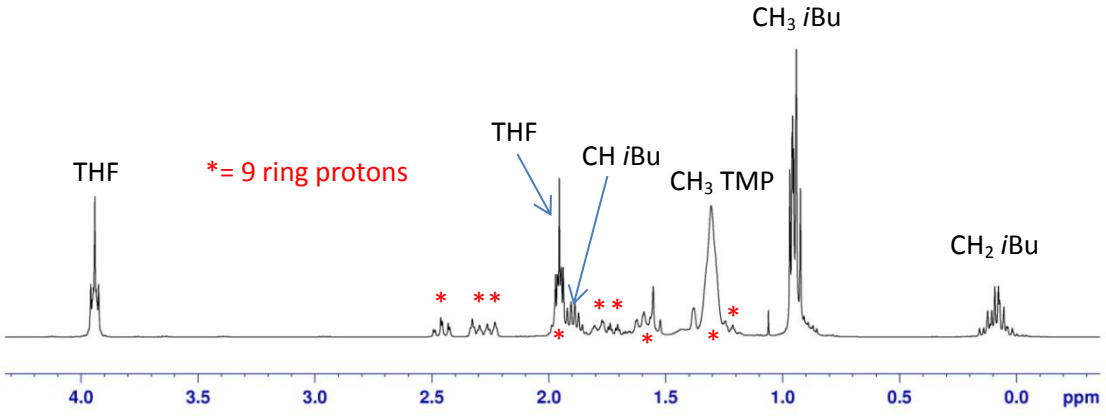

Figure 3.10: ^{1}H NMR spectrum of compound **2.6** [(THF)Li(μ-TMP)(μ-C_5H_9S)Al(*i*Bu)$_2$] in C_6D_{12} solution (β and γCH_2 protons of TMP have been omitted from labelling for clarity).

A search of the CCDB confirms that aluminate **2.6**, to the best of our knowledge, is the only example of a crystallographically characterised metal complex containing an intact deprotonated THTP ring. The lack of such probably reflects the high sensitivity and instability of this heterocyclic anion. In it important to note at this stage that all reactions are carried out at room temperature hence these systems are highly stable. Deprotonation of THT and THTP by Glass[11] required low temperatures to supress the ring opening decomposition of these substrates.

Moving to alternative di-sulphur compounds, 1,3- and 1,4-dithiane were also reacted with **2.1**. 1,3-Dithiane is an important molecule in natural and unnatural product synthesis.[16–20] It is widely used as a protecting group for carbonyl compounds[21–23] and can be used to functionalise such compounds due to the concept of umpolung (reversal of charge) first introduced by Wittig in 1921.[24] Seebach reintroduced this concept in 1974 and described it in terms of a dipole inversion.[25] The carbon atom of a carbonyl group is electrophilic however, once protected by a molecule such as 1,3-dithiane and subsequently lithiated (equivalent to an acyl anion), the carbon atom becomes nucleophilic hence the charge has been revered. This then allows this carbon atom to be subsequently functionalised with a series of electrophiles.[26,27] The carbonyl functionality can be recovered using various methods[28,29] including *N*-halosuccinimide reagents,[30] methyl iodide in wet acetone[31] or *bis*-(trifluoroacetoxy)iodobenzene.[32] Of the reactions tested only the 1,3-dithiane reaction produced a crystalline material which could be crystallographically characterised with the 1,4-dithiane reaction showing only unreacted starting material in the ^{1}H NMR spectrum of the reaction filtrate. 1,3-Dithiane was added to base **2.1** in the usual 1:1 stoichiometry which produced a white precipitate almost immediately. The white solid was filtered and the remaining filtrate was allowed to stand at room temperature. Long colourless needle crystals were grown from this filtrate and subjected to X-ray crystallographic analysis. As expected the compound was revealed to be one incorporating a deprotonated 1,3-dithiane molecule giving [(THF)Li(μ-TMP)(μ-$C_4H_7S_2$)Al(*i*Bu)$_2$] **2.7** in a crystalline yield of 42%. Deprotonation was found to occur at the most acidic methylene site between the two sulphur atoms.

The most important feature of the molecular structure of **2.7** (**Figure 3.11**) is the presence of a deprotonated 1,3-dithiane ring adopting a chair conformation. It embraces this structure so that Li can form a dative bond to both S atoms. In doing so it forms two

distorted 5-element 5-membered LiNAlCS rings. Li and Al are connected in the usual way to the N atom of TMP and also to the opposite bridge by means of one C and two S atoms of the 1,3-dithianyl anion. The sulfur rings of the lithiated 1,3-dithiane compounds [(TMEDA)(THF)Li{C(Ph)-$S_2C_3H_6$}][33] and [(TMEDA)Li{C(Me)-$S_2C_3H_6$}]$_2$[34] also adopt a chair conformation however, there are no dative S-Li bonds showing that the 1,3-dithiane ring, similar to TMP, readily adopts this conformation. Due to the poor quality of the X-ray data a detailed discussion and comparison of bond lengths and angles cannot be given but the molecular structure diagram (**Figure 3.11**) clearly illustrates that it is possible to deprotonate and trap other sulfur containing heterocycles using our *bis*-TMP aluminate base **2.1**. Unlike THT and THTP which cannot be functionalised once deprotonated due to ring opening, 1,3-dithiane doesn't suffer the same limitation and can be readily deprotonated and functionalised at the acidic methylene site between the two S atoms. 2-Substituted 1,3-dithianes can be prepared by various routes either from the reaction of propane-1,3-dithiol with aldehydes,[35] 2-chloro-1,3-dithiane and Grignard reagents[36] or from 2-lithiated 1,3-dithianes and various electrophiles as discussed above.[28]

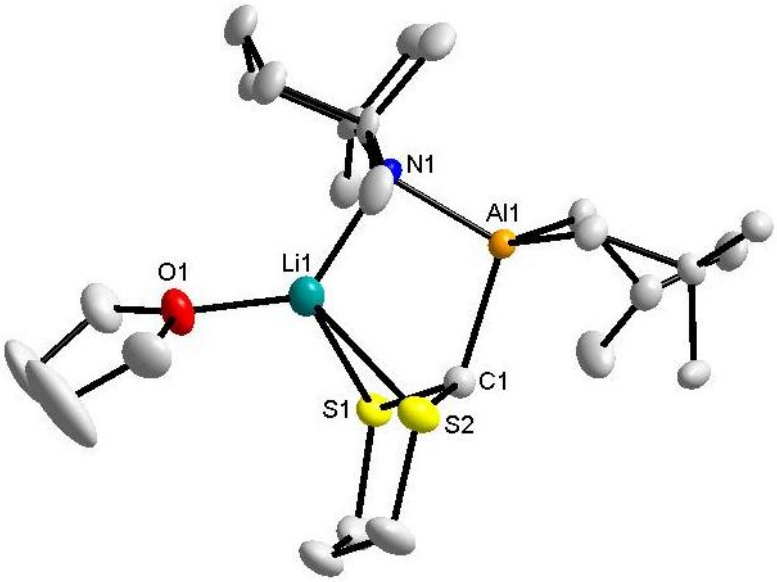

Figure 3.11: Molecular structure of **2.7** [(THF)Li(μ-TMP)(μ-$C_4H_7S_2$)Al(*i*Bu)$_2$] with selective atom labelling. Hydrogen atoms omitted for clarity. Thermal ellipsoids are drawn at 50% probability.

The ^{1}H NMR spectrum of **2.7** (**Figure 3.12**) in C_6D_{12} solution shows the expected CH_2 resonances of the 1,3-dithiane ring at 1.30, 2.06 and 2.37 ppm with the remaining proton between the two sulfur atoms shifted considerably downfield at 3.61 ppm with respect to the CH_2 hydrogen atoms due to shielding by the adjacent Al atom.

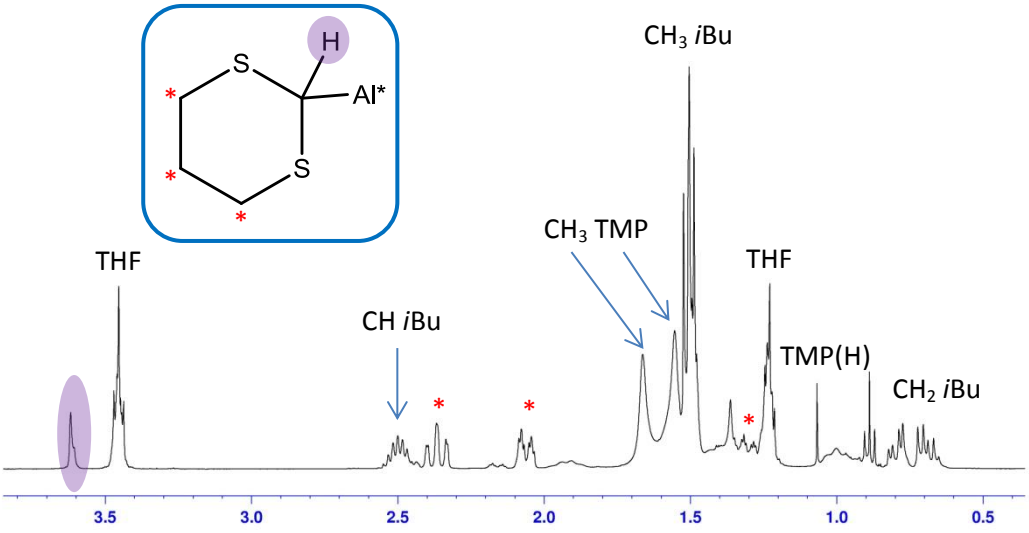

Figure 3.12: ^{1}H NMR spectrum of **2.7** in C_6D_{12} solution (β and γCH_2 protons of TMP have been omitted from labelling for clarity).

Surveying recently reported structurally defined *bis*-TMP aluminate reactions it is clear that the molecular design of the base (**Scheme 3.3**) can be tuned to effect special metallations in different ways. Small ligand caps on the alkali metal (AM) would enable a substrate to pre-coordinate to AM before being pushed into the base zone (**Path A**) to undergo deprotonation and trapping. The new reactions disclosed thus far in this chapter come into this category. Alternatively (**Path B**) a larger cap on a small AM can encroach into the base zone and become deprotonated itself. Combining TMEDA with lithium instigates this reactivity to trap a $Me_2NCH_2CH_2N(Me)CH_2^-$ anion.[6] Enlarging the size of AM can promote a third scenario (**Path C**). Sterically demanding base ligands can collide as the homometallic components approach each other, leading to novel C-H bond activations/cleavages with anions. The strong Brønsted base TMP^- can be transformed to a Brønsted acid through deprotonation of a methyl sidearm by such action to generate a trapped N^-, C^- dianion.[7] All of these structurally engineered deprotonations lead to heteroanionic aluminates. The next challenge will be to find the

best ways to utilise them in C-C bond forming applications[37] and to synthesise homoanionic analogs for maximum atom efficiency.

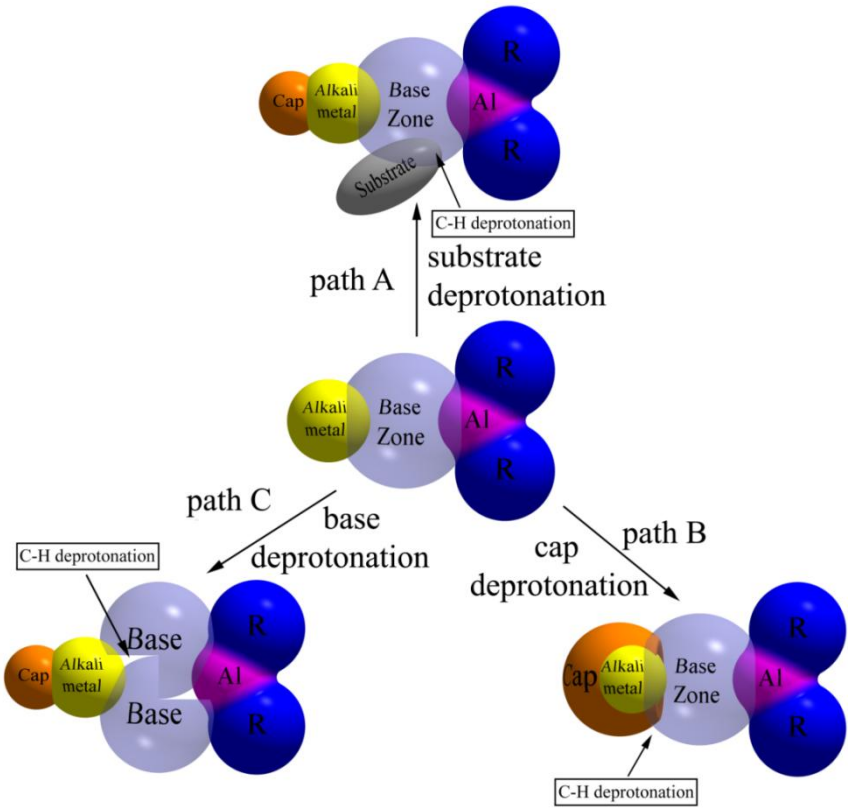

Scheme 3.3: Tuning different selective deprotonations via an alkali metal aluminate motif.

On considering the preceding results in the field of AMM*Al* (*vide supra*) we feel that an important question is worth asking: why is Uchiyama's lithium aluminate [Li(TMP)Al(*i*Bu)$_3$] **2.8** stable indefinitely in THF solution yet a hexane solution of the closely related base **2.1** will deprotonate a stoichiometric amount of THF to yield [(THF)Li(μ-TMP) (μ-OC$_4$H$_7$)Al(*i*Bu)$_2$] **2.2**? To try and elucidate a possible answer we carried out a series of density functional theory (DFT) calculations, which coupled with other experimental observations, allow us to propose a potential rationale for the witnessed reactivity described above. DFT calculations were performed using the Gaussian 03 package with geometry optimization using the B3LYP density functionals[38–40] and the 6-311(*d*,*p*) basis set.[41,42]

Despite the preparation of **2.1** from its component homometallic parts being energetically unfavourable (see **Chapter 2**), a calculation of the same starting materials to give the THF deprotonated species **2.2** was carried out (**Equation 3.1**). This confirms

that the preparation of this complex is favourable and can perhaps be attributed to the formation of a five-membered LiNAlCO ring in place of the open structure proposed for species **2.1** in **Chapter 2**.

$$1/2\ [LiTMP{\cdot}THF]_2 \ + \ THF{\cdot}Al(TMP)iBu_2$$

$$\longrightarrow \ THF{\cdot}Li(TMP)(C_4H_7O)AliBu_2\ (\mathbf{2.2}) \ + \ TMP(H) \qquad (\mathbf{3.1})$$

$$\Delta E \ = \ -5.30\ kcal\ mol^{-1}$$

With this additional information supporting the proposed open structure of **2.1**, we are now in a position to propose a hypothetical mechanism for the synthesis of **2.2**. If **2.1** prevails in an open form such as displayed in **Figure 3.13**, a vacant coordination site on lithium would exist on which a second molecule of THF could attach via its Lewis donating oxygen centre. Consequently, the close proximity of this second THF molecule to the *pseudo*-terminal Al bound TMP anion could result in attack at the α-C-H unit by the amido base, giving the energetically favourable complex **2.2** as the thermodynamic product with elimination of TMP(H).

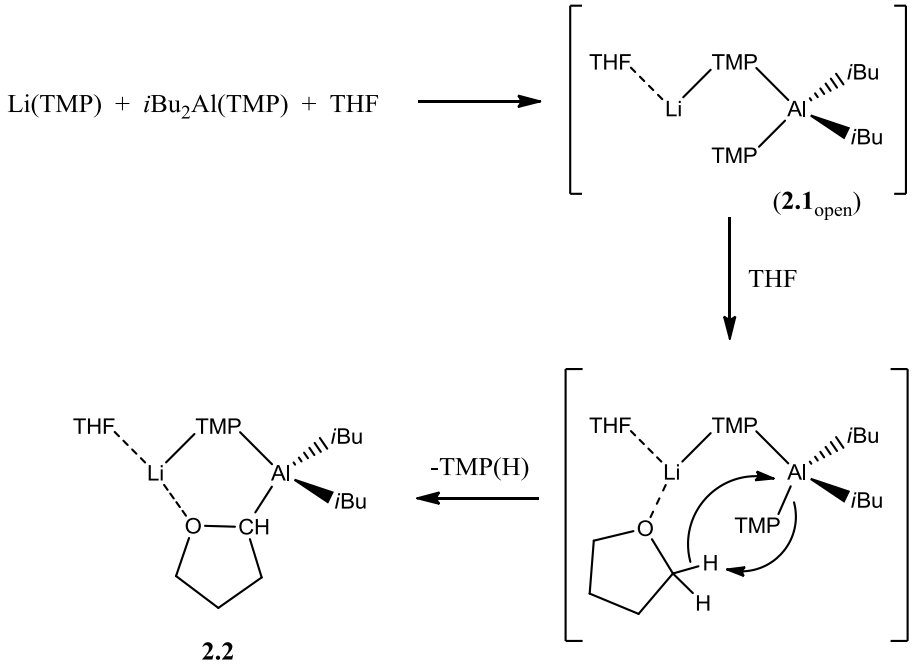

Figure 3.13: Proposed open structure of the putative *bis*-amido *bis*-alkyl lithium aluminate **2.1** with a possible mechanism giving complex **2.2**.

3.2.1 Oxiranes

Due to the successful metallation and trapping of 5- and 6-membered ethers and thioethers the final type of substrate we decided to test with base **2.1** was a series of 3-membered cyclic oxiranes containing an O-CH_2-CH_2 ring. Epoxides (oxiranes) are very important intermediates in organic synthesis as they can be transformed into a variety of functional groups such as alcohols, diols, alkanes, alkenes, aldehydes and ketones.[43] *Trans*-silbene oxide (the oxirane scaffold with two phenyl groups *trans* to one another) was tested first and was added to **2.1** in a 1:1 stoichiometry and left to stir overnight. Colourless crystals were grown from the solution on cooling to -30^{o}C and subjected to X-ray crystallographic analysis. It was thought that the strained 3-membered ring would not remain intact if deprotonated and as expected the compound was found to be one incorporating a deprotonated and ring opened oxirane giving [(THF)Li(μ-TMP)(μ-OCH=CPh_2)Al(*i*Bu)$_2$] **2.9** in an excellent crystalline yield of 74%. The molecular structure of **2.9** (**Figure 3.14**) shows that the phenyl group from C1 has migrated onto C2 resulting in a double bond between the carbon atoms.

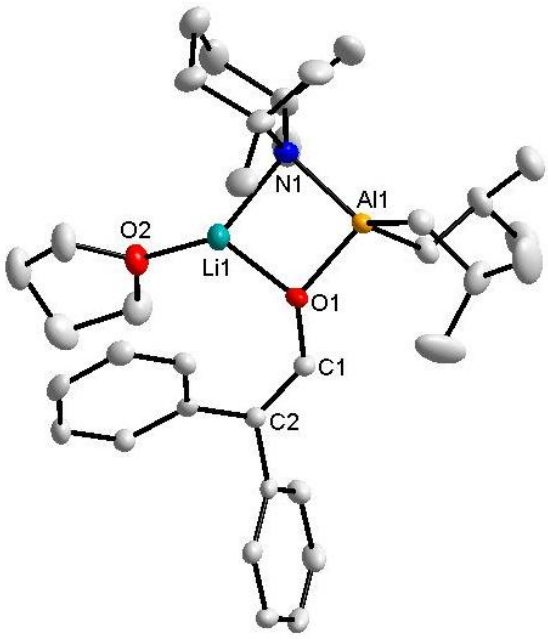

Figure 3.14: Molecular structure of **2.9** [(THF)Li(μ-TMP)(μ-OCH=CPh_2)Al(*i*Bu)$_2$] with selective atom labelling. Hydrogen atoms omitted for clarity. Selected bond lengths [Å] and bond angles [^{o}]: Al1-N1, 1.9423(19); Al1-O1, 1.8465(15); Li1-N1, 2.056(4); Li1-O2, 1.894(4); Li1-O1, 1.886(4); O1-C1, 1.3453(0); C1-C2, 1.3478(0); O1-Al1-C(*i*Bu), 101.0(1); O1-Al1-C(*i*Bu), 112.7(1); N1-Al1-C(*i*Bu), 124.9(1); N1-Al1-C(*i*Bu), 115.7(1); C(*i*Bu)-Al1-C(*i*Bu), 107.9(1); N1-Al1-O1, 91.80(7); Li1-N1-Al1, 85.95(1); O2-Li1-N1, 139.2(2); O2-Li1-O1, 127.0(2); N1-Li1-O1, 87.21(17); Li1-O1-Al1, 93.86(1).

Instead of Al bonding to the deprotonated C as seen before it bonds to the O of the oxirane trapping it as a bridging anion. The rest of the structure is made up in the typical way with terminal *i*Bu groups on Al, a bridging TMP anion between Li and Al and a solvating THF donor ligand on Li.

The ^{1}H NMR spectrum in C_6D_6 solution shows the expected resonances for the *i*Bu and TMP protons at 0.70 and 1.45 ppm respectively. The aromatic protons of the two phenyl rings come at 6.89 ppm for the two *para* protons, 7.05 and 7.14 ppm for the four *meta* protons and 7.35 and 7.58 ppm for the four *ortho* protons. The remaining proton attached to the alkene C adjacent to O comes at 7.50 ppm.

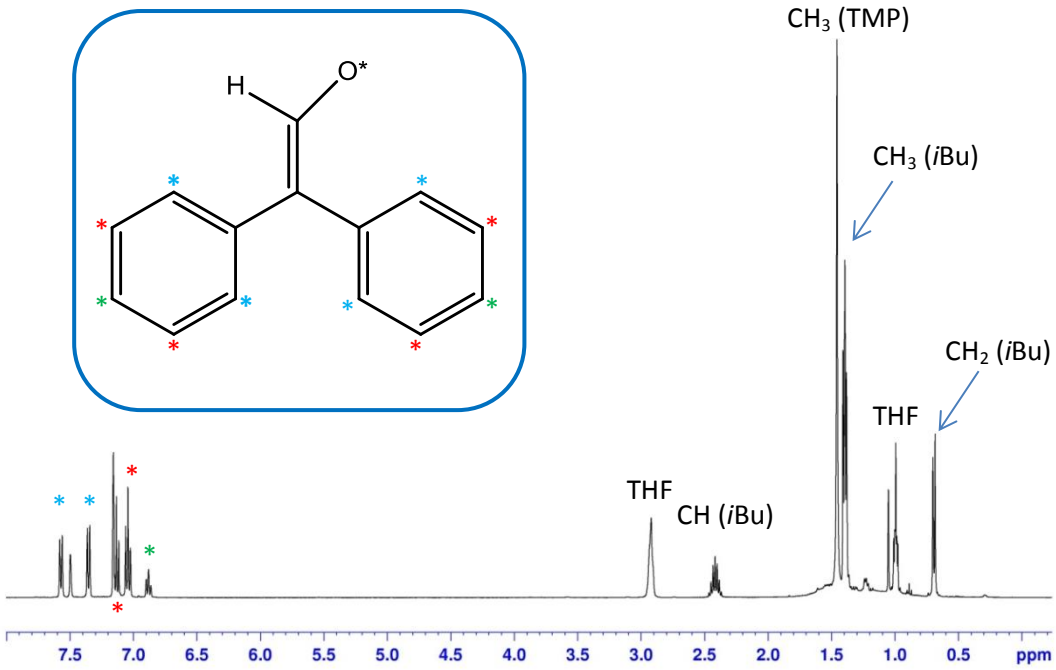

Figure 3.15: ^{1}H NMR spectrum of **2.9** [(THF)Li(μ-TMP)(μ-OCH=CPh$_2$)Al(*i*Bu)$_2$] in C_6D_6 solution (β and γCH$_2$ protons of TMP have been omitted from labelling for clarity.

Although the migration of the phenyl group was initially unexpected a search of the literature revealed that it is known. Acid-catalysed rearrangement of epoxides to carbonyl compounds (Meinwald rearrangement)[44] is well known[45–47] and several reagents have been utilised for this purpose including $BF_3{\cdot}Et_2O$,[48] lithium salts ($LiBr{\cdot}Bu_3PO$, $LiClO_4$ and LiBr·HMPA),[49,50] $Pd(AcO)_2$,[51] $Bi(OTf)_3$,[52] $MgBr_2$,[53] and $InCl_3$.[54] The rearrangement of epoixdes can be utilised in natural product synthesis.[55–58] The product distribution (aldehyde or ketone), regio- and stereoselectivity of the rearrangement is dependent upon the Lewis acid reagent, migrating substituents on the

epoxide and the solvent employed in the reaction.[59] Aldehydes are generated via alkyl or aryl migration and ketones via hydrogen migration. Although many reagents have been exploited for the transformation of epoixdes into ketones only a few examples have been documented on alkyl migration that allows access to aldehydes namely utilising the bulky organoaluminium Lewis acid reagent methylaluminium *bis*(4-bromo-2,6-di-*tert*-butylphenoxide),[60,61] $Ga(OTf)_3$[62] and more recently the catalytic metalloporphyrin complex Cr(TPP)OTf (TPP = tetraphenylporphyrin and OTf = triflate [$CF_3SO_3^-$]).[63]

In addition to acid-catalysed rearrangements, Cope reported the first example of base-catalysed rearrangement of epoxides in 1958 using lithium diethylamide as the base (Cope rearrangement).[64–68] Based on Rickborn's studies using lithium monoalkyl and dialkylamide bases to deprotonate cyclohexene oxide, the major product was revealed to be an allylic alcohol (Schlosser has also used the LICKOR superbase to convert epoxides into allylic alcohols)[69,70] with a ketone being the minor product.[71] The products generated and the ratios of each are dependent upon the lithium amide base employed (in particular the substituent attached to the amide N atom). Base-catalysed rearrangement of epoxides can occur via three pathways (**Scheme 3.4**) (a) cleavage of the strained heterocyclic ring (**Path A**), (b) abstraction of a β-proton to give an allylic alcohol in a process called β-elimination (**Path B**) and (c) removal of an α-proton to generate an α-metalled epoxide (oxiranyl anion) (**Path C**) which can also undergo α-elimination to generate a carbonyl compound.[59,72] Solvent plays an important role in these reactions for example cyclopentene oxide undergoes α-elimination in ether or benzene and β-elimination in HMPA (hexamethylphosphoramide).[73]

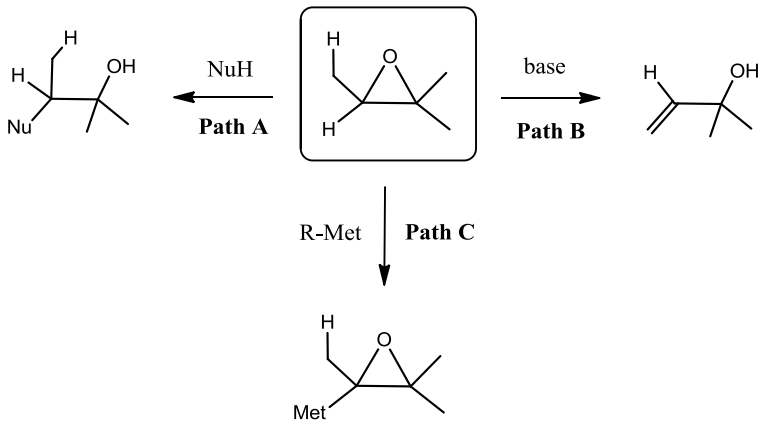

Scheme 3.4: Three different reaction pathways for epoxides.

From **Path C** it is possible to form polysubstituted epoxides (without ring-opening) which are often key intermediates in the construction of structurally complex molecules.[74–78] Boeckman noticed that it was possible to deprotonate epoxides using *n*-butyllithium as long as low temperatures were employed.[79] The generation and reaction of oxiranyllithiums requires very low temperatures because they exhibit carbene-like reactivity and readily undergo decomposition via C-H insertion, 1,2-hydride shift, β-C-H insertion and reductive alkylation.[80–84] *Trans*-stilbene oxide can be lithiated and trapped with electrophiles using *n*-BuLi at -60^{o}C after 2 hours.[85] Unlike the electrophilic chemistry of epoxides, lithiated epoxides as nucleophiles (oxiranyl anions) first studied by Eisch and Galle,[86–88] until recently were far less developed as it required epoxides with an activating substituent.

The base-catalysed rearrangement of *trans*-stilbene oxide is already known using lithium diethylamide as the base.[64] The first step is removal of a proton from the oxirane ring by the diethylamide ion. Ring opening can then occur to give the anion of a carbonyl compound (**Path A**) or rearrangement ensues generating an isomeric product (**Path B**). With *trans*-stilbene oxide as the substrate the phenyl group migrates via **Path B** (see **Scheme 3.5**) to give diphenylacetaldehyde. The migrating phenyl group is the one which is attached to the same carbon which has been deprotonated. Unless there is a structural bias a mixture of products is obtained due to lack of regioselectivity in the ring opening step.

Some of the Lewis acid reagents used for the rearrangement of epoxides mentioned above create a number of environmental disadvantages such as the production of large quantities of toxic and corrosive waste resulting from the use of stoichiometric quantities ($BF_3 \cdot Et_2O$ is corrosive while $InCl_3$ is highly toxic and very expensive). Some rearrangement reactions also need to be carried out at high temperatures over long reaction times hence more 'environmentally friendly' reagents are needed. Reagents such as $BiOClO_4 \cdot H_2O$ have been developed as most bismuth compounds are relatively non-toxic and cheap[89] and acidic zeolite catalysts have been used for milder conditions.[90] Our aluminium reaction provides a system which is also more environmentally friendly as the reaction is carried out at room temperature and aluminium reagents are generally of low toxicity.

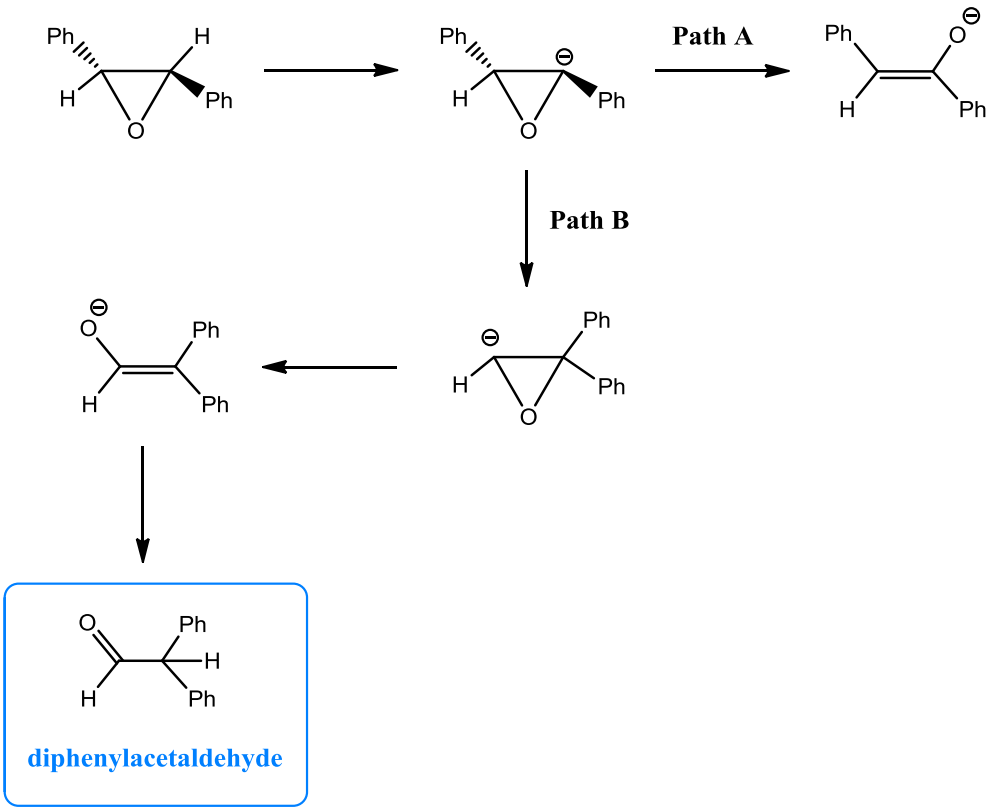

Scheme 3.5: Two possible reaction pathways for the base-catalysed ring opening of *trans*-stilbene oxide.

To convert our ring opened product **2.9** into the corresponding deuterated aldehyde diphenylacetaldehyde the crystals were subjected to a deuterium quench. 1 mL of D_2O was added to a solution of the dissolved crystals in hexane solution. After stirring for 10 mins the solution was dried with magnesium sulphate and concentrated in *vacuo*. The ^1H NMR spectrum of the crude mixture in $CDCl_3$ (**Figure 3.16**) shows the expected aldehyde proton at 9.95 ppm (highlighted in purple) and the aromatic protons of the two phenyl rings just above 7 ppm (highlighted in red) with the only by-product being TMP(D).

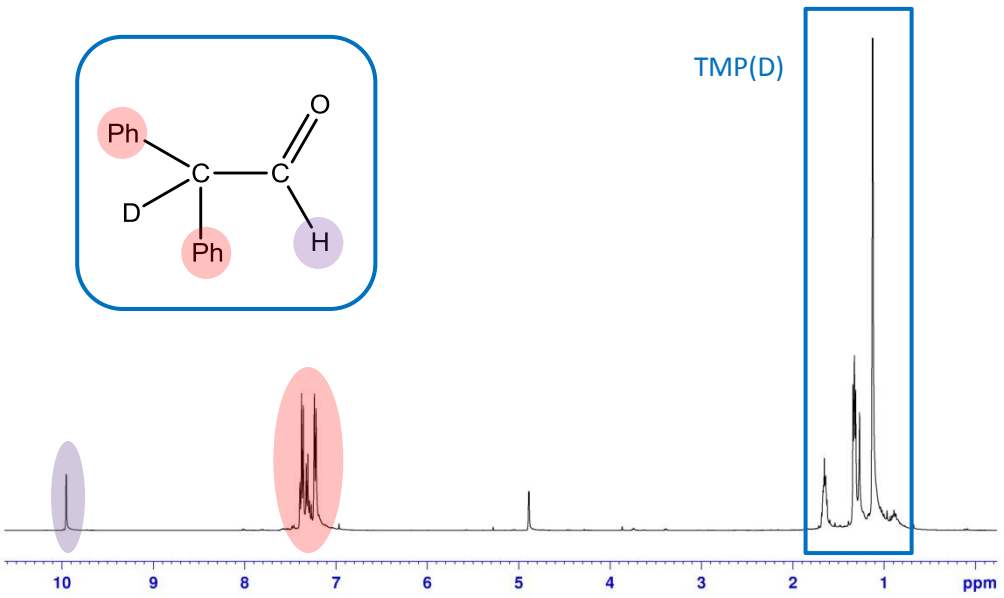

Figure 3.16: ^{1}H NMR spectrum of crude D_2O quench product **2.10** in $CDCl_3$ solution.

The crude mixture was purified using column chromatography using hexane solution as an eluent however, surprisingly in addition to the expected proton peaks for the product, three additional peaks were observed in the ^{1}H NMR spectrum (**Figure 3.17**).

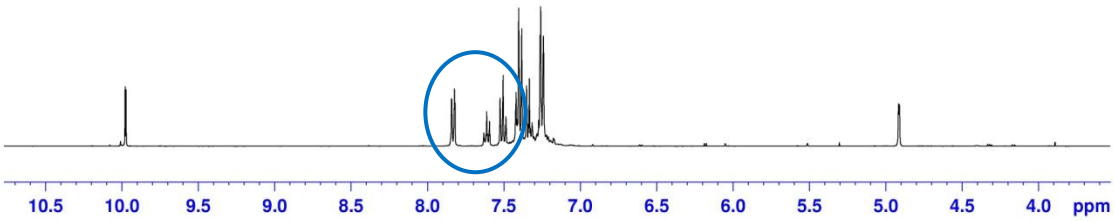

Figure 3.17: ^{1}H NMR spectrum of purified D_2O quench product **2.10** in $CDCl_3$ solution (region highlighted in blue circle is additional peaks observed after purification.

Two triplets at 7.50 and 7.61 ppm and a doublet at 7.82 ppm are now visible in the ^{1}H NMR spectrum and suggest that the product has decomposed in some way generating another product with a phenyl group. These peaks were compared to a series of standards to determine what the additional product was. Comparing the peaks to diphenylethanol and diphenylacetic acid confirmed that the additional product was neither of these compounds formed by possible reduction or oxidation. It was also noticed that if the crude mixture was left for a period of time the additional peaks were once again witnessed in the ^{1}H NMR spectrum so this decomposition is not attributed to

the purification process. The additional product was separated from the desired deuterated diphenylacealdehyde product using column chromatography confirming that it was a separate product (**Figure 3.18**).

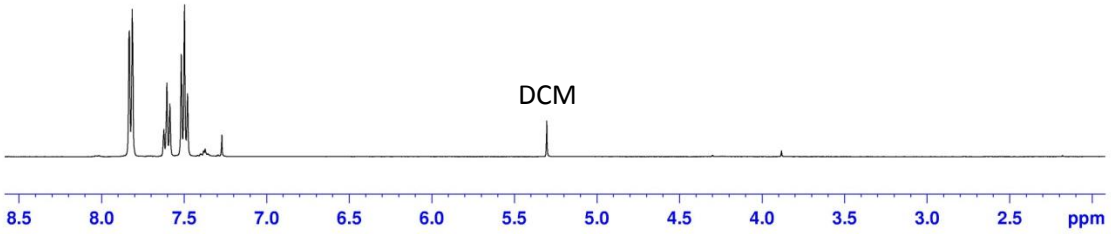

Figure 3.18: ^{1}H NMR spectrum in $CDCl_3$ solution of additional product after separation from desired deuterated diphenylacetaldehyde product.

Future work in this area should focus on determining what the additional product is and why the desired product is decomposing over time. Other oxiranes were tested with **2.1** namely, (a) styrene oxide, (b) 2,3-epoxypropyl benzene, (c) *trans*-2,3-dimethyloxirane and (d) 2,3-epoxy-2-methylbutane (**Figure 3.19**) however, none produced crystalline products.

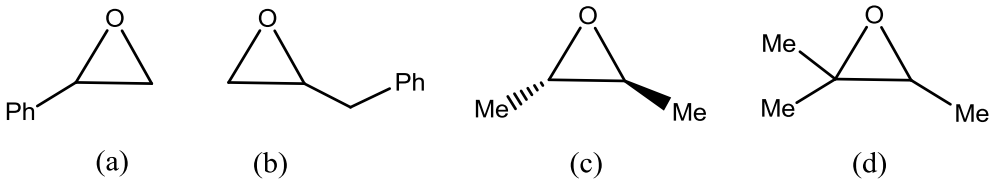

Figure 3.19: Different oxiranes tested with **2.1** (a) styrene oxide, (b) 2,3-epoxypropyl benzene, (c) *trans*-2,3-dimethyloxirane and (d) 2,3-epoxy-2-methylbutane.

The *in situ* mixtures were subjected to a D_2O quench and then worked up as described above. The ^{1}H NMR spectra of the crude mixtures of each of the oxiranes showed no evidence of the expected aldehyde proton so either **2.1** did not react with these substrates or generated the corresponding ketone instead. There was no evidence in the ^{1}H NMR spectra for the OH of an allylic alcohol or peaks to suggest deprotonation of the oxirane had occurred without ring-opening. Future work should focus on revisiting these reactions and testing other oxiranes to establish if it is possible to transform these into aldehydes or ketones. The reaction should also be repeated at low temperature to determine if it is possible to deprotonate the oxirane without ring-opening.

3.3 Contrasting Reactivity of *bis*-TMP 2.1 and *mono*-TMP 2.8 with Donors

3.3.1 Introduction

Our studies have run in parallel with the excellent work of Uchiyama and co-workers who pioneered and have concentrated on the more alkyl-rich lithium aluminate LiAl(TMP)*i*Bu$_3$ **2.8** as previously mentioned which, is also accessed through the co-complexation of homometallic starting materials Li(TMP) and Al*i*Bu$_3$.[91–93] What has consistently been clear throughout the study of these two closely related bimetallic bases is the difference in their reactivity on the substitution of one of the alkyl groups in **2.8** by another equivalent of the bulky secondary amide in **2.1**. While both bases can operate in a 'conventional' manner with respect to functionalized aromatic molecules (see **Chapter 2**) – that is they are potent direct aluminators (C-H to C-Al exchangers) of such molecules via the well-established and understood principles of Directed *ortho*-Metallation (D*o*M)[94–96] – they display marked differences in their reactivity towards non-aromatic, heteroatom containing molecules. This is best displayed by their respective reactivities towards the most common cyclo-ether tetrahydrofuran (THF, donor **A**; **Scheme 3.4a**); **2.8** can be stabilised as a THF solvate **2.8A** and is routinely utilized in this medium;[92] while in contrast **2.1** will deprotonate THF at the methylene group adjacent to the heteroatom via TMP basicity as described above, sedating the resulting highly sensitive cyclic anion in **2.2** without the ether cleavage typically witnessed when a monometallic approach to THF α-deprotonation is attempted. Another pertinent example of the contrasting reactivity of aluminates **2.1** and **2.8** involves the common bidentate donor *N*,*N*,*N'*,*N'*-tetramethylethylenediamine (TMEDA, donor **B**).[6] While both bases will directly aluminate this diamine at one methyl group adjacent to the nitrogen atom, **2.8** will actually metallate a second equivalent to give **2.8B** as depicted in **Scheme 3.4b**. This distinction suggests that the first deprotonation event carried out by **2.8** must occur through TMP and not *i*Bu basicity to give intermediate **2.8B'** (which cannot be isolated), since if the latter situation was operative then this would generate complex **2.1B**, which is inert towards a further equivalent of TMEDA.

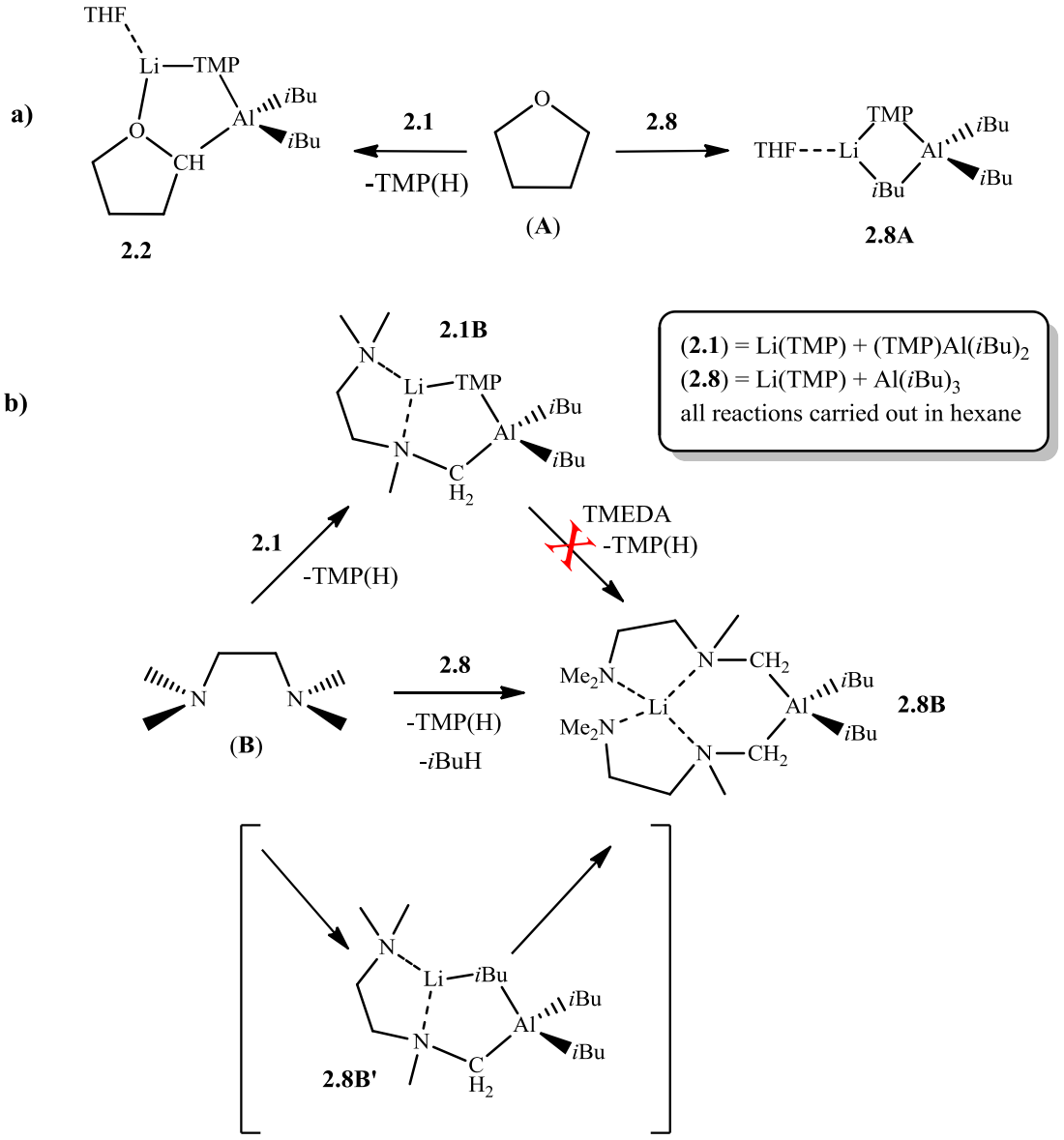

Scheme 3.4: Contrasting reactivity of aluminate bases **2.1** and **2.8** towards (**a**) THF and (**b**) TMEDA.

Interestingly, the solvent plays an important role in any reaction of a base such as **2.8** as demonstrated by its reaction with *N*,*N*-diisopropylbenzamide. In hexane, a simple donor adduct (**2.8**·benzamide) is produced with no deprotonation;[97] whereas in THF *ortho*-deprotonation of the aromatic substrate results in a 94% yield after iodination.[91] When the hexane reaction is repeated in the presence of stoichiometric THF only a negligible amount of *ortho*-deprotonation occurs, while stoichiometric TMEDA yields a product which contains both deprotonated TMEDA and benzamide bridges as well as a ligating neutral benzamide.[98] Furthermore, **2.8**·benzamide will cleave 1,4-dioxane and capture the resulting highly sensitive alkoxy vinyl ether anion;[97] while **2.8** (in the absence of

benzamide) produces the segregATE (solvent-separated ate) $[Li(dioxane)_4]^+$ $[Al(iBu)_4]^-$, presumably from a dismutation process (**Scheme 3.5**).[99]

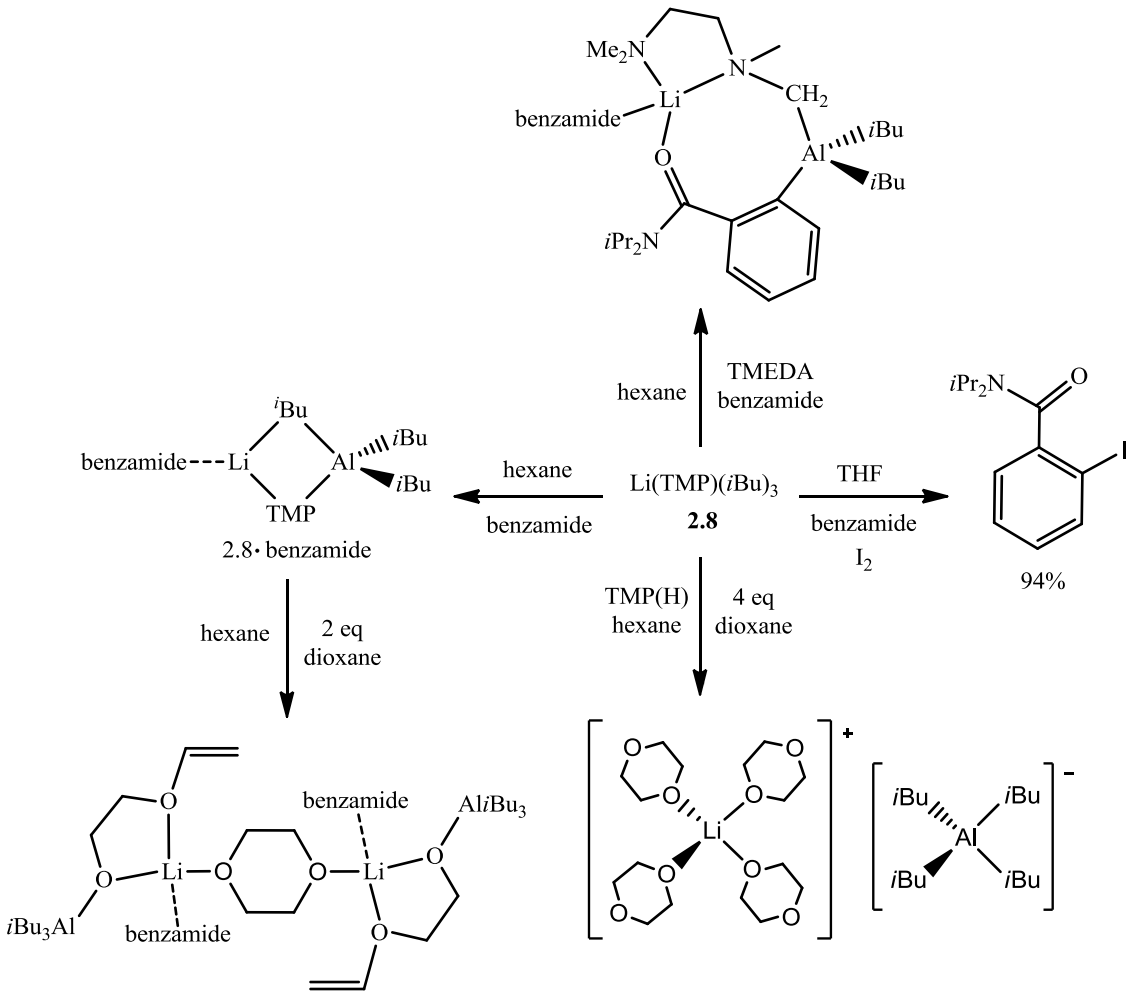

Scheme 3.5: Reactivity of aluminate **2.8** in hexane or THF with benzamide and dioxane.

3.3.2 Results and Discussion

Intrigued by the vagaries in reactivity displayed by the two closely related lithium aluminates **2.1** and **2.8**, we have systematically studied their reactivity with a series of multidentate nitrogen and oxygen containing donor molecules **C-H** (shown in **Figure 3.17**) that offer a variety of donor ligation and/or deprotonation possibilities in an attempt to further understand these important heterometallic reagents.

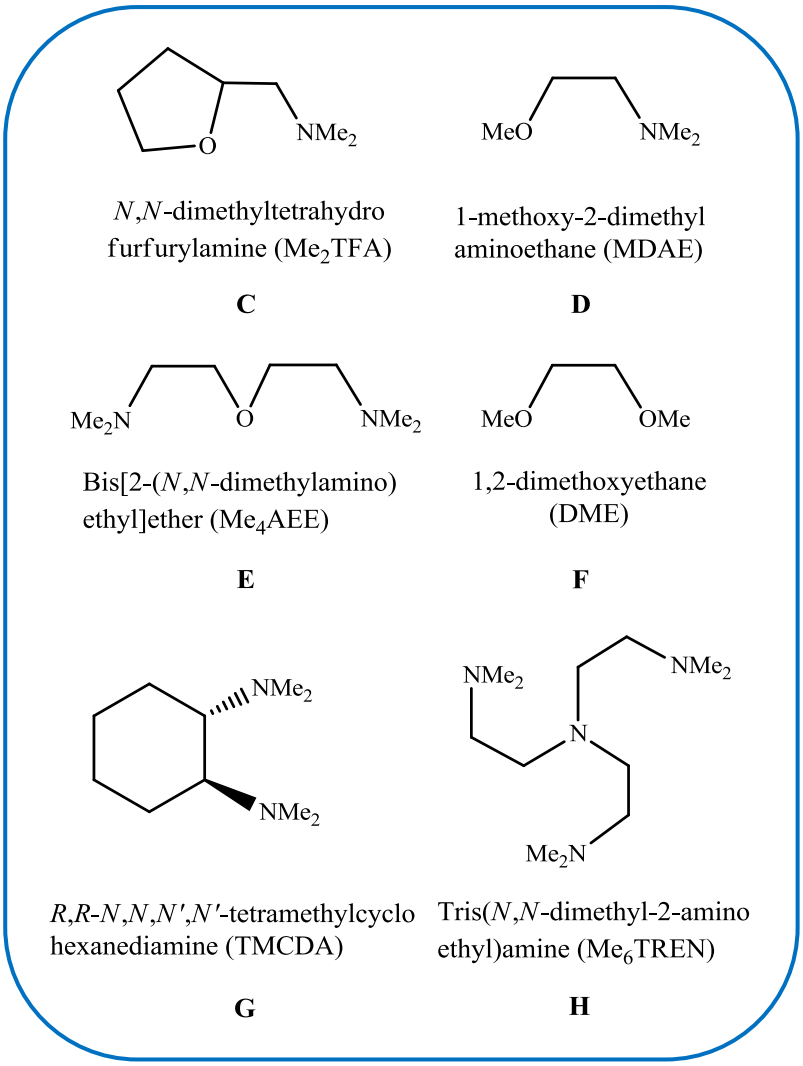

Figure 3.17: Neutral heteroatom containing molecules employed in this study.

3.3.2.1 Solid State

The experimental protocol followed was simply to stir the lithium aluminate bases **2.1** or **2.8** in hexane solution in the presence of an equimolar quantity of each of the neutral Lewis base molecules (**C**-**H**) displayed in **Figure 3.17**. Of the twelve potential organometallic products, seven could be made in crystalline form suitable for single crystal X-ray diffraction analysis. The molecular structure results of these analyses are displayed in **Figures 3.18**, **3.19** and **3.20**. What is instantly clear is, mirroring the THF examples shown in **Scheme 3.4a**, the fully intact donor molecules simply coordinate datively to base **2.8**, contributing to the 4-coordinate, distorted tetrahedral lithium environments **Figure 3.18** (the Li centres have τ_4 values of 0.64, 0.61 and 0.63

respectively according to the method published by Houser,[100] where 1.00 represents an ideal tetrahedral geometry and 0.00 an ideal square planar geometry). In marked constrast the di-TMP base **2.1** C-H deprotonates all of the involved donors via TMP basicity contributing to three coordinate lithium centres and five-membered Li-N-Al-C-O rings (**Figure 3.19**). The one exception to this trend is seen in the reaction of base **2.8** with TMCDA (**Figure 3.20**) – with two molecules of this donor deprotonated via dual *i*Bu/TMP basicity. Such a scenario has been witnessed before using the similar but achiral bidentate *N*,*N* donor TMEDA (**Scheme 3.4b**) and therefore the arguments presented previously for TMEDA are applicable also to this case.[6]

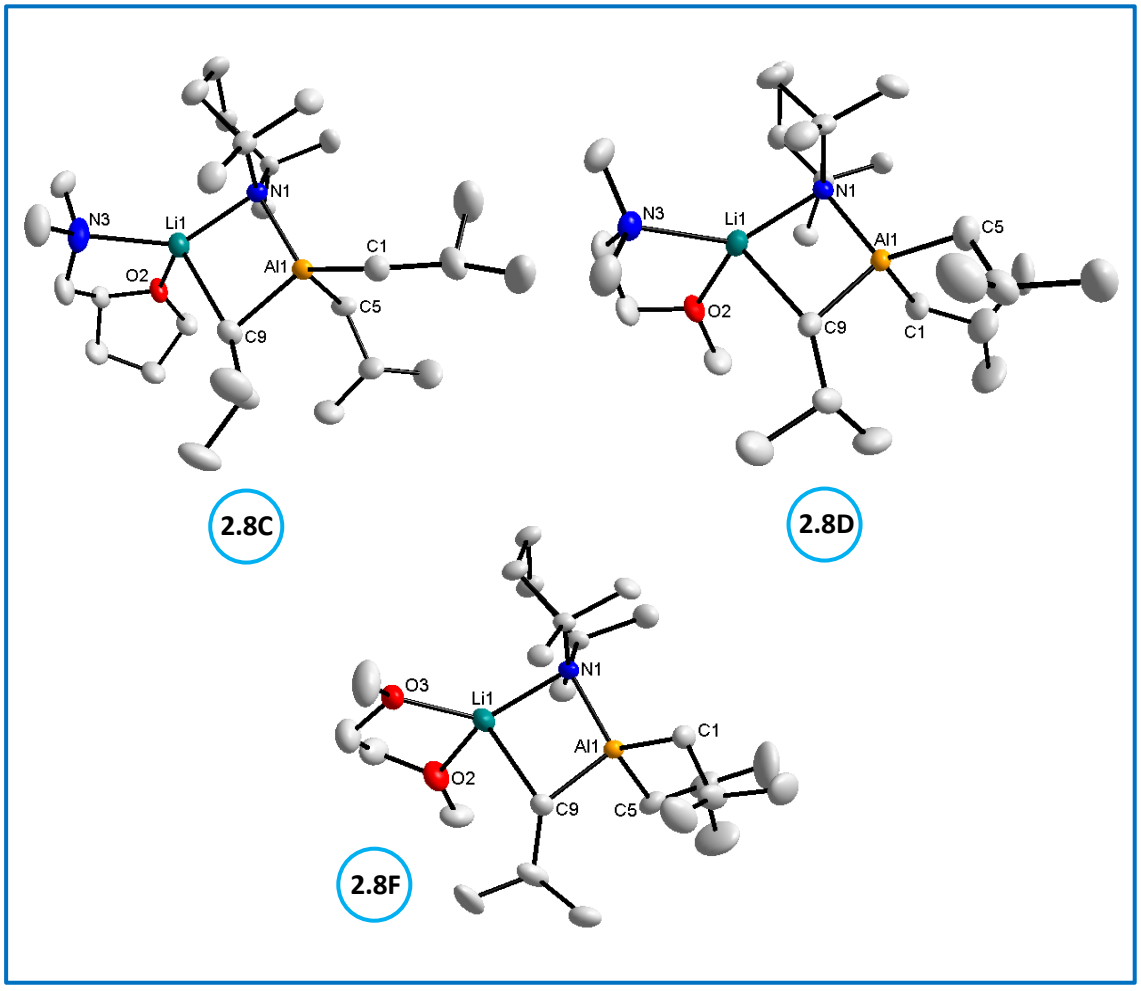

Figure 3.18: Molecular structures of complexes solvated with Me_2TFA **2.8C**, MDAE **2.8D** and DME **2.8F**. Hydrogen atoms omitted for clarity. Thermal ellipsoids drawn at 50% probability.

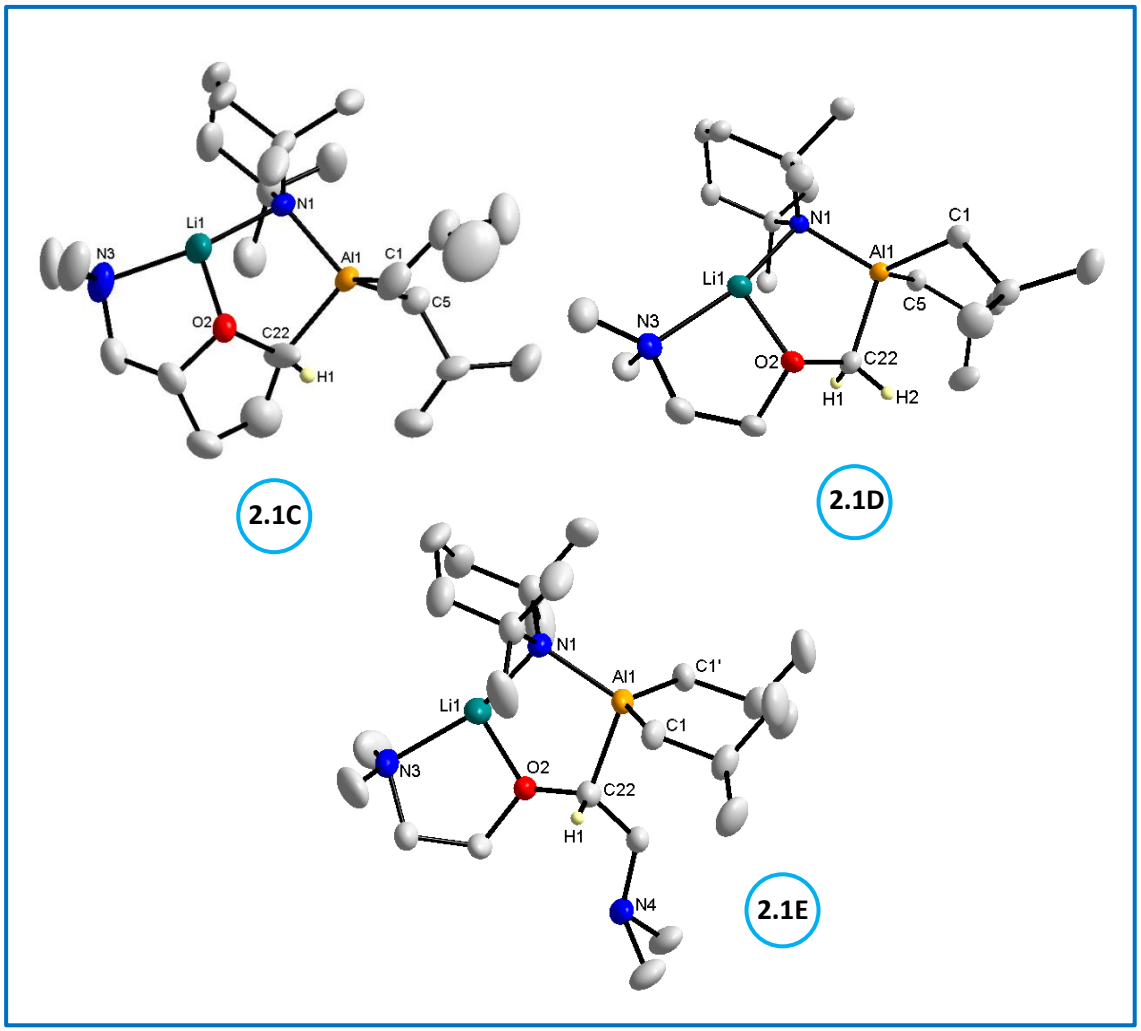

Figure 3.19: Molecular structures of complexes containing α-deprotonated Me_2TFA **2.1C**, MDAE **2.1D** and DME **2.1E**. Hydrogen atoms omitted for clarity. Thermal ellipsoids drawn at 50% probability.

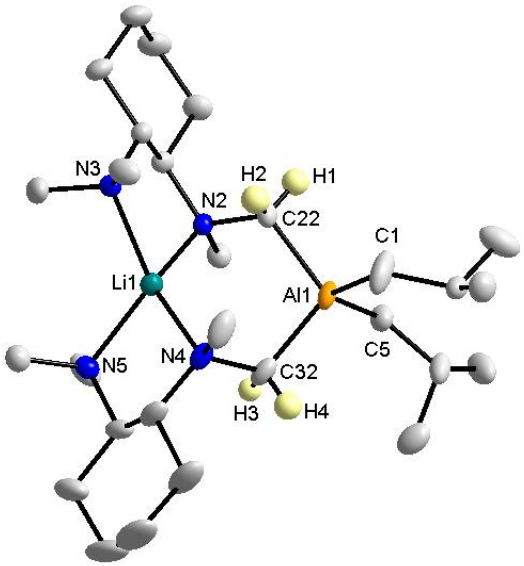

Figure 3.20: Molecular structure of complex containing deprotoaluminated TMCDA **2.8H**. Hydrogen atoms omitted for clarity. Thermal ellipsoids drawn at 50% probability.

As shown in **Figure 3.19**, base **2.1** preferentially deprotonates (aluminates) selectively at the carbon atom adjacent to oxygen rather than nitrogen when given the choice of either position. With the potentially tridentate *N*,*O*,*N* donor Me_4AEE (isoelectronic to the common tridentate *N*,*N*,*N* donor PMDETA – *N*,*N*,*N'*,*N''*,*N''*-pentamethyldiethylenetriamine), deprotonation occurs selectively on one of the methylene groups adjacent to oxygen rather than at a terminal methyl arm, with the ligand then coordinating to lithium in a hypodentate *N*,*O* fashion leaving one CH_2NMe_2 limb swinging free (**2.1E** in **Figure 3.19**).

The three aluminates [Li(μ-$Me_2NCH_2CHCH_2CH_2CHO$)(μ-TMP)Al(*i*Bu)$_2$] **2.1C**, [Li(μ-$Me_2NCH_2CH_2OCH_2$)(μ-TMP)Al(*i*Bu)$_2$] **2.1D** and [Li(μ-$Me_2NCH_2CH_2OCHCH_2NMe_2$)(μ-TMP)Al(*i*Bu)$_2$] **2.1E** with the mono-deprotonated donors are made up of two terminal *i*Bu groups on Al, resulting in a distorted tetrahedral geometry (τ_4 = 0.88, 0.89 and 0.84 for **2.1C**, **2.1D** and **2.1E** respectively), with one TMP bridge connecting Li and Al. The donor ligands are deprotonated in an intramolecular fashion via the most acidic C-H site adjacent to the O atom after prior coordination to Li. The ligand forms the second bridging anion and as a result the deprotonated C and adjacent O complete the central five-element five-membered Al-N-Li-O-C ring. In addition to this multi-element ring each structure is made up of another one or two rings fused onto the central ring.

Compounds **2.1D** and **2.1E** are made up of an additional four-element five-membered N-Li-O-C-C ring, the only major difference between these structures is the pendant CH_2NMe_2 arm attached to the deprotonated C of compound **2.1E**. Compound **2.1C** has two additional fused rings due to the cyclic tetrahydrofuran component of the ligand and NMe_2 dative coordination to Li from the pendant arm forms an additional four-element five-membered N-Li-O-C-C ring.

Di-deprotonated compound [Li(μ-$CH_2NMeC_6H_{10}NMe_2$)$_2$Al(*i*Bu)$_2$] **2.8H** differs only in the replacement of the bridging TMP anion with another deprotonated TMCDA ligand which now occupies the bridging site. The compound contains a central four-element six-membered N-C-Al-C-N-Li ring with two fused three-element five-membered N-C-C-N-Li rings while solvated lithium compounds [(Me_2TFA)Li(μ-*i*Bu)(μ-TMP)Al(*i*Bu)$_2$] **2.8C**, [(MDAE)Li(μ-*i*Bu)(μ-TMP) Al(*i*Bu)$_2$] **2.8D** and [(DME)Li(μ-*i*Bu)(μ-TMP)Al(*i*Bu)$_2$] **2.8F** adopt a similar motif to compounds **2.1C**, **2.1D** and **2.1E** however, this time the second bridging anion is an isobutyl ligand rather than a deprotonated donor molecule and the donor ligand simply solvates the Li atom. It is clear to see from these molecular structure diagrams that no deprotonation of the solvating ligands has occurred; this is further backed up by the ^{1}H NMR spectral data which confirms the presence of an intact donor ligand.

Crystals were also grown from the reaction of *bis*-TMP base **2.1** with the Lewis donor DME; however, these crystals **2.1F** were not of X-ray quality precluding us from obtaining a suitable X-ray crystal structure. The ^{1}H NMR spectrum in C_6D_6 (**Figure 3.21**) however, shows that deprotonation at one of the terminal methyl groups has occurred as two triplets are observed at 2.61 and 2.95 ppm resulting from the loss of symmetry of the CH_2-CH_2 backbone. The signals for the two terminal isobutyl groups can be seen as a multiplet at 0.42-0.70 ppm for the CH_2 protons, two doublets at 1.35 and 1.41 ppm for the CH_3 protons and a septet at 2.32 ppm for the C*H* protons. TMP methyl protons can be seen at 1.42 ppm. The integration of the two singlets at 2.58 and 3.03 ppm are consistent with the methyl and CH_2 protons of a methyl deprotonated DME ligand. The two remaining singlets at 3.00 and 3.37 ppm are consistent with the CH_2 and CH_3 protons of an intact DME molecule.

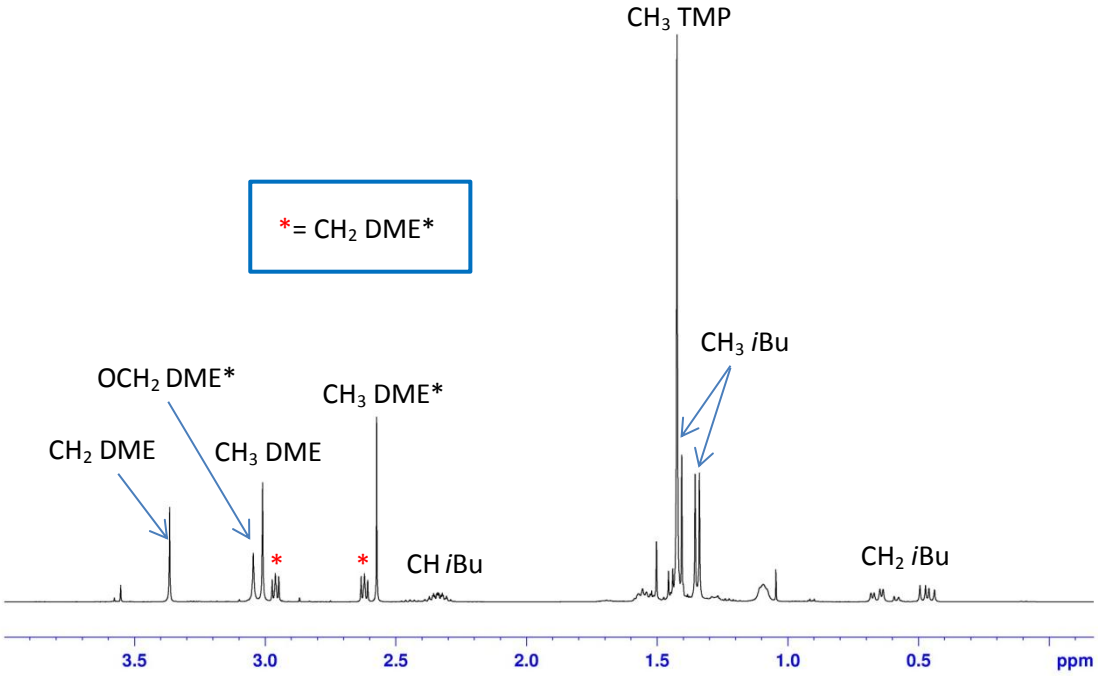

Figure 3.21: ^{1}H NMR spectrum in C_6D_6 of crystalline material from the reaction of base **2.1** with DME (β and γCH_2 protons of TMP have been omitted from labelling for clarity).

The integration of the methyl and C*H*$_2$ protons of the intact DME is 3:2 indicating half a donor DME to one deprotonated DME. As these signals are shifted compared to free DME (methyl 3.40 ppm and CH_2 3.55 ppm) it can be proposed that the structure might contain one donor DME bridging two typical deprotonated motifs to give [(*i*Bu)$_2$Al(μ-TMP)(μ-$CH_3OCH_2CH_2OCH_2$)Li(DME)Li(μ-$CH_2OCH_2CH_2OCH_3$)(μ-TMP)Al(*i*Bu)$_2$] (**Figure 3.22**). Such a structure clearly has similarities with the lithium aluminate dioxane complex (*vide supra*) which also contains a neutral molecule acting as a bridging ligand with deprotonated versions of the same ligand bridging between lithium and aluminium.

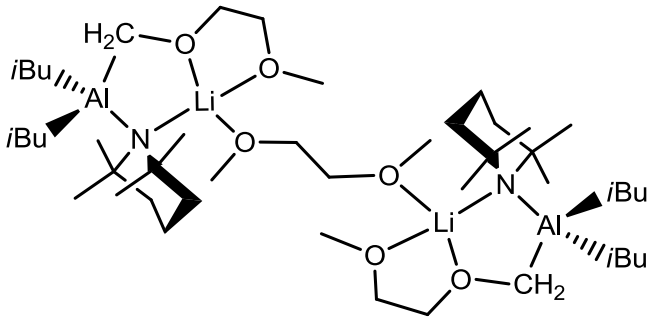

Figure 3.22: Proposed structure of deprotonated DME compound **2.1F** with one donor DME bridging the two molecules containing deprotonated units.

When a solution of **2.1** and DME was allowed to stir for 24 hours another product in addition to **2.1F** was found to co-crystallise in solution. The ^{1}H NMR spectrum shows a mixture of the proposed compound shown above and a second product **2.1FA**. The X-ray crystal data of **2.1FA** is too poor to discuss in any detail however, the data suggests that the product contains a trapped OMe group in the bridging position between Li and Al and a donor fully intact DME on Li instead of a deprotonated DME giving (DME)Li(μ-TMP)(μ-OMe)Al(*i*Bu)$_2$ (**Figure 3.23**). This suggests that after time the deprotonated DME cleaves[101–103] at the MeO-CH$_2$ junction and the methoxy group subsequently becomes trapped although the mechanism through which this occurs is unclear.

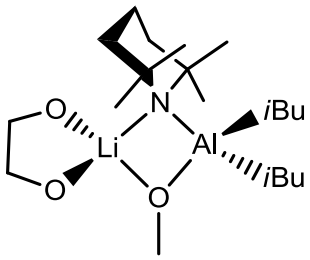

Figure 3.23: Proposed structure of cleaved DME product **2.1FA.**

3.3.2.2 Solution state

A solution state NMR spectroscopic study was initiated on the highly soluble crystalline material obtained (*vide supra*). ^{1}H and ^{13}C spectra in C_6D_6 or D_8-THF were consistent with the molecular structures discussed previously, with complexes **2.1** each displaying a 2:1:1 *i*Bu/TMP/deprotonated-donor ratio and complexes **2.8** each displaying a 3:1:1 *i*Bu/TMP/intact-donor ratio in their ^{1}H resonance integrations. The one exception to this was found in **2.8H**, which displays a 1:1 *i*Bu/deprotonated-TMCDA ratio. In the case of **2.1C**, resonances representing two diastereomers were witnessed (in a 2:1 ratio) as a consequence of deprotonation of the methylene group adjacent to oxygen (C22 of **2.1C** in **Figure 3.19**) in the substituted tetrahydrofuran ring generating a stereogenic carbon centre. This is noteworthy as no distinction between diastereomers was witnessed when a chiral carbon centre was generated in **2.1E** or when THF was the substrate (**2.2**). The most important resonances were those of the hydrogen atoms bonded to the metallated carbon atom as well as the metallated carbon atoms themselves. Specifically, resonances at 3.26/3.37 (diastereomer A/B), 3.20 and 3.28 ppm were witnessed in the

^{1}H NMR spectra of complexes **2.1C**, **2.1D** and **2.1E** respectively [*cf* 3.75/3.86, 3.37 and 3.45 ppm for the corresponding resonances in the free donor ligands]. In the ^{13}C NMR spectra, the resonances of the metallated carbon atom were seen at 84.3/84.5, 78.0 and 82.0 ppm for **2.1C**, **2.1D** and **2.1E** respectively while the non-metallated derivatives **2.8C** and **2.8D** showed these carbon resonances at 68.4 and 59.4 ppm respectively. Meanwhile, the NMR spectra of **2.8F** suggested no deprotonation of the donor ligand had occurred due to the resonances indicating its symmetrical chemical makeup remained. Complex **2.8H** gave a highly complicated NMR spectrum, in part we believe due to the formation of stereogenic centres, which could not be satisfactorily assigned due to overlap of multiple peaks. In each case, further evidence that the crystal structures were representative of the solution state compositions could be gleaned from integration of the anions, with a 3:1 *i*Bu:TMP ratio in structures **2.8** and a 2:1 ratio in structures **2.1** (with the exception of **2.8H** which showed no TMP anions).

Aware that the NMR spectrum of a crop of isolated crystals is not necessarily representative of the whole *in situ* generated reaction mixture from which the crystals were obtained, we also carried out a series of electrophilic quenches on these mixtures to ascertain if the reactivity of **2.1** and **2.8** was consistent towards the other donor molecules. Specifically, a deuterium quench (using D_2O) was carried out with the resulting ^{2}D NMR spectrum consequently compared with the ^{1}H spectrum of the parent donors in an effort to see if the base had removed a proton from them or not.

The deuterium studies reveal some interesting results which cannot be gleaned from the crystal structures in isolation. A comparison of the ^{1}H NMR spectrum of Me_2TFA (donor **C**) with the ^{2}D NMR spectra of the product formed after base **2.8** was reacted with Me_2TFA and then quenched with D_2O (**Figure 3.24a**) shows that some αCH_2O-deprotonation has occurred. There is also a signal consistent with some NMe_2 deprotonation after reaction with base **2.8**. The amount of deprotonation must be negligible as a ^{1}H NMR spectrum of the filtrate solution after the crystals were removed confirms that the major product in solution is consistent with the crystal structure. The ^{2}D NMR spectrum of **2.1** with Me_4AEE (donor **E**) also reveals that a small amount of NMe_2 deprotonation has occurred (**Figure 3.24c**). The ^{2}D NMR spectrum of **2.1** with DME (**Figure 3.24d**) confirms that deprotonation has occurred at the methyl group adjacent to O as observed in the ^{1}H NMR spectrum of the crystals (**Figure 3.21**).

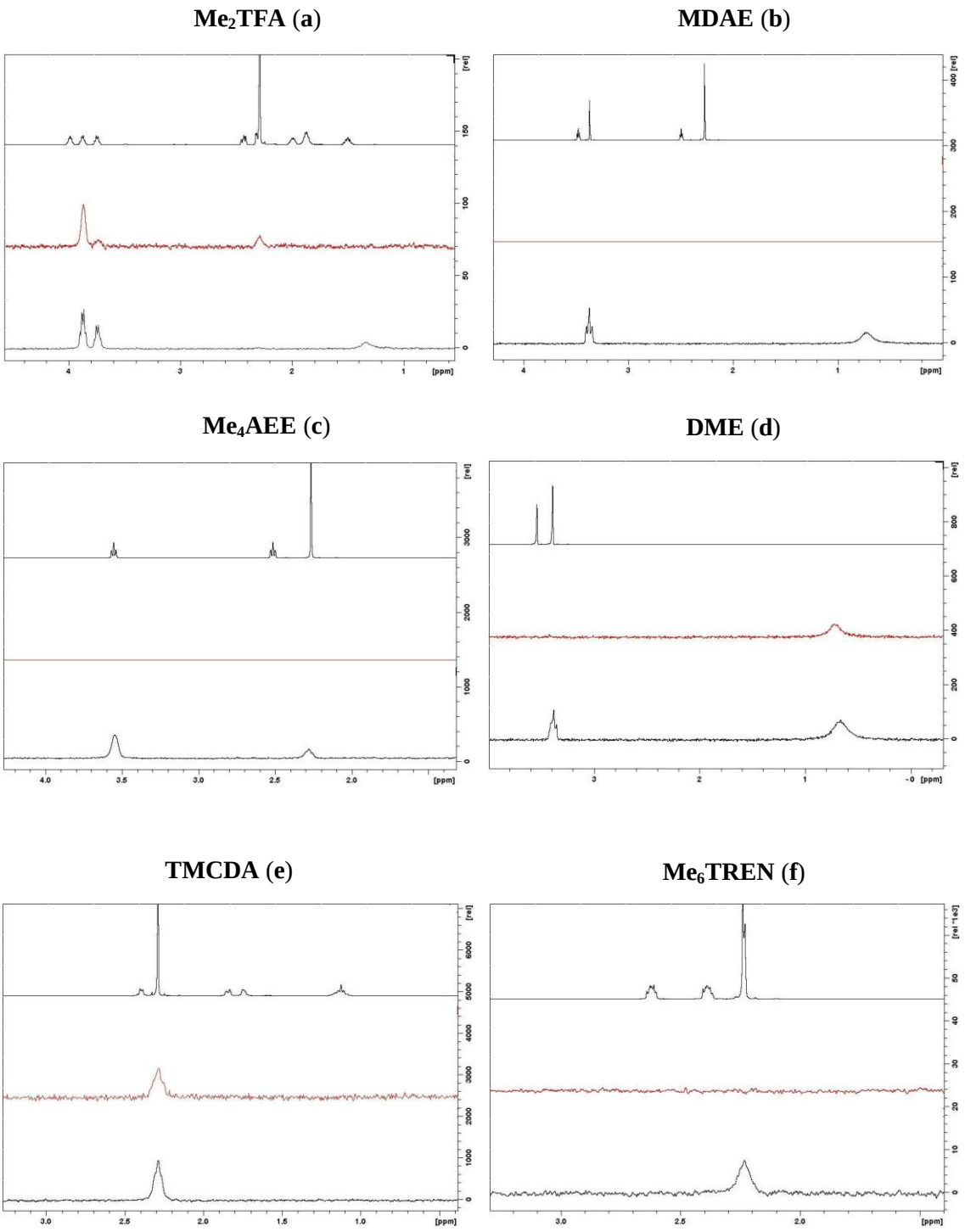

Figure 3.24: (**top**) ^{1}H NMR spectrum of free donor, (**middle**) ^{2}D NMR spectra for the deuterium quench of donor after reaction with base **2.8** or (**bottom**) base **2.1**.

Although crystals structures could not be obtained for the products of the reaction of **2.1** with TMCDA (donor **G**) and **2.1** with Me_6TREN (donor **H**) the D_2O quench experiment revealed that deprotonation at the methyl NMe_2 sites has occurred (**Figure 3.24e** and **f**). Similarly the ^{2}D NMR spectra for the reaction of **2.8** with Me_4AEE (**Figure 3.24c**) or

Me_6TREN (**Figure 3.24f**) confirms that no deprotonation of these ligands has occurred. Overall, aside from the NMe_2 deprotonation of Me_2TFA and Me_4AEE and the αCH_2-deprotonation of Me_2TFA, the D_2O quenches corroborate that the reaction of base **2.1** or **2.8** with each ligand follows the same general trend, **2.1** deprotonates the donor ligand; whereas the ligand simply solvates lithium in **2.8**.

As a representative example Me_4AEE (**E**) was reacted under several quenching protocols to determine if it was possible to selectively functionalise these ligands. The best procedure was found to be cross-coupling deprotonated compound **2.1E** with 4-iodoanisole using $Pd(OAc)_2$/SPhos[104] as a catalyst after transmetallation using zinc acetate [$Zn(OAc)_2$] in THF solution (**Scheme 3.6**). Due to the presence of three sp^3 carbanionic carbon centres (1 x Me_4AEE and 2 x *i*Bu) three equivalents of 4-iodoanisole was added. The new compound **2.1E'** was synthesised in a 62 % yield. To the best of our knowledge this is the first example of the preparation of **2.1E'**.

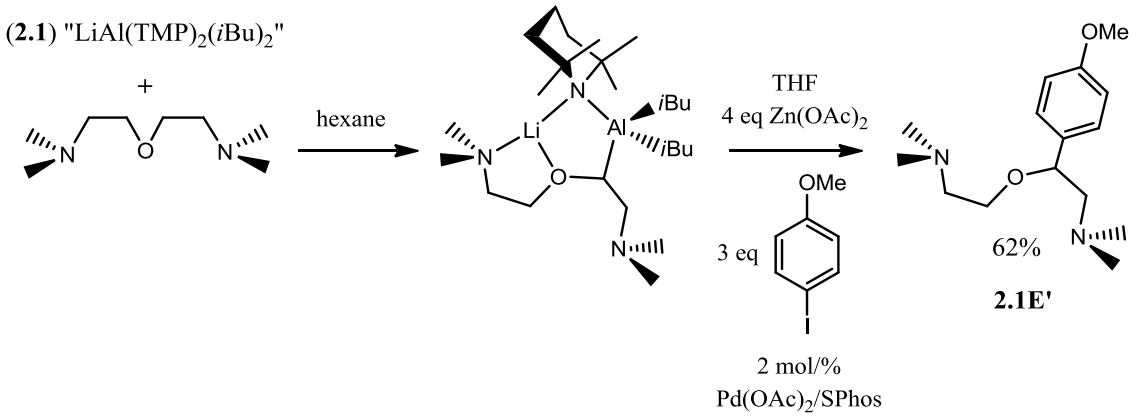

Scheme 3.6: Deprotonation of Me_4AEE with base **2.1**, transmetallation with $Zn(OAc)_2$ and subsequent cross-coupling in THF with 2 mol/% $Pd(OAc)_2$/SPhos and 3 equivalents of 4-iodoanisole to give compound **2.1E'**.

Due to the amine nitrogen's of Me_4AEE the 4-isobutylanisole by-product could be easily removed from the desired product by working-up the solution using ammonium chloride and then removing the organic layer. Ammonia solution and ethyl acetate were then added to the aqueous layer leaving only **2.1E'** and TMP(H) as the crude products in the organic layer. Compound **2.1E'** was purified by removing ethyl acetate and TMP(H) under vacuum.

3.4 Conclusions

The synthetic utility of the lithium aluminate base **2.1** towards alumination of Lewis base donor molecules such as THF, THP, THT and THTP was carried out. Operating at room temperature **2.1** directly aluminates (C-H to C-Al exchange) each donor molecule adjacent of the heteroatom and is able to trap the resulting anion. Each aluminium intermediate was isolated and the structure determined by X-ray crystallography. It was found that a stoichiometric amount of each donor could be deprotonated which is in marked contrast to the deprotonation of THF by a similar zincate base which could only achieve this is bulk quantities.

This chapter also demonstrates that the *bis*-amide $[Li(TMP)_2Al(iBu)_2]$ is a far superior deprotonating agent to the mono-amide analogue $[Li(TMP)Al(iBu)_3]$ and that the deprotonations achieved can be carried out in hexane solution. The aluminium-hydrogen exchange takes place selectively adjacent to the O centre in the mixed N, O ligand sets. In most cases under the conditions studied the mono-amide does not bring about deprotonation but simply engages in a Lewis acid – Lewis base complex with the polydentate donor molecule. A surprising exception to this pattern is that the chiral diamine TMCDA is deprotonated by the weaker aluminating agent at one methyl arm of an NMe_2 group, while the solution investigation shows that the stronger base does this too. Such deprotonations alpha to a nitrogen atom are relatively challenging so this points to possible energetically favourable intramolecular processes. Though the relative deprotonating ability of these synergic lithium – aluminium reagents is made clearer through this chapter, some uncertainty still remains as to the actual constitutions of these reagents in their own right both in hexane and in THF solution.

3.5 Future Work

Any follow on project should focus on trying to electrophilically quench some of the intermediate compounds generated in this chapter such as the THF, THP, THT, THTP products **2.2**, **2.3**, **2.5** and **2.6**. Functionalising these products would be extremely beneficial as they are difficult to trap intact once deprotonated so this would provide an excellent means of generating building blocks to more complex products.

The reaction generating oxirane product **2.9** and subsequent quench with D_2O should be investigated further to establish what the additional product forming after time is and why this is happening. Other oxiranes should be tested with **2.1** [(THF)Li(TMP)$_2$Al(*i*Bu)$_2$] to determine if it is possible to ring-open and selectively trap other epoxides and if the alkyl or aryl group migrates in these particular cases.

3.6 Experimental Section

3.6.1 General Experimental

All reactions and manipulations were carried out under a protective argon atmosphere using either standard Schlenk techniques or a glove box. All solvents were dried over Na/benzophenone and freshly distilled prior to use. *n*BuLi and *i*Bu_2AlCl were purchased from Aldrich and used as received. TMP(H) was purchased from Merck and dried over 4Å molecular sieves prior to use. *i*Bu_2Al(TMP) and Li(TMP) were prepared *in situ*; (Me_2TFA and MDAE),[105] Me_6TREN[106] and TMCDA[107] were prepared by literature methods. THT, THP, 2-methylTHF, THTP, 1,3-dithiane, *trans*-stilbene oxide, Me_4AEE, *i*Bu_3Al (1.0 M in hexane) and DME were purchased from Aldrich and used as received. Data for the X-ray crystal structure determination were obtained with a Nonius Kappa CCD Diffractometer. ^{1}H, ^{13}C NMR and ^{7}Li spectra were recorded on a Bruker AV400 MHz spectrometer (operating at 400.03 MHz for ^{1}H, 100.58 MHz for ^{13}C and 155.50 MHz for ^{7}Li). ^{1}H and ^{13}C NMR chemical shifts are quoted relative to TMS standard at 0.00 parts per million. ^{1}H-^{1}H and ^{1}H-^{13}C correlations were identified using COSY and HSQC NMR techniques respectively. All ^{13}C NMR spectra were proton decoupled.

Procedure for DOSY NMR experiment

The DOSY experiment was performed on a Bruker AVANCE 400 NMR spectrometer operating at 400.13 MHz for proton resonance under TopSpin (version 2.0, Bruker Biospin, Karlsruhe) and equipped with a BBFO-z-atm probe with actively shielded z-gradient coil capable of delivering a maximum gradient strength of 54 G/cm. Diffusion ordered NMR data were acquired using the Bruker pulse program dstegp3s employing a double stimulated echo with three spoiling gradients. Sine-shaped gradient pulses were used with a duration of 2.75 ms (P30) together with a diffusion period of 100 ms (D20). Gradient recovery delays of 200 μs followed the application of each gradient pulse. Data were systematically accumulated by linearly varying the diffusion encoding gradients over a range from 2% to 95% for 64 gradient increment values. The signal decay dimension on the pseudo-2D data was generated by Fourier transformation of the time-domain data. DOSY plots were generated by use of the DOSY processing module of TopSpin. Parameters were optimized empirically to find the best quality of data for presentation purposes. Diffusion coefficients were calculated by fitting intensity data to

the Stejskal-Tanner expression with estimates of errors taken from the variability in the calculated diffusion coefficients by consideration of different NMR responses for the same molecules of interest.

Synthesis of [(THF)Li(μ-TMP)(μ-C_4H_7O)Al(*i*Bu)$_2$] 2.2

Hexane (10 mL) was added to an oven-dried Schlenk tube. Next, 1.6M *n*BuLi (1.25 mL, 2 mmol) was added, followed by TMP(H) (0.34 mL, 2 mmol) at room temperature. The reaction mixture was left to stir for 10 min and then *i*Bu$_2$AlCl (0.38 mL, 2 mmol) was injected into the Schlenk tube, producing a white suspension almost immediately. The reaction was left to stir for 1 hour and was then filtered through Celite and glass wool, which was then washed with more hexane (10 mL). To a separate Schlenk tube containing a solution of freshly prepared LiTMP in hexane (10 mL) [from a mixture of *n*BuLi (1.25 mL, 2 mmol) and TMP(H) (0.34 mL, 2 mmol)], the solution was added through cannula to give a colourless solution. Finally, THF (0.32 mL, 4 mmol) was injected and the reaction mixture was left to stir overnight. Most of the solvent was removed under vacuum and the Schlenk tube was left in the freezer at -30^{o}C. A crop (0.302 g, 35%) of colourless crystals formed which were suitable for X-ray crystallographic analysis.

^{1}H NMR data (400.13 MHz, 298 K, C_6D_{12})

δ = 0.02 [3H, m, CH_2 of *i*Bu], 0.17 [1H, m, CH_2 of *i*Bu], 0.92 [12H, m, CH_3 of *i*Bu], 1.20 [4H, broad s, 2 x βCH_2 of TMP], 1.33 [12H, broad s, 4 x CH_3 of TMP], 1.43 [2H, broad, 1 x γCH_2 of TMP], 1.70 [2H, m, 2 x C_3β' of THF anion], 1.78 [1H, m, 1 x C_2β of THF anion], 1.89 [2H, m, 2 x CH of *i*Bu], 1.95 [4H, m, 2 x βCH_2 of THF], 2.05 [1H, m, 1 x C_2β of THF anion], 2.96 [1H, dd, ^3J(H,H) = 5.4 Hz, 1 x C_1α of THF anion], 3.39 [1H, m, 1 x C_4α' of THF anion], 3.64 [1H, q, ^{3}J(H,H) = 6.5 Hz, 1 x C_4α' of THF anion], 3.89 ppm [4H, m, 2 x αCH_2 of THF].

^{13}C {^{1}H} data (100.62 MHz, 298 K, C_6D_{12})

δ = 18.9 [1 x γCH_2 of TMP], 26.1 [2 x βCH_2 of THF], 27.8, 27.9, 28.3, 28.5, 29.8, 30.2 [4 x CH_3 and 2 x CH of *i*Bu], 28.7 [1 x CH_2 of THF anion], 29.3 [1 x CH_2 of *i*Bu], 30.3 [1 x CH_2 of *i*Bu], 31.8 [1 x CH_2 of THF anion], 36.2 [2 x CH_3 of TMP], 36.5 [2 x CH_3 of TMP], 44.8 [1 x βCH_2 of TMP], 44.9 [1 x βCH_2 of TMP], 52.4 [1 x quaternary C of

TMP], 53.0 [1 x quaternary C of TMP], 68.6 [1 x CH_2 of THF anion], 69.3 [2 x αCH_2 of THF], 84.5 ppm [1 x CH of THF anion].

El. Analysis calc. for $C_{25}H_{51}AlLiNO_2$ (M_r = 431.60) C, 69.57; H, 11.91; N, 3.25; found: C 69.55; H, 11.73; N, 3.24.

Synthesis of [(2-MeTHF)Li(μ-TMP)(μ-C_4H_7O)Al(*i*Bu)$_2$] 2.3

The same procedure as described for **2.2** was employed until the final step where THF (0.16 mL, 2 mmol) and 2-methylTHF (0.20 mL, 2 mmol) were injected and the reaction mixture was left to stir overnight. Upon cooling to -30^{o}C a crop (0.27g, 30%) of colourless crystals formed which were suitable for X-ray crystallographic analysis.

Synthesis of [(THF)Li(μ-TMP)(μ-C_5H_9O)Al(*i*Bu)$_2$] 2.4

The same procedure as described for **2.2** was employed until the final step where THF (0.16 mL, 2 mmol) and THP (0.20 mL, 2 mmol) were injected and the reaction mixture was left to stir overnight. Upon cooling to -30^{o}C a crop (0.30g, 34%) of colourless crystals formed which were suitable for X-ray crystallographic analysis.

^{1}H NMR data (400.13 MHz, 298 K, C_6D_{12})

δ = 0.54 and 0.71 [4H, m, 2 x CH_2 of *i*Bu], 0.87 [2H, βCH_2 of TMP], 1.10 [4H, m, βCH_2 of THF], 1.30 [1H, m, 1 x CH of THP], 1.37 [1H, γCH of TMP], 1.49 [12H, m, 4 x CH_3 of *i*Bu] and [1H, 1 x CH of THP], 1.55 [12H, broad s, 4 x CH_3 of TMP], [1H, γCH of TMP] and [2H, βCH_2 of TMP], 1.60-1.77 [2H, m, CH_2 of THP], 2.01 [1H, m, 1 x CH of THP], 2.27-2.85 [1H, m, 1 x CH of THP], 2.41 [2H, m, 2 x CH of *i*Bu], 3.15 [2H, m, CH_2 of THP], 3.22 [4H, m, αCH_2 of THF], 3.42 ppm [1H, m, 1 x CH(Al) of THP].

Synthesis of [(THF)Li(μ-TMP)(μ-C_4H_7S)Al(*i*Bu)$_2$] 2.5

The same procedure as described for **2.2** was employed until the final step where THF (0.16 mL, 2 mmol) and THT (0.18 mL, 2 mmol) were injected and the reaction mixture was left to stir overnight. Upon cooling to -30^{o}C a crop (0.304 g, 34 %) of colourless crystals formed which were suitable for X-ray crystallographic analysis.

^{1}H NMR data (400.13 MHz, 298 K, C_6D_{12})

0.06 [2H, m, CH_2 of *i*Bu], 0.21 [2H, m, CH_2 of *i*Bu], [2H, m, 2 x CH of *i*Bu], 0.95 [12H, m, 4 x CH_3 of *i*Bu], 1.13 [1H, m, 1 x CH of THT anion], 1.25 [6H, broad s, 2 x CH_3 of TMP], 1.32 [1H, m, 1 x CH of THT anion], 1.41 [6H, broad s, 2 x CH_3 of TMP], 1.56 [4H, broad dd, ^{3}J(H,H) = 10.1 Hz, 2 x βCH_2 of TMP], 1.75 [1H, dd, ^{3}J(H,H) = 3.97 Hz, 1 x CH of THT anion], 1.89 [2H, m, 1 x γCH_2 of TMP], 1.92 [4H, m, 2 x βCH_2 of THF], 2.16 [1H, m, 1 x CH of THT anion], 2.26 [1H, m, 1 x CH of THT anion], 2.63 [1H, dt, ^{3}J(H,H) = 4.4 Hz, 1 x CH of THT anion], 2.74 [1H, t, ^{3}J(H,H) = 9.4 Hz, 1 x CH of THT anion], 3.89 ppm [4H, m, 2 x αCH_2 of THF].

^{13}C {^{1}H} data (100.62 MHz, 298 K, C_6D_{12})

δ = 18.7 [1 x γCH_2 of TMP], 27.9, 28.1, 28.6, 28.8, 29.9, 30.0 [4 x CH_3 and 2 x CH of *i*Bu], 29.8 [1 x CH_2 of *i*Bu], 30.1 [1 x CH_2 of *i*Bu], 31.8 [1 x CH_2 of THT anion], 32.9 [1 x CH_2 of THT anion], 33.3 [1 x CH of THT anion], 37.4 [2 x CH_3 of TMP], 37.8 [2 x CH_3 of TMP], 40.3 [1 x CH_2 of THT anion], 45.0 [1 x βCH_2 of TMP], 45.4 [1 x βCH_2 of TMP], 52.2 [1 x quaternary C of TMP], 52.9 [1 x quaternary C of TMP], 69.3 ppm [2 x αCH_2 of THF].

El. Analysis calc. for $C_{25}H_{51}AlLiNOS$ (M_r = 447.61) C, 67.07; H, 11.48; N, 3.12; found: C 65.14; H, 11.93; N, 2.90. The low C analysis is attributed to the acute air- and moisture- sensitivity of the compound.

Synthesis of [(THF)Li(μ-TMP)(μ-C_5H_9S)Al(*i*Bu)$_2$] 2.6

The same procedure as described for **2.2** was employed until the final step where THF (0.16 mL, 2 mmol) and THTP (0.18 mL, 2 mmol) were injected and the reaction mixture was left to stir overnight. Upon cooling to -30^{o}C a crop (0.55 g, 60%) of colourless crystals formed which were suitable for X-ray crystallographic analysis.

^{1}H NMR data (400.13 MHz, 298 K, C_6D_{12})

δ = 0.09 [4H, m, 2 xCH_2 of *i*Bu], 0.89 [2H, m, 1 x βCH_2 of TMP], 0.95 [12H, m, 4 x CH_3 of *i*Bu], 1.23 [1H, m, 1 x CH of THTP anion], 1.30 [12H, broad s, 4 x CH_3 of TMP], 1.42 [1H, broad, γCH of TMP], 1.56 [2H, m, 1 x βCH_2 of TMP], 1.57 [1H, m, 1 x CH of THTP anion], 1.72 [1H, m, 1 x CH of THTP anion], 1.79 [1H, m, 1 x CH of THTP anion], 1.90 [2H, sept, ^{3}J(H,H) = 6.41 Hz, 2 x CH of iBu] and [1H, γCH of

TMP], 1.96 [4H, m, 2 x βCH$_2$ of THF], 1.99 [1H, m, 1 x CH of THTP anion], 2.27 [2H, m, 2 x CH of THTP anion], 2.46 [1H, m, 1 x CH of THTP anion], 3.94 ppm [4H, m, 2 x αCH$_2$ of THF].

^{13}C {^{1}H} data (100.62 MHz, 298 K, C_6D_{12})

δ = 18.7 [γCH$_2$ of TMP], 26.2 [2 x βCH$_2$ of THF], 27.8 [2 x CH of *i*Bu], 28.0 [2 x CH$_2$ of *i*Bu], 28.9 [4 x CH$_3$ of *i*Bu], 29.4 & 29.5 [2 x CH$_3$ of TMP and 2 x CH of THTP anion], 30.0 [1 x CH of THTP anion], 30.5 [2 x CH of THTP anion], 32.2 [2 x CH of THTP anion], 33.0 [1 x CH of THTP anion], 37.0 [1 x CH$_3$ of TMP], 37.8 [1 x CH$_3$ of TMP], 45.1 [1 x βCH$_2$ of TMP], 45.3 [1 x βCH$_2$ of TMP], 52.5 [1 x quaternary C of TMP], 53.0 [1 x quaternary C of TMP], 69.7 ppm [2 x αCH$_2$ of TMP].

Synthesis of [(THF)Li(μ-TMP)(μ-$C_4H_8S_2$)Al(*i*Bu)$_2$] 2.7

The same procedure as described for **2.2** was employed until the final step where THF (0.16 mL, 2 mmol) and 1,3-dithiane (0.24 g, 2 mmol) was added and the reaction mixture was left to stir overnight. A large amount of white solid formed within 5 minutes of adding 1,3-dithiane. This solid was filtered off and the remaining filtrate was allowed to stand at room temperature. A crop of colourless crystals (0.43g, 45%) formed in solution that were suitable for X-ray crystallographic analysis.

^{1}H NMR data (400.13 MHz, 298 K, C_6D_6)

δ = 0.64-0.83 [4H, m, 2 x CH$_2$ of *i*Bu], 1.22 [4H, m, βCH$_2$ of THF], 1.30 [2H, m, CH$_2$ of ring], 1.51 [12H, m, 4 x CH$_3$ of *i*Bu], 1.55 [6H, broad s, 2 x CH$_3$ of TMP], 1.65 [6H, broad s, 2 x CH$_3$ of TMP], 2.06 [2H, m, CH$_2$ of ring], 2.37 [2H, m, CH$_2$ of ring], 2.50 [2H, m, 2 x CH of *i*Bu], 3.45 [4H, m, 2 x αCH$_2$ of THF], 3.61 ppm [1H, s, CH between S atoms]. β and γCH$_2$ of TMP could not be assigned due to absence of HSQC spectrum.

Synthesis of [(THF)Li(μ-TMP)(μ-OC(H)=CPh$_2$)Al(*i*Bu)$_2$] 2.9

The same procedure as described for **2.2** was employed until the final step where THF (0.16 mL, 2 mmol) and *trans*-stilbene oxide (0.39 g, 2 mmol) was added and the reaction mixture was left to stir overnight. Upon cooling to -30^{o}C a crop (0.82g, 74%) of colourless crystals formed which were suitable for X-ray crystallographic analysis.

^{1}H NMR data (400.13 MHz, 298 K, C_6D_{12})

δ = 0.70 [4H, d, ^{3}J(H,H) = 6.79 Hz, 2 x CH_2 of *i*Bu], 1.00 [4H, m, 2 x βCH_2 of THF], 1.40 [12H, m, 4 x CH_3 of *i*Bu], 1.45 [12H, s, 4 x CH_3 of TMP], 2.41 [2H, sept, ^{3}J(H,H) 6.55 = Hz, 2 x CH of *i*Bu], 2.91 [4H, m, 2 x αCH_2 of THF], 6.89 [1H, t, ^{3}J(H,H) = 7.76 Hz, 1 x aromatic H], 7.05 [2H, t, ^{3}J(H,H) = 8.00 Hz, 2 x aromatic H], 7.14 [2H, t, ^{3}J(H,H) = 8.00 Hz, 2 x aromatic H], 7.35 [2H, d, ^{3}J(H,H) = 7.76 Hz, 2 x aromatic H], 7.50 [1H, s, C=C(H)], 7.58 ppm [2H, d, ^{3}J(H,H) = 7.52 Hz, 2 x aromatic H].

^{13}C {^{1}H} NMR data (100.62 MHz, 298 K, C_6D_{12})

δ = 18.3 [γCH_2 of TMP], 24.8 [βCH_2 of THF], 27.4 [CH of *i*Bu], 28.5 [CH_2 of *i*Bu], 29.5 [CH_3 of TMP], 29.8 [CH_3 of *i*Bu], 44.6, 52.2, 68.1 [αCH_2 of THF], 119.7, 125.7 [1 x aromatic C], 126.0 [2 x aromatic C], 130.4 [2 x aromatic C], 145.8 ppm [C=C(H)].

Synthesis of [Li(μ-TMP)(μ-Me_2TFA*)Al(*i*Bu)$_2$] 2.1C

Hexane (10 mL) was injected into an oven-dried Schlenk tube. Next, 1.6M *n*BuLi (1.25 mL, 2 mmol) was added, followed by TMP(H) (0.34 mL, 2 mmol) at room temperature. The reaction mixture was left to stir for 10 min and then *i*Bu_2AlCl (0.38 mL, 2 mmol) was introduced, producing a white suspension almost immediately. The reaction was left to stir for 1 hour and was then filtered through Celite and glass wool, which was then washed with more hexane (10 mL). To a separate Schlenk tube containing a solution of freshly prepared LiTMP in hexane (10 mL) [from a mixture of *n*BuLi (1.25 mL, 2 mmol) and TMP(H) (0.34 mL, 2 mmol)], the solution of *i*Bu_2Al(TMP) was added via cannula. Finally, Me_2TFA (0.28 mL, 2 mmol) was added by injection and the reaction mixture was left to stir overnight. The solution was left to stand in the freezer at -30 ^{o}C. A crop (0.24 g, 29%) of colourless crystals formed in solution which were suitable for X-ray crystallographic analysis.

^{1}H NMR data (400.13 MHz, THF-D_8, 298 K)

Diastereomer A: Diastereomer B is 2:1

Diastereomer A: δ = -0.17 (1H, d, ^{3}J(H, H) = 6.5 Hz, CH_2 of *i*Bu), -0.08 (3H, d, ^{3}J(H, H) = 6.3 Hz, CH_2 of *i*Bu), 0.92 (12H, m, CH_3 of *i*Bu), 1.23 (1H, m, γCH_2 of TMP), 1.25 (6H, s, CH_3 of TMP), 1.27 (1H, m, AlCHCH_2 of Me_2TFA*), 1.30 (6H, s, CH_3 of TMP), 1.51 (1H, m, AlCHCH_2CH_2 of Me_2TFA*), 1.64 (1H, m, γCH_2 of TMP), 1.79 (1H, m, AlCHCH_2CH_2 of Me_2TFA*), 1.90 (2H, m, CH of *i*Bu), 1.92 (1H, m, AlCHCH_2 of

Me_2TFA*), 2.06 (1H, m, CH_2NMe_2 of Me_2TFA*), 2.24 (6H, s, CH_3 of Me_2TFA*), 2.33 (1H, m, CH_2NMe_2 of Me_2TFA*), 3.26 (1H, dd, ^3J(H, H) = 13.0 Hz, ^4J(H, H) = 5.9 Hz, AlC*H* of Me_2TFA*), 3.94 ppm (1H, m, C*H*CH_2N of Me_2TFA*).

Diastereomer B: δ = 0.00 (4H, m, CH_2 of *i*Bu)], 0.89 (12H, m, CH_2 of *i*Bu), 1.22 (6H, s, CH_3 of TMP), 1.24 (6H, s, CH_3 of TMP), 1.27 (1H, m, γCH_2 of TMP), 1.28 (1H, m, AlCHCH_2CH_2 of Me_2TFA*), 1.29 (1H, m, AlCHCH_2 of Me_2TFA*), 1.58 (1H, m, γCH_2 of TMP), 1.85 (2H, m, CH of *i*Bu), 1.95 (1H, m, AlCHCH_2CH_2 of Me_2TFA*), 2.05 (1H, m, AlCHCH_2 of Me_2TFA*), 2.17 (1H, m, CH_2NMe_2 of Me_2TFA*), 2.23 (6H, s, CH_3 of Me_2TFA*), 2.43 (1H, m, CH_2NMe_2 of Me_2TFA*), 3.37 (1H, dd, ^3J(H, H) = 12.6 Hz, ^4J(H, H) = 5.8 Hz, AlC*H* of Me_2TFA*), 3.98 ppm (1H, m, C*H*CH_2N of Me_2TFA*). Due to a complex spectrum of overlapping signals the βCH_2 of TMP could not be seen.

^{13}C {^{1}H} NMR data (100.62 MHz, THF-D_8, 298 K)

Diastereomer A: δ = 19.2 (γ*C*H_2 of TMP), 28.0 (*C*H of *i*Bu), 28.1 (*C*H of *i*Bu), 32.8 (AlCHCH_2*C*H_2 of Me_2TFA*), 33.7 (*C*H_3 of TMP), 44.6 (AlCH*C*H_2 of Me_2TFA*), 46.3 (*C*H_3 of Me_2TFA*), 52.7 (*C*Me_2 of TMP), 66.7 (CH*C*H_2NMe_2 of Me_2TFA*), 76.1 (*C*HCH_2NMe_2 of Me_2TFA*), 84.3 ppm (Al*C*H of Me_2TFA*).

Diastereomer B: δ = 19.6 (γCH_2 of TMP), 28.2 (*C*H of *i*Bu), 28.3 (*C*H of *i*Bu), 33.0 (AlCH*C*H_2 of Me_2TFA*), 34.4 (*C*H_3 of TMP), 34.6 (*C*H_3 of TMP), 44.2 (AlCH*C*H_2 of Me_2TFA*), 46.1 (*C*H_3 of Me_2TFA*), 52.5 (*C*Me_2 of TMP), 65.8 (CH*C*H_2NMe_2 of Me_2TFA*), 76.5 (*C*HCH_2NMe_2 of Me_2TFA*), 84.5 ppm (Al*C*H of Me_2TFA*).

Diastereomer A/B: δ = 30.4 (*C*H_2 of *i*Bu), 29.9 (*C*H_2 of *i*Bu), 29.0 (*C*H_2 of *i*Bu), 28.7 ppm (*C*H_2 of *i*Bu). Due complex ^{1}H and ^{13}C NMR spectra the *C*H_3 of *i*Bu and β*C*H_2 of TMP could only be assigned to 29.4, 29.7, 30.1 and 31.2 ppm and could not be differentiated.

^{7}Li NMR data (155.50 MHz, THF-D_8, 298 K)

δ = 0.33 ppm.

Synthesis of [Me_2TFA·Li(μ-TMP)(μ-*i*Bu)Al(*i*Bu)$_2$] 2.8C

Hexane (10 mL) was added to an oven-dried Schlenk tube. Next, 1.6M *n*BuLi (1.25 mL, 2 mmol) was added, followed by TMP(H) (0.34 mL, 2 mmol) at room temperature. The reaction mixture was left to stir for 10 min and then *i*Bu_3Al (2 mL, 2 mmol) was injected. Finally, Me_2TFA (0.28 mL, 2 mmol) was added and the reaction mixture was

left to stir overnight. The solution was left to stand at -30 ^{o}C. A crop (0.58 g, 61%) of colourless crystals formed in solution which were suitable for X-ray crystallographic analysis.

^{1}H NMR data (400.13 MHz, THF-D$_8$, 298 K)

δ = -0.34 (1H, m, CH_2 of *i*Bu), -0.20 (5H, d, ^{3}J(H, H) = 6.3 Hz, CH_2 of *i*Bu), 0.84 (15H, d, ^{3}J(H, H) = 6.4 Hz, CH_3 of *i*Bu), 0.89 (3H, d, ^{3}J(H, H) = 6.4 Hz, CH_3 of *i*Bu), 1.22 (4H, m, βCH_2 of TMP), 1.22 (12H, s, CH_3 of TMP), 1.52 (2H, m, γCH_2 of TMP), 1.54 (1H, m, OCHCH_2 of Me_2TFA), 1.81 (2H, m, OCH_2CH_2 of Me_2TFA), 1.89 (3H, m, CH of *i*Bu), 1.93 (1H, m, OCHCH_2 of Me_2TFA), 2.20 (6H, s, NCH_3 of Me_2TFA), 2.30 (2H, m, C$H_2$$NMe_2$ of Me_2TFA), 3.64 (1H, m, αCH_2 of Me_2TFA), 3.78 (1H, m, αCH_2 of Me_2TFA), 3.90 ppm (1H, m, αC*H* of Me_2TFA).

^{13}C {^{1}H} NMR data (100.62 MHz, THF-D$_8$, 298 K)

δ = 20.2 (γ*C*H_2 of TMP), 26.2 (OCH_2*C*H_2 of Me_2TFA), 30.0 (*C*H_2 of *i*Bu), 28.7 (*C*H of *i*Bu), 30.2 (*C*H_3 of *i*Bu), 30.8 (OCH*C*H_2 of Me_2TFA), 34.6 (Me of TMP), 45.3 (β*C*H_2 of TMP), 46.5 (NMe_2 of Me_2TFA), 52.5 (*C*Me_2 of TMP), 64.8 (*C*$H_2$$NMe_2$ of Me_2TFA), 68.4 (O*C*H_2 of Me_2TFA), 78.7 ppm (O*C*H of Me_2TFA).

^{7}Li NMR data (155.50 MHz, THF-D$_8$, 298 K)

δ = -0.43 ppm

Synthesis of [Li(μ-TMP)(μ-MDAE*)Al(*i*Bu)$_2$] 2.1D

This was prepared as per complex **2.1C** but with 1-methoxy-2-dimethylaminoethane (MDAE) (0.25 mL, 2 mmol) injected to the *in situ* generated lithium aluminate base. The solution was left to stand in the freezer at -30 ^{o}C. A crop (0.63 g, 81%) of colourless crystals formed in solution which were suitable for X-ray crystallographic analysis.

^{1}H NMR data (400.13 MHz, THF-D$_8$, 298 K)

δ = -0.12 (4H, m, CH_2 of *i*Bu), 0.88 (6H, d, ^{3}J(H, H) = 6.4 Hz, CH_3 of *i*Bu), 0.90 (6H, d, ^{3}J(H, H) = 6.4 Hz, CH_3 of *i*Bu), 1.25 (4H, m, βCH_2 of TMP), 1.25 (12H, s, CH_3 of TMP), 1.59 (2H, m, γCH_2 of TMP), 1.86 (2H, m, CH of *i*Bu), 2.26 (6H, s, NMe_2 of MDAE*), 2.46 (2H, m, Me_2NCH_2 of MDAE*), 3.20 (2H, s, AlCH_2 of MDAE*), 3.57 ppm (2H, m, $AlCH_2OCH_2$ of MDAE*).

^{13}C {^{1}H} NMR data (100.62 MHz, THF-D_8, 298 K)

δ = 19.6 (γ*C*H_2 of TMP), 28.3 (*C*H of *i*Bu), 29.2 (*C*H_3 of *i*Bu), 30.0 (*C*H_3 of *i*Bu), 30.8 (*C*H_2 of *i*Bu), 33.9 (*C*H_3 of TMP), 45.0 (β*C*H_2 of TMP), 45.5 (NMe_2 of MDAE*), 52.6 (*C*Me_2 of TMP), 60.0 (Me_2N*C*H_2 of MDAE*), 71.7 (AlCH_2O*C*H_2 of MDAE*), 78.0 ppm (Al*C*H_2 of MDAE*).

^{7}Li NMR data (155.50 MHz, THF-D_8, 298 K)

δ = 0.19 ppm.

Synthesis of [MDAE·Li(μ-TMP)(μ-*i*Bu)Al(*i*Bu)$_2$] 2.8D

This was prepared as per complex **2.8C** but with 1-methoxy-2-dimethylaminoethane (MDAE) (0.25 mL, 2 mmol) injected to the *in situ* generated lithium aluminate base. The solution was left to stand in the freezer at -30 ^{o}C. A crop (0.30 g, 33%) of colourless crystals formed in solution which were suitable for X-ray crystallographic analysis.

^{1}H NMR data (400.13 MHz, 298 K, C_6D_6)

δ = 0.27 (6H, d, ^{3}J(H, H) = 6.50 Hz, 3 x CH_2 of *i*Bu), 1.40 (2H, m, 1 x βCH_2 of TMP), 1.42 (15H, d, ^{3}J(H, H) = 6.50 Hz, 5 x CH_3 of *i*Bu), 1.46 (3H, d, ^{3}J(H, H) = 6.50 Hz, 1 x CH_3 of *i*Bu), 1.50 (12H, broad s, 4 x CH_3 of TMP), 1.70 (6H, s, N$(CH_3)_2$ of MDAE), 1.76 (2H, t, ^{3}J(H, H) = 5.18 Hz, NCH_2 of MDAE), 2.43 (3H, m, 3 x CH of *i*Bu), 2.64 (2H, s, OCH_2 of MDAE), 2.93 ppm (3H, s, OCH_3 of MDAE).

^{13}C {^{1}H} NMR data (100.62 MHz, 298 K, C_6D_6)

δ = 18.8 (γ*C*H_2 of TMP), 27.7 (*C*H of *i*Bu), 27.8 (β*C*H_2 of TMP), 28.6 (*C*H_3 of TMP), 29.4 (*C*H_3 of TMP), 29.7 (*C*H_3 of *i*Bu), 29.9 (*C*H_2 of *i*Bu), 45.0 (β*C*H_2 of TMP), 45.1 (N*C*H_3 of MDAE), 52.8 (*C*Me_2 of TMP), 57.8 (N*C*H_2 of MDAE), 59.4 (O*C*H_3 of MDAE), 68.2 ppm (O*C*H_2 of MDAE).

^{7}Li NMR data (155.50 MHz, 298 K, C_6D_6)

δ = - 0.34 ppm

Synthesis of [Li(μ-TMP)(μ-Me_4AEE*)Al(*i*Bu)$_2$] 2.1E

This was prepared as per complex **2.1C** but with Bis[2-(*N*,*N*-dimethylamino)ethyl]ether (Me_4AEE) (0.38 mL, 2 mmol) injected to the *in situ* generated lithium aluminate base,

producing a white precipitate which dissolved on gentle heating. A crop (0.38 g, 42%) of colourless crystals formed in solution while cooling to room temperature.

^{1}H NMR data (400.13 MHz, 298 K, C_6D_6)

δ = 0.48-0.54 (4H, m, 2 x CH_2 of *i*Bu), 1.34 (1H, m, γCH of TMP), 1.36-1.46 (12H, m, 4 x CH_3 of *i*Bu), 1.51 (12H, broad s, CH_3 of TMP), 1.55 (1H, m, OCH_2CH_2 of Me_4AEE*), 1.60 (6H, s, $N(CH_3)_2$ of Me_4AEE*), 1.84 (1H, m, γCH of TMP), 2.02 (1H, m, OCH_2CH_2 of Me_4AEE*), 2.25 (6H, s, $N(CH_3)_2$ of Me_4AEE*), 2.35 (2H, m, 2 x CH of *i*Bu), 2.66 (1H, d, ^{3}J(H, H) = 14.4 Hz, $OCHCH_2$ of Me_4AEE*), 3.15 (1H, m, OCH_2 of Me_4AEE*), 3.28 (1H, m, OCH of Me_4AEE*), 3.50 (1H, d, ^{3}J(H, H) = 11.1Hz, $OCHCH_2$ of Me_4AEE*), 4.48 ppm (1H, m, OCH_2 of Me_4AEE*).

^{13}C {^{1}H} NMR data (100.62 MHz, 298 K, C_6D_6)

δ = 18.3 (γCH_2 of TMP), 27.6 (CH of *i*Bu), 27.8 (CH of *i*Bu), 29.0 (CH_2 of *i*Bu), 28.6 (CH_3 of *i*Bu), 29.4 (CH_3 of *i*Bu), 29.6 (CH_3 of *i*Bu), 35.7 (CH_3 of TMP), 30.2 (CH_3 of *i*Bu), 43.2 (CH_3 of Me_4AEE*), 45.4 (CH_3 of Me_4AEE*), 46.12 (CH_3 of Me_4AEE*), 60.1 (OCH_2CH_2 of Me_4AEE*), 68.2 ($OCHCH_2$ of Me_4AEE*), 69.7 (OCH_2 of Me_4AEE*), 82.0 ppm (O*C*H of Me_4AEE).

^{7}Li NMR data (155.50 MHz, 298K, C_6D_6)

δ = 1.34 ppm.

Synthesis of [(DME)Li(μ-TMP)(μ-*i*Bu)Al(*i*Bu)$_2$] 2.8F

This was prepared as per complex **2.8C** but with dimethoxyethane (DME) (0.21 mL, 2 mmol) injected to the *in situ* generated lithium aluminate base. The Schlenk tube was left to stand at 0^{o}C where a crop (0.42 g, 48%) of colourless crystals formed in solution that were suitable for X-ray crystallographic analysis.

^{1}H NMR data (400.13 MHz, C_6D_6, 298 K)

δ = 0.21 (1H, m, CH_2 of *i*Bu), 0.29 (5H, d, ^{3}J(H, H) = 6.1 Hz, CH_2 of *i*Bu), 1.40 (18H, d, ^{3}J(H, H) = 6.6 Hz, CH_3 of *i*Bu), 1.52 (12H, broad s, CH_3 of TMP), 2.40 (3H, m, CH of *i*Bu), 2.68 (4H, s, CH_2 of DME), 2.86 ppm (6H, s, CH_3 of DME).

^{13}C {^{1}H} NMR data (100.62 MHz, C_6D_6, 298 K)

δ = 18.9 (γ*C*H_2 of TMP), 27.8 (*C*H_3 of *i*Bu), 27.8 (*C*H of *i*Bu), 29.7 (*C*H_3 of TMP), 44.8 (β*C*H_2 of TMP), 52.8 (*C*Me_2 of TMP), 59.0 (*C*H_3 of DME), 69.7 ppm (*C*H_2 of DME).

^{7}Li NMR data (155.50 MHz, C_6D_6, 298 K)

δ = -0.45 ppm.

Synthesis of [Li($Me_2NC_6H_{10}NMeCH_2$)$_2$Al(*i*Bu)$_2$] 2.8H

This aluminate was prepared analogously to complex **2.8C** but with (R,R)-*N,N,N',N'*-tetramethylcyclohexanediamine (TMCDA) (0.38 mL, 2 mmol) injected to the *in situ* generated lithium aluminate base. The Schlenk tube was left in the freezer at -30^{o}C. A crop (0.27 g, 28%) of colourless crystals formed in solution that were suitable for X-ray crystallographic analysis. The rational synthesis of **2.8H** was attempted (0.76 mL, 4 mmol of TMCDA) however, an oil formed in solution and no crystals could be grown.

Synthesis of [$NMe_2CH_2CH_2OCH(C_6H_4OCH_3)CH_2NMe_2$] 2.1E'

Compound **2.1E** was synthesised on a 2 mmol scale as described above. Hexane was removed in *vacuo* and 10 mL of dry THF was added. 4 equivalents of Zn(OAc)$_2$ (8 mmol, 1.48 g) was added and allowed to stir overnight. In a separate Schlenk tube 2 mol/% (0.009 g) of Pd(OAc)$_2$ was added together with 4 mol/% (0.03 g) of 2-dicyclohexylphosphino-2',6'-dimethoxybiphenyl to give Pd(OAc)$_2$/SPhos. THF (5 mL) was added and the solution was allowed to stir until the solid had completely dissolved. 3 equivalents of 4-iodoanisole was added and this solution was added to the first solution via cannula. This combined solution was left to stir overnight. A saturated solution of ammonium chloride (20 mL) was added and the organic layer was separated from the aqueous layer, washing twice with ethyl acetate. Ammonia solution and ethyl acetate were added to the aqueous layer and the organic layer was once again separated from the aqueous layer. The organic layer was concentrated in *vacuo* to leave **2.1E'** and TMP(H) as a crude product. The TMP(H) was removed under vacuum to give **2.1E'** in 62 % (0.27 g) yield.

^{1}H NMR data (400.13 MHz, $CDCl_3$, 298 K)

δ = 2.23 (6H, s, N{CH_3}$_2$), 2.31 (6H, s, N{CH_3}$_2$), 2.29 (1H, m, CH of CH_2), 2.43 (1H, m, CH of CH_2), 2.55 (1H, m, CH of CH_2), 2.76 (1H, m, CH of CH_2), 3.35 (2H, m, CH_2),

3.79 (3H, s, OCH_3), 4.38 (1H, dd, ^3J(H, H) = 9.04, 3.51 Hz, CH next to O), 6.86 (2H, d, ^3J(H, H) = 8.7 Hz, 2 x CH aromatic), 7.22 ppm (2H, d, ^3J(H, H) = 8.7 Hz, 2 x CH aromatic).

$^{13}C\{^1H\}$ NMR data (100.62 MHz, $CDCl_3$, 298 K)

δ = 45.5 ($N\{CH_3\}_2$), 45.8 ($N\{CH_3\}_2$), 55.2 (OCH_3), 59.0 (CH_2), 65.9 (CH_2), 66.4 (CH_2), 79.9 (*C*H next to O), 113.9 (2 x *C*H of aromatic), 127.9 (2 x *C*H of aromatic), 133.86 (quaternary *para C* of aromatic), 159.2 (quaternary *C* of aromatic next to OMe).

Crystallographic Analysis

Crystallographic data was collected at 123(2) K on Oxford Diffraction instruments with a Nonius Kappa CCD Diffractometer. Structures were solved using the *SHELXS-97* program[108] and were refined to convergence against F^2 against all independent reflections by the full-matrix least-squares method using the *SHELXL-97* program.[108] Selected crystallographic and refinement parameters are given in **Tables 3.1** and **3.2**.

Table 3.1: Crystallographic data and refinement details for compounds **2.2**, **2.5**, **2.6** and **2.9**.

	2.2	**2.5**	**2.6**	**2.9**
Empirical formula	$C_{25}H_{51}AlLiNO_2$	$C_{25}H_{51}AlLiNOS$	$C_{26}H_{53}AlLiNOS$	$C_{35}H_{55}AlLiNO_2$
Mol. Mass	431.59	447.65	461.67	555.72
Crystal system	Orthorhombic	Triclinic	Triclinic	Monoclinic
Space group	*Pca*2$_1$	*P*1	*P*-1	*P*21/*c*
a [Å]	16.7981(5)	10.7592(8)	10.5809(10)	19.8968(6)
b [Å]	10.6516(4)	11.0807(9)	10.7800(17)	8.9744(2)
c [Å]	15.5481(6)	13.5715(11)	14.2255(18)	19.5140(5)
α [°]	90	90.902(7)	67.845(13)	90
β [°]	90	104.045(7)	89.196(9)	100.870(3)
γ [°]	90	117.173(8)	70.173(11)	90
V [Å^3]	2781.97(17)	1381.3(2)	1401.6(3)	3421.94(16)
Z	4	2	2	4
Measured reflections	8272	17857	15296	16427
Unique reflections	3146	6844	6738	7792
R_{int}	0.0309	0.0490	0.0759	0.0330

GooF	1.041	0.915	1.119	1.026
R [on *F*, obs reflns only]	0.0594	0.0500	0.0703	0.0646
wR [on F^2, all data]	0.1567	0.1259	0.2298	0.1634
Largest diff. peak/hole [e $Å^{-3}$]	0.482/-0.306	0.614/-0.433	0.568/-0.574	0.694/-0.341

Table 3.2: Crystallographic data and refinement details for compounds **2.1C**, **2.8C**, **2.1D**, **2.8D**, **2.1E**, **2.8F** and **2.8H**.

	2.1C	**2.8C**	**2.1D**	**2.8D**	**2.1E**	**2.8F**	**2.8H**
Empirical formula	$C_{24}H_{50}AlLiN_2O$	$C_{28}H_{60}AlLiN_2O$	$C_{22}H_{48}AlLiN_2O$	$C_{26}H_{58}AlLiN_2O$	$C_{25}H_{55}AlLiN_3O$	$C_{25}H_{55}AlLiNO_2$	$C_{28}H_{60}AlLiN_4$
Mol. Mass	416.58	474.70	390.54	448.66	447.64	435.62	486.72
Crystal system	triclinic	monoclinic	monoclinic	triclinic	orthorhombic	monoclinic	orthorhombic
Space group	P-1	P 21/c	P 21/n	P-1	Pmn21	C c	P21 21 21
a [Å]	9.4546(5)	11.0214(3)	14.2282(5)	10.9349(4)	12.8948(8)	9.5982(3)	11.5071(2)
b [Å]	10.4989(3)	17.0744(4)	10.5076(4)	17.4597(7)	11.0717(5)	18.7837(7)	13.3712(3)
c [Å]	14.9340(6)	17.1403(5)	16.7736(7)	17.8521(8)	10.1824(5)	16.1448(6)	19.9303(6)
α [°]	72.798(3)	90	90	118.629(4)	90	90	90
β [°]	87.420(4)	106.104(3)	90.171(5)	90.683(3)	90	99.987(3)	90
γ [°]	69.720(4)	90	90	97.080(3)	90	90	90
V [Å^3]	1325.6(2)	3098.93(17)	2507.71(17)	2959.1(2)	1453.71(13)	2866.64(18)	3066.55(13)
Z	2	4	4	4	2	4	4
Measured reflections	26903	16787	9718	30177	5099	6393	17148

Unique reflections	5179	7289	5330	12880	2513	4179	7145
R_{int}	0.0317	0.0271	0.0278	0.0521	0.0365	0.0229	0.0213
Obs. reflns. [$I > 2\sigma(I)$]	4215	5283	4448	6838	2041	3728	6282
GooF	1.043	1.019	1.023	1.026	1.041	1.027	1.048
R [on F, obs reflns only]	0.0921	0.0549	0.0435	0.0931	0.0472	0.0472	0.0446
wR [on F^2, all data]	0.2583	0.1441	0.0961	0.2907	0.1208	0.1173	0.1053
Largest diff. peak/hole [e Å^{-3}]	1.827/-0.825	0.412/-0.346	0.208/-0.156	1.210/-0.402	0.385/-0.210	0.684/-0.277	0.329/-0.238

References

[1] A. R. Kennedy, J. Klett, R. E. Mulvey, D. S. Wright, *Science* **2009**, *326*, 706.

[2] R. B. Bates, L. M. Kroposki, D. E. Potter, *J. Org. Chem.* **1972**, *37*, 560.

[3] R. E. Mulvey, V. L. Blair, W. Clegg, A. R. Kennedy, J. Klett, L. Russo, *Nature Chemistry* **2010**, *2*, 588.

[4] A. Maercker, *Angew. Chem. Int. Ed.* **1987**, *26*, 972.

[5] S. J. Geier, D. W. Stephan, *J. Am. Chem. Soc.* **2009**, *131*, 3476.

[6] B. Conway, J. Garcia-Alvarez, E. Hevia, A. R. Kennedy, R. E. Mulvey, S. D. Robertson, *Organometallics* **2009**, *28*, 6462.

[7] B. Conway, A. R. Kennedy, R. E. Mulvey, S. D. Robertson, J. Garcia-Alvarez, *Angew. Chem. Int. Ed.* **2010**, *49*, 3182.

[8] D. Li, I. Keresztes, R. Hopson, P. G. Williard, *Acc. Chem. Res.* **2009**, *42*, 270.

[9] S. Merkel, D. Stern, J. Henn, D. Stalke, *Angew. Chem.* **2009**, *121*, 6468.

[10] W. Bauer, P. von R. Schleyer, *Magn. Reson. Chem.* **1988**, *26*, 827.

[11] Y. Liu, R. S. Glass, *Tetrahedron Lett.* **1997**, *38*, 8615.

[12] V. L. Blair, A. R. Kennedy, R. E. Mulvey, C. T. O'Hara, *Chem. Eur. J.* **2010**, *16*, 8600.

[13] F. H. Allen, *Acta Crystallogr.* **2002**, *B58*, 380.

[14] R. A. Adams, M. P. Pompeo, W. Wu, J. H. Yamamoto, *J. Am. Chem. Soc.* **1993**, *115*, 8207.

[15] S. A. Vinogradov, A. E. Mistrukov, I. P. Beletskaya, *J. Chem. Soc. Dalton Trans.* **1995**, 2679.

[16] M. Yus, C. Najera, F. Foubelo, *Tetrahedron* **2003**, *59*, 6147.

[17] K. C. Nicolaou, K. Ajito, A. P. Patron, H. Khatuya, P. K. Richter, P. Bertinato, *J. Am. Chem. Soc.* **1996**, *118*, 3059.

[18] P. U. Park, C. A. Broka, B. F. Johnson, Y. Kishi, *J. Am. Chem. Soc.* **1987**, *109*, 6205.

[19] G. Adam, R. Zibuck, D. Seebach, *J. Am. Chem. Soc.* **1987**, *109*, 6176.

[20] A. B. Smith, C. M. Adams, *Acc. Chem. Res.* **2004**, *37*, 365.

[21] K. K. Rana, C. Guin, S. Jana, S. C. Roy, *Tetrahedron Lett.* **2003**, *44*, 8597.

[22] A. Kamal, G. Chouhan, K. Ahmed, *Tetrahedron Lett.* **2002**, *43*, 6947.

[23] A. Lalitha, K. Pitchumani, C. Srinivasan, *Green Chem.* **1999**, 173.

[24] G. Wittig, P. Davis, G. Koenig, *Chem. Ber.* **1951**, *84*, 627.

[25] D. Seebach, M. Kolb, *Chem. Ind.* **1974**, *7*, 687.

[26] E. J. Corey, D. Seebach, *Angew. Chem. Int. Ed.* **1965**, *4*, 1075.

[27] E. J. Corey, D. Seebach, *Angew. Chem. Int. Ed.* **1965**, *4*, 1077.

[28] B. T. Grobel, D. Seebach, *Synthesis* **1977**, 357.

[29] T. W. Greene, P. G. M. Wuts, *Protective Groups in Organic Synthesis*, John Wiley & Sons, New York, **1999**.

[30] E. J. Corey, B. W. Erickson, *J. Org. Chem.* **1971**, *36*, 3553.

[31] M. Fetizon, M. Jurion, *J. Chem. Soc., Chem. Commun.* **1972**, 382.

[32] G. Stork, K. Zhao, *Tetrahedron Lett.* **1989**, *30*, 287.

[33] R. Amstutz, J. D. Dunitz, D. Seebach, *Angew. Chem. Int. Ed.* **1981**, *20*, 465.

[34] R. Amstutz, D. Seebach, P. Seiler, B. Schweizer, J. D. Dunitz, *Angew. Chem. Int. Ed.* **1980**, *19*, 53.

[35] D. Seebach, E. J. Corey, *J. Org. Chem.* **1975**, *40*, 231.

[36] C. G. Kruse, A. Wijsman, A. van der Gen, *J. Org. Chem.* **1979**, *44*, 1847.

[37] S. Kawamura, K. Ishizuka, H. Takaya, M. Nakamura, *Chem. Commun.* **2010**, *46*, 6054.

[38] W. Kohn, A. D. Becke, R. G. Parr, *J. Phys. Chem.* **1996**, *100*, 12974.

[39] A. D. Becke, *Phys. Rev. A.* **1988**, *38*, 3098.

[40] C. T. Lee, W. Yang, R. G. Parr, *Phys. Rev. B.* **1988**, *37*, 785.

[41] A. D. McLean, G. S. Chandler, *J. Chem. Phys.* **1980**, 5639.

[42] R. Krishnan, J. S. Binkley, R. Seeger, J. A. Pople, *J. Chem. Phys.* **1980**, *72*, 650.

[43] E. N. Jacobsen, M. H. Wu, *Comprehensive Asymmetric Catalysis II*, Springer-Verlag, New York, **1999**.

[44] J. Meinwald, S. S. Labana, M. S. Chadha, *J. Am. Chem. Soc.* **1963**, *85*, 582.

[45] J. G. Smith, *Synthesis* **1984**, *8*, 629.

[46] R. E. Parker, N. S. Issacs, *Chem. Rev.* **1959**, *59*, 737.

[47] A. S. Rao, S. K. Paknikar, J. G. Kirtane, *Tetrahedron* **1983**, *39*, 2323.

[48] H. O. House, *J. Am. Chem. Soc.* **1955**, *70*, 3070.

[49] B. Rickborn, R. M. Gerkin, *J. Am. Chem. Soc.* **1968**, *90*, 4193.

[50] B. Rickborn, R. M. Gerkin, *J. Am. Chem. Soc.* **1971**, *93*, 1693.

[51] S. Kulasegaram, R. J. Kulawiec, *J. Org. Chem.* **1997**, *62*, 6547.

[52] K. A. Bhatia, K. J. Eash, N. M. Leonard, M. C. Oswald, R. S. Mohan, *Tetrahedron Lett.* **2001**, *42*, 8129.

[53] Y. Kita, S. Kitagaki, Y. Yoshida, S. Mihara, D. F. Fang, M. Kondo, S. Okamoto, R. Imai, S. Akai, H. Fujioka, *J. Org. Chem.* **1997**, *62*, 4991.

[54] B. C. Ranu, U. Jana, *J. Org. Chem.* **1998**, *63*, 8212.

[55] Y. Kita, J. Futamura, Y. Ohba, Y. Sawama, J. K. Ganesh, H. Fujioka, *J. Org. Chem.* **2003**, *68*, 5917.

[56] T. Bando, K. Shishido, *Chem. Commun.* **1996**, 1357.

[57] M. Matsushita, H. Maeda, M. Kodama, *Tetrahedron Lett.* **1998**, *39*, 3749.

[58] T. Kimura, N. Yamamoto, Y. Suzuki, K. Kawano, Y. Norimine, K. Ito, S. Nagato, Y. Limura, M. Yonaga, *J. Org. Chem.* **2002**, *67*, 6228.

[59] B. Rickborn, *Comprehensive Organic Synthesis, Carbon-Carbon Bond Formation*, Pergamon, Oxford, **1991**.

[60] K. Maruoka, T. Ooi, H. Yamamoto, *J. Am. Chem. Soc.* **1989**, *111*, 6431.

[61] K. Maruoka, N. Murase, R. Bureau, T. Ooi, H. Yamamoto, *Tetrahedron* **1994**, *50*, 3663.

[62] X.-M. Deng, X.-L. Sun, Y. Tang, *J. Org. Chem.* **2005**, *70*, 6537.

[63] K. Suda, T. Kikkawa, S. Nakajima, T. Takanami, *J. Am. Chem. Soc.* **2004**, *126*, 9554.

[64] A. C. Cope, P. A. Trumbull, E. R. Trumbull, *J. Am. Chem. Soc.* **1958**, *80*, 2844.

[65] A. C. Cope, H. H. Lee, H. E. Petree, *J. Am. Chem. Soc.* **1958**, *80*, 2849.

[66] A. C. Cope, M. Brown, H. E. Petree, *J. Am. Chem. Soc.* **1958**, *80*, 2852.

[67] A. C. Cope, M. Brown, H. H. Lee, *J. Am. Chem. Soc.* **1958**, *80*, 2855.

[68] A. C. Cope, J. K. Heeren, *J. Am. Chem. Soc.* **1965**, *87*, 3125.

[69] A. Mordini, E. Benrayana, C. Margot, M. Schlosser, *Tetrahedron* **1990**, *46*, 2401.

[70] A. Mordini, S. Pecchi, G. Capozzi, A. Capperucci, A. Degl'Innocenti, G. Reginato, A. Ricci, *J. Org. Chem.* **1994**, *59*, 4784.

[71] C. L. Kissel, B. Rickborn, *J. Org. Chem.* **1972**, *37*, 2060.

[72] J. K. Crandall, M. Apparu, *Org. React.* **1983**, *29*, 345.

[73] K. M. Morgan, J. J. Gajewski, *J. Org. Chem.* **1996**, *61*, 820.

[74] J. Lertvorachon, Y. Thebtaranonth, T. Thongpanchang, P. Thonyoo, *J. Org. Chem.* **2001**, *66*, 4692.

[75] Y. Mori, K. Yaegashi, H. Furukawa, *J. Am. Chem. Soc.* **1997**, *119*, 4557.

[76] Y. Mori, K. Yaegashi, H. Furukawa, *Tetrahedron* **1997**, *53*, 12917.

[77] Y. Mori, K. Yaegashi, H. Furukawa, *J. Org. Chem.* **1998**, *63*, 6200.

[78] Y. Mori, *Heteroat. Chem.* **1997**, *17*, 183.

[79] J. R. K. Boeckman, *Tetrahedron Lett.* **1977**, 4281.

[80] E. Doris, L. Dechoux, C. Mioskowski, *Tetrahedron Lett.* **1994**, *35*, 7943.

[81] K. M. Morgan, M. J. O'Connor, J. L. Humphrey, K. E. Buschman, *J. Org. Chem.* **2001**, *66*, 1600.

[82] D. M. Hodgson, E. H. M. Kirton, S. M. Miles, S. L. M. Norsikian, N. J. Reynolds, *Org. Biomol. Chem.* **2005**, *3*, 1893.

[83] D. M. Hodgson, N. S. Kaka, *Angew. Chem.* **2008**, *120*, 10106.

[84] D. M. Hodgson, S. L. M. Norsikian, *Org. Lett.* **2001**, *3*, 461.

[85] S. Florio, V. Aggarwal, A. Salomone, *Org. Lett.* **2004**, *6*, 4191.

[86] J. J. Eisch, J. E. Galle, *J. Am. Chem. Soc.* **1976**, *98*, 4646.

[87] J. J. Eisch, J. E. Galle, *J. Organomet. Chem.* **1976**, *121*, C10.

[88] J. J. Eisch, J. E. Galle, *J. Org. Chem.* **1990**, *55*, 4835.

[89] A. M. Anderson, J. M. Blazek, P. Garg, B. J. Payne, R. S. Mohan, *Tetrahedron Lett.* **2000**, *41*, 1527.

[90] K. Smith, G. A. El-Hiti, M. Al-Shamali, *Catalysis Letters* **2006**, *109*, 77.

[91] M. Uchiyama, H. Naka, Y. Matsumoto, T. Ohwada, *J. Am. Chem. Soc.* **2004**, *126*, 10527.

[92] H. Naka, M. Uchiyama, Y. Matsumoto, A. E. H. Wheatley, M. McPartlin, J. V. Morey, Y. Kondo, *J. Am. Chem. Soc.* **2007**, *129*, 1921.

[93] H. Naka, J. V. Morey, J. Haywood, D. J. Eisler, M. McPartlin, F. Garcia, H. Kudo, Y. Kondo, M. Uchiyama, A. E. H. Wheatley, *J. Am. Chem. Soc.* **2008**, *130*, 16193.

[94] H. W. Gschwend, H. R. Rodriguez, *Org. React.* **1979**, *26*, 1.

[95] V. Snieckus, *Chem. Rev.* **1990**, *90*, 879.

[96] M. C. Whisler, S. MacNeil, V. Snieckus, P. Beak, *Angew. Chem. Int. Ed.* **2004**, *43*, 2206.

[97] J. Garcia-Alvarez, E. Hevia, A. R. Kennedy, J. Klett, R. E. Mulvey, *Chem. Commun.* **2007**, 2402.

[98] J. Garcia-Alvarez, D. V. Graham, A. R. Kennedy, R. E. Mulvey, S. Weatherstone, *Chem. Commun.* **2006**, 3208.

[99] B. Conway, E. Hevia, J. Garcia-Alvarez, D. V. Graham, A. R. Kennedy, R. E. Mulvey, *Chem. Commun.* **2007**, 5241.

[100] L. Yang, D. R. Powell, R. P. Houser, *Dalton Trans.* **2007**, 955.

[101] P. H. Kasai, *J. Phys. Chem. A.* **2002**, *106*, 83.

[102] C. A. Bradley, L. F. Veiros, P. J. Chirik, *Organometallics* **2007**, *26*, 3191.

[103] G. B. Deacon, P. C. Junk, G. J. Moxey, *Z. Anorg. Allg. Chem.* **2008**, *634*, 2789.

[104] T. E. Barder, S. D. Walker, J. R. Martinelli, S. L. Buchwald, *J. Am. Chem. Soc.* **2005**, *127*, 4685.

[105] H. J. Reich, W. S. Goldenberg, A. W. Sanders, *ARKIVOC* **2004**, *xiii*, 97.

[106] G. J. P. Britovsek, J. England, A. J. P. White, *Inorg. Chem.* **2005**, *44*, 8125.

[107] J.-C. Kizirian, N. Cabello, L. Pinchard, J.-C. Caille, A. Alexakis, *Tetrahedron* **2005**, *61*, 8939.

[108] G. M. Sheldrick, *Acta Crystallogr., Sect. A: Found. Crystallogr.* **2008**, *64*, 112.

Chapter 4: Halogen Substituted Aromatics

4.1 Introduction: 3-iodoanisole

A particularly attractive facet of Alkali-Metal-Mediated Alumination (AMM*Al*) is the high halogen tolerance which has been documented by the bases $(TMP)_3Al{\cdot}3LiCl$ (**3.1**, made by Knochel)[1] and $i Bu_3Al(TMP)Li$[2] (**3.2**, made by Uchiyama – the first reported base of this type). Heterometallic alkali-metal aluminate bases will generally carry out directed *ortho*-metallation (metal-hydrogen exchange) reactions of halo-substituted aromatic molecules in preference to metal-halogen exchange. The ability of these bases to form aryl aluminium species should also be noted as the conventional procedures used to prepare these compounds, namely transmetallation of the corresponding organolithium or Grignard reagents with appropriate aluminium salts, are of limited use due to poor functional group tolerance. While alkyl-amido base **3.2** and our alkyl *bis*-TMP base $i Bu_2Al(TMP)_2Li$ **3.3** are clearly constitutionally very similar, they can display markedly different reactivity; Uchiyama's base is stable in THF, a solvent in which it is routinely utilized, while **3.3** deprotonates a stoichiometric amount of THF in bulk hexane solution (see **Chapter 3**). With this in mind and inspired by Uchiyama's recent report of thermally controlled *ortho*-deprotonation of 3-bromo-*N*,*N*-diisopropylbenzamide with mono-TMP base **3.2**,[3] we investigated whether *bis*-TMP base **3.3** can likewise *ortho*-deprotonate 3-halogenated *ortho*-directing substituted aromatics. Focusing on 3-haloanisoles, we learn much about the fate of the different metals and different ligands following their *ortho*-alumination.

4.2 Results and Discussion

The attempted deprotonation of 3-iodoanisole by lithium aluminate **3.3** to give complex **3.4** was carried out in bulk hexane solution as depicted in **Scheme 4.1**.

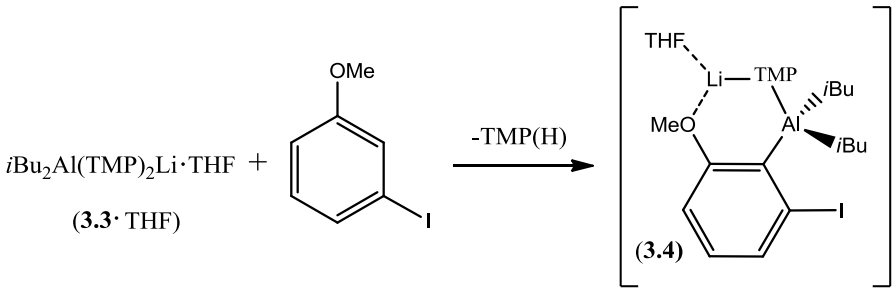

Scheme 4.1: Attempted deprotonation of 3-iodoanisole by **3.3** to give complex **3.4**.

Even at a subambient temperature as low as -78°C, the mixture instantly precipitated a white solid. This solid was removed by vacuum filtration and the resulting solution was kept overnight at -35°C, yielding a reasonable large crop of colourless crystals. A single crystal structural determination revealed that this crystalline product was in fact the C_2 symmetric amine solvated lithium iodide cubane $[LiI{\cdot}TMP(H)]_4$, **3.5** (**Figure 4.1**, see **Table 4.1** for selected bond parameters).

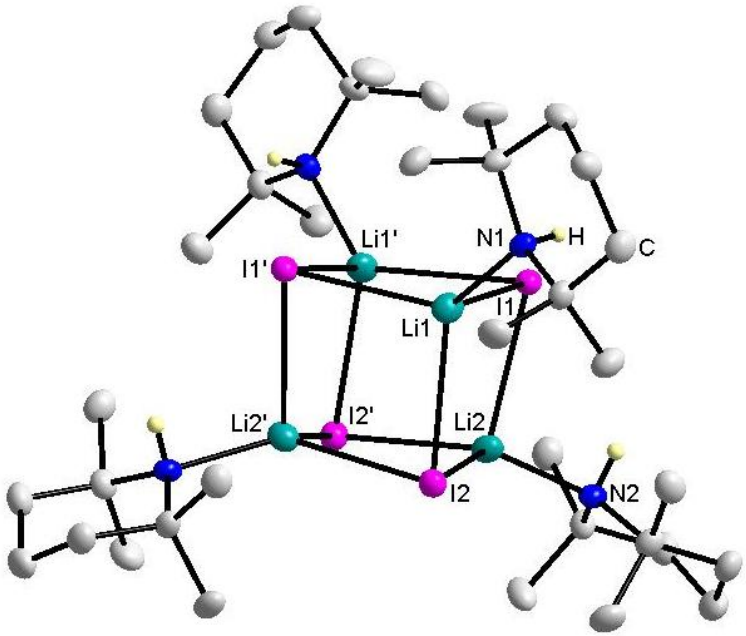

Figure 4.1: Molecular structure of tetrameric **3.5**. Thermal ellipsoids are drawn at the 50% probability level and all carbon bound H atoms have been removed for clarity. Primed atom labels represent symmetry generated atoms via symmetry operation –x, y, 0.5-z.

Table 4.1: Selected bond lengths (Å) and bond angles (°) of complex **3.5**.

Li-I				Li-N	
Li1-I1	2.879(8)	Li2-I1	2.843(7)	Li1-N1	2.111(9)
Li1-I1’	2.843(7)	Li2-I2	2.799(9)	Li2-N2	2.097(6)
Li1-I2	2.907(7)	Li2-I2’	2.814(7)		
I-Li-I		Li-I-Li		N-Li-I	
I1-Li1-I1’	102.3(2)	Li1-I1-Li1’	77.1(2)	N1-Li1-I1	102.4(3)
I1-Li1-I2	98.4(2)	Li1-I1-Li2	79.0(2)	N1-Li1-I1’	126.0(4)
I1’-Li1-I2	97.7(2)	Li1’-I1-Li2	80.4(2)	N1-Li1-I2	124.9(3)
I1-Li2-I2	101.9(2)	Li1-I2-Li2	79.3(2)	N2-Li2-I1	101.1(3)
I1-Li2-I2’	99.9(2)	Li1-I2-Li2’	79.8(2)	N2-Li2-I2	125.1(3)
I2-Li2-I2’	97.1(3)	Li2-I2-Li2’	81.8(2)	N2-Li2-I2’	126.6(3)

Since Snaith first reported a HMPA (hexamethylphosphoramide) solvated LiCl cubane tetramer in 1984,[4] examples of Lewis donor-solvated (D) alkali-metal halide cubanes [$(MX{\cdot}D)_4$] have sporadically graced the literature. Surprisingly, only lithium examples with alkali-metal bound Lewis donors are known, including those of Et_2O,[5–7] Et_3N,[8] $HN{=}PR_3$ (R = ^{t}Bu, Ph)[9] and $O{=}PH(^t Bu)_2$.[10] While heavier alkali-metal halide cubanes including those of KF or CsF are known, these are stabilized via halide-Lewis acid interactions involving trisalkyl gallium or indium species.[11–13]

Like its predecessors mentioned above, *pseudo*-cubane **3.5** consists of interpenetrating Li_4 and I_4 tetrahedra, with lone pair donation from the TMP(H) nitrogen atoms to the Lewis acidic lithium cations giving Li a distorted tetrahedral environment overall. From the seminal ring-stacking principle developed by Snaith, which is widely applicable throughout lithium structural chemistry, **3.5** could be alternatively described as a face-to-face stack of two $(LiI)_2$ dimeric rings.[14–16] Due to its considerable bulk (and expense) secondary amine TMP(H) is not a common Lewis donor towards electron deficient metals, with most crystallographically authenticated examples involving either late transition metals[17–20] or group 13 metals.[21–26] However, TMP(H) solvation of lithium is precedented, with both a derivative of base **3.2**[27] and a dilithium zincate[28] having been stabilised via a Li···N(TMPH) interaction. The two distinct TMP(H) ligands in **3.5**, which both reside in the more typical chair conformation, each lie tilted towards one of the adjacent iodide anions as displayed by their one smaller (mean 101.7^o) and two larger N-Li-I bond angles (mean 125.6^o). The NH bond (note that the H atom was located and independently refined in the crystallographic study) lies almost parallel to the Li-I bond representing the smaller angle (H-N-Li-I torsion angle = 5.8/2.2^o for Li1 and Li2 respectively) with an N(H)···I distance of 3.42(3) and 3.34(2)Å for H1-I1 and H2-I2 respectively. The cubane itself is highly distorted [I-Li-I, 97.1(3)-102.3(2)^o; Li-I-Li, 77.1(2)-81.8(2)^o] with Li-I bond lengths [range 2.799(9)-2.907(7)Å; mean 2.847 Å] in accord with those in previously reported LiI cubanes, as are the dative Li···N distances when compared to those in the tertiary amine solvated $[LiI{\cdot}NEt_3]_4$.

As far as we can ascertain complex **3.5** surprisingly represents the first example of a secondary amine stabilised alkali-metal halide cubane. Lack of solubility in common non-donating NMR solvents is a problem for **3.5**, precluding us from obtaining such spectra of it. Polar THF-d_8 was used as an alternative solvent but this displaced TMP(H)

as the donor, giving a spectrum of the free secondary amine. Infra-red characterisation to confirm the presence of the secondary amine functionality was also attempted; however this proved uninformative due to either the hygroscopic nature of the product resulting in peaks masking the region of interest or the inherently weak absorptions of the functionality in question.

Interestingly, all attempts at a rational synthesis of **3.5** were unsuccessful. For example, LiI would not dissolve in non-polar solvents in the presence of stoichiometric amounts of TMP(H) or even in neat TMP(H) while *in situ* generated LiI (either from Me_3SiI and MeLi or NH_4I and *n*BuLi) immediately precipitated from the mixture. When polar THF was used as a solvent, not surprisingly TMP(H) failed to displace this with the only tangible product identified being the known solvate LiI·3THF.[29]

An NMR spectroscopic study on both the white precipitate isolated initially and the subsequently grown crystals of **3.5** suggest that these two products are identical. This result implies that the putative metallated product **3.4** must rapidly decompose, almost certainly via a benzyne mechanism, and that unlike Uchiyama's protocol with base **3.2**, the suppression of this decomposition is not possible since it cannot be stopped even at the extreme temperature of -78°C. The fact that a product containing a Li-I fragment is produced, even though it is almost certain that alumination occurs *ortho* to the halide, allows us to propose a potential pathway by which the decomposition of the putative aluminated intermediate occurs (**Scheme 4.2**). Comparison with the *ortho*-aluminated substituted aromatics shown in **Chapter 2** provides us with confidence that it is an alumination, that is, formation of **3.4**, which occurs first.

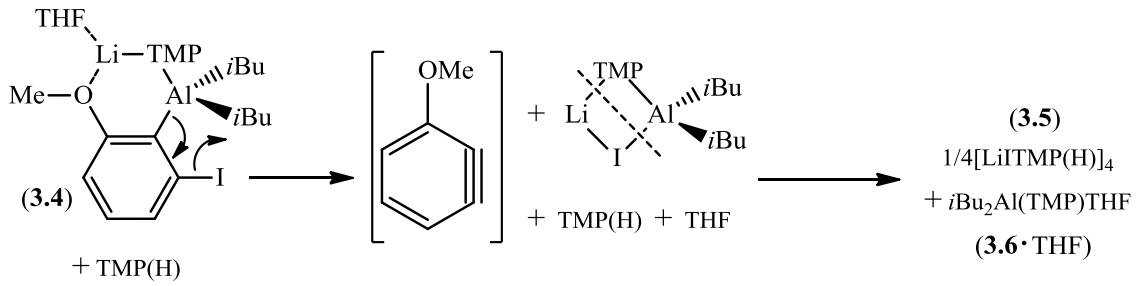

Scheme 4.2: Potential pathway for decomposition of the putative aluminated intermediate.

While there are many documented examples of complexes of general formula "Li(μ-anion)$_2$Al(anion)$_2$", from a search of the Cambridge Structural Database[30] surprisingly

none of them involve a mixed organic anion/iodide anion bridging set,[31,32] perhaps in part due to the appreciably different M-I and M-C/M-N bond lengths which would lead to a severely distorted M-I-M-C/N four atom ring. It is therefore highly likely that putative Li(μ-I)(μ-TMP)Al*i*Bu$_2$ rapidly disproportionates to **3.5** and **3.6**·THF.[33–36] Since the Lewis bases TMP(H) and THF are only present in stoichiometric quantities it is conceivable that the less sterically bulky donor (THF) will bind preferentially to the more sterically encumbered stronger Lewis acidic metal (in this case Al), leaving only TMP(H) available to solvate the electron-poor lithium.

This pathway was further supported by a ^{1}H NMR spectrum of the residue remaining after **3.5** had been isolated which showed resonances consistent with the neutral dialkylaluminium amide **3.6**·THF. The synthesis of *i*Bu$_2$AlTMP as an oil is discussed in **Chapter 1** which was shown to exist as a monomer by DOSY NMR spectroscopy, almost certainly because of the short Al-N$_{TMP}$ distance, coupled with the steric bulk around the TMP nitrogen, which meant that dimerization to give four-coordinate Al centres could not occur.[37] Consequently we prepared an authentic sample of **3.6**·THF by simply adding a molar equivalent of THF to pre-prepared *i*Bu$_2$AlTMP in hexane. Upon cooling to -35^{o}C, the resultant crystals were confirmed as being the desired product via a combination of X-ray crystallography (**Figure 4.2**) and NMR spectroscopy [^{1}H and ^{13}C] (^{1}H NMR spectrum shown **Figure 4.3**).

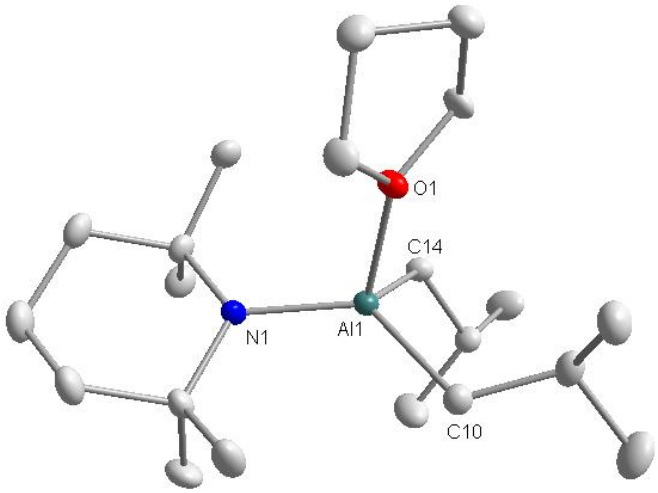

Figure 4.2: Molecular structure of **3.6**·THF. Thermal ellipsoids are drawn at the 50% probability level and all H atoms have been removed for clarity. Selected bond lengths (Å) and angles (^{o}): Al1-N1 1.865(1), Al1-O1 1.951(1), Al1-C10 1.992(2), Al1-C14 2.011(2); N1-Al1-O1 100.99(6), N1-Al1-C10

122.11(7), N1-Al1-C14 119.67(7), O1-Al1-C10 99.45(7), O1-Al1-C14 101.98(7), C10-Al1-C14 107.80(7).

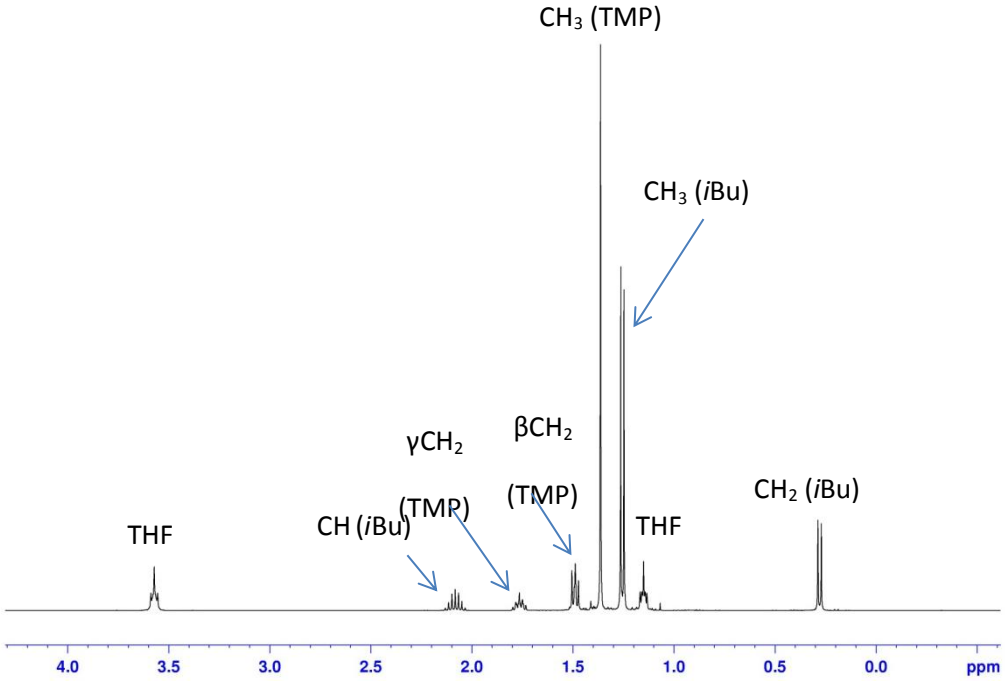

Figure 4.3: ^{1}H NMR spectrum of *i*Bu$_2$Al(TMP)THF **3.6**.

To verify that benzyne formation is a key step during this process, we repeated this reaction and then attempted to trap any benzyne formed via a Diels-Alder cyclisation by adding a diene (1,3-diphenylisobenzofuran) at -78^{o}C, before allowing the reaction to warm to room temperature (**Scheme 4.3**). After work up and purification crystals of 1-methoxy-9-10-diphenyl-9-10-epoxyanthracene (**3.7**) were obtained in near quantitative yield. ^{1}H and ^{13}C NMR spectroscopy (see **Figure 4.4** for the assigned ^{13}C spectrum) plus elemental analysis established that **3.7** was the final product. In particular, the ^{13}C NMR spectrum displayed all 23 expected resonances which could be easily assigned to one of five environments – methyl (orange), quaternary aliphatic (red), aromatic C-H (green), *ortho*/*meta* C-H (blue) and aromatic C (black). The identity of the product was corroborated by a single crystal molecular structure determination (see inset of **Figure 4.4**).

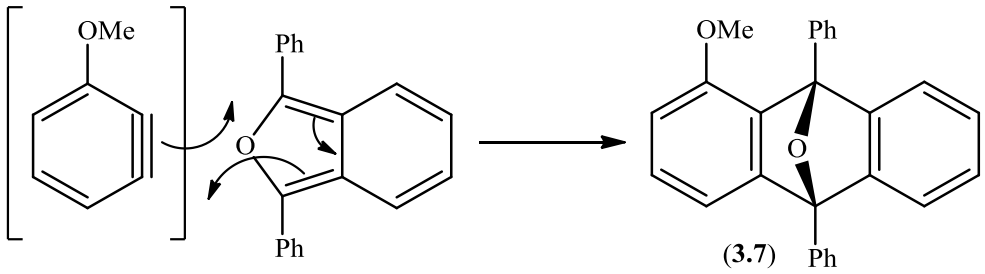

Scheme 4.3: Diels Alder cyclisation with the OMe-substituted benzyne intermediate to give **3.7**.

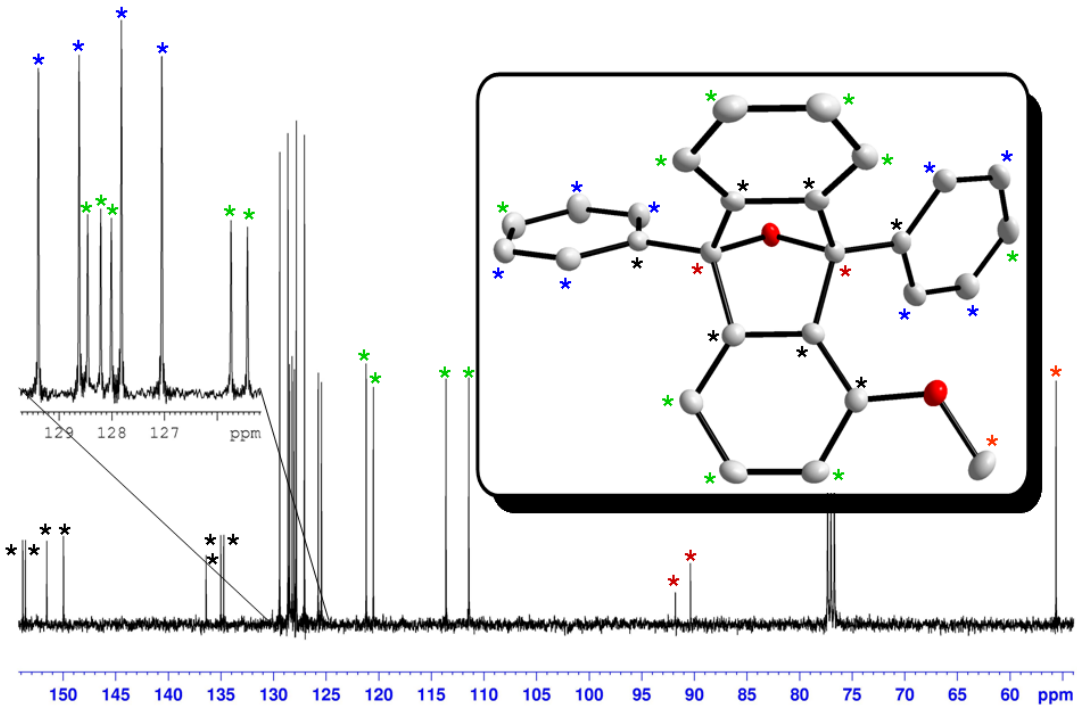

Figure 4.4: $^{13}C\{^{1}H\}$ NMR spectrum of **3.7** with molecular structure inset (thermal ellipsoids at 50% probability level and H atoms omitted for clarity. Oxygen atoms are shaded red).

The results outlined thus far show that bases **3.2** and **3.3** display contrasting reactivities towards 3-halogenated substituted aromatic substrates, since Uchiyama *et al.* utilized a low temperature regime to sedate their aluminated product prior to electrophilic quenching.

An interesting parallel can be drawn here with alkali-metal mediated zincations. Bisalkyl TMP zincates formulated as "$R_2Zn(TMP)Li$"[38–40] (which are also effective at performing chemoselective deprotonations in both typical[38,41] and atypical[42,43] positions) display contrasting reactivity in the zincation of 3-halogenated substituted aromatic molecules; with the metallated product extruding benzyne when R = Me but

not when R = *t*Bu, suggesting steric bulk is a critical factor in preventing benzyne formation (**Scheme 4.5a**).[44,45] It is pertinent to note that heteroleptic alkyl/amido alkali-metal zincates depend on the identity of the alkali-metal and Lewis donor for their reactivity and can operate via a two-step mechanism whereby the initial deprotonation occurs via TMP basicity [generating TMP(H)]; this amine is subsequently deprotonated by an alkyl group of the deprotonated substrate containing intermediate resulting in re-integration of TMP into the framework and permanent loss of alkane (**Scheme 4.5b**).[46–50] This however relies on accessibility of the zinc centre by the Lewis donating TMP(H) and is prevalent in lighter alkali-metal congeners (Li, Na) which tend to be monomeric with coordinatively unsaturated 3-coordinate Zn as opposed to heavier potassium zincates which oligomerize and have 4-coordinate inaccessible Zn centres of diminished Lewis acidity.[51]

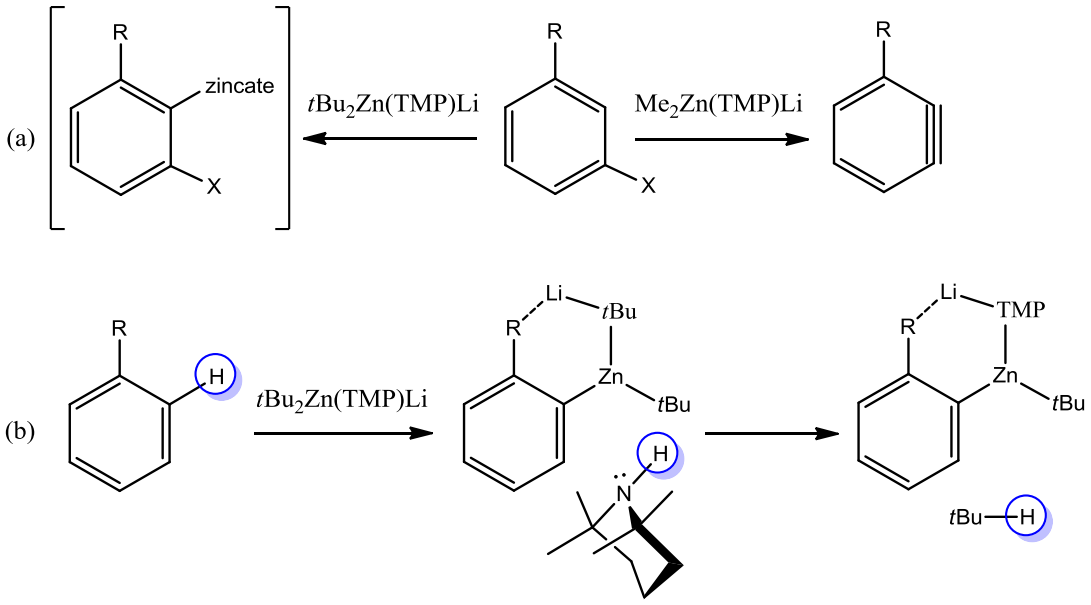

Figure 4.5a: (top) contrasting reactivity of bisalkyl lithium TMP zincates and **4.5b** (bottom) two-step mechanism of bisalkyl alkali-metal TMP zincate displaying overall alkyl basicity. R = *ortho* directing group, X = halide.

An analogous two step mechanism can be ruled out for the lithium aluminates **3.2** and **3.3** discussed thus far since apart from deprotonated substrate, the only other anions present when **3.2** executes a deprotonation are *i*Bu groups, and if alkyl induced deprotonation were to occur at any stage then volatile *i*Bu-H would be irreversibly lost from the system negating its re-entry. The presence of a TMP anion bound to a

coordinatively saturated (4 coordinate) Al centre in our system here would thus appear to be key to the high reactivity of this intermediate and may explain why this breaks down with extrusion of a benzyne. However, while it is tempting at this stage to unequivocally assign the reactivity to anionic effects, it is important to remember that solvent (polar THF versus non-polar hexane) in the zincate systems above plays a highly important role. Likewise, **3.2** is routinely used as a THF solution, while **3.3** is used in hexane as it α-deprotonates THF, *vide supra*. Consequently, we decided to repeat the attempted synthesis of complex **3.4** in THF at -78°C, anticipating firstly that the low temperature would suppress THF deprotonation and secondly that the more acidic 3-iodoanisole would be preferentially deprotonated. In practice, no white precipitate was seen when 3-iodoanisole was introduced to a stirring solution of pre-prepared **3.3** in THF at -78°C. After stirring for two hours, a stoichiometric solution of elemental iodine in THF was introduced in an attempt to prepare 2,3-diiodoanisole.[52] After work-up and purification via column chromatography, a crystalline product (**3.8**) was obtained. A molecular structure determination (**Figure 4.6**) and a ^{1}H NMR spectrum (**Figure 4.7**) showed the identity of **3.8** to in fact be the hitherto unknown N-substituted TMP compound 1-(2-iodo-3-methoxyphenyl)-2,2,6,6-tetramethylpiperidide in a moderate yield of 48%.

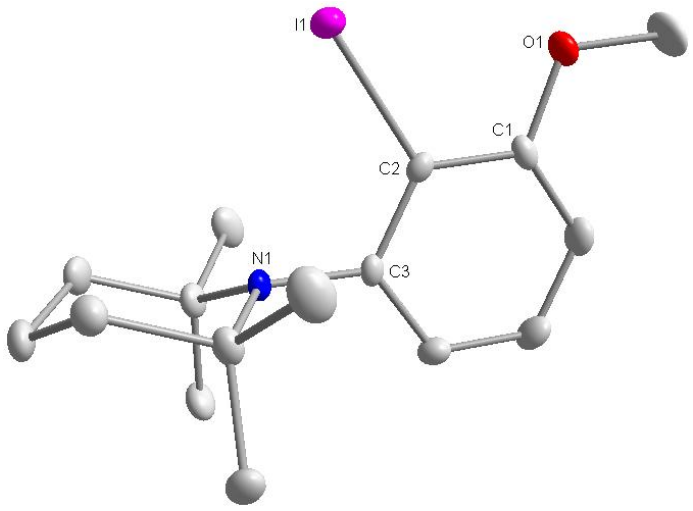

Figure 4.6: Molecular structure of N-substituted TMP derivative **3.8**. Thermal ellipsoids are drawn at the 50% probability level and all H atoms have been removed for clarity. Selected bond lengths (Å) and angles (°): C1-O1 13.71(3), C2-I1 2.107(2), C3-N2 1.436(3); O1-C1-C2 116.4(2), C1-C2-I1 117.6(2), C3-C2-I1 120.7(2), C2-C3-N1 119.6(2).

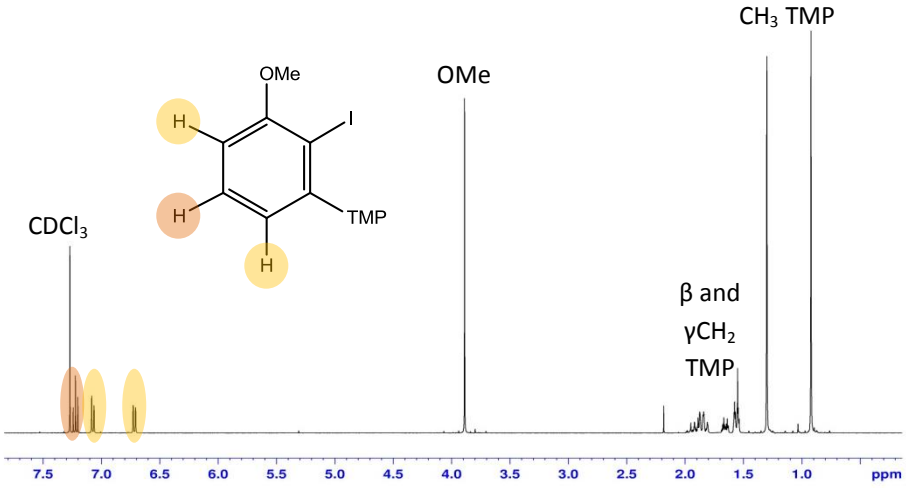

Figure 4.7: ^{1}H NMR spectrum of 1-(2-iodo-3-methoxyphenyl)-2,2,6,6-tetramethylpiperidide **3.8**.

Heterotri-substituted benzene **3.8** can be regarded as the product of Li-TMP addition across the benzyne functionality, followed by replacement of the lithium atom via an iodine quench. The ^{1}H NMR spectrum of **3.8** suggests that the TMP chair is conformationally locked since the methyl, β and γ environments are all resolved into twice the number of resonances typically anticipated for a coordinatively flexible TMP compound. This cascade process involving metallation of *meta*-halogenated substituted aromatics, elimination of metal halide/formation of benzyne and then LiTMP addition across the benzynyl functionality has previously been documented by Mortier[53,54] amongst others.[55,56]

It should be noted here that prior to column purification, a ^{1}H NMR spectrum of the crude product was obtained whose aromatic region showed product **3.8** to be present in about an equimolar amount to the starting substrate, 3-iodoanisole. On the basis of this unexpected result we can propose a final hypothesis for the fate of the benzyne generated once LiI is expelled from the putative metallated product **3.4**. If the benzyne reacts with the LiTMP component of the base **3.3** faster than the base can deprotonate the remaining substrate, then additional *i*Bu$_2$Al(TMP)·THF (**3.6**·THF) will be generated along with 1-(2-lithio-3-methoxyphenyl)-2,2,6,6-tetramethylpiperidide (which itself is simply quenched with iodine). As a consequence of the base being consumed this way, 50% of the 3-iodoanisole will remain unreacted, as seen here. This allows us to propose a modification of **Scheme 4.2** showing the fate of all the intermediate products (**Scheme 4.4**).

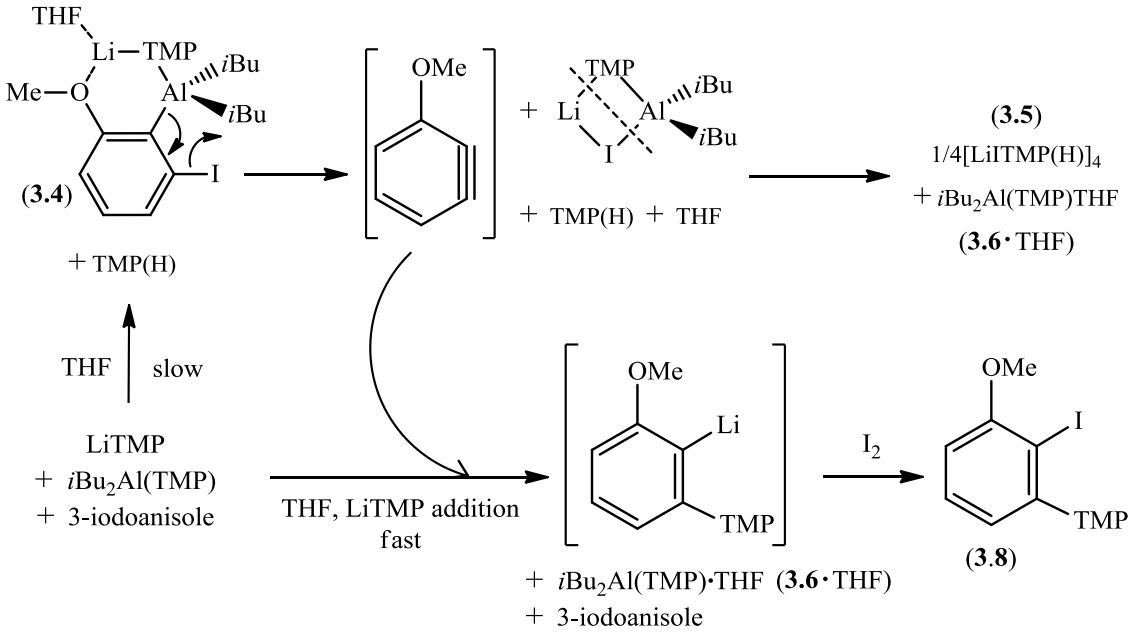

Scheme 4.4: Modified expanded version of **Scheme 4.2** showing the effect of changing the solvent from hexane to THF.

It is reasonable to presume that the relatively weak C-I bond was responsible for the failure to *ortho* deprotonate the substrate without causing further decomposition reactions, so consequently we turned our attention to the more strongly bonded 3-bromo- and 3-chloroanisole congeners. However, on moving to the bromo congener an analogous reactivity was witnessed. A different outcome was observed with the chloro-substituted derivative. It yielded 2-iodo-3-chloroanisole (**3.9**)[57] in only 25% yield after being subjected to metallation with one molar equivalent of base **3.3** at -78°C for 2 hours followed by electrophilic quenching with iodine. A longer reaction time (8 hours) had no significant effect on the yield however, using a four-fold excess of base **3.3** furnished a near-quantitative yield of 98% of **3.9** (^{1}H NMR spectrum **Figure 4.8**).

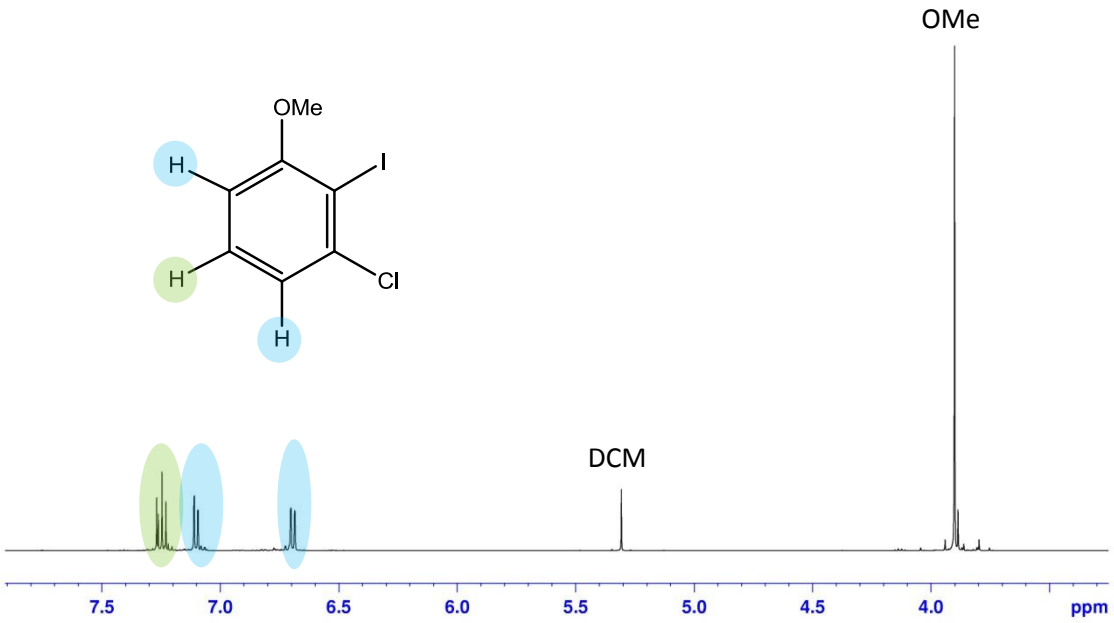

Figure 4.8: ^{1}H NMR spectrum of 2-iodo-3-chloroanisole product **3.9**.

4.3 Introduction: 4-iodoanisole

Owing to the different relative strengths of carbon-halogen bonds, hetero-halogen substituted aromatics can be regioselectively functionalised in different ways at distinct sites.[58,59] For example, Knochel has demonstrated this through the stepwise selective functionalisation of the heterotrihalogenated heterocycle 2-chloro-4-bromo-6-iodo-pyrimidine to yield the fungicide Mepanipyrim.[60] Aryl halides are a fundamentally important, synthetically useful class of organic compounds hence they are utilised in the synthesis of a broad range of commercially important materials such as natural products,[61,62] biologically active materials[63,64] and pharmaceuticals.[65–70] Participation of aryl halides in transition metal-catalysed cross coupling reactions,[71–75] metal-halogen exchange reactions[76] and in the synthesis and applications of organometallic compounds such as Grignard reagents[77] are just some of their important leading applications.

4.4 Results and Discussion

Inspired by the importance of halogenated aromatics and the halogen tolerance of our base **3.3** we investigated the possible sequential regioselective alumination followed by electrophilic halogenation (**Scheme 4.5**) of 4-iodo **3.10a**, 4-bromo **3.10b** and 4-chloroanisole **3.10c** respectively to form the new synthetically useful

triheterohalogenated isomers 2-bromo-4-iodo-6-chloroanisole **3.12a**, 2-iodo-4-bromo-6-chloroanisole **3.12b** and 2-iodo-4-chloro-6-bromoanisole **3.12c** (**Table 4.2**).[78–80]

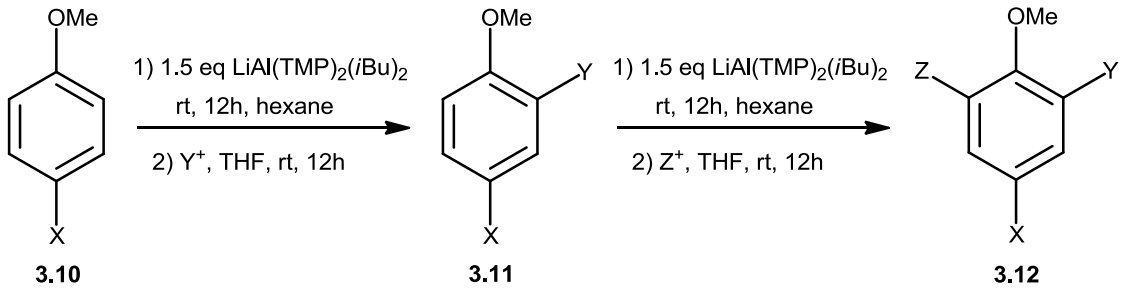

Scheme 4.5: Sequential aluminations and halogenations of 4-haloanisole to yield the new triheterohalogenated derivative **3.12**. Y^+ and Z^+ are electrophilic halides.

Table 4.2: Halogenation of various halo-anisoles with *N*-bromosuccinimide, iodine and sulfuryl chloride after alkali-metal-mediated alumination.

Entry	Aryl Halide	Product	Yield (%)
1	**3.10a** 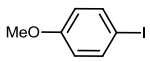 [a] 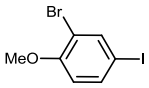 **3.11a**		93
2	**3.10b** 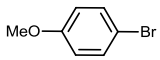 [b] 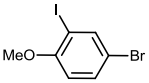 **3.11b**		91
3	**3.10c** 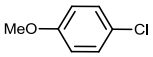 [b] 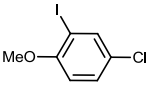 **3.11c**		88
4	**3.11a** 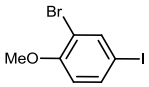 [c] 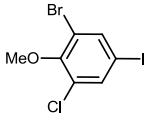 **3.12a**		90
5	**3.11b** 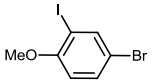 [c] 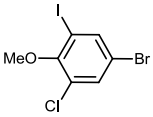 **3.12b**		86
6	**3.11c** 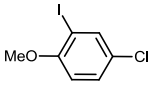 [d] 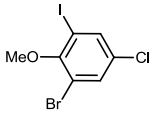 **3.12c**		89

[a] Y^+ used = *N*-bromosuccinimide ($CH_2C\{=O\}NBrC\{=O\}CH_2$), [b] Y^+ used = iodine (I_2), [c] Z^+ used = sulfuryl chloride (SO_2Cl_2), [d] Z^+ used = *N*-bromosuccinimide

Y^+ and Z^+ are electrophilic halide reagents used.

Utilising **3.3** in a 1.5:1.5:1 stoichiometric reaction with THF and 4-iodoanisole in hexane solution gave the *ortho*-aluminated compound **3.10-int** [(THF)Li(μ-TMP)(μ-{1-OMe-2-Al(*i*Bu)$_2$-4-I-C$_6$H$_3$}] in a reasonable crystalline yield of 71%. The molecular structure of **3.10-int** (**Figure 4.9**) features a five-element, six-atom LiNAlCCO ring with TMP and *ortho*-deprotonated 4-iodoanisole (O bonded to Li; C bonded to Al) occupying bridging sites between Li and Al. The Al centre displays a distorted tetrahedral geometry made up of three C atoms, from two terminal *i*Bu ligands and one deprotonated 4-iodoanisole molecule, with the fourth atom the TMP N. Contact from Al to the Li atom is through one amido (TMP) N atom and one metallated 4-iodoanisole molecule where coordination occurs through the O atom of the methoxy group. Li is also coordinated to the O atom of a donor THF molecule to complete a distorted trigonal planar geometry.

It can be postulated that the first step in AMM*Al* is coordination of the O atom of the OMe group to the cationic Li atom resulting in the *ortho* C-H bond lying in close proximity to the *pseudo*-terminal TMP (see **Chapter 2**). The second step involves an intramolecular deprotonation of the aromatic substrate to form TMP(H). Deprotonation occurs *ortho* to the OMe group as it is a superior directing group to I. As a result, Li is far removed from I so benzyne formation is inhibited. Formation of benzyne by deprotonation adjacent to a halogen has been demonstrated using **3.3** as previously described and also seen with a similar zincate base [(TMEDA)Li(μ-TMP)(μ-CH$_2$SiMe$_3$)Zn(CH$_2$SiMe$_3$)]. This latter reaction affords a zwitterionic compound from chlorobenzene by addition of *bis*-silylalkylzincate Zn(CH$_2$SiMe$_3$)$_2$ and TMEDA across the benzyne triple bond and subsequent deprotonation of one TMEDA methyl arm.[33] Uchiyama *et. al.* and Knochel *et. al.* have also aluminated 4-iodoanisole; however Uchiyama's preparation involves 2.2 equivalents of the base [LiAl(TMP)(*i*Bu)$_3$] with the substrate.[2] Knochel also uses sub-ambient temperatures to prepare their aluminate base [(C$_{12}$H$_{26}$N)$_3$Al·3LiCl].[1]

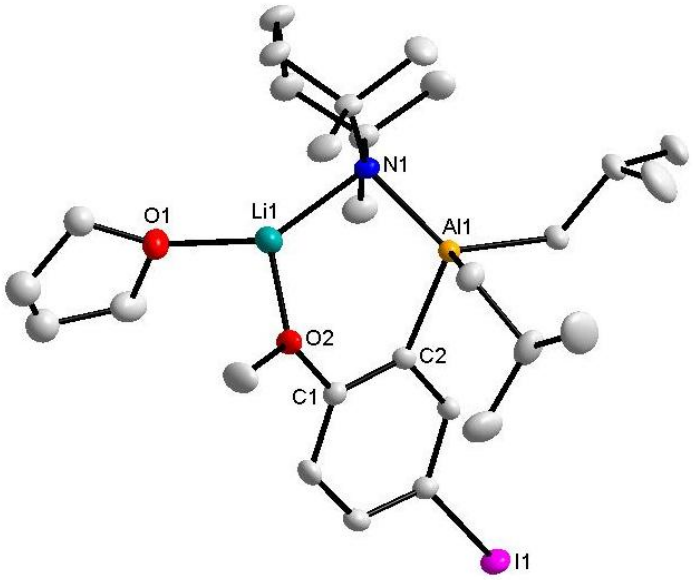

Figure 4.9: Molecular structure of **3.10-int** with thermal ellipsoids drawn at 50% probability level. Hydrogen atoms and minor disordered components on THF have been omitted for clarity.

Aluminium intermediate **3.10-int** was subjected to an excess of *N*-bromosuccinimide to form 2-bromo-4-iodoanisole **3.11a** in a 93% yield after purification by column chromatography (see the ^{1}H NMR spectrum in **Figure 4.10**).

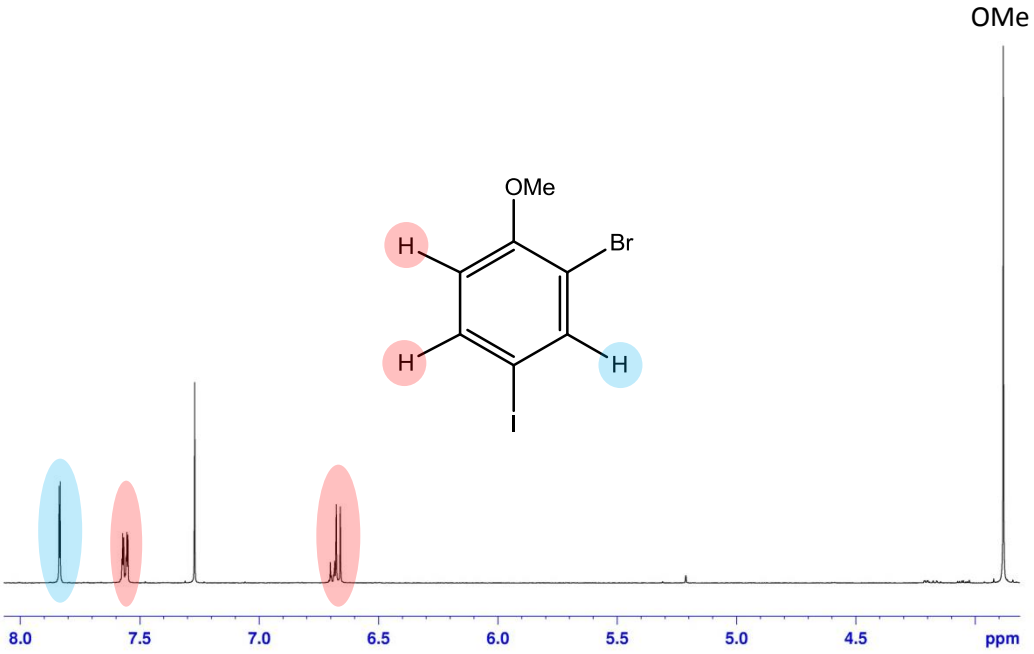

Figure 4.10: ^{1}H NMR spectrum of 2-bromo-4-iodoanisole quench product **3.11a**.

Next dihalo compound **3.11a** was added to a freshly prepared hexane solution of **3.3** to ascertain if a second deprotonation on the trisubstituted benzene ring was possible. It

was found that alumination took place in the 6-position producing the tetrasubstituted benzene [(THF)Li(μ-TMP)(μ-{1-OMe-2-Al(*i*Bu)$_2$-4-I-6-Br-C$_6$H$_2$}] **3.11-int** in a crystalline yield of 33% though overall the yield is near quantitative (as evidenced by the ^{1}H NMR spectrum of the filtrate solution). The molecular structure of **3.11int** (**Figure 4.11**) is analogous to that of **3.10-int** except that the *ortho*-deprotonated 4-iodoanisole bridge between Li and Al carries a Br substituent in the 2-position. As now expected alumination occurs *ortho* to the stronger coordinating OMe group.

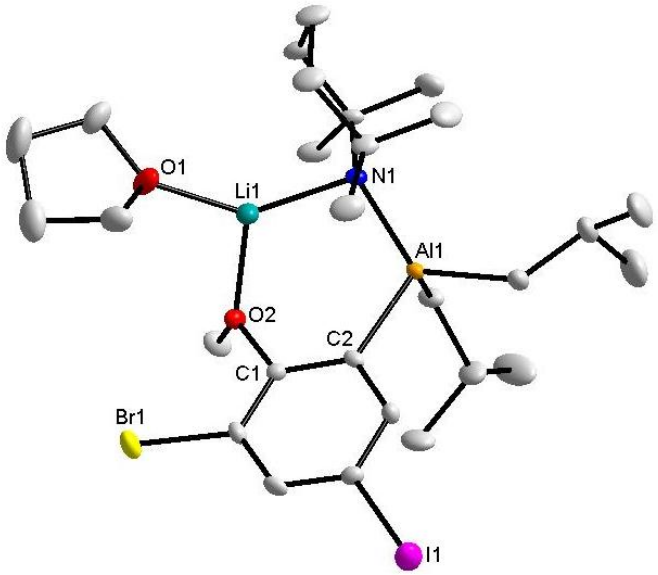

Figure 4.11: Molecular structure of one of two independent molecules of compound **3.11-int** with thermal ellipsoids drawn at 50% probability level. Hydrogen atoms have been omitted for clarity.

As the bond lengths and bond angles in **3.10-int** and **3.11-int** (**Table 4.3**) are similar and are generally consistent with those of previously discussed deprotonated substrates (compounds **1.2-1.6** in **Chapter 2**) these will not be discussed further as there are no extra distinguishing features. The ^{1}H NMR spectra of **3.10-int** and **3.11-int** (**Figure 4.12**) suggest that both retain their structural integrity in solution as the resonances are consistent with those expected from the crystal structure.

Table 4.3: A comparison of selected bond parameters of complexes **3.10-int** and **3.11-int** with those in 2-iodoanisole complex **1.6** from **Chapter 2** (in Å and °).

	3.10-int	3.11-int	1.6
Al1-N1	1.9675(14)	1.978(2)	1.974(3)
N1-Li1	2.021(3)	2.019(5)	2.015(6)
Li1-O1	1.904(3)	1.908(5)	1.906(7)
Li1-O2	1.917(3)	1.917(5)	1.904(6)
C2-Al1	2.0499(15)	2.061(2)	2.047(3)
O1-Li1-O2	103.04(15)	103.4(2)	102.0(3)
O1-Li1-N1	142.35(18)	141.9(3)	140.2(3)
N1-Li1-O2	114.59(16)	114.6(2)	117.7(3)
Li1-N1-Al1	42.06(7)	103.09(16)	98.7(2)

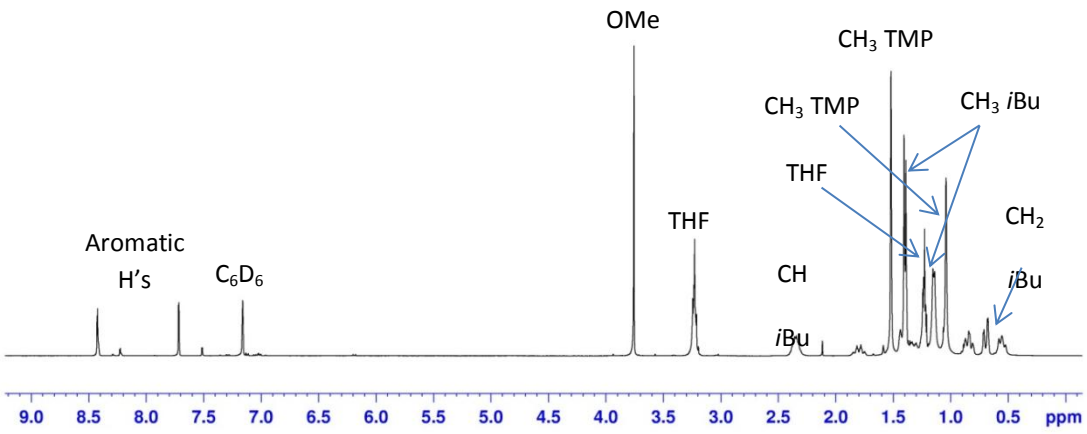

Figure 4.12: ^{1}H NMR spectrum in C_6D_6 solution of aluminated 2-bromo-4-iodoanisole compound **3.11-int** (β and γCH_2 protons of TMP have been omitted from labelling for clarity).

To generate a triheterohalo compound, **3.11-int** was subjected to an excess of sulfuryl chloride, forming the new multi-heterohalogenated 2-bromo-4-iodo-6-chloroanisole **3.12a** in an excellent 90% yield. **Figure 4.13** illustrates the molecular structure of **3.12a**. Although the molecular structure shows the presence of a Br atom in the 2-position and a Cl atom in the 6-position scrambling was observed between these atoms. GC-MS studies were carried out on **3.12a** to confirm that the molecular weight was consistent with a compound containing the three different halogen atoms Cl, Br and I.

The parent ion found at 347.86 m/z is consistent with the molecular weight of **3.12a** (347.38g) (**Figure 4.14**). The ^{1}H NMR spectrum of **3.12a** (**Figure 4.15**) is also consistent with two different halogen atoms in the 2- and 6-positions as the two remaining *meta*-protons exhibit w-coupling [^{4}J(H, H) = 2.04 and 2.02 Hz].

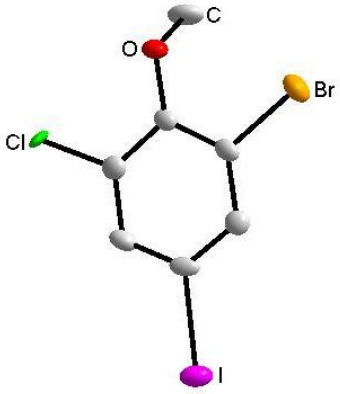

Figure 4.13: Molecular structure of trihalo compound **3.12a** with thermal ellipsoids drawn at 50% probability level. Hydrogen atoms have been omitted for clarity.

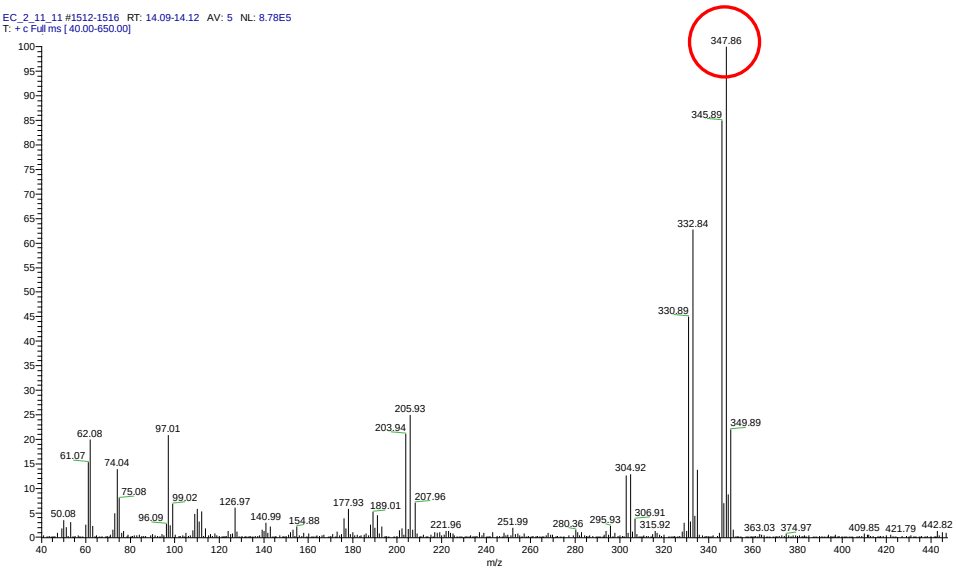

Figure 4.14: Mass spectrum of compound **3.12a** highlighting parent ion peak at 347 m/z.

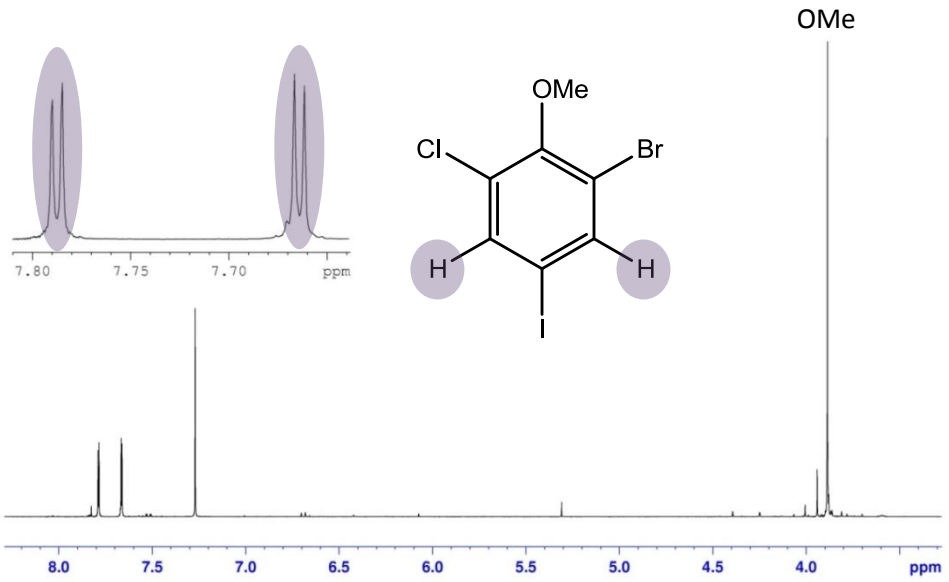

Figure 4.15: ^{1}H NMR spectrum in $CDCl_3$ solution of 2-bromo-4-iodo-6-chloroanisole **4a** (inset shows the two distinct aromatic H resonances).

Brominating and chlorinating agents were also tested to establish the best halogenation reagents (**Table 4.4**). As is the case with *N*-bromosuccinimide, bromine was found to be a moderately good brominating agent producing **3.11a** from **3.10-int** in a 81% yield. A small amount (approximately 10%) of the halogen exchange product 2-bromo-4-bromoanisole was observed in the crude ^{1}H NMR spectrum reducing the yield of product **3.11a** (**Figure 4.16**). 1,2-Dibromotetrachloroethane on the other hand was found to be a poor brominating agent producing none of the desired product. Sulfuryl chloride was found to be the best chlorinating agent (yield = 90%) as *N*-chlorosuccinimide produced **3.12a** in a lower 48% yield while hexachloroethane did not react at all.

Table 4.4: Brominating and chlorinating agents tested for the conversion of **3.10-int** to **3.11a** and **3.11-int** to **3.12a** respectively and yields obtained.

Brominating agent	**Yield (%)**	**Chlorinating agent**	**Yield (%)**
Br_2	81	SO_2Cl_2	90
N-bromosuccinimide	93	*N*-chlorosuccinimide	48
$Cl_2BrC\text{-}CBrCl_2$	0	$Cl_3C\text{-}CCl_3$	0

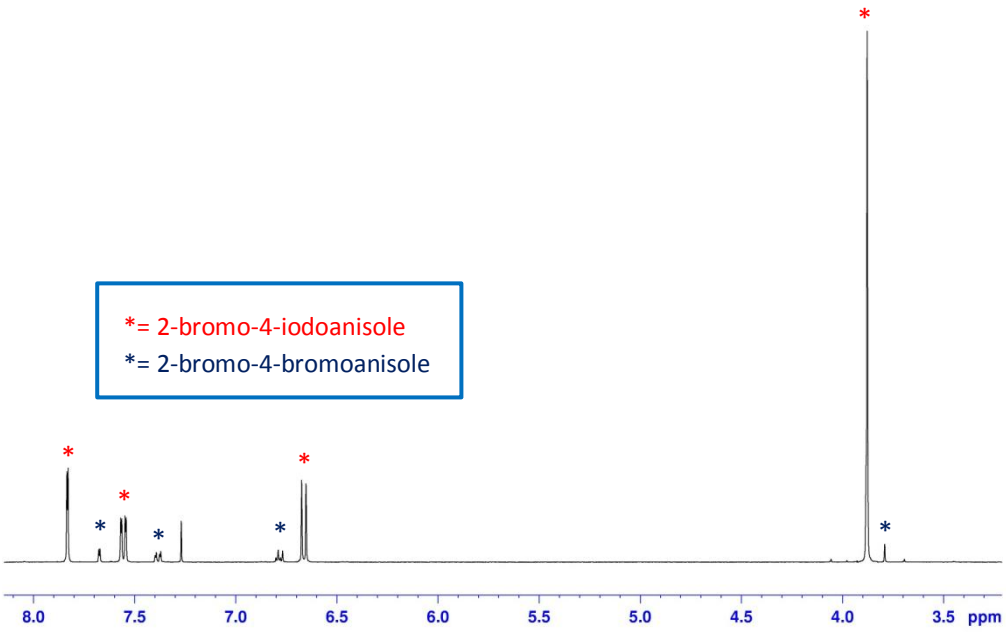

Figure 4.16: ^{1}H NMR spectrum of 2-bromo-4-iodoanisole using bromine as a brominating agent. A trace amount of the bromine exchange product 2-bromo-4-bromoanisole is visible.

Two isomers of triheterohalogenated **3.12a**, 2-iodo-4-bromo-6-chloroanisole **3.12b** and 2-bromo-4-chloro-6-iodoanisole **3.12c** were also synthesised via a similar route starting from 4-bromo **3.10b** and 4-chloroanisole **3.10c** respectively. They were synthesised using the optimal brominating and chlorinating reagents as well as elemental iodine. Compound **3.12b** and the new compound **3.12c** were prepared in a 86% and 89% yield respectively. Though compound **3.12b** was first reported as long ago as 1927, its characterisation was limited.[81] GC-MS characterisation was also carried out on compounds **3.12b** and **3.12c**. Analogous to the situation with **3.12a** the parent ion was found at 347.86 m/z and 347.91 m/z which is consistent with the molecular weight of compounds **3.12b** and **3.12c** (^{1}H NMR spectra with a mass spectrum insert are shown in **Figures 4.17** and **4.18**). ^{1}H NMR data for each multi-heterohalogenated compound including the informative w-coupling for isomers **3.12a**, **3.12b** and **3.12c** is shown in **Table 4.5**.

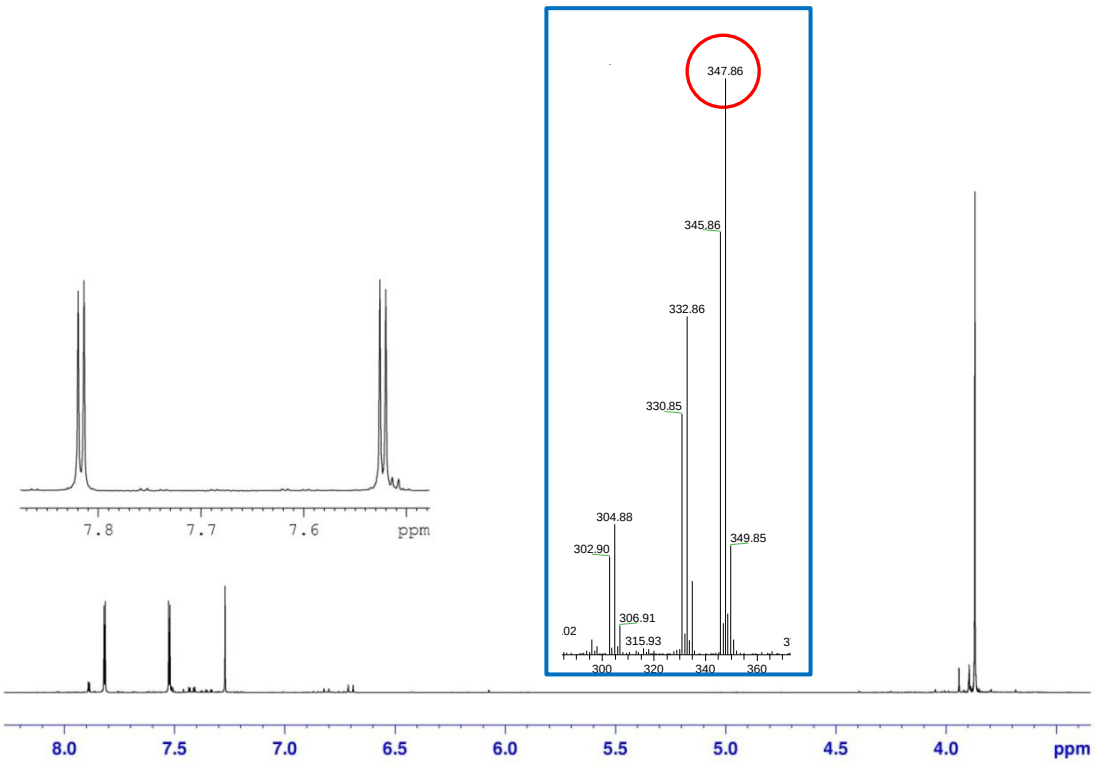

Figure 4.17: ^{1}H NMR spectrum in $CDCl_3$ solution and mass spectrum (in blue inset) of 2-iodo-4-bromo-6-chloroanisole product **3.12b**.

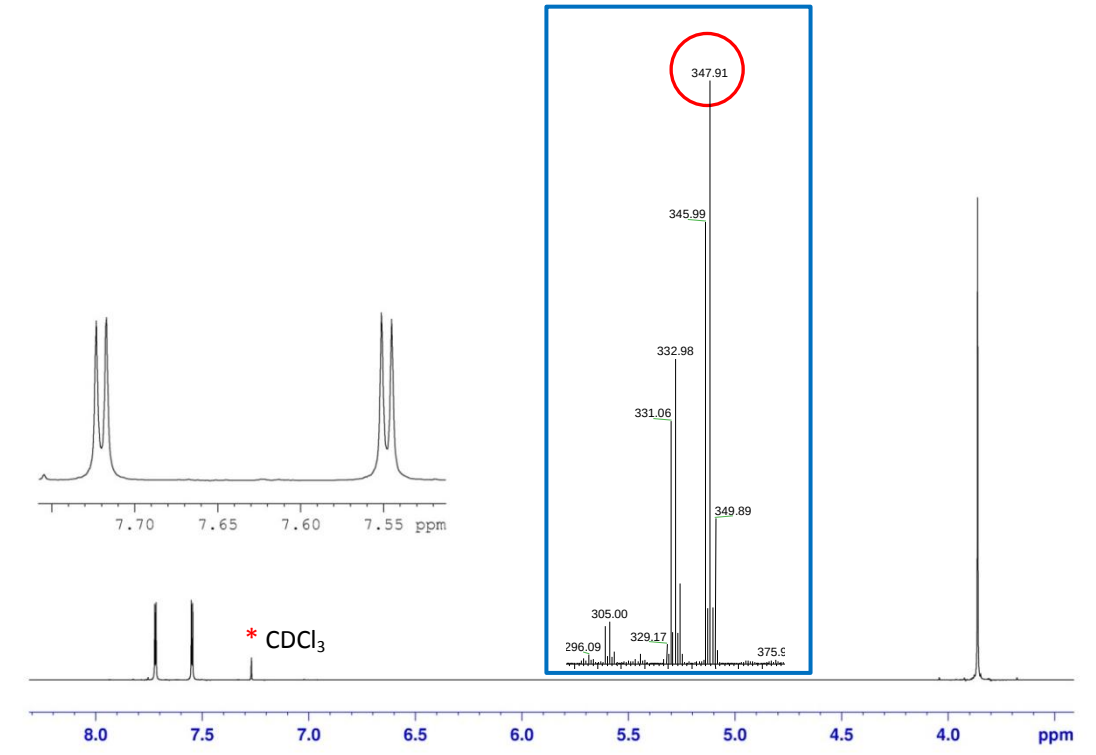

Figure 4.18: ^{1}H NMR spectrum in $CDCl_3$ solution and mass spectrum (in blue inset) of 2-iodo-4-chloro-6-bromoanisole product **3.12c**.

Table 4.5: ^{1}H NMR data in $CDCl_3$ solution including coupling constants for multi-heterohalogenated compounds **3.11a-c and 3.12a-c**.

	3.11a	**3.11b**	**3.11c**	**3.12a**	**3.12b**	**3.12c**	
X **Y** **Z**	Br I H	I Br H	I Cl H	Br I Cl	I Br Cl	I Cl Br	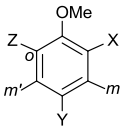
OMe	3.88	3.87	3.87	3.89	3.86	3.87	
o	6.66, d, 8.65 Hz	6.69, d, 8.78 Hz	6.74, d, 8.75 Hz	-	-	-	
m	7.83	7.89	7.75	7.67, d, 2.04 Hz	7.52, d, 2.27 Hz	7.55, d, 2.46 Hz	
m'	7.55, d, 8.61 Hz	7.42, d, 8.88 Hz	7.29, d, 8.67 Hz	7.79, d, 2.02 Hz	7.82, d, 2.29 Hz	7.72, d, 2.45 Hz	

The individual metal components of **3.3** [*i*Bu_2AlTMP and LiTMP] were also tested with 4-iodoanisole **3.10a** to determine if any metallation would occur in the absence of an mixed-metal effect. As anticipated the weak base *i*Bu_2AlTMP did not metallate 4-iodoanisole (observe the main spectrum in **Figure 4.19**) and LiTMP only deprotonated 4-iodoanisole to a very limited extent as evidenced by the ^{1}H NMR spectrum after quenching with iodine (spectrum in blue inset in **Figure 4.19**).

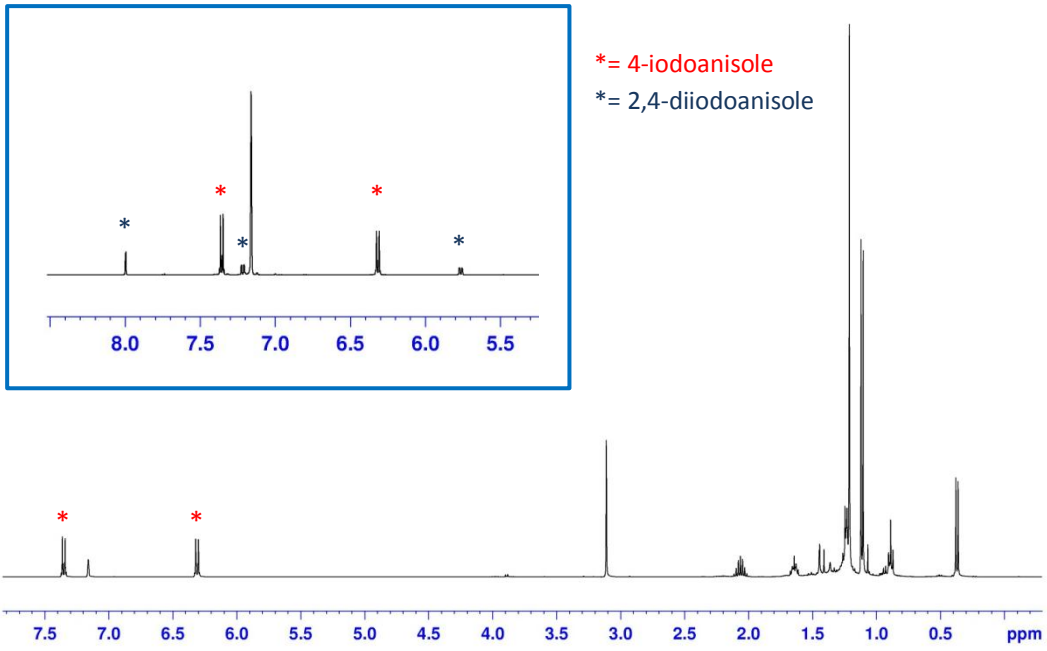

Figure 4.19: (main spectrum) ^{1}H NMR spectrum of reaction between *i*Bu_2AlTMP and 4-iodoanisole and (spectrum in blue inset) LiTMP and 4-iodoanisole after iodine quench.

4-Iodo-*N*,*N*-dimethylaniline was also prepared by a known literature method[82] and reacted with **3.3** to test whether substrates with weaker *ortho*-directing groups would

allow metal-halogen exchange instead of directed *ortho*-metallation. It was found that the base did not react at all atwith 4-iodo-*N*,*N*-dimethylaniline.

Future work in this area should focus on taking the triheterohalogenated isomers **3.12a**, **3.12b** and **3.12c** and reacting them with **3.3** to establish if it is possible to achieve a third alumination on the ring. Alternatively, because the *meta*-protons are not as accessible do we get metal-halogen exchange instead? It is probable that due to the halogen tolerant nature of the base and inaccessible protons that no reaction will occur. It is also worth halogenating aluminated 2-iodoanisole compound **1.6** from **Chapter 1** and reacting it further with **3.3** to see if we get any additional metallation.

4.5 Conclusions

In this part of the project it has been shown that seemingly innocuous changes to a bimetallic framework [in this specific case switching from the alkyl rich Li(TMP)Al(*i*Bu)$_3$ to the more amide rich Li(TMP)$_2$Al(*i*Bu)$_2$] can dramatically alter the pathway that a metallation reaction will follow. While *ortho*-deprotonation at the 2-position of 3-halogenated anisoles is facile with the former, the increased reactivity of the latter (due to the presence of an active TMP anion in the deprotonated intermediate not present in the former) causes breakdown of the trapped deprotonated intermediate complex resulting in a series of different homometallic and organic products due to competing reactions. By mapping these products we have shed new light on the processes and potential pitfalls one may encounter when embarking on a deprotonative journey using such heterometallic low-polarity metallators. While factors such as solvent and temperature play a vital role in controlling these reactions, what is clear is that aluminium TMP bases are generally highly tolerant of halogen functionality, preferring metal-hydrogen exchange over often competitive metal-halogen exchange.

Additionally, it has been discovered that **3.3** can regioselectively functionalise 4-halogen-substituted anisoles via a series of sequential *ortho*-aluminations and electrophilic halogenations. The synthetically useful 2,4,6-halosubstituted anisoles were made starting from 4-iodo, 4-bromo and 4-chloroanisole. *N*-Bromosuccinimide and sulfuryl chloride were the best brominating and chlorinating agent respectively for these novel reactions.

4.6 Future Work

Any follow on project should focus on investigating other 3-haloaromatics with different directing groups - do we always get alumination between the groups generating benzyne with 3-iodoaromatics or can we switch to the opposite *ortho*-position?

Likewise other 4-haloaromatics should be tested so that we can synthesise other useful multiple halogen aromatic compounds. Triheterohalogenated isomers **3.12a**, **3.12b** and **3.12c** should be reacted with **3.3** further to establish if it is possible to achieve a third alumination on the ring. Alternatively, because the *meta*-protons are not as accessible do we get metal-halogen exchange instead? It is probable that due to the halogen tolerant nature of the base and inaccessible protons that no reaction will occur. It is also worth halogenating aluminated 2-iodoanisole compound **1.6** from **Chapter 1** and reacting it further with **3.3** to see if we get any additional metallation.

4.7 Experimental

4.7.1 General Methods

As a consequence of the air and moisture sensitivity of the metal compounds involved in this project, all reactions and manipulations were performed under a protective argon atmosphere using either standard Schlenk techniques or a glove box (Faircrest). All solvents were dried over Na/benzophenone and freshly distilled prior to use. [(THF)Li(TMP)$_2$Al(*i*Bu)$_2$] **3.3** and *i*Bu$_2$AlTMP were prepared *in situ* as described in **Chapter 2**. 3-Iodoanisole, 1,3-diphenylisobenzofuran, 4-iodoanisole, 4-bromoanisole, 4-chloroanisole, sulfuryl chloride, *N*-chlorosuccinimide, *N*-bromosuccinimide, hexachloroethane, 1,2-dibromotetrachloroethane, bromine and iodine were purchased from Aldrich and used as received without additional purification. ^{1}H and ^{13}C NMR spectra were recorded on a Bruker AV400 MHz spectrometer (operating at 400.03 MHz for ^{1}H and 100.58 MHz for ^{13}C). All ^{13}C NMR spectra were proton decoupled. Elemental analyses were performed using a Perkin Elmer 2400 Series II CHN/S Analyser. Gas chromatography-mass spectrometry (GC-MS) was performed using Thermo Finnigan Polaris Q GCMS (ion trap).

Synthesis of [LiI·TMP(H)]$_4$ 3.5

A pre-prepared solution of **3.3** in hexane solution was cooled to -78^{o}C to which 3-iodoanisole was added via syringe. Lithium iodide TMP(H) solvate **3.5** precipitated immediately as a white powder and was collected by vacuum filtration. The filtrate was left overnight at -35^{o}C affording a batch of X-ray quality crystals of **3.5** (combined yield of powder and crystals: 0.45 g, 82 %).

El. Analysis calc. for $C_{36}H_{76}I_4Li_4N_4$ (M_r = 1100.40) C, 39.29; H, 6.96; N, 5.09; found: C, 39.73; H, 7.22; N, 4.24%.

Synthesis of *i*Bu$_2$Al(TMP)·THF (3.6·THF)

Pre-prepared *i*Bu$_2$Al(TMP) (0.28 g, 1 mmol) was added to an aliquot of hexane (5 mL) and THF (0.08 mL, 1 mmol) was introduced via syringe. This solution was left overnight at -34^{o}C to yield the final product as colourless crystals (0.25 g, 71%).

^{1}H NMR data (400.13 MHz, 298 K, C_6D_6)

δ = 0.28 [4H, d, ^{3}J(H,H) = 6.40 Hz, Al-CH_2], 1.15 [4H, m, THF], 1.25 [12H, d, ^{3}J(H,H) = 6.40 Hz, ^{i}Bu CH_3], 1.36 [12H, s, TMP CH_3], 1.48 [4H, t, ^{3}J(H,H) = 6.29 Hz, TMP β], 1.76 [2H, m, TMP γ], 2.08 [2H, sept, ^{3}J(H,H) = 6.53 Hz, ^{i}Bu CH], 3.57 ppm [4H, m, THF].

^{13}C{^{1}H} NMR data (100.62 MHz, 298 K, C_6D_6)

δ = 18.7 [TMP γ], 24.9 [THF], 26.8 [^{i}Bu CH], 28.5 [^{i}Bu CH_2], 28.9 [^{i}Bu CH_3], 34.5 [TMP CH_3], 41.6 [TMP β], 51.9 [TMP α], 69.7 ppm [THF].

El. Analysis calc. for $AlC_{21}H_{44}NO$ (M_r = 353.56) C, 71.34; H, 12.54, N, 3.96; found: C, 70.98; H, 13.21, N 4.15%.

Synthesis of 1-methoxy-9-10-diphenyl-9-10-epoxyanthracene 3.7

3-Iodoanisole (0.24 mL, 2 mmol) was added to a prepared solution of **3.3** in hexane at -78^{o}C. 1,3-diphenylisobenzofuran (0.54 g, 2 mmol) was added after a few minutes and the mixture was allowed to stir and to warm to room temperature overnight. Saturated aq. NH_4Cl (40 mL) was added to quench the reaction and the mixture was extracted with $CHCl_3$ (30 mL x 3). The mixture was dried over $MgSO_4$ and the solvent evaporated under reduced pressure. The residue was purified by SiO_2 column chromatography using petroleum ether (100%), diethyl ether:petroleum ether (1:10) and diethyl ether:petroleum ether (1:5) as an eluent to give 1-methoxy-9-10-diphenyl-9-10-epoxyanthracene (0.69 g, 92%).

^{1}H NMR data (400.13 MHz, 298 K, C_6D_{12})

δ = 3.66 [3H, s, OCH_3], 6.66 [1H, d, ^{3}J(H,H) = 7.46 Hz], 7.02-7.12 [4H, m], 7.37 [1H, d, ^{3}J(H,H) = 7.05 Hz], 7.47-7.58 [7H, m], 7.92 [2H, m], 8.01 ppm [2H, m].

^{13}C{^{1}H} NMR data (100.62 MHz, 298 K, C_6D_{12})

δ = 55.6 [OCH_3], 90.4 [quaternary C], 91.8 [quaternary C], 111.4 [aromatic CH], 113.6 [aromatic CH], 120.5 [aromatic CH], 121.2 [aromatic CH], 125.4 [aromatic CH], 125.7 [aromatic CH], 127.1 [2C, phenyl CH], 127.8 [2C, phenyl CH], 128.0 [aromatic CH], 128.2 [aromatic CH], 128.5 [aromatic CH], 128.6 [2C, phenyl CH], 129.4 [2C, phenyl

CH], 134.7 [aromatic C], 135.0 [aromatic C], 136.4 [aromatic C], 150.0 [aromatic C], 151.5 [aromatic C], 153.6 [aromatic C], 153.8 ppm [aromatic C].

El. Analysis calc. for $C_{27}H_{20}O_2$ (M_r = 376.46) C, 86.14; H, 5.36; found: C, 85.57; H, 5.33%.

Synthesis of 1-(2-iodo-3-methoxyphenyl)-2,2,6,6-tetramethylpiperidide 3.8

LiTMP was prepared from TMP(H) (0.17 mL, 1 mmol) and *n*BuLi (0.63 mL, 1.6 M in hexanes, 1 mmol) in THF (5 mL) and cooled to -78°C. A -78°C solution of *i*Bu_2Al(TMP) in THF (5mL) was added via cannula to give an *in situ* solution of **3.3**. 3-iodoanisole (0.12 mL, 1 mmol) in THF at -78°C was added and this was stirred for 2 h. I_2 (5 mL of a 1 M solution, 5 mmol) in dry THF was added to the reaction mixture and stirred overnight. The mixture was diluted with saturated aq. $NaHS_2O_3$ (20 mL) and saturated aq. NH_4Cl (40 mL) and extracted with $CHCl_3$ (30 mL x 3). The organic layer was dried over $MgSO_4$ and solvent removed under reduced pressure. The residue was purified by SiO_2 column chromatography using hexane (100%) as an eluent to give 1-(2-iodo-3-methoxyphenyl)-2,2,6,6-tetramethylpiperidide (0.36 g, 48 %).

^{1}H NMR data (400.13 MHz, 298 K, $CDCl_3$)

δ = 0.93 [6H, s, 2 x CH_3 of TMP], 1.30 [6H, s, 2 x CH_3 of TMP], 1.54-1.58 [2H, m, 1 x βCH_2 of TMP], 1.63-1.69 [1H, m, 1 x γCH of TMP], 1.81-1.98 [2H, m, 1 x βCH_2 of TMP] and [1H, m, 1 x γCH of TMP], 3.89 [3H, s, OCH_3], 6.71 [1H, d, ^3J(H,H) = 8.16 Hz, 1 x aromatic C-H], 7.07 [1H, d, ^3J(H,H) = 7.94 Hz, 1 x aromatic C-H], 7.22 ppm [1H, t, ^3J(H,H) = 8.02 Hz, 1 x aromatic C-H].

^{13}C{^{1}H} NMR data (100.62 MHz, 298 K, $CDCl_3$)

δ = 18.7 [1 x γ<u>C</u>H of TMP], 25.7 [1 x <u>C</u>H_3 of TMP], 31.4 [1 x <u>C</u>H_3 of TMP], 41.2 [1 x β<u>C</u>H_2 of TMP], 56.1 [1 x γ<u>C</u>H of TMP], 56.5 [1 x O<u>C</u>H_3], 106.2 [1 x aromatic <u>C</u>], 108.6 [1 x aromatic <u>C</u>H], 124.3 [1 x aromatic <u>C</u>H], 127.9 [1 x aromatic <u>C</u>H], 150.9 [1 x aromatic <u>C</u>], 159.3 ppm [1 x aromatic <u>C</u>].

El. Analysis calc. for $C_{16}H_{24}NOI$ (M_r = 373.28) C, 51.48; H, 6.48; N, 3.75; found: C, 52.13; H, 6.85; N, 3.76%.

Synthesis of [(THF)Li(μ-TMP){1-OMe-2-Al(*i*Bu)$_2$-4-I-C$_6$H$_3$}] 3.10-int

Hexane (10 mL) was added to an oven-dried Schlenk tube. Next, 1.6M *n*BuLi (2.8 mL, 4.5 mmol) was added, followed by TMP(H) (0.77 mL, 4.5 mmol) at room temperature. The reaction mixture was left to stir for 10 min and then *i*Bu$_2$AlCl (0.86 mL, 4.5 mmol) was injected into the Schlenk tube, producing a white suspension almost immediately. The reaction was left to stir for 1 hour and was then filtered through Celite and glass wool, which was then washed with more hexane (10 mL). To a separate Schlenk tube containing a solution of freshly prepared LiTMP in hexane (10 mL) [from a mixture of *n*BuLi (2.8 mL, 4.5 mmol) and TMP(H) (0.77 mL, 4.5 mmol)], the solution was added through cannula to give a colourless solution. Finally, THF (0.36 mL, 4.5 mmol) and 4-iodoanisole (0.70 g, 3 mmol) were injected and the reaction mixture was left to stir overnight. A white suspension formed which dissolved on addition of 25 mL of toluene. The Schlenk tube was left in the freezer at -30^{o}C. A crop (1.27 g, 71%) of colourless crystals formed in solution that were suitable for X-ray crystallographic analysis.

^{1}H NMR data (400.13 MHz, 298 K, C$_6$D$_{12}$)

δ = 0.54-0.75 [4H, m, 2 x CH$_2$ of *i*Bu], 0.85 [2H, m, 1 x βCH$_2$ of TMP], 1.06 [4H, m, 2 x βCH$_2$ of THF], 1.15 [6H, d, ^3J(H,H) = 6.48 Hz, 2 x CH$_3$ of *i*Bu], 1.24 [6H, s, 2 x CH$_3$ of TMP], 1.35 [6H, d, ^3J(H,H) = 6.47 Hz, 2 x CH$_3$ of *i*Bu], 1.36 [1H, m, 1 x γCH of TMP], 1.50 [2H, m, 1 x βCH$_2$ of TMP], 1.58 [6H, s, 2 x CH$_3$ of TMP], 1.86 [1H, m, 1 x γCH of TMP], 2.29 [2H, m, 2 x CH of *i*Bu], 2.94 [4H, m, 2 x αCH$_2$ of THF], 3.19 [3H, s, CH$_3$O of 4-iodoanisole], 6.11 [1H, d, ^3J(H,H) = 8.53 Hz, 1 x aromatic CH], 7.50 [1H, dd, ^3J(H,H) = 8.49 Hz, ^4J(H,H) = 2.30 Hz, 1 x aromatic CH], 8.49 ppm [1H, d, ^4J(H,H) = 2.30 Hz, 1 x aromatic CH].

^{13}C{^{1}H} NMR data (100.62 MHz, 298 K, C$_6$D$_{12}$)

δ = 18.7 [γ*C*H$_2$ of TMP], 25.0 [2 x β*C*H$_2$ of THF], 27.5 [2 x *C*H of *i*Bu], 28.0 [2 x *C*H$_3$ of *i*Bu], 28.5 [2 x *C*H$_2$ of *i*Bu], 30.2 [2 x *C*H$_3$ of TMP], 30.8 [2 x *C*H$_3$ of *i*Bu], 37.4 [2 x *C*H$_3$ of TMP], 44.2 [2 x β*C*H$_2$ of TMP], 53.2 [2 x quaternary *C* of TMP], 55.6 [*C*H$_3$O of 4-iodoanisole], 68.5 [2 x α*C*H$_2$ of THF], 90.6 [1 x quaternary *C*-I of 4-iodoanisole], 112.6 [1 x aromatic *C*H], 136.2 [1 x aromatic *C*H], 149.2 [1 x aromatic *C*H], 162.5 ppm [1 x quaternary *C*-OMe of 4-iodoanisole].

El. Analysis calc. for $C_{28}H_{50}AlLiO_2IN$ (M_r = 593.54) C, 56.66; H, 8.49; N, 2.36; found: C, 55.22; H, 8.02; N, 1.95%.

Synthesis of 2-bromo-4-iodoanisole 3.11a

10 mL of THF was added to dissolve the white precipitate (**3.10-int**) and an excess of *N*-bromosuccinimide (~3.2 g) was added to the reaction mixture at 0°C and stirred overnight. The mixture was diluted with saturated aq. $NaHS_2O_3$ (40 mL) and saturated aq. NH_4Cl (20 mL) and extracted with ethyl acetate (30 mL x 3). The organic layer was dried over $MgSO_4$ and solvent removed under reduced pressure. The residue was purified by SiO_2 column chromatography using hexane as an eluent to give 2-bromo-4-iodoanisole (0.87 g, 93%).

^{1}H NMR data (400.13 MHz, 298 K, $CDCl_3$)

δ = 3.88 [3H, s, OCH_3], 6.66 [1H, d, ^3J(H,H) = 8.65 Hz, 1 x aromatic C-H], 7.55 [1H, d, ^3J(H,H) = 8.61 Hz, 1 x aromatic C-H], 7.83 ppm [1H, s, 1 x aromatic C-H].

^{13}C{^{1}H} NMR data (100.62 MHz, 298 K, $CDCl_3$)

δ = 56.3 [O*C*H_3], 82.4 [1 x aromatic *C*-I], 113.0 [1 x aromatic *C*-Br], 113.8 [1 x aromatic *C*-H], 137.3 [1 x aromatic *C*-H], 141.0 [1 x aromatic *C*-H], 156.0 ppm [1 x aromatic *C*-OCH_3].

El. Analysis calc. for C_7H_6OBrI (M_r = 312.93) C, 26.87; H, 1.93; found: C, 27.86; H, 1.97%.

Synthesis of [(THF)Li(μ-TMP){1-OMe-2-Al(*i*Bu)$_2$-4-I-6-Br-C_6H_2}] 3.11-int

Same procedure as **3.10-int** except this time **3.3** was prepared on a 3 mmol scale. THF (0.24 mL, 3 mmol) and 2-bromo-4-iodoanisole (0.63 g, 2 mmol) were injected and the reaction mixture was left to stir overnight. A white solid formed which was dissolved on addition of 25 mL of toluene. The solution was filtered and the Schlenk tube placed in the freezer at -30°C. A crop (0.44 g, 33%) of colourless crystals formed in solution that were suitable for X-ray crystallographic analysis.

^{1}H NMR data (400.13 MHz, 298 K, C_6D_6)

δ = 0.58 [2H, m, 1 x CH_2 of *i*Bu], 0.69 [2H, m, 1 x CH_2 of *i*Bu], 0.84 [2H, m, 1 x βCH_2 of TMP], 1.04 [6H, s, 2 x CH_3 of TMP], 1.15 [6H, m, 2 x CH_3 of *i*Bu], 1.23 [4H, m, 2 x

βCH$_2$ of THF], 1.32 [1H, m, 1 x γCH of TMP], 1.40 [6H, m, 2 x CH$_3$ of *i*Bu], 1.44 [2H, m, 1 x βCH$_2$ of TMP], 1.52 [6H, s, 2 x CH$_3$ of TMP], 1.79 [1H, m, 1 x γCH of TMP], 2.35 [2H, m, 2 x CH of *i*Bu], 3.23 [4H, m, 2 x αCH$_2$ of THF], 3.76 [3H, s, OMe], 7.72 [1H, s, 1 x aromatic C-H], 8.43 ppm [1H, s, 1 x aromatic C-H].

^{13}C{^{1}H} NMR data (100.62 MHz, 298 K, C$_6$D$_6$)

δ = 18.5 [1 x γ*C*H$_2$ of TMP], 25.2 [2 x β*C*H$_2$ of THF], 27.3 [2 x *C*H$_3$ of *i*Bu], 27.4 [2 x *C*H of *i*Bu], 29.8 [2 x *C*H$_3$ of TMP], 31.3 [2 x *C*H$_3$ of *i*Bu], 37.7 [2 x *C*H$_3$ of TMP], 43.9 [2 x β*C*H$_2$ of TMP], 62.0 [O*C*H$_3$], 68.7 [2 x α*C*H$_2$ of THF], 93.3 [1 x aromatic *C*-I], 115.1 [1 x aromatic *C*-Br], 139.5 [1 x aromatic *C*-H], 147.5 [1 x aromatic *C*-H], 157.8 ppm [1 x aromatic *C*-OCH$_3$].

El. Analysis calc. for C$_{28}$H$_{49}$AlLiO$_2$NIBr (M$_r$ = 672.43) C, 50.01; H, 7.35; N, 2.08; found: C, 49.23; H, 7.15; N, 1.98%.

Synthesis of 2-bromo-4-iodo-6-chloroanisole 3.12a

10 mL of THF was added to dissolve the white precipitate **3.11-int** and an excess of sulfuryl chloride (~1 mL) was added to the reaction mixture at 0^{o}C and stirred overnight. The mixture was diluted with saturated aq. NaHS$_2$O$_3$ (40 mL) and saturated aq. NH$_4$Cl (20 mL) and extracted with ethyl acetate (30 mL x 3). The organic layer was dried over MgSO$_4$ and solvent removed under reduced pressure. The residue was purified by SiO$_2$ column chromatography using hexane as an eluent to give 2-bromo-4-iodo-6-chloroanisole (0.62 g, 90%).

^{1}H NMR data (400.13 MHz, 298 K, CDCl$_3$)

δ = 3.89 [3H, s, OCH$_3$], 7.67 [1H, d, ^{4}J(H,H) = 2.04 Hz, 1 x aromatic C-H], 7.79 ppm [1H, d, ^{4}J(H,H) = 2.02 Hz, 1 x aromatic C-H].

^{13}C{^{1}H} NMR data (100.62 MHz, 298 K, CDCl$_3$)

δ = 60.7 [O*C*H$_3$], 86.9 [1 x aromatic *C*-I], 119.5 [1 x aromatic *C*-Br], 130.2 [1 x aromatic *C*-Cl], 138.0 [1 x aromatic *C*-H], 139.9 [1 x aromatic *C*-H], 153.5 ppm [1 x aromatic *C*-OCH$_3$].

El. Analysis calc. for C$_7$H$_5$OIBrCl (M$_r$ = 347.38) C, 24.20; H, 1.45; found: C, 24.49; H, 1.38%.

Synthesis of 2-iodo-4-bromo-6-chloroanisole 3.12b

Same procedure as **3.10-int** for the preparation of **3.3**. THF (0.36 mL, 4.5 mmol) and 4-bromoanisole **3.10b** (0.38 mL, 3 mmol) were injected and the reaction mixture was left to stir overnight. A white precipitate formed which dissolved on addition of 10 mL of THF. I_2 (18 mL of a 1M solution, 18 mmol) was added and the reaction was left to stir overnight. The mixture was diluted with saturated aq. $NaHS_2O_3$ (40 mL) and saturated aq. NH_4Cl (20 mL) and extracted with ethyl acetate (30 mL x 3). The organic layer was dried over $MgSO_4$ and solvent removed under reduced pressure. The residue was purified by SiO_2 column chromatography using hexane as an eluent to give 2-iodo-4-bromoanisole **3.11b** (0.81 g, 86%).

^{1}H NMR data (400.13 MHz, 298 K, $CDCl_3$)

δ = 3.87 [3H, s, OCH_3], 6.69 [1H, d, ^3J(H,H) = 8.78 Hz, 1 x aromatic C-H], 7.42 [1H, d, ^3J(H,H) = 8.88 Hz, 1 x aromatic C-H], 7.89 ppm [1H, s, 1 x aromatic C-H].

3 mmol of **3.3** was prepared as described and 2-iodo-4-bromoanisole (0.63 g, 2 mmol) was added and left to stir overnight. Sulfuryl chloride (~1 mL) was added to the resulting solution at 0^{o}C and left to stir overnight. The reaction mixture was worked-up as described above. The residue was purified by SiO_2 column chromatography using hexane as an eluent to give 2-iodo-4-bromo-6-chloroanisole **3.12b** (0.62 g, 89%).

^{1}H NMR data (400.13 MHz, 298 K, $CDCl_3$)

δ = 3.87 [3H, s, OCH_3], 7.52 [1H, d, ^4J(H,H) = 2.27 Hz, 1 x aromatic C-H], 7.82 ppm [1H, d, ^4J(H,H) = 2.29 Hz, 1 x aromatic C-H].

^{13}C{^{1}H} data (100.62 MHz, 298 K, $CDCl_3$)

δ = 60.6 [O*C*H_3], 93.1 [1 x aromatic *C*-I], 117.6 [1 x aromatic *C*-Br], 128.4 [1 x aromatic *C*-Cl], 133.3 [1 x aromatic *C*-H], 139.8 [1 x aromatic *C*-H], 155.2 ppm [1 x aromatic *C*-OCH_3].

El. Analysis calc. for $C_7H_5OIBrCl$ (M_r = 347.38) C, 24.20; H, 1.45; found: C, 24.45; H, 1.37%.

Synthesis of 2-iodo-4-chloro-6-bromoanisole 3.12c

Same procedure as **3.10-int** for the preparation of **3.3**. THF (0.36 mL, 4.5 mmol) and 4-chloroanisole (0.37 mL, 3 mmol) were injected and the reaction mixture was left to stir overnight. A white precipitate formed in solution which was dissolved on addition of 10 mL of THF. I_2 (18 mL of a 1M solution, 18 mmol) was added and the reaction was left to stir overnight. The mixture was diluted with saturated aq. $NaHS_2O_3$ (40 mL) and saturated aq. NH_4Cl (20 mL) and extracted with ethyl acetate (30 mL x 3). The organic layer was dried over $MgSO_4$ and solvent removed under reduced pressure. The residue was purified by SiO_2 column chromatography using hexane as an eluent to give 2-iodo-4-chloroanisole **3.11c** (0.72 g, 89%).

^{1}H NMR data (400.13 MHz, 298 K, $CDCl_3$)

δ = 3.87 [3H, s, OCH_3], 6.74 [1H, d, ^3J(H,H) = 8.75 Hz, 1 x aromatic C-H], 7.29 [1H, d, ^3J(H,H) = 8.67 Hz, 1 x aromatic C-H], 7.75 ppm [1H, s, 1 x aromatic C-H].

3 mmol of **3.3** was prepared as described and 2-iodo-4-chloroanisole (0.54 g, 2 mmol) was added to the mixture and it was left to stir overnight. *N*-bromosuccinimide (~3.2 g) was added to the resulting solution at 0^{o}C and it was left to stir overnight. The reaction mixture was worked-up as described above. The residue was purified by SiO_2 column chromatography using hexane as an eluent to give 2-iodo-4-chloro-6-bromoanisole **3.12c** (0.60 g, 86%).

^{1}H NMR data (400.13 MHz, 298 K, $CDCl_3$)

δ = 3.86 [3H, s, OCH_3], 7.55 [1H, d, ^4J(H,H) = 2.46 Hz, 1 x aromatic C-H], 7.72 ppm [1H, d, ^4J(H,H) = 2.45 Hz, 1 x aromatic C-H].

^{13}C{^{1}H} NMR data (100.62 MHz, 298 K, $CDCl_3$)

δ = 60.7 [O*C*H$_3$], 92.1 [1 x aromatic *C*-I], 116.6 [1 x aromatic *C*-Br], 130.7 [1 x aromatic *C*-Cl], 133.3 [1 x aromatic *C*-H], 137.9 [1 x aromatic *C*-H], 155.6 ppm [1 x aromatic *C*-OCH$_3$].

El. Analysis calc. for $C_7H_5OIBrCl$ (M_r = 347.38) C, 24.20; H, 1.45; found: C, 24.55; H, 1.43%.

Table 4.6: Crystallographic data and refinement details for compounds **3.5**, **3.6·THF**, **3.7**, **3.8**, **3.10-int** and **3.11-int**.

	3.5	**3.6·THF**	**3.7**	**3.8**	**3.10-int**	**3.11-int**
Empirical Formula	$C_{36}H_{76}I_4Li_4N_4$	$C_{21}H_{44}AlNO$	$C_{27}H_{20}O_2$	$C_{16}H_{24}INO$	$C_{28}H_{50}AlLiO_2IN$	$C_{28}H_{49}AlLiO_2NIBr$
M_r	1100.37	353.55	376.43	373.26	593.54	= 672.43
Crystal System	Monoclinic	Orthorhombic	Monoclinic	Orthorhombic	Triclinic	Triclinic
Space Group	*C*2/*c*	*Pbca*	*P*21/*n*	*Fdd*2	*P*-1	*P*-1
a [Å]	25.5194(9)	10.4710(2)	10.7897(3)	12.8821(5)	11.9465(4)	11.9465(4)
b [Å]	10.7301(2)	12.1167(2)	17.0361(4)	59.0714(18)	14.3366(6)	14.3366(6)
c [Å]	19.8807(6)	35.1416(2)	11.4052(3)	8.4330(4)	13.7161(12)	19.2013(6)
β [°]	118.682(4)	90	110.652(3)	90	101.603(3)	101.603(3)
V [Å^3]	4775.9(2)	4458.55(14)	1961.72(9)	6417.2(4)	1529.2(2)	3152.4(2)
Z	4	8	4	16	2	4
P_{calcd} [g cm^{-3}]	1.530	1.053	1.275	1.545	1.289	1.417
Reflns Measured	11422	16838	9138	15680	16599	33478
Unique Reflns	5807	5203	4795	4065	8298	15453
R int	0.0354	0.0294	0.0217	0.0335	0.0241	0.0225
GooF	1.082	1.092	1.017	1.083	1.035	1.039

R [on F, obs rflns only]	0.0409	0.0559	0.0460	0.0212	0.0267	0.0342
wR [on F^2, all data]	0.0794	0.1126	0.1044	0.0473	0.0666	0.0846
Largest diff. peak/hole [e$Å^{-3}$]	1.070/-0.600	0.308/-0.238	0.327/-0.237	0.444/-0.388	0.720/-0.645	1.005/-1.082

4.6 References

[1] S. H. Wunderlich, P. Knochel, *Angew. Chem. Int. Ed.* **2009**, *48*, 1501.

[2] M. Uchiyama, H. Naka, Y. Matsumoto, T. Ohwada, *J. Am. Chem. Soc.* **2004**, *126*, 10527.

[3] H. Naka, M. Uchiyama, Y. Matsumoto, A. E. H. Wheatley, M. McPartlin, J. V. Morey, Y. Kondo, *J. Am. Chem. Soc.* **2007**, *129*, 1921.

[4] D. Barr, W. Clegg, R. E. Mulvey, R. Snaith, *J. Chem. Soc., Chem. Commun.* **1984**, 79.

[5] F. Neumann, F. Hampel, P. v. R. Schleyer, *Inorg. Chem.* **1995**, *34*, 6553.

[6] N. W. Mitzel, C. Lustig, *Z. Naturforsch., B: Chem. Sci.* **2001**, *56*, 443.

[7] M. Brym, C. Jones, P. C. Junk, M. Kloth, *Z. Anorg. Allg. Chem.* **2006**, *632*, 1402.

[8] C. Doriat, R. Köppe, E. Baum, G. Stösser, H. Köhnlein, H. Schnöckel, *Inorg. Chem.* **2000**, *39*, 1534.

[9] S. Courtenay, P. Wei, D. W. Stephan, *Can. J. Chem.* **2003**, *81*, 1471.

[10] B. R. Aluri, M. K. Kindermann, P. G. Jones, I. Dix, J. Helnicke, *Inorg. Chem.* **2008**, *47*, 6900.

[11] B. Werner, T. Kräuter, B. Neumüller, *Inorg. Chem.* **1996**, *35*, 2977.

[12] B. Werner, B. Neumüller, *Chem. Ber.* **1996**, *129*, 355.

[13] H. Krautscheid, O. Kluge, *Acta Cryst. E.* **2007**, *63*, m2690.

[14] D. Barr, W. Clegg, R. E. Mulvey, R. Snaith, *J. Chem. Soc., Chem. Commun.* **1989**, 57.

[15] N. D. R. Barnett, R. E. Mulvey, W. Clegg, P. A. O'Neil, *J. Am. Chem. Soc.* **1993**, *115*, 1573.

[16] R. E. Mulvey, *Chem. Soc. Rev.* **1991**, *20*, 167.

[17] P. C. Healy, C. Pakawatchai, C. L. Raston, B. W. Skelton, A. H. White, *J. Chem. Soc. Dalton Trans.* **1983**, 1905.

[18] P. C. Healy, J. D. Kildea, A. H. White, *Aust. J. Chem.* **1989**, *42*, 137.

[19] B. Ahrens, P. G. Jones, A. K. Fischer, *Eur. J. Inorg. Chem.* **1999**, 1103.

[20] G. A. Bowmaker, Effendy, K. C. Lim, B. W. Skelton, D. Sukarianingsih, A. H. White, *Inorg. Chim. Acta* **2005**, *358*, 4342.

[21] D. C. Bradley, H. Dawes, D. M. Frigo, M. B. Hursthouse, B. Hussein, *J. Organomet. Chem.* **1987**, *325*, 55.

[22] D. A. Atwood, V. O. Atwood, D. F. Carriker, A. H. Cowley, F. P. Gabbai, R. A. Jones, M. R. Bond, C. J. Carrano, *J. Organomet. Chem.* **1993**, *463*, 29.

[23] J. L. Atwood, G. A. Koutsantonis, F.-C. Lee, C. L. Raston, *J. Chem. Soc., Chem. Commun.* **1994**, 91.

[24] I. Krossing, H. Nöth, H. Schwenk-Kircher, T. Seifert, C. Tacke, *Eur. J. Inorg. Chem.* **1998**, 1925.

[25] L. A. Mîinea, S. Suh, D. M. Hoffman, *Inorg. Chem.* **1999**, *38*, 4447.

[26] K. Knabel, H. Nöth, *Z. Naturforsch., B: Chem. Sci.* **2005**, *60*, 1027.

[27] J. Garcia-Alvarez, E. Hevia, A. R. Kennedy, J. Klett, R. E. Mulvey, *Chem. Commun.* **2007**, 2402.

[28] D. R. Armstrong, A. M. Drummond, L. Balloch, D. V. Graham, E. Hevia, A. R. Kennedy, *Organometallics* **2008**, *27*, 5860.

[29] H. Noth, R. Waldhor, *Z. Naturforsch. B: Chem. Sci.* **1998**, *53*, 1525.

[30] F. H. Allen, *Acta Crystallogr.* **2002**, *B58*, 380.

[31] H. H. Karsch, K. Zellner, G. Müller, *J. Chem. Soc., Chem. Commun.* **1991**, 466.

[32] X. Tian, R. Fröhlich, N. W. Mitzel, *Dalton Trans.* **2005**, 380.

[33] D. R. Armstrong, L. Balloch, W. Clegg, S. H. Dale, P. Garcia-Alvarez, E. Hevia, L. M. Hogg, A. R. Kennedy, R. E. Mulvey, C. T. O'Hara, *Angew. Chem. Int. Ed.* **2009**, *48*, 8675.

[34] A. C. Hoepker, L. Gupta, Y. Ma, M. F. Faggin, D. B. Collum, *J. Am. Chem. Soc.* **2011**, *133*, 7135.

[35] R. E. Mulvey, E. Hevia, *Angew. Chem. Int. Ed.* **2011**, *50*, 6448.

[36] P. Garcia-Alvarez, D. V. Graham, E. Hevia, A. R. Kennedy, J. Klett, R. E. Mulvey, C. T. O'Hara, S. Weatherstone, *Angew. Chem. Int. Ed.* **2008**, *47*, 8079.

[37] A. R. Kennedy, R. E. Mulvey, D. E. Oliver, S. D. Robertson, *Dalton Trans.* **2010**, *39*, 6190.

[38] Y. Kondo, M. Shilai, M. Uchiyama, T. Sakamoto, *J. Am. Chem. Soc.* **1999**, *121*, 3539.

[39] H. R. L. Barley, W. Clegg, S. H. Dale, E. Hevia, G. W. Honeyman, A. R. Kennedy, R. E. Mulvey, *Angew. Chem. Int. Ed.* **2005**, *44*, 6018.

[40] W. Clegg, S. H. Dale, E. Hevia, G. W. Honeyman, R. E. Mulvey, *Angew. Chem. Int. Ed.* **2006**, *45*, 2370.

[41] L. Balloch, A. R. Kennedy, R. E. Mulvey, T. Rantanen, S. D. Robertson, V. Snieckus, *Organometallics* **2011**, *30*, 145.

[42] D. R. Armstrong, J. Garcia-Alvarez, D. V. Graham, G. W. Honeyman, E. Hevia, A. R. Kennedy, R. E. Mulvey, *Chem. Eur. J.* **2009**, *15*, 3800.

[43] D. R. Armstrong, L. Balloch, E. Hevia, A. R. Kennedy, R. E. Mulvey, C. T. O'Hara, S. D. Robertson, *Beilstein J. Org. Chem.* **2011**, *7*, 1234.

[44] M. Uchiyama, T. Miyoshi, Y. Kajihara, T. Sakamoto, Y. Otani, T. Ohwada, Y. Kondo, *J. Am. Chem. Soc.* **2002**, *124*, 8514.

[45] M. Uchiyama, Y. Kobayashi, T. Furuyama, S. Nakamura, Y. Kajihara, T. Miyoshi, T. Sakamoto, Y. Kondo, K. Morokuma, *J. Am. Chem. Soc.* **2008**, *130*, 472.

[46] P. C. Andrikopoulos, D. R. Armstrong, H. R. L. Barley, W. Clegg, S. H. Dale, E. Hevia, G. W. Honeyman, A. R. Kennedy, R. E. Mulvey, *J. Am. Chem. Soc.* **2005**, *127*, 6184.

[47] M. Uchiyama, Y. Matsumoto, D. Nobuto, T. Furuyama, K. Yamaguchi, K. Morokuma, *J. Am. Chem. Soc.* **2006**, *128*, 8748.

[48] D. Nobuto, M. Uchiyama, *J. Org. Chem.* **2008**, *73*, 1117.

[49] W. Clegg, B. Conway, E. Hevia, M. D. McCall, L. Russo, R. E. Mulvey, *J. Am. Chem. Soc.* **2009**, *131*, 2375.

[50] D. R. Armstrong, V. L. Blair, W. Clegg, S. H. Dale, J. Garcia-Alvarez, G. W. Honeyman, E. Hevia, R. E. Mulvey, L. Russo, *J. Am. Chem. Soc.* **2010**, *132*, 9480.

[51] W. Clegg, B. Conway, D. V. Graham, E. Hevia, A. R. Kennedy, R. E. Mulvey, L. Russo, D. S. Wright, *Chem. Eur. J.* **2009**, *15*, 7074.

[52] J. Hine, S. Hahn, D. E. Miles, K. Ahn, *J. Org. Chem.* **1985**, *50*, 5092.

[53] F. Gohier, A.-S. Castanet, J. Mortier, *Org. Lett.* **2003**, *5*, 1919.

[54] F. Gohier, J. Mortier, *J. Org. Chem.* **2003**, *68*, 2030.

[55] S. Tripathy, R. LeBlanc, T. Durst, *Org. Lett.* **1999**, *1*, 1973.

[56] T. Truong, O. Daugulis, *J. Am. Chem. Soc.* **2011**, *133*, 4243.

[57] R. Sanz, M. P. Castroviejo, V. Guilarte, A. Pérez, F. J. Fañanás, *J. Org. Chem.* **2007**, *72*, 5113.

[58] I. Bytschkov, H. Siebeneicher, S. Doye, *Eur. J. Org. Chem.* **2003**, *2888*.

[59] D. J. Michaelis, T. A. Dineen, *Tetrahedron Lett.* **2009**, *50*, 1920.

[60] P. Knochel, M. Mosrin, *Chem. Eur. J.* **2009**, *15*, 1468.

[61] P. Ploypradith, W. Jinaglueng, C. Pavaro, S. Ruchirawat, *Tetrahedron Lett.* **2003**, *44*, 1363.

[62] J. Boukouvalas, R. P. Loach, *J. Org. Chem.* **2008**, *73*, 8109.

[63] B. L. Eriksen, P. Vedso, M. Begtrup, *J. Org. Chem.* **2001**, *66*, 8344.

[64] M. Aso, T. Kaneko, M. Nakamura, N. Koga, H. Suemune, *Chem. Commun.* **2003**, 1094.

[65] T. A. Jensen, D. Tanner, X. Liang, N. Skjaerbaek, *J. Org. Chem.* **2004**, *69*, 4936.

[66] J. R. Gage, W. R. Perrault, T.-J. Poel, R. C. Thomas, *Tetrahedron Lett.* **2000**, *41*, 4301.

[67] P. M. Herrinton, C. E. Owen, J. R. Gage, *Org. Process Res. Dev.* **2001**, *5*, 80.

[68] T. Mase, I. N. Houpis, A. Akao, I. Dorziotis, K. Emerson, T. Hoang, T. Iida, T. Itoh, K. Kamei, S. Kato, et al., *J. Org. Chem.* **2001**, *66*, 6775.

[69] N. Ikemoto, R. A. Miller, F. J. Fleitz, J. Liu, D. E. Petrillo, J. F. Leone, J. Laquidara, B. Marcune, S. Karady, J. D. Armstrong, et al., *Tetrahedron Lett.* **2005**, *46*, 1867.

[70] S. J. Dolman, F. Gosselin, P. D. O'Shea, I. W. Davies, *Tetrahedron* **2006**, *62*, 5092.

[71] E. Negishi, *Angew. Chem. Int. Ed.* **2011**, *50*, 2.

[72] D. Zhao, J. You, C. Hu, *Chem. Eur. J.* **2011**, *17*, 5466.

[73] F. Bellina, R. Rossi, *Chem. Rev.* **2010**, *110*, 1082.

[74] K. C. Nicolaou, P. G. Bulger, D. Sarlah, *Angew. Chem. Int. Ed.* **2005**, *44*, 4442.

[75] J. Hassan, M. Sevignon, C. Gozzi, E. Schulz, M. Lemaire, *Chem. Rev.* **2002**, *102*, 1359.

[76] M. Schlosser, *Angew. Chem. Int. Ed.* **2005**, *44*, 376.

[77] P. Knochel, W. Dohle, N. Gommermann, F. F. Kneisel, F. Kopp, T. Korn, I. Sapountzis, V. A. Vu, *Angew. Chem. Int. Ed.* **2003**, *42*, 4302.

[78] K. Smith, G. A. El-Hiti, *Green Chem.* **2011**, *13*, 1579.

[79] G. I. Borodkin, V. G. Shubin, *Russ. J. Org. Chem.* **2006**, *42*, 1745.

[80] K. Smith, *J. Chem. Technol. Biotechnol.* **1997**, *68*, 432.

[81] M. Kohn, J. J. Sussmann, *Monatsh. Chem.* **1927**, *48*, 193.

[82] T. Yamamoto, K. Toyota, N. Morita, *Tetrahedron Lett.* **2010**, *51*, 1364.

Chapter 5: Comparison Between *bis*-TMP and *mono*-TMP Base

5.1 Introduction

So far some key differences have been observed between our *bis*-TMP base [Li(TMP)$_2$Al(*i*Bu)$_2$] **4.1** and Uchiyama's *mono*-TMP varient [Li(TMP)Al(*i*Bu)$_3$] **4.2**. For one, **4.2** is reported to be stable in neat THF solution where it is utilised for the deprotonation of a number of aromatic and heteroaromatic substrates[1] yet **4.1** will deprotonate a stoichiometric amount of THF in hexane solution and trap its resulting anion (see **Chapter 3**). When other donor ligands are added in place of THF in hexane solution such as Me$_2$TFA, MDAE and Me$_4$AEE the donor will merely solvate Li in the case of **4.2** yet **4.1** will effectively deprotonate each donor ligand at the most acidic methyl site (see **Chapter 3**).

In light of these observations and based on a previous report on the reactivity of **4.2** (**Scheme 5.1** and **5.2**)[2] we decided to carry out a comprehensive investigation of these two aluminate bases in order to attempt to understand their differences in reactivity. It was reported that **4.2** gives [{Li(THF)$_4$}$^+${Al(TMP)(*i*Bu)$_3$}$^-$] when prepared *in situ* in THF solution which is considered to be the active component as adding an equivalent of *N*,*N*-diisopropylbenzamide results in direct *ortho*-alumination as evidenced by the isolation of compound **4.4** (**Scheme 5.1**).

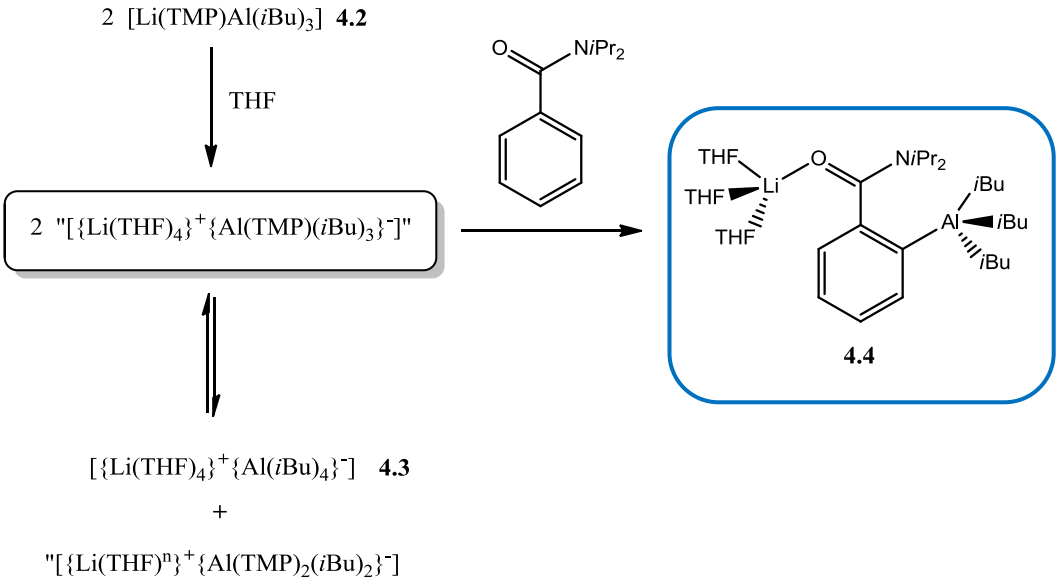

Scheme 5.1: Postulated pathway for formation of *ortho*-aluminated *N*,*N*-diisopropylbenzamide.

It was also stated that the seemingly active component $[\{Li(THF)_4\}^+\{Al(TMP)(iBu)_3\}^-]$ must disproportionate depending on the reaction time involved, as crystals were isolated from the solution and their ^1H NMR spectrum revealed a solvent-separated homoleptic alkyl aluminate $[\{Li(THF)_4\}^+\{Al(iBu)_4\}^-]$ **4.3** with four *iso*-butyl groups, although a crystal structure was never determined. If **4.2** does disproportionate in this way, balancing the stoichiometry means that $[\{Li(THF)_n\}^+\{Al(TMP)_2(iBu)_2\}^-]$ could be left in solution which is the formula of our *bis*-TMP aluminium base **4.1**.

The report also concluded that the homoleptic aluminate **4.3** was completely unreactive and if **4.2** was prepared in hexane solution rather than THF solution it did not react with *N*,*N*-diisopropylbenzamide. Direct alumination was only observed when **4.2** was prepared *in situ* in THF solution prior to adding the carbonyl containing substrate (**Scheme 5.2**).

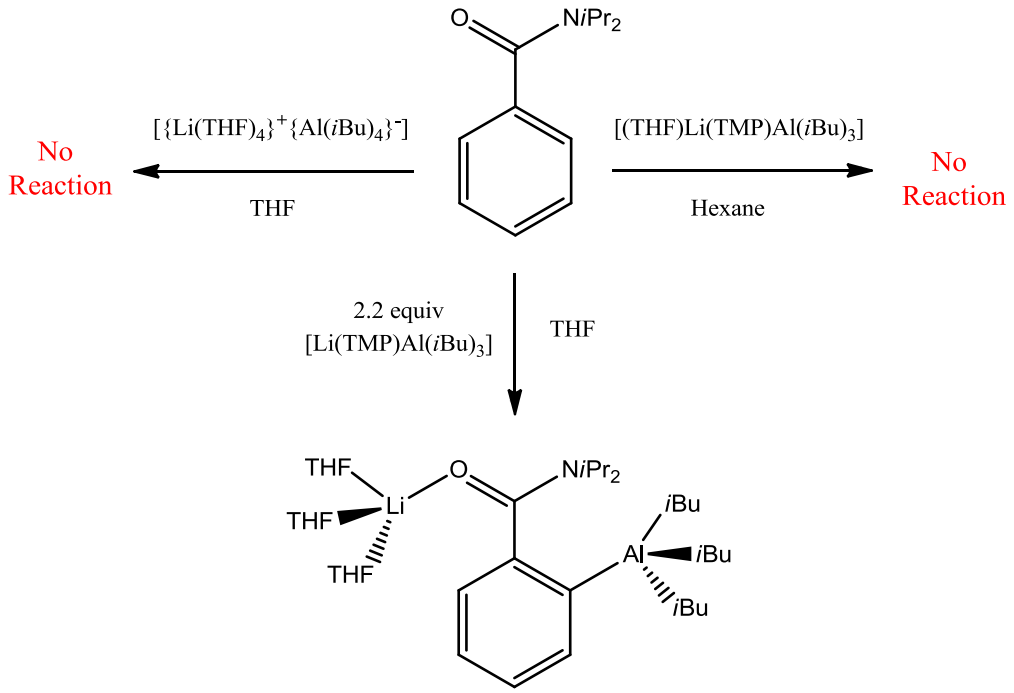

Scheme 5.2: How the aluminate reagent identity greatly influences the course of the direct alumination reaction.

We therefore decided to investigate these observations further in order to establish if $[\{Li(THF)_4\}^+\{Al(TMP)(iBu)_3\}^-]$ is the active component or whether our putative *bis*-TMP base **4.1** dissolved in THF solution $[\{Li(THF)_n\}^+\{Al(TMP)_2(iBu)_2\}^-]$ is the active base. We also wanted to shed more light on the reactivity of **4.2** in non-polar hexane solution and how this differs from its reactivity in polar THF solution. The results from

this part of the project will be discussed in four sections – 1) crystalline **4.2**, 2) *in situ* **4.2** in THF solution, 3) **4.1** in THF solution and 4) comparison of **4.1** and **4.2**. Some conclusions will be drawn on the observations and results obtained. Additionally, the reactivity of the sodium versions of both bases will also be considered for comparison.

5.2 Results and Discussion

5.2.1 Crystalline 4.2 [(THF)Li(TMP)(*i*Bu)$_3$]

As it was observed that **4.2** disproportionates in THF solution when prepared *in situ*, it was expected that crystals of **4.2** obtained from hexane solution in its THF solvate form would also disproportionate when dissolved in THF solution. To explore this possibility, crystals of **4.2** were added to a NMR tube and dissolved in D_8-THF. However, it was found that crystalline **4.2** does not disproportionate in D_8-THF even after 24 hours (**Figure 5.1**). This suggests that the molecular structure in which the Lewis acidic Li centre is solvated by a Lewis basic THF ligand, once formed, cannot disproportionate as it has formed a stable four-atom four-membered LiNAlC ring which cannot be broken under these conditions (see inset of **Figure 5.1**).

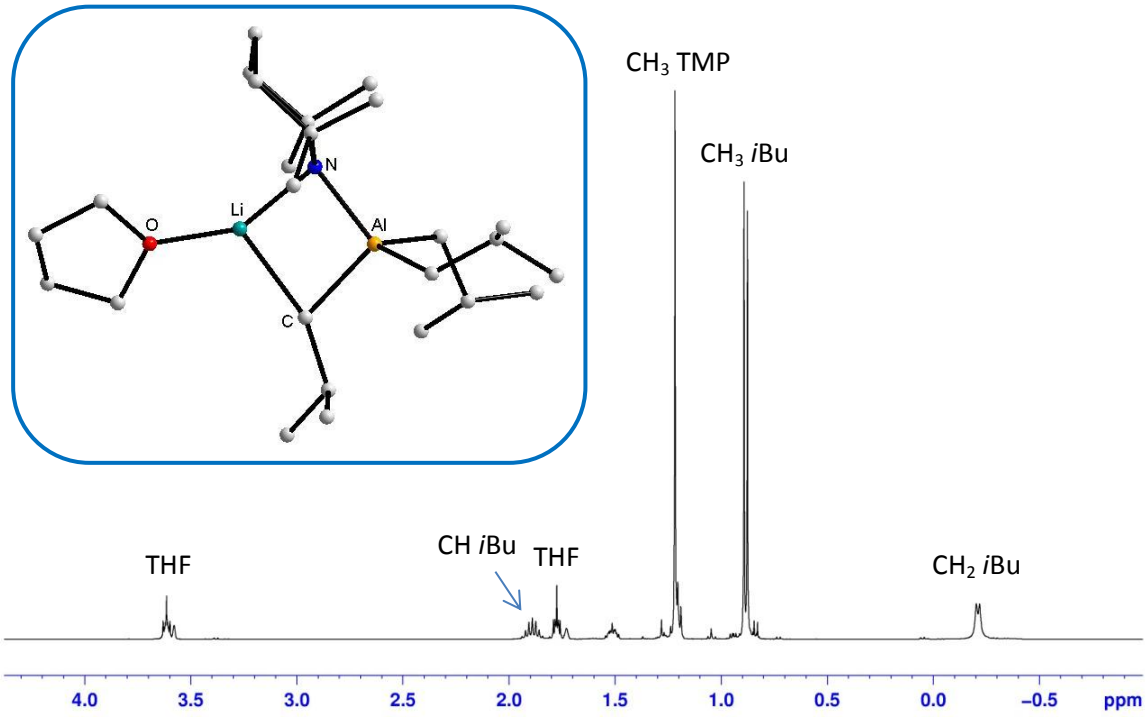

Figure 5.1: ^{1}H NMR spectrum in D_8-THF of crystalline [(THF)Li(TMP)Al(*i*Bu)$_3$] **4.2.** Molecular structure is shown inset.

If mono-TMP aluminate **4.2** was to disproportionate in THF solution then it would be expected that the ^{1}H NMR spectrum (**Figure 5.1**) would show more than one type of *i*Bu and TMP resonance as there are potentially three distinct species in solution all in equilibrium with one another, namely the homoleptic aluminate **4.3**, *bis*-TMP base **4.1** and *mono*-TMP base **4.2**.

Crystalline **4.2** was also heated in an NMR tube in D_8-THF solution to temperatures of 300, 310, 320 and 330K to determine if the base would disproportionate at an elevated temperature. As observed in the ^{1}H NMR spectra in **Figure 5.2** crystalline **4.2** does not disproportionate at higher temperature as there was no change in the spectra on increasing the temperature, establishing that once the base is crystallised from hexane solution with formula [(THF)Li(TMP)Al(*i*Bu)$_3$] it is not the same base as that prepared *in situ* in THF solution. Although Uchiyama reports the molecular structure of the base as that shown in **Figure 5.1**, on the basis of these observations this cannot be the active base in solution.

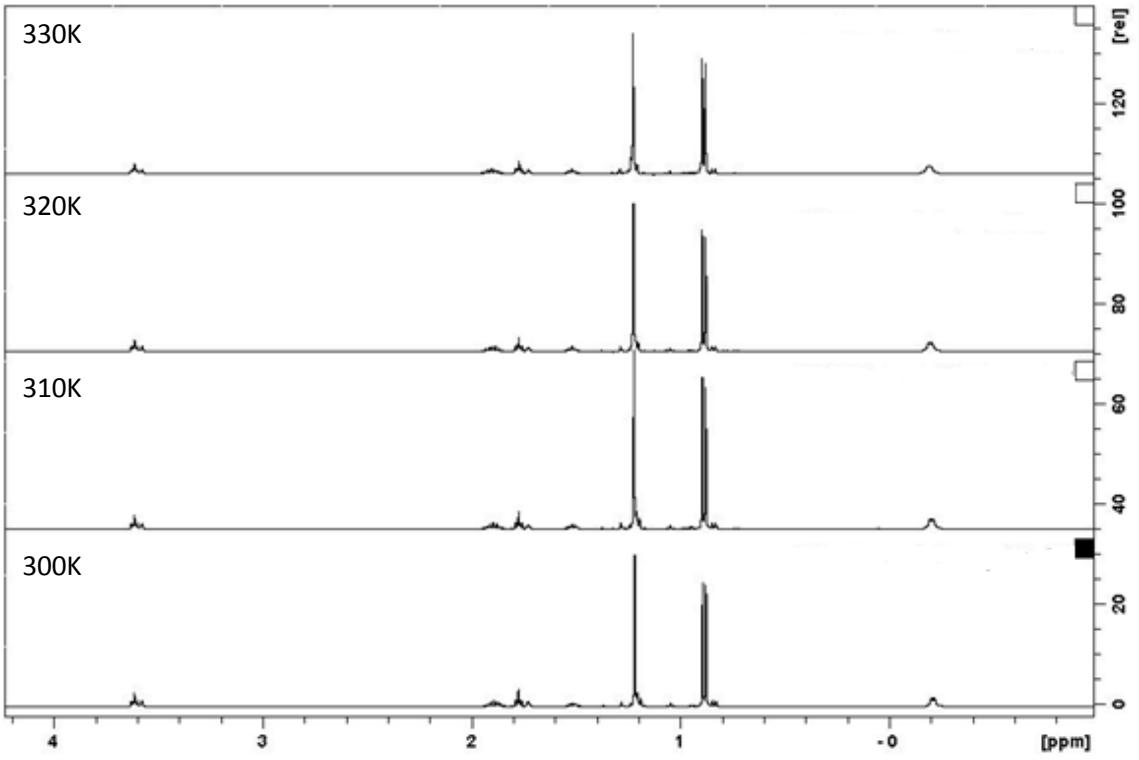

Figure 5.2: Variable temperature ^{1}H NMR spectra in D_8-THF solution of crystalline **4.2**.

To verify that the contact ion-pair aluminate [(THF)Li(TMP)Al(*i*Bu)$_3$] shown in **Figure 5.1** retains its structure or at least its anionic [(TMP)Al(*i*Bu)$_3$]$^-$ ate moiety in D_8-THF

solution, a DOSY NMR spectrum[3–11] was carried out on the crystalline compound. As can be seen from the DOSY NMR spectrum (**Figure 5.3**) all of the resonances consistent with the compound (that is C$\underline{H}_2$ of *i*Bu at -0.20 ppm, C$\underline{H}_3$ of *i*Bu at 0.91 ppm, C$\underline{H}$ of *i*Bu at 1.90 ppm, C$\underline{H}_3$ of TMP at 1.22 ppm, γC$\underline{H}_2$ of TMP at 1.51 ppm and βC$\underline{H}_2$ of TMP at 1.22 ppm) seemingly lie along the same line, implying that they all must belong to the same compound hence it does not disproportionate. The only other resonances observed belong to THF at 1.80 ppm for the αC$\underline{H}_2$ protons and 3.60 ppm for the βC$\underline{H}_2$ protons. THF is labile hence will coordinate and de-coordinate in D_8-THF solution. These peaks appear further down the spectrum as THF has a lower molecular weight and hence higher diffusion coefficient than crystalline **4.2**. TMP(H) is also observed in the spectrum at 1.06 ppm due to a small amount of hydrolysis. As this is not part of the structure it also appears as a separate peak in the spectrum due to its higher diffusion coefficient.

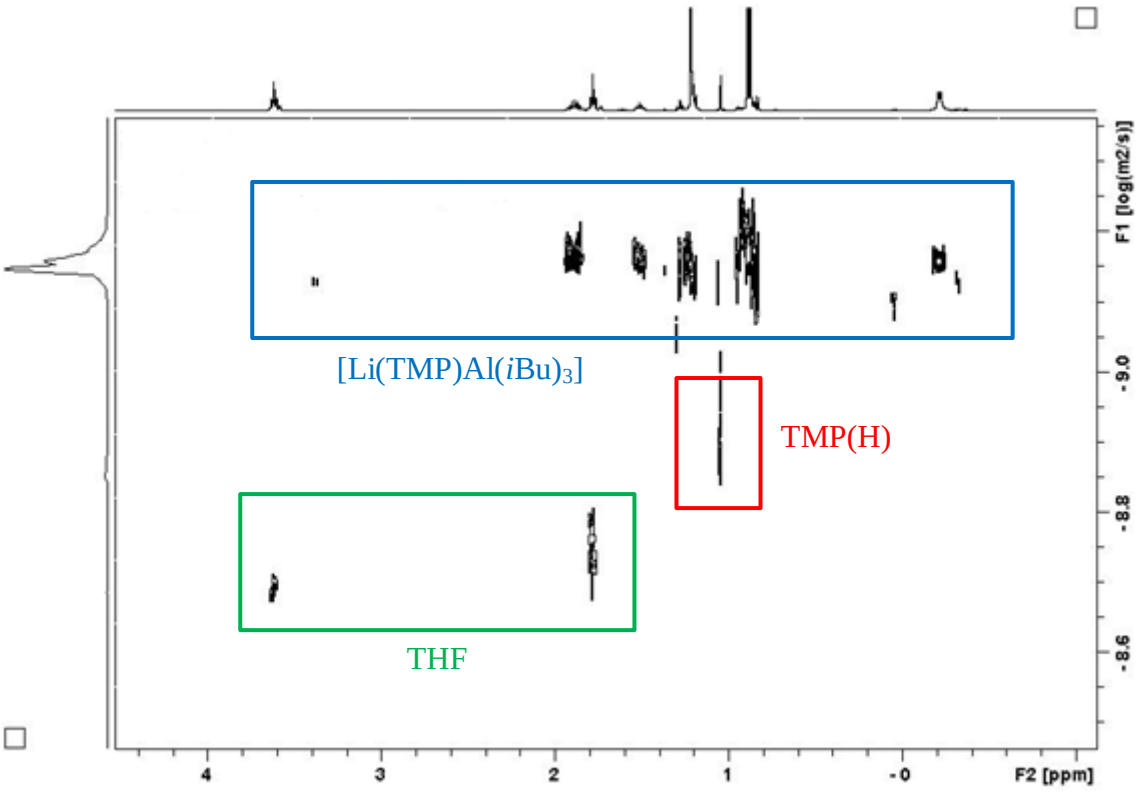

Figure 5.3: ^{1}H DOSY NMR spectrum in D_8-THF solution of crystalline **4.2**.

To investigate further that crystalline **4.2** may not be the same as *in situ* **4.2** in THF solution and is therefore not the active base, it was dissolved in THF solution and mixed with anisole. It was found that crystalline **4.2** was completely inert towards anisole in

THF solution as evidenced by the ^{1}H NMR spectrum of the reaction mixture (**Figure 5.4**). The aromatic region only shows unreacted anisole. We know that *in situ* **4.2** in THF solution is reactive towards anisole as Uchiyama reports the iodinated product, formed via alumination of anisole and electrophilic quenching with iodine, in good yield.[1]

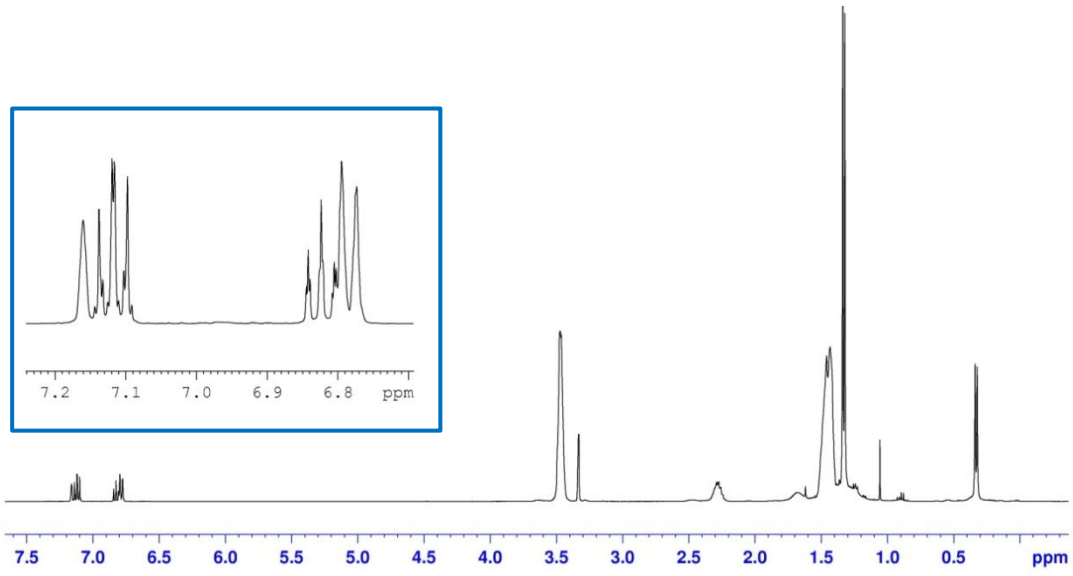

Figure 5.4: ^{1}H NMR spectrum in C_6D_6 solution of reaction mixture from the reaction of crystalline **4.2** and anisole in THF solution (aromatic region shown inset).

It was proposed that once the contact ion-pair structure of **4.2** is formed all deprotonative reactivity of the mixture is lost. To probe whether this is the case, **4.2** was also prepared *in situ* in hexane (that is made from its constituent parts *i*Bu_3Al, LiTMP and one equivalent of THF) and again combined with anisole. It transpires that even this *in situ* generated base in hexane solution was inert towards anisole. We can therefore conclude with a degree of certainty that **4.2** crystallised from hexane solution is not the same base in bulk as that prepared and reacted *in situ* in THF solution.

5.2.2 *In situ* 4.2 [Li(TMP)Al(*i*Bu)$_3$] in THF Solution

For comparison purposes the reactivity of the *in situ* base **4.2** in THF solution was tested with anisole. As expected, *in situ* **4.2** was found to effectively deprotonate anisole, though only a 50% conversion was achieved (**Figure 5.5**). Our reaction was carried out using a 1:1 stoichiometry of **4.2** and anisole which led us to ask the question why does Uchiyama use 2.2 equivalents of *in situ* **4.2** in the reported deprotonation reactions? We postulated at this stage that a suitable explanation for this stoichiometry

was the fact that 50% of the base is the active component with the other 50% being completely unreactive. This rationale is plausible as we already know that **4.2** disproportionates to give the homoleptic aluminate $[\{Li(THF)_4\}^+\{Al(iBu)_4\}^-]$ **4.3** which we already know to be unreactive towards *N*,*N*-diisopropylbenzamide (**Scheme 5.2**). So another question to ask was "is the other component after disproportionation $[\{Li(THF)_n\}^+\{Al(TMP)_2(iBu)_2\}^-]$ (that is, our *bis*-TMP **4.1**) and is this the active base?"

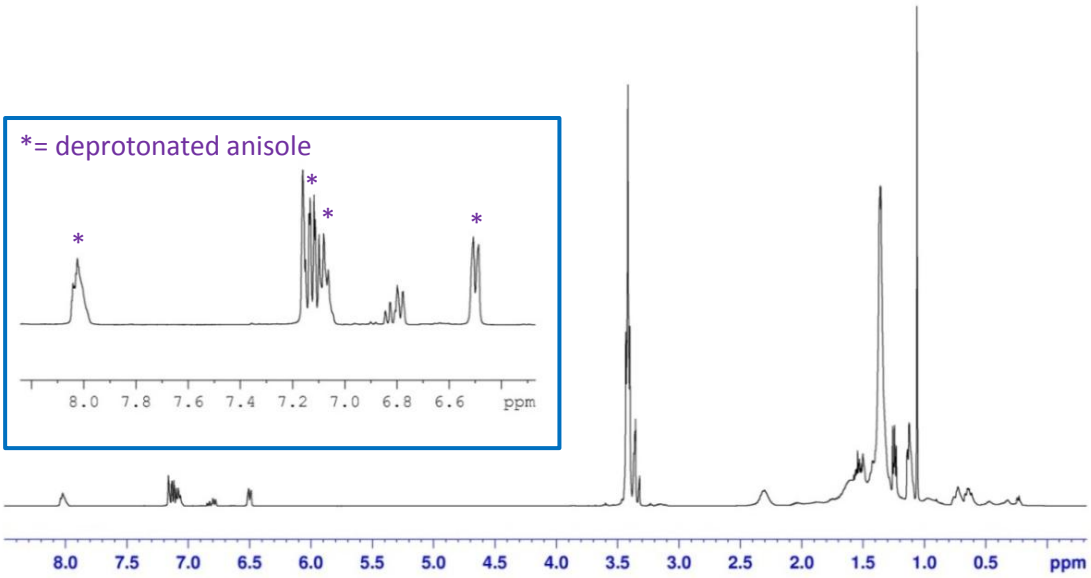

Figure 5.5: ^{1}H NMR spectrum in C_6D_6 of reaction mixture obtained from reaction of **4.2** with anisole in THF solution.

We decided to test the reactivity of *in situ* **4.2** in THF solution with anisole at 0^{o}C and room temperature to determine if there was an equilibrium occurring between the different species in solution and whether this would result in a kinetic versus thermodynamic basicity. Would the reactivity of the base be altered by varying the temperature? When 2.2 molar equivalents of *in situ* **4.2** was reacted with anisole at room temperature and the reaction mixture was then quenched with iodine, both anisole and 2-iodoanisole were observed in the ^{1}H NMR spectrum in a 1:1 ratio (**Figure 5.6** shows aromatic region of this spectrum).

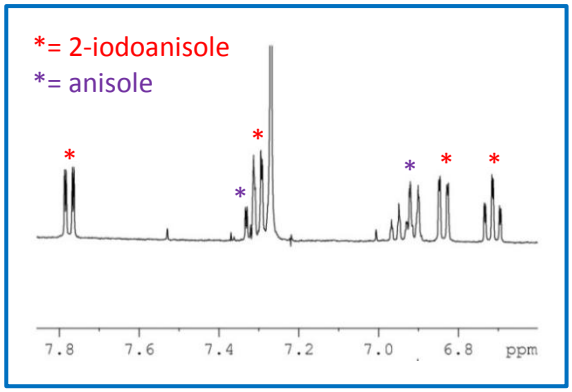

Figure 5.6: Aromatic region from the ^{1}H NMR spectrum in $CDCl_3$ solution of crude product generated after *in situ* **4.2** was reacted with anisole at room temperature in THF solution and quenched with iodine.

When this reaction was repeated at 0^{o}C only 2-iodoanisole was observed in the ^{1}H NMR spectrum, with no evidence of unreacted anisole (**Figure 5.7**). It therefore appears that **4.2** is more reactive at 0^{o}C than it is at room temperature which suggests that the kinetic component of the aluminate is more reactive and as the temperature increases the reactivity diminishes. This could be due to the equilibrium lying more in favour of the homoleptic aluminate **4.3** and *bis*-TMP **4.1** (see **Scheme 5.1**) which is possibly the active base. Uchiyama prepares **4.2** at -78^{o}C and adds each substrate at 0^{o}C which could be the reason why his procedure produces such high yields of iodinated product.

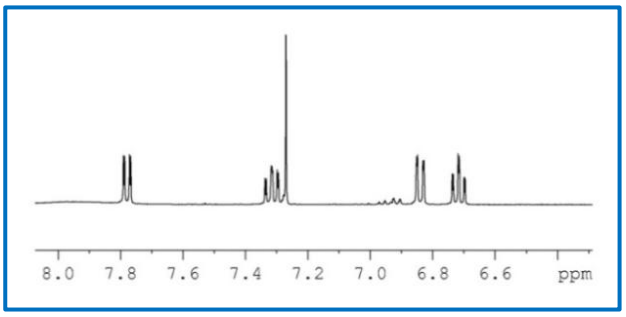

Figure 5.7: Aromatic region from the ^{1}H NMR spectrum in $CDCl_3$ solution of crude product generated after *in situ* **4.2** was reacted with anisole at 0^{o}C in THF solution and quenched with iodine.

If the reactivity is altered by varying the temperature there clearly must be different species present in THF solution. In order to determine the number of species present and their identities, **4.2** was prepared again *in situ* in THF solution and the ^{27}Al NMR spectrum was recorded as shown in **Figure 5.8**.

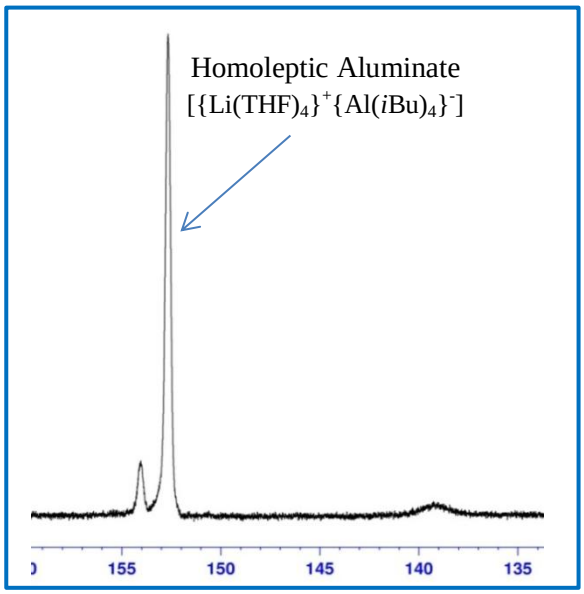

Figure 5.8: ^{27}Al NMR spectrum of **4.2** in D_8-THF solution.

The sharp signal located at 152.5 ppm was confirmed to be the homoleptic aluminate $[\{Li(THF)_4\}^+\{Al(iBu)_4\}^-]$ **4.3** by comparison with the ^{27}Al NMR spectrum of an authentic sample. A smaller peak was observed at 154.0 ppm which was thought to correspond to **4.1** due to the large signal corresponding to **4.3**. Another broader peak was also visible at 139.0 ppm.

The identity of the additional peaks in the ^{27}Al NMR spectrum of **4.2** was sought by comparison with the ^{27}Al NMR spectra of the different aluminium starting reagents of **4.1** and **4.2** (that is iBu_2AlTMP and iBu_3Al respectively) and **4.1** itself in THF solution (**Figure 5.9**). However, due the quadrapolar ^{27}Al nuclei, the signals are far too broad to be observed except for the broad resonance in **4.1** spectrum. The small peak in **Figure 5.8** must therefore belong to another species. It is thought that the homoleptic aluminate **4.3** appears as a sharp resonance in the ^{27}Al NMR spectrum as it is considered to have a high degree of tetrahedral symmetry based on a similar dioxane analogue $[\{Li(dioxane)_4\}^+\{Al(iBu)_4\}^-]$ which has been crystallographically characterised.[12] Given that the small resonance at 154.0 ppm lies close to the large one at 152.5 ppm and looks just as sharp suggests it is probably a closely related tetrahedral species. As there is also a broad resonance in the ^{27}Al NMR spectrum of **4.1** in THF solution at the same shift as that observed in **Figure 5.8**, this is highly likely to be **4.1** due to the disproportionation of **4.2** in THF solution.

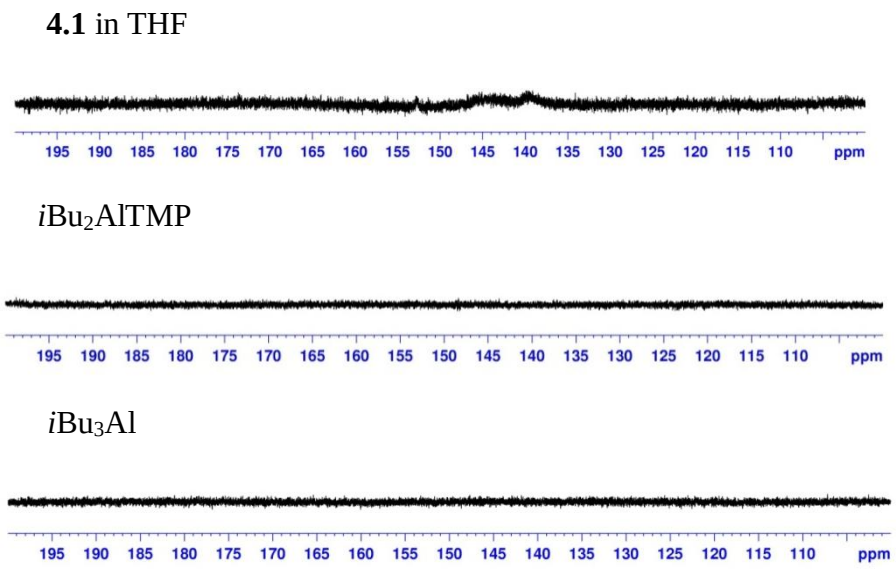

Figure 5.9: ^{27}Al NMR spectra of **4.1** in THF (top), *i*Bu_2AlTMP (middle) and *i*Bu_3Al (bottom).

The ^{7}Li NMR spectrum of *in situ* **4.2** in THF solution was also considered to help determine the number of lithium species present in solution (**Figure 5.10**). A total of four resonances were observed including a large signal at -0.35 ppm which is consistent with tetra-alkyl **4.3** as found from a comparison with its ^{7}Li NMR spectrum. Another species which could be present is LiTMP as it is one of the components of **4.2** however; a direct comparison with the ^{7}Li NMR spectrum of LiTMP showed no resonances consistent with those observed in **Figure 5.10**. The three resonances could suggest that there is an equilibrium between lithium species in solution. We know that LiTMP forms a monomer-dimer equilibrium in THF solution[13,14] hence the three ^{7}Li signals bunched together at 1.29, 1.65 and 1.98 ppm could suggest that they might belong to similar formulated species such as LiTMP·xTHF (monomer) and $[LiTMP{\cdot}xTHF]_2$ (dimer). Alternatively, two of these ^{7}Li NMR resonances could correspond to mono-TMP **4.2** and *bis*-TMP **4.1**.

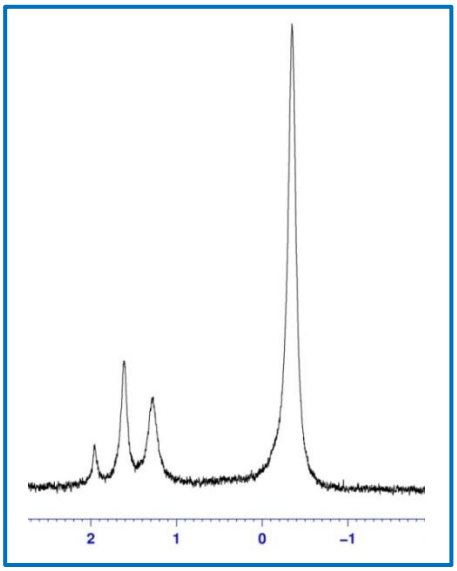

Figure 5.10: ^{7}Li NMR spectrum of **4.2** in THF solution showing a sharp resonance consistent with $[\{Li(THF)_4\}^+\{Al(iBu)_4\}^-]$ **4.3** and three smaller unknown resonances.

The ^{7}Li NMR spectrum of **4.1** (**Figure 5.11**) was compared to that in **Figure 5.10**. It shows a resonance at 3.50 ppm which is consistent with that of LiTMP[15,16] which is one of the starting materials and another at 2.00 ppm which could correspond to **4.1**. This resonance is consistent with the small one located at 2.00 ppm in **Figure 5.10.** If these resonances both correspond to **4.1** this provides us with some more evidence consistent with the disproportionation of **4.2** in THF solution to give **4.1**. The presence of another yet unidentified lithium containing species cannot be ruled out, such as a THF solvated LiTMP aggregate.

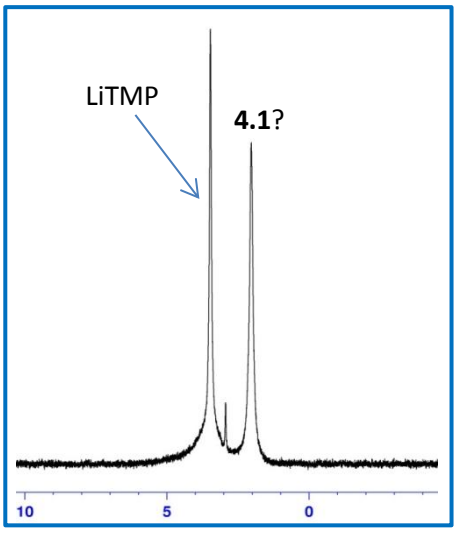

Figure 5.11: ^{7}Li NMR spectrum of **4.1** in D_8-THF solution.

To help confirm the presence of **4.1** as one of the disproportionation products and back-up our theory that it is the active base component within **4.2**, *in situ* **4.2** was left to stir for 24 hours in THF solution before adding anisole. We know that **4.1** will deprotonate THF (see **Chapter 3**) so if **4.1** was present in solution after disproportionation, the reactivity of **4.2** should diminish as it will have preferentially deprotonated THF. As expected, it did not react with anisole hence after 24 hours the base is no longer active in THF solution. This is further evidence to suggest that **4.1** could be the active base.

5.2.3 4.1 [Li(TMP)$_2$Al(*i*Bu)$_2$] in THF Solution

To compare the reactivity of **4.1** with **4.2** the former was was also tested with anisole in bulk THF solution. The molecular structure of aluminated anisole formed from **4.1** in hexane has been discussed in **Chapter 2** (compound **1.2**) however, until now no reactivity study of this base has been carried out in THF solution. As witnessed in the ^{1}H NMR spectrum of the reaction mixture, **4.1** also deprotonates anisole in bulk THF solution.

As discussed in **Chapter 3**, mixture **4.1** will deprotonate a stoichiometric amount of THF in hexane solution. However, its ability or otherwise to deprotonate THF in a bulk solution medium has not been probed. Hence **4.1** was allowed to stir in THF solution for 24 hours at ambient temperature before taking a NMR spectrum of the resulting mixture. Resonances consistent with compound **2.2** [(THF)Li(μ-TMP)(μ-OC$_4$H$_7$)Al(*i*Bu)$_2$] in **Chapter 3** were witnessed in the ^{1}H NMR spectrum (**Figure 5.12** shows the characteristic resonances inset).

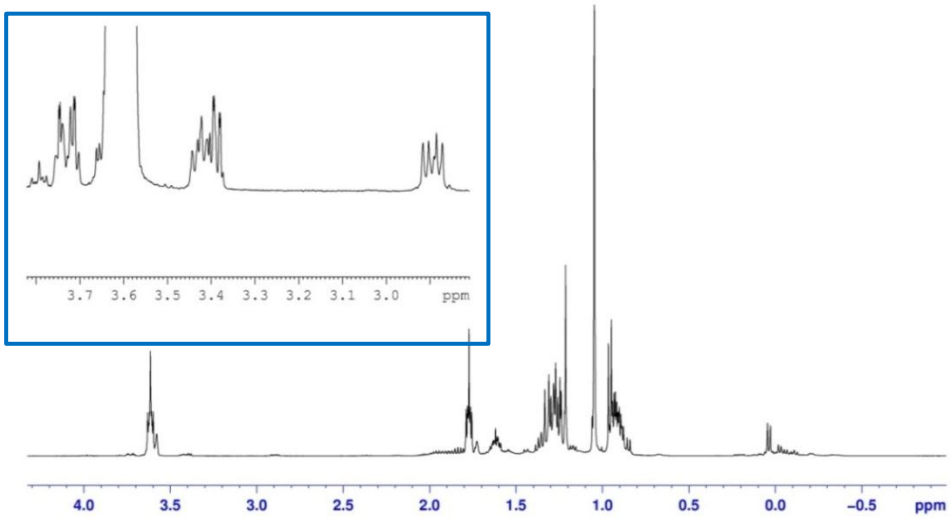

Figure 5.12: ^{1}H NMR spectrum of reaction mixture of **4.1** after stirring for 24 hours in THF solution (signals consistent with deprotonated THF compound are shown in inset).

The characteristic C-H hydrogen atoms on the deprotonated THF ring come at 2.90 ppm, 3.42 ppm and 3.74 ppm and these are clearly visible in the ^{1}H NMR spectrum in **Figure 5.12**. However, these resonances were only visible when the spectrum was magnified. A significantly larger signal was observed for TMP(H) at 1.06 ppm suggesting that in bulk THF solution **4.1** will deprotonate THF but it probably also decomposes via one of the common decomposition pathways discussed in **Chapter 3**, most likely breaking down to ethene and the enolate of acetaldehyde.[17]

If **4.1** is the active base of *in situ* **4.2** then allowing it to stir for any length of time in THF solution will result in the activity of the base to decrease due to THF deprotonation. To rule out the possibility that once formed, the deprotonated THF compound [(THF)Li(μ-TMP)(μ-OC_4H_7)Al(*i*Bu)$_2$] is a base itself, it was crystallised from hexane solution (for synthesis see **Chapter 3**) and dissolved in THF solution. Anisole was then added and the solution was left to stir for 24 hours. As can be seen from the ^{1}H NMR spectrum of the resulting reaction mixture, the THF compound does not act as a base, since unreacted anisole can be observed in the aromatic region highlighted in **Figure 5.13**.

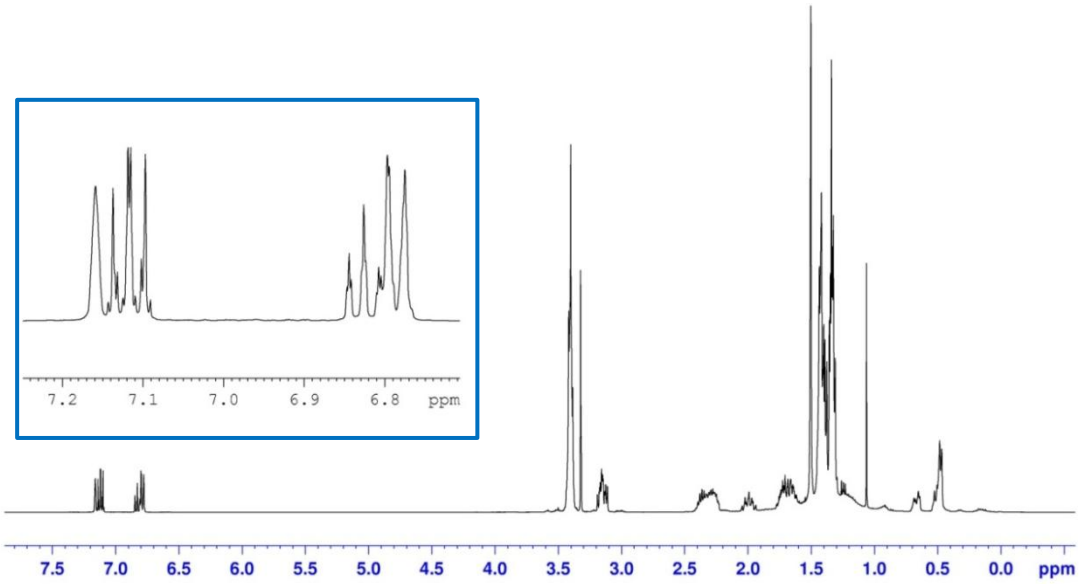

Figure 5.13: ^{1}H NMR spectrum of reaction mixture after reacting deprotonated THF compound with anisole and stirring for 24 hours.

To determine if the same is true for the reactivity of **4.1** in THF solution, that is, reacting **4.1** in THF solution for 24 hours before adding anisole, a ^{1}H NMR spectrum of the reaction mixture was carried out. We know that **4.1** will deprotonate bulk THF solution so it should no longer react with anisole after 24 hours. As expected no deprotonation was observed. In addition to the characteristic THF peaks discussed previously, a large signal for TMP(H) was observed. We can conclude that if left to stir for a period of time in THF solution, **4.1** will deprotonate THF and become inactive towards further deprotonation. This is consistent with our observation that **4.2** becomes inactive in THF solution after 24 hours.

We were also curious about the constitution of **4.1** itself in THF solution and how the ^{1}H NMR resonances of the base mixture differ from its constituent parts LiTMP and *i*Bu$_2$AlTMP. A comparison of the ^{1}H NMR spectra of **4.1**, *i*Bu$_2$AlTMP and LiTMP in THF solution is shown in **Figure 5.14**.

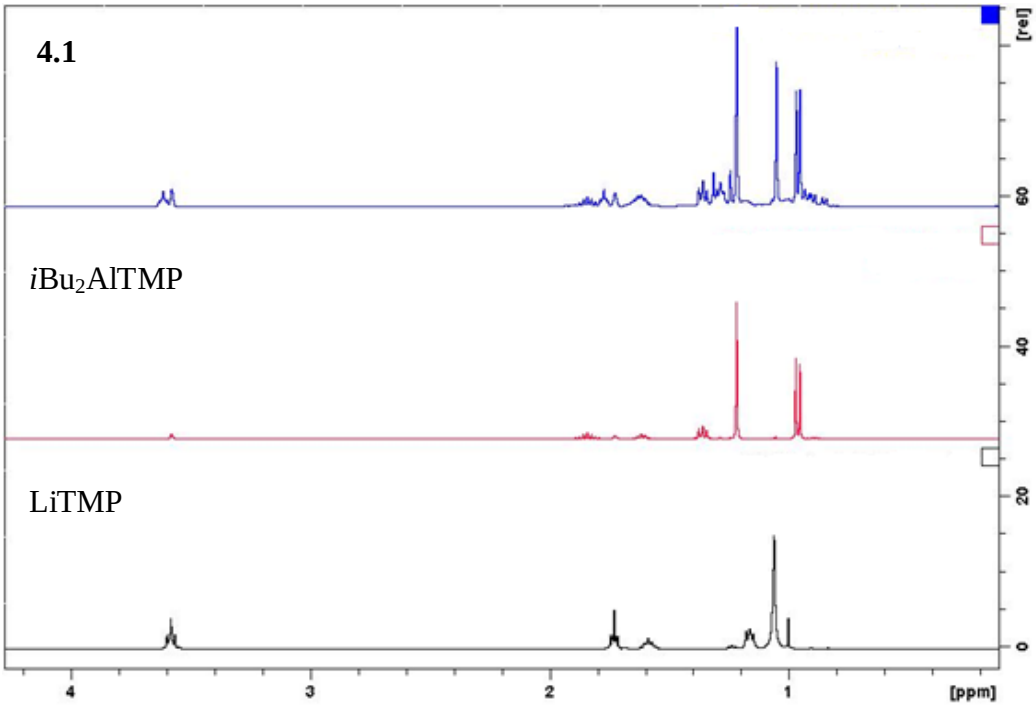

Figure 5.14: ^{1}H NMR spectra of **4.1** (top), *i*Bu_2AlTMP (middle) and LiTMP (bottom) in D_8-THF solution.

On close inspection of these spectra it appears that **4.1** remains as separate components in THF solution rather than a mixed-metal species. There are no shifts in the resonances of the base mixture **4.1** when compared to those of the starting materials. This suggests that it could be LiTMP which carries out the deprotonation of the substrate and *i*Bu_2AlTMP then traps the deprotonated substrate to generate a mixed-metal species.

If **4.1** is not actually a mixed-metal species, LiTMP must be deprotonating THF rather than **4.1** as discussed above. To establish whether this is the case, LiTMP was dissolved in C_6D_6 in an NMR tube to which a few drops of THF were added. A ^{1}H NMR spectrum was taken after 30 minutes and after 24 hours (**Figure 5.15**). A signal was observed at 5.25 ppm which is consistent with ethene which would come from the cleavage and ring opening of THF. This signal increases after a period of 24 hours. When **4.1** is left to stir in bulk THF solution for 24 hours a small amount of the deprotonated THF compound [(THF)Li(μ-TMP)(μ-OC_4H_7)Al(*i*$Bu)_2$] is observed, so this is either due to a mixed-metal base rather than just LiTMP or another more plausible explanation could be that LiTMP probably in its more reactive monomeric

form deprotonates THF and the anionic THF rapidly co-complexes with *i*Bu_2AlTMP before cleaving.

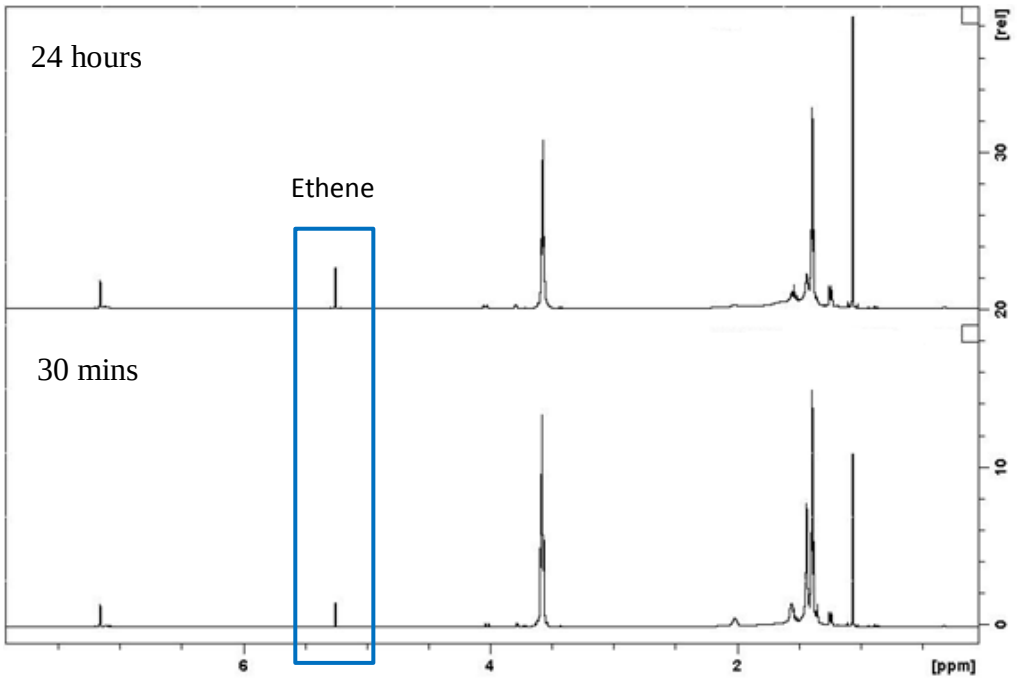

Figure 5.15: ^{1}H NMR spectra of LiTMP in C_6D_6 solution after addition of a few drops of THF in an NMR tube – (bottom) after 30 mins and (top) after 24 hours.

As we have been unable to determine with absolute certainty that it is LiTMP or a particular form of it that is doing the deprotonating we decided to ascertain whether it was possible to co-complex lithiated anisole (white solid prepared from *n*BuLi and anisole in hexane solution) with *i*Bu_3Al in THF solution. The ^{1}H NMR spectrum shows a mixture of lithiated anisole and the expected aluminated anisole product confirming that it is possible for lithiated anisole to undergo a transmetallation process with the alkylaluminium reagent *i*Bu_3Al. The ^{1}H NMR spectrum of this reaction was compared to that of the product generated after **4.2** was reacted with anisole in THF solution at 0^{o}C. This confirms that the products are the same (**Figure 5.16**).

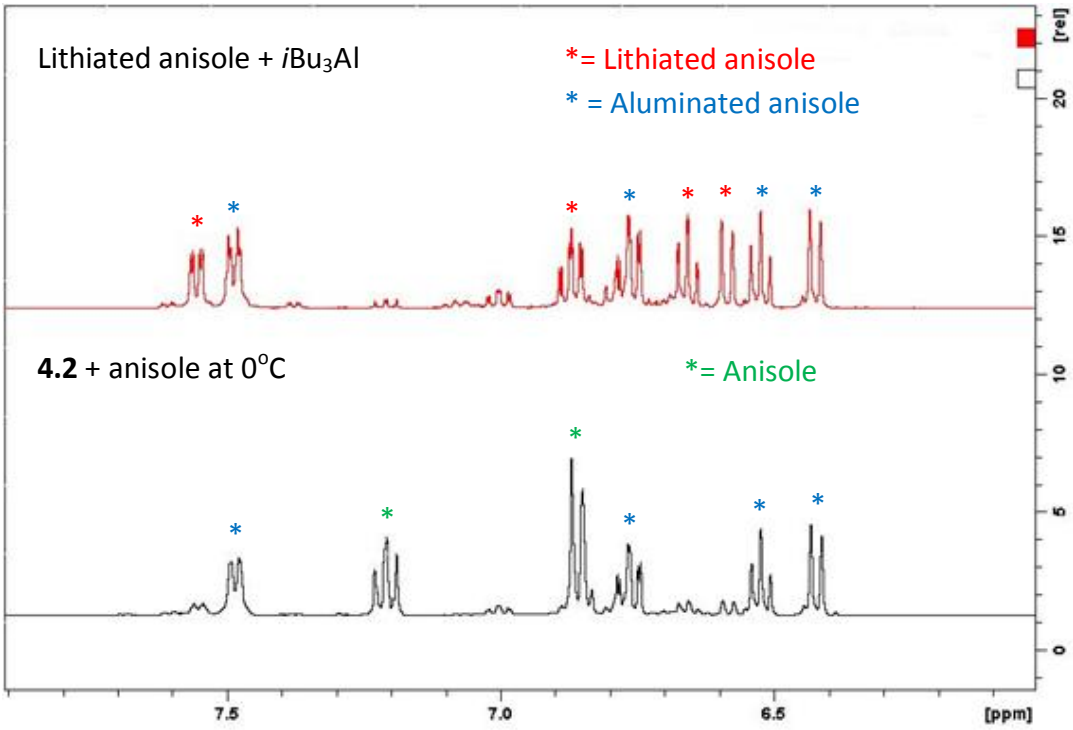

Figure 5.16: Comparison of the ^{1}H NMR spectra in D_8-THF of lithiated anisole reacted with *i*Bu_3Al and **4.2** reacted with anisole at 0°C.

It is therefore possible that LiTMP could be carrying out the deprotonation and the aluminium reagent co-complexing to form the aluminated product that contains an *ortho*-deprotonated anisole. In theory if **4.2** breaks down to the tetra-alkyl aluminate **4.3** and the monometallic component of **4.1** (*i*Bu_2AlTMP) as shown in **Scheme 5.3**, then the lithiated anisole could be trapped by either the lithium aluminate **4.3** or neutral aluminium species *i*Bu_2AlTMP leading to Li(anisole*) and Al(*i*Bu)$_3$ or Li(anisole*) and *i*Bu_2Al(TMP) species.

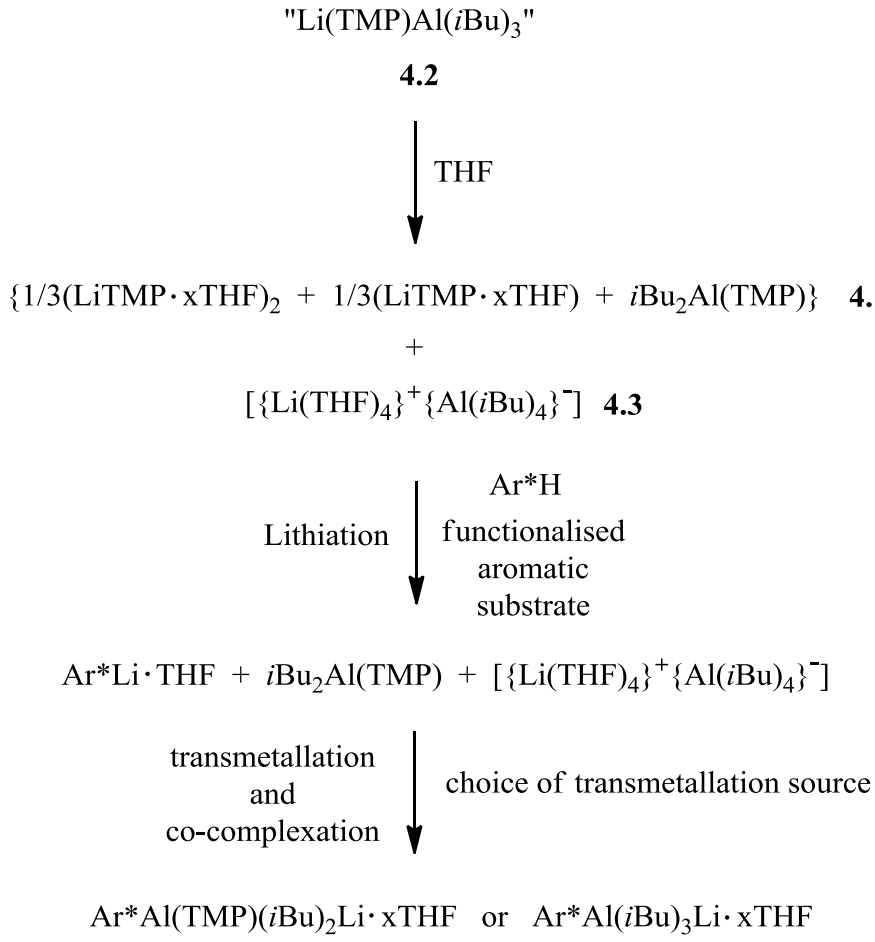

Scheme 5.3: Disproportionation of **4.2** into **4.1** and **4.3** showing that lithiated aromatic substrate can transmetallate/co-complex with either **4.3** or *i*Bu$_2$AlTMP.

In order to prove and try to rationalise why Uchiyama uses 2.2 equivalents of **4.2** in his reactions we decided to react **4.1** in hexane solution with a 1:1 solution of anisole and THF to determine which would be deprotonated preferentially and if there was any competition between the two substrates. If **4.1** is a disproportionation product of mixture **4.2** and anisole is added, a competition between anisole and THF could result in the need to increase the amount of base required. As anticipated **4.1** was found to deprotonate anisole preferentially and there was no sign of THF deprotonation. Only 50% of aluminated anisole was observed in the ^{1}H NMR spectrum as the reaction was only left to stir for 30 minutes (**Figure 5.17**).

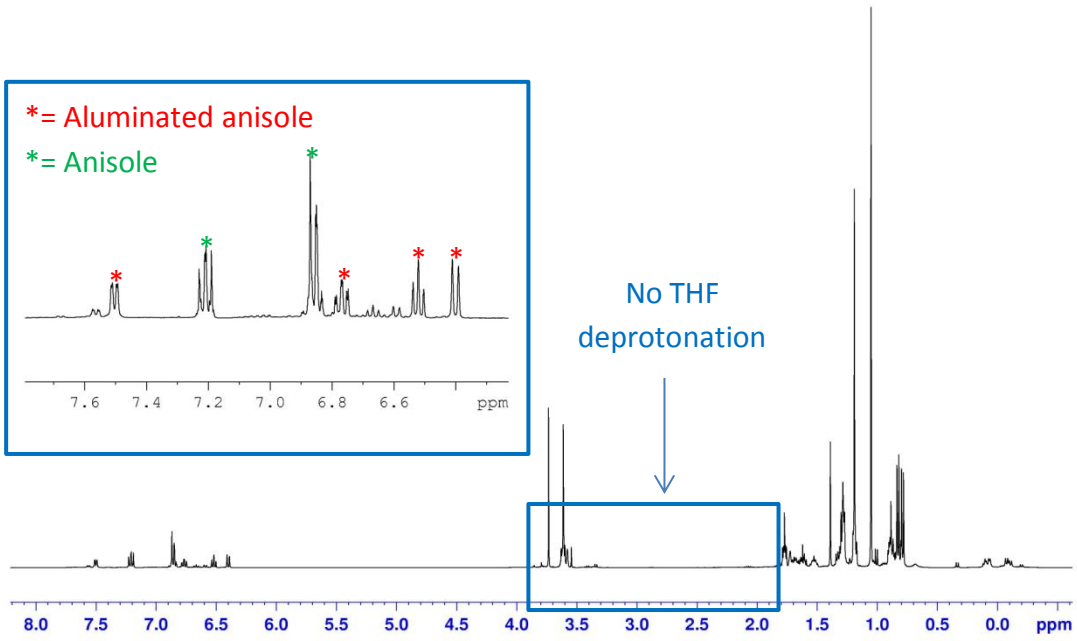

Figure 5.17: ^{1}H NMR spectrum in D_8-THF of reaction filtrate from the reaction of **4.1** with a 1:1 solution of anisole and THF.

It can be concluded that there is no competition between anisole and THF. Anisole is deprotonated preferentially as it is more acidic than THF due to the inductive directing effect of its methoxy substituent. The reason why Uchiyama uses 2.2 equivalents of **4.2** must therefore lie in the fact that it disproportionates to give the inert homoleptic aluminate $[\{Li(THF)_4\}^+\{Al(i\text{Bu})_4\}^-]$ **4.3** and **4.1**, leaving only 50% of active base left in solution.

Another way we wanted to determine whether **4.1** is present as a component of **4.2** in THF solution was to crystallise the homoleptic aluminate **4.3** and remove it from solution and then react the remaining solution with anisole. In theory this would leave **4.1** in solution which should react with anisole if it is the active base. Removing the homoleptic aluminate **4.3** drives the equilibrium further towards the formation of **4.1**. The ^{1}H NMR spectrum of the reaction mixture showed that the remaining mixture did not deprotonate anisole and resonances consistent with THF deprotonation were observed. This was due to the long period of time required to crystallise the homoleptic aluminate before anisole could be added. This observation is still consistent with **4.1** being present in the mixture as it readily deprotonates THF. We know that **4.2** is stable in THF solution for up to two weeks as stated by Uchiyama,[1] so it is very likely that

4.1 is present as the disproportionation product and it is **4.1** which is the active base whether due to a mixed-metal species or lithiation/transmetallation.

One aspect which was particularly puzzling to us was the formation of the aluminated *N*,*N*-diisopropylbenzamide product [(THF)$_3$Li(*i*Pr$_2$NC(=O)C$_6$H$_4$)Al(*i*Bu$_3$)] **4.4** shown in **Scheme 5.4** (also shown in **Scheme 5.2**) as previously reported.[2] Significantly this product has three *i*Bu groups attached to aluminium suggesting that it is **4.2** which is the active base.

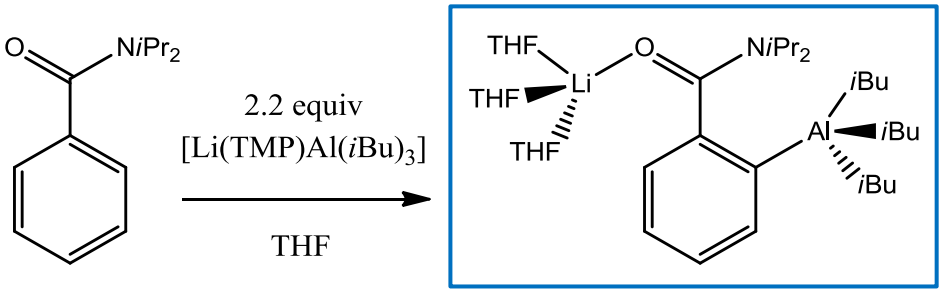

Scheme 5.4: Formation of aluminated *N*,*N*-diisopropylbenzamide [(THF)$_3$Li(*i*Pr$_2$NC(=O)C$_6$H$_4$) Al(*i*Bu$_3$)] **4.4** from reaction of **4.2** with *N*,*N*-diisopropylbenzamide in THF solution.

In order to determine if it is possible to exchange a TMP ligand for an *i*Bu group and if **4.1** in THF solution could form **4.4**, we reacted **4.1** with *N*,*N*-diisopropylbenzamide. The ^{1}H NMR spectrum of the reaction mixture shows a doublet at 8.60 ppm and a second much smaller doublet at 8.45 ppm (top spectrum in **Figure 5.18**). This would suggest that there are two very similar aluminated *N*,*N*-diisopropylbenzamide products. The reaction of **4.2** in THF solution with *N*,*N*-diisopropylbenzamide was also carried out to determine which of the doublets belonged to **4.4**. The ^{1}H NMR spectrum (bottom spectrum in **Figure 5.18**) revealed that the smaller doublet observed in the reaction of **4.1** and *N*,*N*-diisopropylbenzamide (8.45 ppm) is consistent with **4.4** containing three *i*Bu groups. There is also evidence of a smaller doublet at 8.60 ppm which matches the main product observed in the top spectrum of **Figure 5.18**. This is likely to be one containing two *i*Bu groups and one TMP ligand. On the basis of these observations it is likely that in the case of **4.1** the lithiated *N*,*N*-diisopropylbenzamide is trapped by the sole aluminium compound present, namely *i*Bu$_2$AlTMP, whereas in the case of **4.2** it is the lithium tetra-alkyl aluminate **4.3** which does the trapping predominately (**Scheme 5.3**).

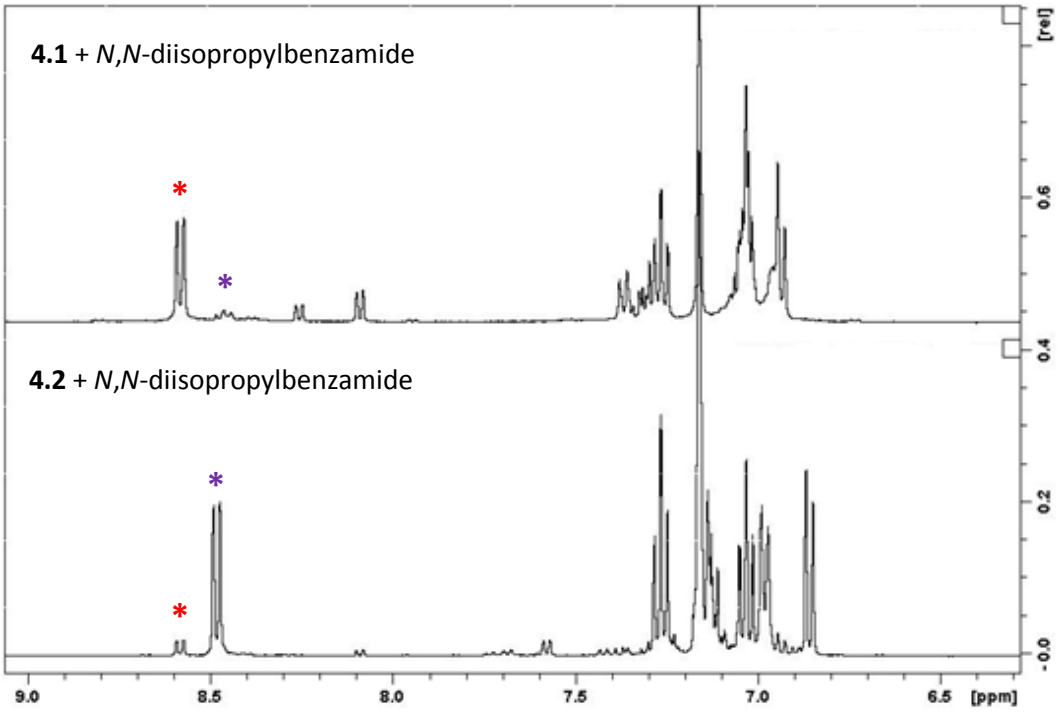

Figure 5.18: Comparison of ^{1}H NMR spectra of reaction mixtures in C_6D_6 of **4.1** and **4.2** with *N*,*N*-diisopropylbenzamide in THF solution.

5.2.4 Further Comparison of 4.1 [Li(TMP)$_2$Al(*i*Bu)$_2$] and 4.2 [Li(TMP)Al(*i*Bu)$_3$]

To strengthen our argument that **4.2** disproportionates to give **4.1** we carried out a comparison of the ^{1}H NMR spectra of each base in THF solution to determine if there were any similarities. The characteristic resonances for the homoleptic aluminate [{Li(THF)$_4$}$^{+}${Al(*i*Bu)$_4$}$^{-}$] **4.3**, which is the other disproportionation product, is highlighted in **Figure 5.19**. A broad low frequency resonance is observed at -0.85 ppm and a doublet at 0.82 ppm for the C$\underline{H}_2$ and C$\underline{H}_3$ hydrogen atoms of the *i*Bu group respectively. From the rest of the spectrum it is clear that there are no major differences between the bases and it is very probable to assume that **4.2** in THF solution could disproportionate to give **4.1**. For comparison the ^{1}H NMR spectrum of an authentic freshly prepared sample of **4.3** is shown in **Figure 5.20**.

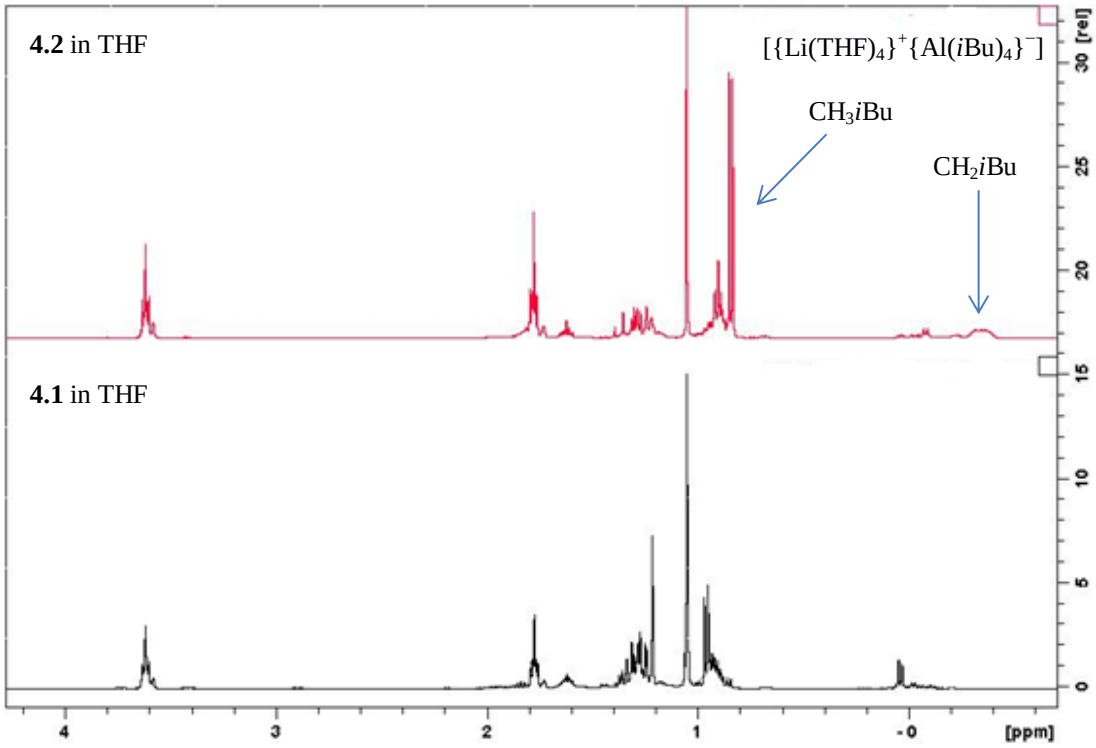

Figure 5.19: A comparison of the ^{1}H NMR spectra in d_8-THF of **4.2** (top) and **4.1** (bottom).

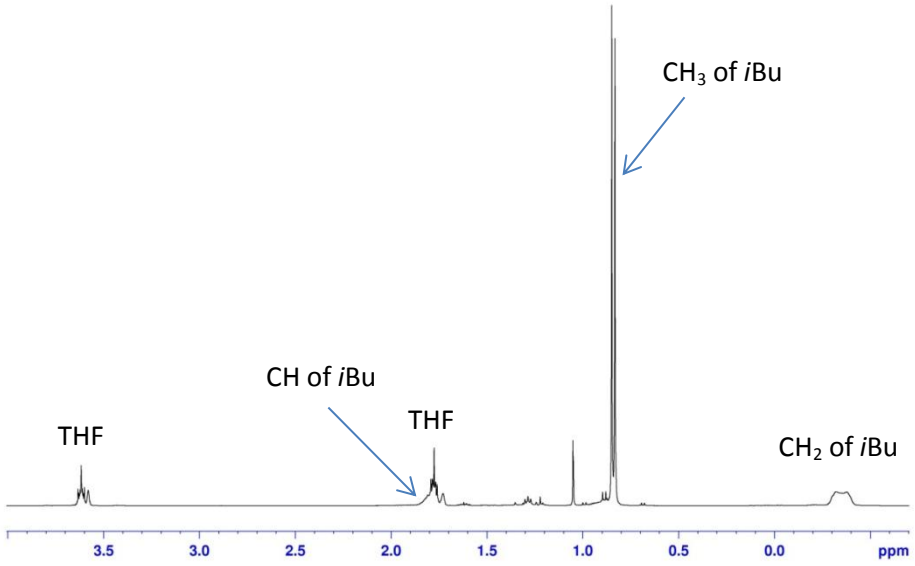

Figure 5.20: ^{1}H NMR spectrum in D_8-THF of homoleptic aluminate [{Li(THF)$_4$}$^{+}${Al(*i*Bu)$_4$}$^{-}$].

5.2.5 Investigation of Sodium Versions of 4.1 and 4.2

We also decided to investigate the sodium version of **4.2** ([Na(TMP)Al(*i*Bu)$_3$] **4.5**) to test its reactivity and determine if there are any differences in reactivity when compared to the lithium version. The sodium base **4.5** was prepared in hexane solution by mixing together NaTMP (prepared from *n*BuNa and TMPH) and *i*Bu$_3$Al with TMEDA added as the donor solvent. A molar equivalent of anisole was then added and the solution was allowed to stir for two hours. From the ^{1}H NMR spectrum of the reaction mixture (**Figure 5.22**) it was found that **4.5** was completely inert and did not react at all with anisole. This was expected as we have already shown that when the lithium base **4.2** is prepared in hexane first and forms the contact ion-pair molecular structure it too is completely unreactive.

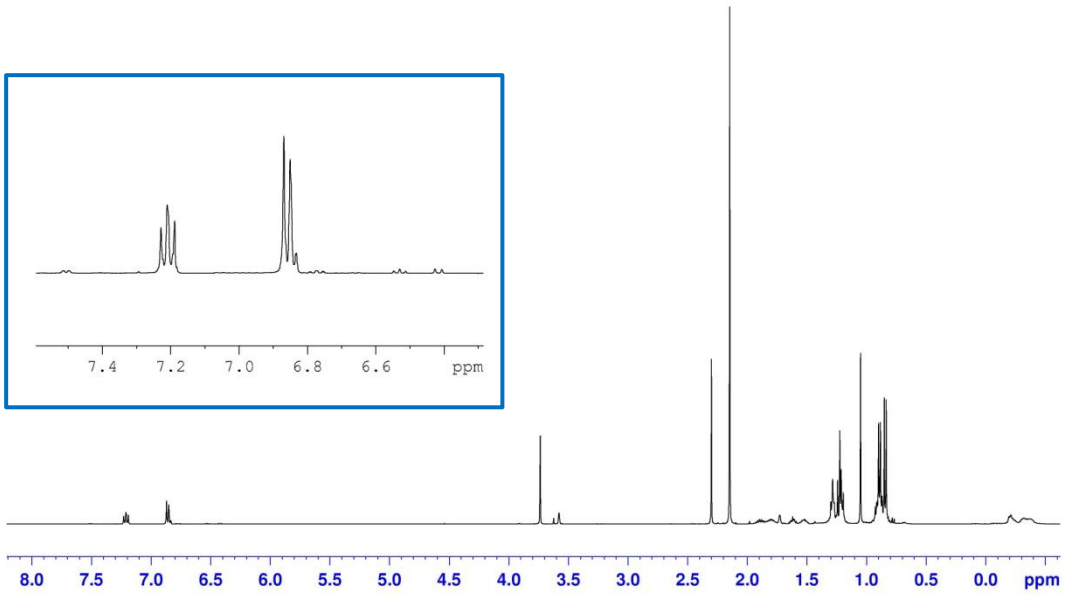

Figure 5.22: ^{1}H NMR spectrum in C_6D_6 of reaction mixture after **4.5** is prepared in hexane solution and combined with anisole.

If the sodium version of **4.1** is prepared in hexane solution ([Na(TMP)$_2$Al(*i*Bu)$_2$] **4.6**) by mixing together NaTMP, *i*Bu$_2$AlTMP, TMEDA and then treated with anisole it also does not deprotonate the ether as evidenced by the ^{1}H NMR spectrum of the reaction mixture. This is in contrast to lithium base **4.1** which readily deprotonates a range of substrates in hexane solution (see **Chapter 2**). This distinction could be due to the formation of a similar contact ion-pair molecular structure as that seen for **4.2** with a closed ring-motif which we know to be completely unreactive in hexane solution and

also when dissolved in THF solution. A contact ion-pair molecular structure could form when substituting lithium for sodium as sodium is a much larger alkali metal so forces the bond between sodium and the TMP N atom to lengthen relieving some of the steric strain of a bulky, high branched TMP bridge. Although we can postulate the likely structure of **4.6** to be [(THF)Na(μ-TMP)$_2$Al(*i*Bu)$_2$] with two bridging TMP anions, we were unable to crystallise a product from hexane solution. However, if **4.6** were to form this closed ring-motif it is more than likely to be unreactive.

In order to test the possibility of monometallic NaTMP deprotonating anisole and sodiated anisole then getting trapped with the aluminium reagent via transmetallation to generate the aluminated product, NaTMP and anisole were reacted in hexane solution for two hours before adding TMEDA and *i*Bu$_3$Al. Unlike the reactions discussed above, we observed deprotonation of anisole in the ^{1}H NMR spectrum (**Figure 5.23**).

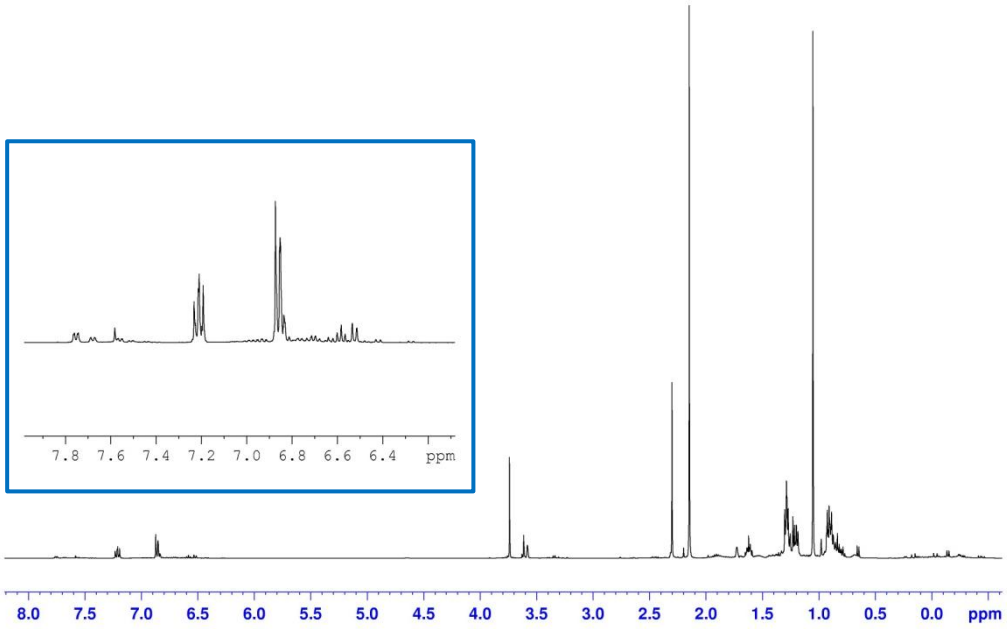

Figure 5.23: ^{1}H NMR spectrum in C_6D_6 of reaction filtrate after NaTMP and anisole were reacted for two hours before adding TMEDA and *i*Bu$_3$Al.

From a previous report by our group on a cadmium ate base,[18] it suggests that LiTMP will only deprotonate anisole to a small extent. Once some anisole has been deprotonated by LiTMP and co-complexed with the secondary metal reagent this drives the equilibrium towards formation of the product. This results in more anisole being deprotonated by LiTMP hence generating a high yield of product. To evaluate whether this scenario was happening in our NaTMP system, the sodium amide was reacted with

anisole for two hours in hexane solution and the ^{1}H NMR spectrum of the reaction mixture was recorded. This confirmed that anisole was only deprotonated in a very small amount (< 10%). When the reaction was repeated but this time TMEDA was added it was found that anisole was deprotonated to a greater extent. This is because TMEDA can coordinate to the sodium increasing its reactivity by forming a smaller complexed NaTMP molecule which can attack the *ortho*-position of anisole which is activated inductively by the OMe group. The reaction was then repeated again but this time adding the aluminium reagent *i*Bu$_2$AlTMP and TMEDA after reacting NaTMP and anisole for two hours. As expected mostly the desired deprotonated product was observed in the ^{1}H NMR spectrum of the reaction mixture with only a small amount of unreacted anisole. The same was true when switching the aluminium reagent to *i*Bu$_3$Al. It was therefore found that both the sodium aluminium bases **4.5** and **4.6** were completely unreactive and a deprotonation was only observed when the substrate was reacted with NaTMP first before co-complexing with the aluminium reagent. The reactivity of these bases should also be considered in THF solution for a full comparison.

5.2.6 Observed Reactivity of 4.2

Based on the observations obtained within this Chapter we can propose a scheme in order to describe the reactivity observed for **4.2** (**Scheme 5.5**). When LiTMP, *i*Bu$_3$Al and one equivalent of THF are added to hexane, Complex **A** with its contact ion-pair structure was found to be completely inert towards metallation. It was found to be totally unreactive whether crystallised and reacted directly or prepared *in situ* first. We also found that crystalline **4.2** when dissolved in THF solution does not form the same base as that formed by preparing **4.2** *in situ* in THF solution (hence Complex **B**), so you cannot form Complex **B** from Complex **A**. When LiTMP and *i*Bu$_3$Al are added to THF solution to form complex **B**, it appears to disproportionate to give the homoleptic aluminate [{Li(THF)$_4$}$^+${Al(*i*Bu)$_4$}$^-$] **4.3** which is completely unreactive towards metallation and a mixture of LiTMP, probably in dimeric and monomeric forms as well as *i*Bu$_2$AlTMP. These final two components equate to **4.1**. We also know that when left to stir in the absence of a substrate **4.1** will deprotonate THF so becomes inactive towards metallation.

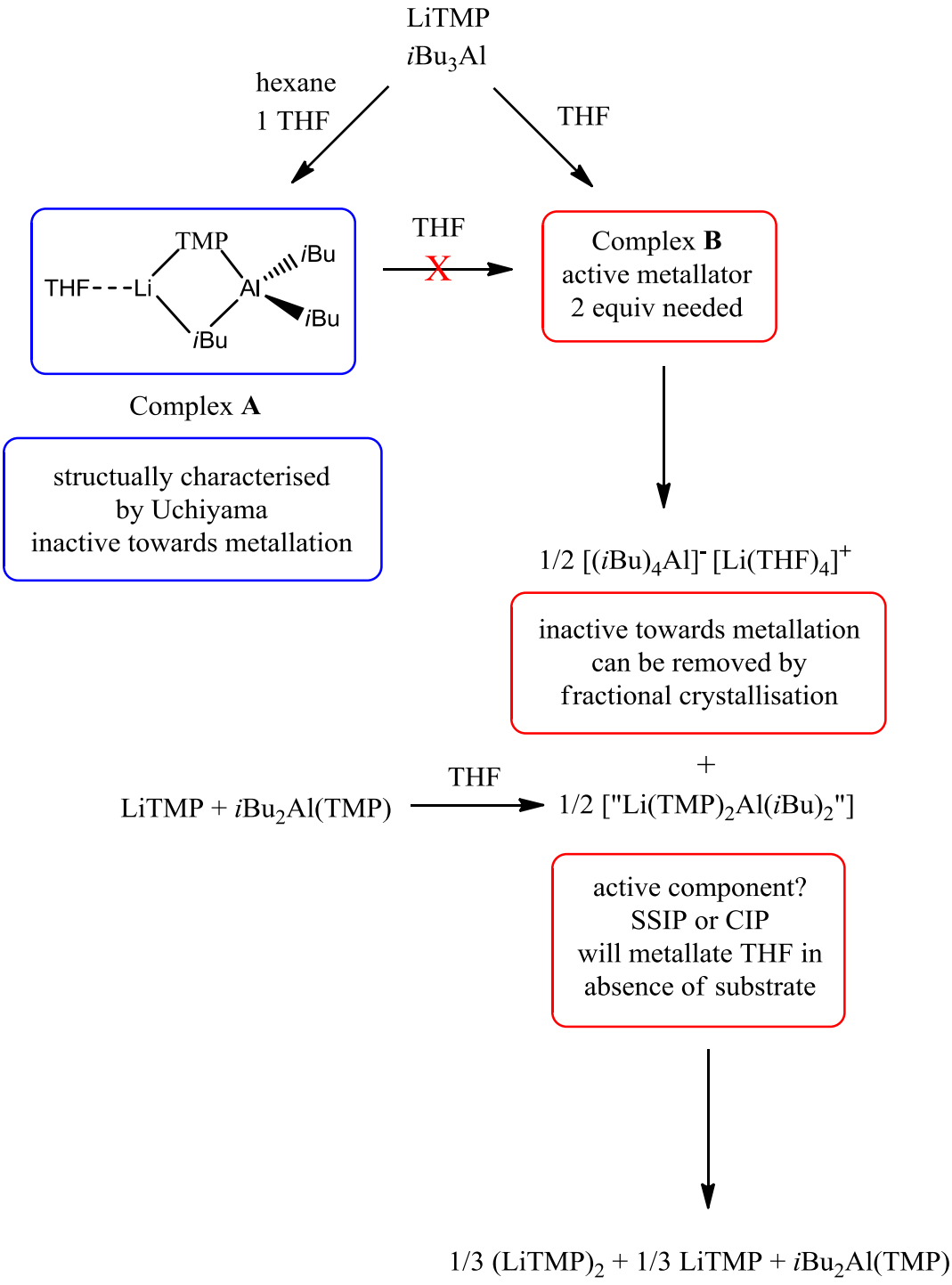

Scheme 5.5: Explanation for the observed reactivity of **4.2** and the conclusions drawn from the experimental observations made.

5.3 Conclusions

Taking the individual reagents separately, the key observations and facts obtained from this study are as follows:

5.3.1 Crystalline 4.2

- The base with a well-defined contact ion-pair structure does not disproportionate in D_8-THF even after 1 week or by heating or cooling the solution.
- It does not react with anisole when dissolved in THF.
- If it is prepared *in situ* in hexane it also does not react with anisole.

These observations strongly argue that **4.2** crystallised from hexane solution using a stoichiometric amount of THF is not the same base as that prepared *in situ* in THF solution. It also suggests that once this closed ring structure is formed it renders the complex completely unreactive as it can no longer deprotonate anisole.

5.3.2 4.2 prepared *in situ* in THF solution

- Mixture **4.2** appears to be more reactive at 0^oC than at room temperature suggesting degradation of THF at ambient temperature.
- When the homoleptic aluminate **4.3** is removed from a solution of the **4.2** mixture there is evidence of THF deprotonation in the ^1H NMR spectrum.
- If **4.2** is allowed to stir for 24 hours at ambient temperature before adding anisole it does not deprotonate.
- When lithiated anisole and iBu$_3$Al were added together in THF solution the ^1H NMR spectrum shows a mixture of lithiated anisole and aluminated anisole. This is also consistent with the product formed if *in situ* **4.2** and anisole are reacted at 0^oC.

These observations suggest that there is more of the active base present at 0^oC than at room temperature implying that either the active component is the kinetic product of the disproportionation and as the temperature increases the thermodynamic product begins to form decreasing the reactivity of the base towards anisole or alternatively that the active base is LiTMP, probably in monomeric form, which is unstable in THF over time. After removing the homoleptic aluminate **4.3** from solution, THF deprotonation is observed. This is a key indication that **4.1** is one of the disproportionation products formed as a previous report by Uchiyama states that **4.2** is stable in THF solution even

after 2 weeks. When the homoleptic component is removed this shifts the equilibrium in favour of **4.1** which subsequently deprotonates THF. The observation by Uchiyama that the base is stable in THF solution after 2 weeks is questionable as allowing **4.2** to stir for 24 hours and then testing its reactivity with anisole confirms that if left over time the base becomes inactive.

5.3.3 4.1 prepared *in situ* in THF solution

- **4.1** deprotonates anisole in THF solution.
- From a comparison of the ^{1}H NMR spectra of **4.1** and its components it looks like it does not form a mixed-metal species but rather LiTMP and *i*Bu$_2$AlTMP swimming separately in solution.
- After stirring for 24 hours in bulk THF solution there is evidence of THF deprotonation/degradation.
- The deprotonated THF compound [(THF)Li(μ-TMP)(μ-OC$_4$H$_7$)Al(*i*Bu)$_2$] does not deprotonate anisole.
- If **4.1** is allowed to stir for 24 hours before adding anisole there is only a very small amount of deprotonation probably due to competitive attack of THF.
- **4.1** in hexane preferentially deprotonates anisole over THF if a 1:1 mixture is used.
- Resonances in the ^{27}Al NMR spectra of **4.1** and starting aluminium reagents *i*Bu$_3$Al and *i*Bu$_2$AlTMP are broadened so much they are essentially invisible due to the quadrupolar nature of ^{27}Al nuclei. Only the homoleptic aluminate gives a sharp signal as it is thought to be highly symmetrical.

These observations strongly point to the fact that **4.1** is actually just the separate components LiTMP and *i*Bu$_2$AlTMP in THF solution rather than a mixed-metal base. **4.1** will deprotonate anisole if it is added within 5 mins otherwise it will begin to attack bulk THF solution. The deprotonated THF compound [(THF)Li(μ-TMP) (μ-OC$_4$H$_7$)Al(*i*Bu)$_2$] does not act as a base so when **4.1** deprotonates/attacks THF it loses its basicity. This is consistent with **4.1** being the active base of **4.2** as it also loses its reactivity if allowed in stir in THF for a long period of time. **4.1** will deprotonate anisole preferentially over THF, there is no competition between these substrates. A competition between THF and anisole cannot be used as an explanation for why 2.2 equivalents of the base are used. We can conclude that this stoichiometry is due to the

disproportionation of **4.2** to give **4.1** and **4.3** hence only 50% of the active base remains. The ^{27}Al NMR spectra of **4.1** and **4.2** along with the starting materials were uninformative as these species cannot be detected due to the quadrapolar ^{27}Al nuclei. Only the homoleptic aluminate **4.3** was detected as it is symmetrical.

5.3.4 Concluding Explanations

There are two possible explanations for the observations discussed within this chapter namely:

1. The *in situ* prepared **4.2** [Li(TMP)Al(*i*Bu)$_3$] in THF solution disproportionates to give **4.1** [Li(TMP)$_2$Al(*i*Bu)$_2$] which is the active base. This disproportionation explains why Uchiyama uses 2.2 molar equivalents of **4.2** because it disproportionates into **4.1** and the homoleptic aluminate **4.3** [{Li(THF)$_4$}$^+${Al(*i*Bu)$_4$}$^-$] which has been confirmed to be unreactive towards deprotonation.
2. If **4.1** is indeed the active base it is actually just the separate species LiTMP and *i*Bu$_2$AlTMP present in THF solution, that is there is no formation of a mixed-metal lithium aluminate complex. It is actually LiTMP which carries out the deprotonation, probably in its active monomeric form (LiTMP·THF) which has previously been reported and lithiated anisole is subsequently trapped by the more carbophilic *i*Bu$_2$AlTMP which drives the equilibrium to form a high yield of product. The homoleptic aluminate **4.3** could also potentially trap the deprotonated aromatic substrate.

5.4 Future Work

Assuming deprotonation is via lithiation, what species does the lithiated aryl (e.g. lithiated anisole) perform the transmetallation/co-complexation with? A few reactions for future work include reacting lithiated anisole with *i*Bu$_2$AlTMP (**Equation 1**) and reacting lithiated anisole with the homoleptic aluminate **4.3** (**Equation 2**).

(1) (Anisolyl)Li + *i*Bu$_2$Al(TMP) $\xrightarrow{\text{THF}}$ (Anisolyl)Al(TMP)(*i*Bu)$_2$Li(THF)

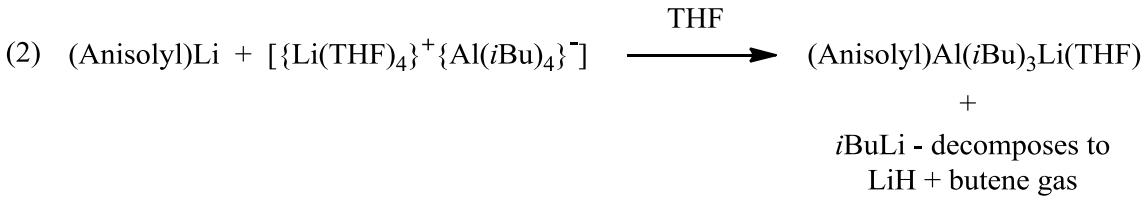

The ^{1}H NMR spectra of the products generated from these reactions should be compared to the ^{1}H NMR spectrum of the product generated when **4.2** is prepared *in situ* in THF solution and reacted with anisole. Which of these species carries out the transmetallation?

The last reaction to carry out would be to react *i*Bu$_2$AlTMP with the homoleptic aluminate **4.3** (**Equation 3**) to see if this could generate Al(*i*Bu)$_3$ which could carry out the transmetallation/co-complexation.

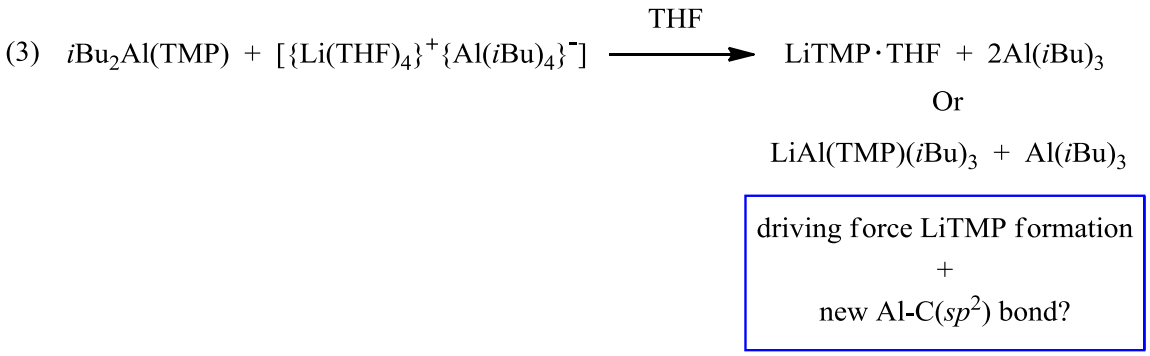

Hence the transmetallating/co-complexing species could be either Al(*i*Bu)$_3$, *i*Bu$_2$Al(TMP) or [{Li(THF)$_4$}$^+${Al(*i*Bu)$_4$}$^-$].

5.5 Experimental

5.5.1 General Methods

As a consequence of the air and moisture sensitivity of the metal compounds involved in this project, all reactions and manipulations were performed under a protective argon atmosphere using either standard Schlenk techniques or a glove box (Faircrest). All solvents were dried over Na/benzophenone and freshly distilled prior to use. Anisole and *N*,*N*-diisopropylbenzamide was purchased from Aldrich and used as received without additional purification. ^{1}H NMR spectra were recorded on a Bruker AV400 MHz spectrometer operating at 400.03 MHz. ^{1}H NMR chemical shifts are quoted relative to TMS standard at 0.00 parts per million. ^{7}Li NMR spectra were recorded on a

Bruker AV400 MHz spectrometer operating at 155.50 MHz. ^{7}Li NMR chemical shifts are quoted relative to LiCl standard at 0.00 parts per million.

Procedure for DOSY NMR experiment

DOSY experiments were performed on a Bruker AVANCE 400 NMR spectrometer operating at 400.13 MHz for proton resonance under TopSpin (version 2.0, Bruker Biospin, Karlsruhe) and equipped with a BBFO-z-atm probe with actively shielded z-gradient coil capable of delivering a maximum gradient strength of 54 G/cm. Diffusion ordered NMR data were acquired using the Bruker pulse program dstegp3s employing a double stimulated echo with three spoiling gradients. Sine-shaped gradient pulses were used with a duration of 4 ms (P30) together with a diffusion period of 100 ms (D20). Gradient recovery delays of 200 μs followed the application of each gradient pulse. Data were systematically accumulated by linearly varying the diffusion encoding gradients over a range from 2% to 95% for 64 gradient increment values. The signal decay dimension on the pseudo-2D data was generated by Fourier transformation of the time-domain data. DOSY plots were generated by use of the DOSY processing module of TopSpin. Parameters were optimised empirically to find the best quality of data for presentation purposes. Diffusion coefficients were calculated by fitting intensity data to the Stejskal-Tanner expression with estimates of errors taken from the variability in the calculated diffusion coefficients by consideration of different NMR responses for the same molecules of interest.

Preparation of 4.1 in THF solution

LiTMP was prepared as follows: hexane (50 mL) was added to an oven-dried Schlenk tube. Next, 1.6M *n*BuLi (12.5 mL, 20 mmol) was added, followed by TMP(H) (3.4 mL, 20 mmol) at room temperature. The reaction mixture was left to stir for 30 minutes before freezing in liquid nitrogen and placing in the Schlenk flask in the freezer at -30^{o}C. A white solid formed in solution which was isolated by filtration and the solid was stored inside the glove box.

*i*Bu$_2$Al(TMP) was prepared as follows: hexane (50 mL) was added to an oven-dried Schlenk tube. Next, 1.6M *n*BuLi (12.5 mL, 20 mmol) was added, followed by TMP(H) (3.4 mL, 20 mmol) at room temperature. The reaction mixture was left to stir for 10 minutes before adding *i*Bu$_2$AlCl (3.8 mL, 20 mmol) which produced a white suspension

almost immediately. The reaction was left to stir for 1 hour and was then filtered through Celite and glass wool, which was then washed with more hexane (20 mL). The solution was removed under vacuum to give a pale yellow oil which was stored inside the glove box.

Before every reaction involving **4.1**, LiTMP (0.29g, 2 mmol) and *i*Bu_2Al(TMP) (0.56g, 2 mmol) were added to an oven dried Schlenk tube inside the glove box. 10 mL of THF were added to give the base **4.1** in THF solution.

Preparation of 4.2 in THF solution

Before every reaction involving **4.2**, LiTMP (0.29g, 2 mmol) was added to an oven dried Schlenk tube inside the glove box. 10 mL of THF was then added at 0^oC before adding *i*Bu_3Al (2 ml, 2 mmol) to give the base **4.2** in THF solution.

Synthesis of crystalline 4.2

Hexane (50 mL) was added to an oven-dried Schlenk tube. Next, 1.6M *n*BuLi (12.5 mL, 20 mmol) was added, followed by TMP(H) (3.4 mL, 20 mmol) at room temperature. The reaction mixture was left to stir for 10 minutes before adding *i*Bu_3Al (20 ml, 20 mmol) and one molar equivalent of THF (1.6 ml, 20 mmol). The Schlenk tube was placed in the freezer at -30^oC affording colourless crystals in solution. The crystals were isolated and stored within the glove box.

^{1}H NMR data (400.13 MHz, 298 K, D_8-THF)

δ = -0.21 [6H, d, 3 x CH_2 of *i*Bu], 0.88 [18H, d, 6 x CH_3 of *i*Bu], 1.20 [12H, s, 4 x CH_3 of TMP], 1.20 [4H, m, 2 x βCH_2 of TMP], 1.51 [2H, m, γCH_2 of TMP], 1.78 [4H, m, 2 x CH_2 of THF], 1.90 [3H, m, 3 x CH of *i*Bu], 3.61 ppm [4H, m, 2 x CH_2 of THF].

Synthesis of Homoleptic Aluminate 4.3

4.2 was prepared as described above. The Schlenk flask was placed in the freezer at -30^oC, after a few days colourless crystals formed in solution. The crystals were isolated by filtration and stored inside the glove box.

^{1}H NMR data (400.13 MHz, 298 K, D_8-THF)

δ = -0.85 [8H, d, 4 x CH_2 of *i*Bu], 0.82 [24H, d, 8 x CH_3 of *i*Bu], 1.79 [CH_2 of THF], 1.81 [4H, m, 4 x CH of *i*Bu], 3.61 ppm [CH_2 of THF].

Preparation of [(THF)Na(TMP)Al(*i*Bu)$_3$] 4.5

*n*BuNa (0.16 g, 2 mmol) was added to an oven dried Schlenk tube followed by 10 mL of hexane (10 mL). TMP(H) (0.34 mL, 2 mmol) was added at room temperature generating NaTMP which was left to stir for 30 minutes. *i*Bu_3Al (2 mL, 2 mmol) was added followed by one molar equivalent of THF (0.16 mL, 2 mmol).

Preparation of [(THF)Na(TMP)$_2$Al(*i*Bu)$_2$] 4.6

*n*BuNa (0.16 g, 2 mmol) was added to an oven dried Schlenk tube followed by 10 mL of hexane (10 mL). TMP(H) (0.34 mL, 2 mmol) was added at room temperature generating NaTMP which was left to stir for 30 minutes. *i*Bu_2AlTMP (0.56 g, 2 mmol) was added followed by one molar equivalent of THF (0.16 mL, 2 mmol).

5.6 References

[1] M. Uchiyama, H. Naka, Y. Matsumoto, T. Ohwada, *J. Am. Chem. Soc.* **2004**, *126*, 10527.

[2] B. Conway, E. Hevia, J. Garcia-Alvarez, D. V. Graham, A. R. Kennedy, R. E. Mulvey, *Chem. Commun.* **2007**, 5241.

[3] D. Li, I. Keresztes, R. Hopson, P. Williard, *Acc. Chem. Res.* **2009**, *42*, 270.

[4] A. Macchioni, G. Ciancaleoni, C. Zuccaccia, D. Zuccaccia, *Chem. Soc. Rev.* **2008**, *37*, 479.

[5] B. Antalek, *Concepts Magn. Reson., Part A* **2007**, *30*, 219.

[6] T. Brand, E. J. Cabrita, S. Berger, *Mod. Magn. Reson.* **2006**, *1*, 131.

[7] M. Nilsson, G. A. Morris, *Magn. Reson. Chem.* **2006**, *44*, 655.

[8] Y. Cohen, L. Avram, L. Frish, *Angew. Chem. Int. Ed.* **2005**, *44*, 520.

[9] J. S. Gounarides, A. Chen, M. J. Shapiro, *J. Chromatogr. B* **1999**, *725*, 79.

[10] E. O. Stejskal, J. E. Tanner, *J. Chem. Phys.* **1965**, *42*, 288.

[11] K. F. Morris, C. S. J. Johnson, *J. Am. Chem. Soc.* **1992**, *114*, 3139.

[12] J. Garcia-Alvarez, E. Hevia, A. R. Kennedy, J. Klett, R. E. Mulvey, *Chem. Commun.* **2007**, 4202.

[13] P. Renaud, M. A. Fox, *J. Am. Chem. Soc.* **1988**, *110*, 5702.

[14] D. R. Armstrong, P. Garcia-Alvarez, A. R. Kennedy, R. E. Mulvey, S. D. Robertson, *Chem. Eur. J.* **2011**, *17*, 6725.

[15] F. E. Romesberg, D. B. Collum, *J. Am. Chem. Soc.* **1992**, *114*, 2112.

[16] J. H. Gilchrist, D. B. Collum, *J. Am. Chem. Soc.* **1992**, *114*, 794.

[17] A. Maercker, *Angew. Chem. Int. Ed.* **1987**, *26*, 972.

[18] D. R. Armstrong, A. R. Kennedy, R. E. Mulvey, J. A. Parkinson, S. D. Robertson, *Chem. Sci.* **2012**, *3*, 2700.

Chapter 6: General Experimental

6.1 Schlenk Techniques

As organoalkali metal and organoaluminium compounds are thermodynamically unstable in the presence of moisture and oxygen, all the synthetic chemistry was performed under a protective dry inert argon atmosphere. High-vacuum Schlenk techniques using a vacuum/argon double manifold (**Figure 7.1**) set up were employed routinely to perform this sensitive synthetic work. An argon filled glove box was utilised for the manipulation and storage of all air-sensitive starting materials and products.

Figure 6.1: Standard experiment Schlenk line set-up.

The Schlenk apparatus consists of two separate lines: one line is connected to a vacuum pump while the other is to a supply of dry oxygen-free argon. Five glass taps are positioned along the line which can in turn allow the entry or removal of gas from the system by opening to cylinder argon or vacuum respectively. To ensure an air-tight environment all taps and joints are lubricated with high vacuum grease. An outlet oil-filled Dreschel bottle is positioned at one end of the line to prevent gas overpressure. At the opposite end of the line a vacuum trap is placed in a Dewar flask of liquid nitrogen to prevent solvent contaminating the vacuum pump after removal from the reaction vessel. Before an air-sensitive reaction each Schlenk tube is placed under vacuum for approximately 5 minutes to remove oxygen. The Schlenk tube is subsequently flushed

with dry, oxygen-free argon gas. This procedure is repeated at least three times to ensure that as much oxygen as possible has been removed from the system.

6.2 Glove Box with Gas Recirculation/Purification System

In order to prevent new compounds and starting materials from decomposing, every compound sensitive to air and moisture was stored within a glove box. In addition, NMR spectroscopic and microanalysis samples were also prepared within the glove box as well as the weighing of starting materials and isolated products. The glove box (**Figure 7.2**) contains two evacuable ports (small and large) and is fitted with butyl rubber gloves.

Figure 6.2: A standard glove box with gas recirculation and purification system.

The argon atmosphere is maintained by gas circulation, where the gas is circulated via a pumping system between the glove box and the H_2O/O_2 gas purification system. Oxygen and moisture levels (ppm values) are monitored by sensors inside the box and can be easily read off a dial situated at the top of the box. The box was regenerated approximately once every 2-3 months as required. In order to prevent air and moisture entering the box the port was evacuated for a minimum of 10 minutes before flushing with argon. This procedure was done in triplicate to ensure an oxygen-free port and allow the inner port door to be opened without introducing oxygen or moisture to the glove box. Solid compounds inside an argon-filled Schlenk flask can be taken into the box as long as the flask is placed under vacuum and the taps are well greased. Starting

materials can also be removed from the glove box after clean, dry glassware (with open taps) have been placed in the port and evacuated three times as previously mentioned.

6.3 Reagents Used

The majority of reagents and solvents used within this PhD project were purchased from the Aldrich Chemical Company. This includes anisole, 2-iodoanisole, 1-methoxynapthalene, *m*-tolunitrile, ferrocene, *n*BuLi (1.6 M solution in hexane), *i*Bu_2AlCl, THT, 2-methylTHF, THTP, 1,3-dithiane, *trans*-stilbene oxide, Me_4AEE, *i*Bu_3Al (1.0 M in hexane), DME, 3-iodoanisole, 1,3-diphenylisobenzofuran, 4-iodoanisole, 4-bromoanisole, 4-chloroanisole, sulfuryl chloride, *N*-chlorosuccinimide, *N*-bromosuccinimide, hexachloroethane, 1,2-dibromotetrachloroethane, bromine and iodine. 1,3-dimethoxybenzene, *N*,*N*-diisopropylbenzamide and *cis*-DMP(H) were purchased from Alfa Aesar and used as received. TMP(H) was purchased from Merck and stored over 4Å molecular sieves prior to employment. *N*,*N*-dimethylbenzylamine was purchased from Aldrich and distilled over calcium hydride prior to use. *i*Bu_2Al(TMP) and Li(TMP) were prepared *in situ*; (Me_2TFA and MDAE),[1] Me_6TREN[2] and TMCDA[3] were prepared by literature methods. All solvents (THF, hexane, toluene, THP, benzene and diethyl ether) were dried over Na/benzophenone and freshly distilled prior to use (discussed in detail below).[4] All reagents were purchased at the highest purity available.

6.4 Solvent and Reagent Purification

Many of the solvents and reagents required prior purification before they were used due to many containing small amounts of dissolved moisture and oxygen hence these were distilled and degassed before taking part in any preparation/reaction.

The distillation of solvents was carried out under an inert nitrogen atmosphere. The solvents were dried over a sodium metal and benzophenone solution. Sodium hydroxide and hydrogen gas are the products formed when the sodium metal reacts with dissolved water.[4] The remaining sodium metal reacts with benzophenone and forms the blue ketal radical. The blue coloured solution is an indicator that the solvent is dry. Some of the reagents mentioned above also required prior distillation in the presence of calcium

hydride (CaH_2). The distilled solution was subsequently stored over 4Å molecular sieves.

A freeze-pump-thaw methodology[5] was used to remove any dissolved oxygen from solvents such as deuterated benzene, THF, toluene and cyclohexane. This degassing technique involved freezing the solvent in liquid nitrogen, placing the vial under vacuum and then allowing it to thaw to room temperature. This was repeated three times to ensure a completely oxygen free solution. Similarly, all degassed solvents were stored over 4Å molecular sieves to avoid moisture contamination.

6.5 Standardisation of Reagents

Standardisation is a procedure employed to check the molarity of a solution. Reagents such as *n*-butyllithium can react with trace amounts of moisture and air or loss of solvent can occur and hence the molarity of their solutions change over time. It is therefore essential that the reagent is standardised so that an accurate molarity of the reagent is added into a reaction. Standardisation is carried out by titration of the reagent with salicylaldehyde phenylhydrazone in dry THF.[6] The formation of a red coloured solution indicates the end point. The molarity of the reagent can then be calculated.

To standardise *n*BuLi, salicylaldehyde phenylhydrazone is weighed into a Schlenk flask (0.6 g) and is dried under vacuum. 10 mL of dry THF is added and the resulting solution is titrated against *n*BuLi until a red colour is formed indicating the end point (**Figure 6.3**). The molarity of the *n*BuLi solution can be calculated as follows:

Moles of salicylaldehyde phenylhydrazone = 0.6/212.25 = X

1 mole of indicator reacts with 1 mole of *n*BuLi so Molarity of solution (mol/L) = X/Titration volume x 1000

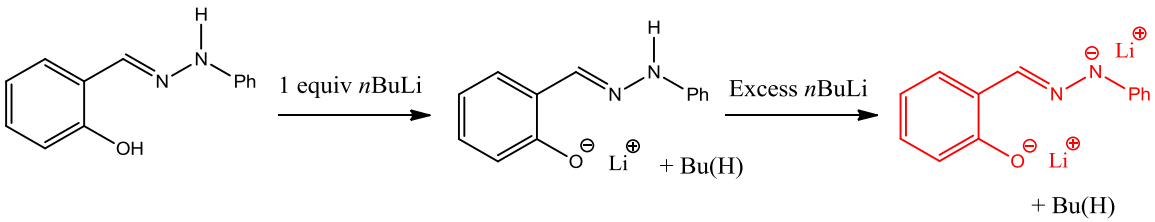

Figure 6.3: Standardisation of *n*BuLi with salicylaldehyde phenylhydrazone.

6.6 Preparation of Commonly Used Starting Materials

6.6.1 Synthesis of LiTMP

Hexane (50 mL) was added to an oven-dried Schlenk tube. Next, 1.6M *n*BuLi (12.5 mL, 20 mmol) was introduced, followed by TMP(H) (3.4 mL, 20 mmol) at room temperature. The Schlenk flask was frozen in liquid nitrogen and placed in the freezer at -30^{o}C. An off white solid formed in solution which was isolated by filtration and stored in the glove box.

6.6.2 Synthesis of *i*Bu$_2$AlTMP

Hexane (50 mL) was added to an oven-dried Schlenk tube. Next, 1.6M *n*BuLi (12.5 mL, 20 mmol) was added, followed by TMP(H) (3.4 mL, 20 mmol) at room temperature. The reaction mixture was left to stir for 10 min and then *i*Bu$_2$AlCl (3.8 mL, 20 mmol) was injected into the Schlenk tube, producing a white suspension almost immediately. The reaction was left to stir for 1 hour and was then filtered through Celite and glass wool, which was then washed with more hexane (20 mL). Hexane was removed under vacuum leaving a pale yellow oil which was stored in the glove box.

6.7 Analytical Procedures

6.7.1 Nuclear Magnetic Resonance Spectroscopy

All NMR spectroscopic samples were prepared either in the glove box or on the Schlenk line via an NMR manifold to ensure an oxygen and moisture free environment. Deuterated solvents such as benzene, cyclohexane and THF were dried over 4Å molecular sieves and were used to dissolve the sample. The NMR tube was kept free from air using a cap tightly wound with Parafilm. ^{1}H, ^{7}Li and ^{13}C NMR spectra were recorded on a Bruker AV400 MHz spectrometer (operating at 400.03 MHz for ^{1}H, 155.50 MHz for ^{7}Li and 100.58 MHz for ^{13}C). All ^{13}C NMR spectra were proton decoupled. All ^{1}H and ^{13}C chemical shifts were quoted relative to a TMS standard at 0.00 parts per million. ^{7}Li chemical shifts were quoted related to a LiCl standard at 0.00 parts per million. ^{1}H-^{1}H and ^{1}H-^{13}C correlations were identified using COSY and HSQC NMR techniques respectively.

6.7.2 X-ray Crystallography

All crystals were grown under an inert argon atmosphere at temperatures ranging from 20 to -30^{o}C. The remaining filtrate was removed via syringe and the crystals dried under vacuum for a few minutes. Crystals suitable for X-ray diffraction were obtained with a Nonius Kappa CCD Diffractometer using graphite monochromated Mo-K_{α} radiation (λ = 0.71073Å) and data was checked so that it was suitable for publication by Dr A. Kennedy at the University of Strathclyde.

6.7.3 Microanalysis

The percentage elemental composition was determined using microanalysis measurements. The percentage of carbon, hydrogen and nitrogen in the compounds was calculated using a Perkin Elmer 2400 Series II CHN/S Analyser and performed by Denise Gilmour at the University of Strathclyde. The samples were analysed in triplicate and stored in an air-tight container after manipulation inside the glove box. Due to the air-sensitive nature of the samples being analysed it was not always possible to obtain completely accurate measurements despite repeated attempts.

6.7.4 GC-MS Analysis

Gas chromatography-mass spectrometry (GC-MS) was performed using Thermo Finnigan Polaris Q GCMS (ion trap) by Patricia Keating at the University of Strathclyde.

6.7.5 DOSY NMR experiments

DOSY NMR experiments were performed on a Bruker AVANCE 400 NMR spectrometer operating at 400.13 MHz for proton resonance under TopSpin (version 2.0, Bruker Biospin, Karlsruhe) and equipped with a BBFO-z-atm probe with actively shielded z-gradient coil capable of delivering a maximum gradient strength of 54 G/cm. Diffusion ordered NMR data were acquired using the Bruker pulse program dstegp3s employing a double stimulated echo with three spoiling gradients. Sine-shaped gradient pulses were used with a duration of 2.75 ms (P30) together with a diffusion period of 100 ms (D20). Gradient recovery delays of 200 μs followed the application of each gradient pulse. Data were systematically accumulated by linearly varying the diffusion encoding gradients over a range from 2% to 95% for 64 gradient increment values. The

signal decay dimension on the pseudo-2D data was generated by Fourier transformation of the time-domain data. DOSY plots were generated by use of the DOSY processing module of TopSpin. Parameters were optimized empirically to find the best quality of data for presentation purposes. Diffusion coefficients were calculated by fitting intensity data to the Stejskal-Tanner expression with estimates of errors taken from the variability in the calculated diffusion coefficients by consideration of different NMR responses for the same molecules of interest.

6.8 References

[1] H. J. Reich, W. S. Goldenberg, A. W. Sanders, *ARKIVOC* **2004**, *xiii*, 97.

[2] G. J. P. Britovsek, J. England, A. J. P. White, *Inorg. Chem.* **2005**, *44*, 8125.

[3] J.-C. Kizirian, N. Cabello, L. Pinchard, J.-C. Caille, A. Alexakis, *Tetrahedron* **2005**, *61*, 8939.

[4] D. F. Shriver, M. A. Derezdzon, *The Manipulation of Air-Sensitive Compounds*, Wiley And Sons, New York, **1986**.

[5] D. F. Shriver, M. A. Derezdzon, *The Manipulation of Air-Sensitive Compounds*, Wiley And Sons, New York, **1986**.

[6] B. E. Love, E. G. Jones, *J. Org. Chem.* **1999**, *64*, 3755.